

## CANADIAN THESES ON MICROFICHE

I.S.B.N.

## THESES CANADIENNES SUR MICROFICHE



National Library of Canada  
Collections Development Branch

Canadian Theses on  
Microfiche Service

Ottawa, Canada  
K1A 0N4

Bibliothèque nationale du Canada  
Direction du développement des collections

Service des thèses canadiennes  
sur microfiche

### NOTICE

The quality of this microfiche is heavily dependent upon the quality of the original thesis submitted for microfilming. Every effort has been made to ensure the highest quality of reproduction possible.

If pages are missing, contact the university which granted the degree.

Some pages may have indistinct print especially if the original pages were typed with a poor typewriter ribbon or if the university sent us a poor photocopy.

Previously copyrighted materials (journal articles, published tests, etc.) are not filmed.

Reproduction in full or in part of this film is governed by the Canadian Copyright Act, R.S.C. 1970, c. C-30. Please read the authorization forms which accompany this thesis.

THIS DISSERTATION  
HAS BEEN MICROFILMED  
EXACTLY AS RECEIVED

### AVIS

La qualité de cette microfiche dépend grandement de la qualité de la thèse soumise au microfilmage. Nous avons tout fait pour assurer une qualité supérieure de reproduction.

S'il manque des pages, veuillez communiquer avec l'université qui a conféré le grade.

La qualité d'impression de certaines pages peut laisser à désirer, surtout si les pages originales ont été dactylographiées à l'aide d'un ruban usé ou si l'université nous a fait parvenir une photocopie de mauvaise qualité.

Les documents qui font déjà l'objet d'un droit d'auteur (articles de revue, examens publiés, etc.) ne sont pas microfilmés.

La reproduction, même partielle, de ce microfilm est soumise à la Loi canadienne sur le droit d'auteur, SRC 1970, c. C-30. Veuillez prendre connaissance des formules d'autorisation qui accompagnent cette thèse.

LA THÈSE A ÉTÉ  
MICROFILMÉE TELLE QUE  
NOUS L'AVONS REÇUE

DETAILED MORPHOLOGY AND LATE QUATERNARY  
SEDIMENTATION OF THE NOVA SCOTIAN SLOPE,  
SOUTH OF HALIFAX

by



Philip R. Hill

Submitted in partial fulfillment of the requirements for the  
degree of Doctor of Philosophy at Dalhousie University,  
November, 1981.

i

TABLE OF CONTENTS

	PAGE
Table of Contents	i
List of Figures	iv
List of Tables	xi
Abstract	xii
Acknowledgements	xiv
<u>CHAPTER 1 INTRODUCTION</u>	1
General	1
Structural and Morphological Settings	1
Sedimentary Processes	6
Thesis Objectives	6
Regional Setting	10
Physical Oceanography	12
Late Quaternary Events	21
Equipment Materials and Methods	27
<u>CHAPTER 2 SLOPE MORPHOLOGY</u>	34
Introduction	34
The Scotian Gulf Area	41
Air Gun Record	41
Bathymetry	46
Interpretation of Specific Morphological Features from GLORIA II Sidescan and High Resolution Seismic Profiles	49
The Nature of the Mid-Slope Area: Erosion vs Deposition	75
Summary: Morphology of the Scotian Gulf Area	77
The Western Bank Area	80
<u>CHAPTER 3 CONTEMPORARY SEDIMENT DYNAMICS</u>	85
Data	85
Current Meter Observations	90
Grain Size Distribution	95
Sediment Transport Paths	109
Deposition of Muds below 600 metres Depth	119

	PAGE
<u>CHAPTER 4 STRATIGRAPHY</u>	125
Lithostratigraphy	125
Biostratigraphy	133
Chronostratigraphy	140
Comparison with Shelf Stratigraphy	151
Paleo-oceanographic Implications	156
<u>CHAPTER 5 ARGILLACEOUS FACIES</u>	162
Descriptions	
Mud Types, Sources and Transport Paths	175
Rates of Sediment Supply and Deposition	185
Facies Associations	188
Facies 2,4,5: Turbidite Association	188
Facies 1 and 3: Hemipelagic Association	198
<u>CHAPTER 6 ARENACEOUS AND RUDACEOUS FACIES</u>	212
Descriptions	
Interpretation of Coarse-Grained Facies	217
(a) Turbidite Deposits	217
(b) Debris Flow Deposits	225
(c) Slump Deposits	231
<u>CHAPTER 7 DISTRIBUTION OF FACIES IN THE SCOTTIAN GULF AREA</u>	232
Upper Slope and Channel Association	235
Mid-Slope Facies Association	240
Degraded Channel Margin or Lobe Facies Association	246
Constructional Slope Association	251
Summary and Interpretations	251
<u>CHAPTER 8 DISCUSSION: CONSTRUCTIONAL SLOPE PROCESSES</u>	257
(a) Sediment Supply Rates	258
(b) Sediment Transport Paths	260
(c) Slope Transport Mechanisms	262
The Role of Constructional Slope Channels	264
An Ancient Analogue: The Rio Dell Formation	267
Comparison of Scotian Slope and Rio Dell Formation Sequences	272
<u>CHAPTER 9 DISCUSSION: DESTRUCTIONAL SLOPE PROCESSES</u>	275
Slumping	276
Debris Flows	278
Turbidity Currents	288

	PAGE
(a) Initiation	288
(b) Transport Paths	294
(c) Depositional Sites	299
<u>CHAPTER 10</u> CONCLUSIONS	306
<u>REFERENCES</u>	316
<u>APPENDIX 1</u> Markov Sequence Analysis of Fine-Grained Facies	332

## LIST OF FIGURES

	PAGE
1-1 Structural settings of continental slopes of the Atlantic Ocean.	2
1-2 Bathymetric chart of the Nova Scotian continental margin.	5
1-3 Bathymetric features of the Nova Scotian shelf and slope.	9
1-4 Major elements of the surface circulation in the Northwest Atlantic Ocean.	14
1-5 Salinity-temperature relationships between Labrador Current Core Water (LCCW), North Atlantic Deep Water (NADW) and Labrador Current Water (LCW).	16
1-6 Salinity-temperature plots for four sections across the Scotian Slope at 50 m depth.	19
1-7 Cross section through slope Water Region (Gulf Stream, 60, Section III) showing approximate positions of the two Slope Water zones.	20
1-8 Continuous vector diagram for currents at 1500 metres depth (approximately 62°W) on the Scotian Slope.	22
1-9 Effects of sea-level lowering on the continental margin of Nova Scotia.	25
2-1 Schematic illustration of the characteristics shown by constructional and destructional slopes.	35
2-2 Location of survey lines in the Scotian Gulf area.	38
2-3 Location of V-fin seismic survey lines in the Western Bank area.	39
2-4 Line drawings of air-gun records from the Scotian Gulf area.	42
2-5 Schematic illustration of the four seismic units identified from the air-gun records shown in Figure 2-4.	43

	PAGE
2-6 Bathymetric map of the Scotian Gulf area.	48
2-7 12 KHz echo-sounder profiles run perpendicular to the slope contours, Scotian Gulf area.	50
2-8 Morphological features of the Scotian Gulf area.	53
2-9 Features traced from GLORIA profile A-A'.	55
2-10 Features traced from GLORIA profile B-B'.	57
2-11 Features traced from GLORIA profile C-C'.	59
2-12 Seismic profiles G-G', K-K', Q-Q', R-R'.	61
2-13 Seismic profiles L-L', M-M', O-O', P-P'.	62
2-14 Seismic profiles H-H', I-I', J-J', N-N'.	63
2-15 12 KHz echo-sounder profile S-S'.	66
2-16 Variation in main channel dimensions (to scale) measured from seismic and 12 KHz profiles.	69
2-17 Line drawing showing detail of seismic line Q-Q', over the depositional lobe, Scotian Gulf area.	71
2-18 Line drawings from upper-slope seismic profiles, showing details of valleys between slide-blocks, Scotian Gulf area.	73
2-19 Line drawings of profiles from the mid-slope area.	76
2-20 Line drawing of downslope profiles from just outside the Scotian Gulf study area.	78
2-21 Block diagram illustrating the main morphological features of the Scotian Gulf area.	79
2-22 Line drawings of seismic profiles U-U', V-V', T-T', Western Bank area.	81
2-23 Line drawings of seismic profiles W-W', X-X', Y-Y', Z-Z'.	82
2-24 Sketch map of morphological features in the Western Bank area.	83

	PAGE
3-1 Location of surficial sediment samples (a) Scotian Gulf (b) Western Bank.	89
3-2 Current meter records for three stations shown in Figure 3-1.	92
3-3 Cumulative grain size distributions of selected samples from the N.S. Shelf break and slope.	98
3-4 Size distribution of samples from the Scotian Gulf area, dissected according to the method of Dalrymple (1977).	101
3-5 Size distribution of samples shown in Figure 3-4, dis- sected by removal of central subpopulation.	103
3-6 Criteria for initial movement and suspension of quartz grains in water at 20°C.	105
3-7 Size distributions of samples from the Western Bank area, dissected by removal of central subpopulation.	110
3-8 Cumulative grain-size distribution of three typical samples from the Scotian Gulf Shelf.	111
3-9 Map of part of the Nova Scotian margin showing u <sub>s</sub> con- tours derived from sediment texture in the two study areas, and schematic illustration of sediment trans- port routes.	114
3-10 Proportions of various size intervals plotted against water depth.	121
4-1 Type stratigraphic core (11) from the Western Bank area.	127
4-2 Variation in Unit 1 sequences along the Nova Scotian continental slope.	129
4-3 Unit 2 members in gravity cores from the Western Bank area.	132
4-4 Foraminiferan assemblages in five cores from the Scotian Slope.	138
4-5 Downcore variation of the foraminiferan species <u>Elphidium excavatum</u> f. <u>clavata</u> and <u>Cassidulina crassa</u> in two cores from the Scotian Slope.	139
4-6 Carbon-14 dates (yrs B.P.) on cores from the Scotian Slope.	147

	PAGE
4-7 Accumulation rates in the dated cores of Figure 4-6.	150
4-8 Stratigraphic summary of Scotian Slope cores and comparison to Scotian Shelf stratigraphy of Mudie (1980).	153
4-9 Correlation of Mudie's Emerald Basin cores by carbon-14 dating.	154
4-10 Salinity-temperature diagram with superimposed density ( $\sigma_t$ ) isolines.	160
5-1 Important characteristics of the argillaceous facies (1 to 5).	164
5-2 Representative cumulative grain-size distributions for the fine-grained facies.	165
5-3 Representative x-radiographs of Facies 1 bioturbated muds.	167
5-4 Representative x-radiographs of Facies 2 parallel laminated muds.	169
5-5 Representative x-radiographs of Facies 3 wispy-laminated muds.	172
5-6 Representative x-radiographs of Facies 4 homogeneous muds.	174
5-7 Representative x-radiographs of Facies 5 silt/mud couplets.	177
5-8 Heavy mineral, clay mineral and chemical compositions of olive grey, dark yellow brown, brown and red-brown mud types.	179
5-9 Facies sequence analysis.	191
5-10 Typical turbidite mud sequences observed in slope cores.	193
5-11 Wispy laminae of Facies 3 with line drawings to illustrate possible ripple-drift cross-lamination.	197
5-12 Mechanisms of fine sediment transport across the shelfbreak and slope.	200

6-1	Important characteristics of the arenaceous and rudaceous facies (6-10).	204
6-2	Occurrence of Facies 6 thick-bedded sand units in three piston cores.	205
6-3	<u>Grain size variation through Facies 6 thick sand bed.</u>	206
6-4	Grain size variation through Facies 7 well-sorted thin sand beds.	208
6-5	Representative x-radiographs of Facies 7 well-sorted, thin sand beds.	210
6-6	Representative grain-size distribution of Facies 8 muddy sand.	211
6-7	Representative x-radiographs of Facies 8 muddy sand beds.	213
6-8	Representative x-radiograph of Facies 9 gravelly sandy mud bed.	216
6-9	Grain size distributions in some gravelly sandy mud beds.	219
6-10	Sketches of deformed structures from visual inspection and x-radiographs of Facies 10 slumped beds.	221
6-11	Orientation of elongate clasts $> -1 \phi$ in vertical section of thin gravelly sandy mud beds from cores 55 and 63.	230
7-1	Location of piston cores in the Scotian Gulf area with respect to major morphological features.	234
7-2	Key to Figures 7-3 to 7-8, indicating reliability of survey navigation and core positioning.	237
7-3	Facies sequences and locations of cores from the upper slope and main channel.	239
7-4	Facies sequences and locations of cores from the mid-slope area, along seismic profile N-N'.	242
7-5	Facies sequences and locations of cores 52, 55 and 60 from south of profile N-N'.	245

	PAGE
7-6 Facies sequences of cores 63, 77 and 78 from east of the main channel.	248
7-7 Facies sequences and locations of cores 61, 79 and 80 from the depositional lobe area.	250
7-8 Facies sequences and locations of cores from the constructional slope area.	253
7-9 Summary of morphological regions and their characteristic facies association, Scotian Gulf area.	254
8-1 Wisconsinan transport paths of red-brown mud.	261
8-2 Slope transport mechanisms for red-brown and olive-grey sediment.	263
8-3 Location map for Rio Dell Formation in northern California.	268
8-4 Generalised stratigraphic section for the Rio Dell Formation.	269
8-5 Detailed measured sections in the Rio Dell Formation.	271
8-6 Field sketch of trough-shaped scour surfaces and dark mudstone drape and fill.	273
9-1 (a) Field sketch from Miocene Potamoula shale, Greece showing three thin pebbly beds in shale sequence. (b) Cumulative grain-size distribution of a sample from the uppermost bed in (a).	282
9-2 Four thin debris-flow bed-geometries recognised from ancient deposits.	285
9-3 Speculative model of small-scale debris flows in the destructional slope setting.	287
9-4 Criteria for initial movement and suspension of quartz grains in water at 20°C with autosuspension criterion plotted for various slope angles.	290
9-5 Speculative mechanism for generation of turbidity currents by cross-channel currents.	293

	PAGE
9-6 Conceptual illustration of the flow paths of midslope turbidity currents.	297
9-7 Model of thin-bedded channel fill sequences of Mutti (1977).	303
9-8 Schematic illustration of the mode of inter-slump depression fill on the Nova Scotian slope (Scotian Gulf destructional area).	305

## LIST OF TABLES

	PAGE
1-1 List of core and grab-sample locations.	31
3-1 Mooring data for the three current meters.	58
3-2 Estimates of shear velocity ( $u_*$ ) from observed currents and grain size distributions at the shelfbreak and slope.	107
3-3 Long term averages of hourly current vectors, indicating net drift directions as average vectors.	117
4-1 List of main species comprising foraminiferan assemblages A and B.	135
4-2 List of Carbon 14 dates on Scotian Slope cores.	142
4-3 Estimated content of reworked ("dead") carbon in the dated samples, with potential error in absolute ages.	145
5-1 Difference matrix, Markov sequence analysis of fine- grained sediments.	190
6-1 Criteria for distinguishing paratills and debris flows.	228
A-1 Transition Count matrix, Markov sequence analysis of fine-grained sediments.	314
A-2 Transition Probability matrix, Markov sequence analysis of fine-grained sediments.	314
A-3 Probability Independent Trials matrix, Markov sequence analysis of fine-grained sediments.	315

ABSTRACT

A detailed bathymetric, seismic and sidescan survey in a small intercanyon area of the Nova Scotian continental slope reveals a complex surficial morphology. On the upper slope, large scale slumping has left a steep 150 m escarpment, below which a chaotic mass of slumped debris has accumulated. Large coherent blocks of sediment up to 50m thick lie within the debris resulting in the characteristically irregular relief of the upper slope. In the mid-slope area, the relief is less; mass-movements on the scale of tens of metres control the morphology, resulting in a disjunct system of hummocks and depressions. An erosive channel, some 50 m deep and 1 km wide traverses the upper and middle slopes, rapidly decreasing in depth and width below 800 m water depth, where it crosses a broad depositional lobe. The lobe is similar in profile and dimensions to the suprafan of a small submarine fan and is thought to have been deposited during an early stage in the channel development. A small part of the study area shows a very smooth morphology and has been largely unaffected by destructional processes.

Detailed textural analysis indicates that surficial sand at the shelfbreak and on the upper slope is in equilibrium with the modern current regime. Active sediment transport of sand in suspension is dominantly alongslope with a small, but important downslope component. Finer sediment remains in suspension for longer periods and is finally deposited in quieter downslope environments.

Gravity and piston cores indicate that this sedimentation pattern has remained essentially similar during the last 18,000 years.

As a result, the post-glacial stratigraphic sequence is very uniform over much of the Nova Scotian slope. Sedimentation patterns in the late Wisconsinan were, in contrast, very complex and were largely related to the meso-scale morphology of the area. Gravity-driven processes of slumping, debris flow and turbidity flow were important and resulted in a greater variety of sediment facies.

Distinct facies associations are defined for the upper slope, middle slope and channel margin / depositional lobe environments. Mid-slope hummocks and depressions also show distinguishable facies associations which are thought to reflect the differential fill of the depressions by morphologically diverted turbidity currents. These facies associations are probably applicable to other destructional slopes. The area lay close to the late Wisconsinan ice margin; it is not clear whether this ice margin had any significant effect on the types of facies developed.

ACKNOWLEDGMENTS

My sincere thanks go to David Piper for originally suggesting this project, for his sage advice, support and encouragement. I would also like to thank Tony Bowen, Basil Cooke and Franco Mediolini for similar help with particular avenues of research. Discussions with other colleagues, particularly Ali Aksu, Peta Mudie, Charlie Barrie, Mark Williamson, David Scott, Ann Miller, Paul Schenk and Anita de Iure are much appreciated.

The study has greatly relied on the co-operation and generosity of D.E.T. Bidgood and colleagues (Nova Scotia Research Foundation Corporation) who supplied V-fin seismic profiles, and D.G. Roberts (Institute of Oceanographic Sciences, U.K.) who diverted Starella to survey the study area with GLORIA II. Brian Petrie (Bedford Institute of Oceanography) supplied current meter records and much advice on their interpretation. The masters and crews of Dawson, Starella and Pandora II made shipboard operations as efficient and comfortable as possible.

Particular thanks go to Tom Duffett and Bob Iulucci for assistance in the preparation and execution of many cruises. A very large amount of help was given by a great many people at BIO. Although they are too numerous to list, their help is much appreciated. Diane Crouse typed the thesis in record time. Carmen Braund helped with drafting.

Funding for the research was provided by grants from NSERC Canada and Imperial Oil Ltd. to D.J. W. Piper, while I have been supported by a Dalhousie Graduate Fellowship.

Many friends have made my studies at Dalhousie pleasant and memorable. I'd like to thank Marie-Claude Blanchard, Mark Williamson,

Carmen Braund, Denise Poley, Charlie and Aleks Barrie, Randell Stephenson, Terry McDonald and Norman Lyttle for their friendship. The thesis would not have been completed in full sanity without M-C, Mark and Denny.

Finally, this work is dedicated to my parents, whose love and support has been constant.

## CHAPTER 1

## INTRODUCTION

GENERAL

The continental slope marks the transition from shelf to deep basin environments. Most sedimentology texts do not give very comprehensive treatment to the slope environment (see for example Friedman and Sanders, 1978; Blatt et al., 1980; Reading, 1978), largely reflecting the wide gap of knowledge concerning the slope. Relatively few studies of ancient sedimentary sequences have specifically concentrated on slope environments (Piper et al., 1976 and Carter, 1979 are notable exceptions). Modern slopes have recently become the focus of considerable interest, partly out of scientific curiosity, but greatly stimulated by the exploration for oil and gas on the outer continental margin. This interest is shown by the proliferation of symposia and related volumes on the outer margin and on slopes in particular (eg. Stanley and Swift, 1976; Bouma et al., 1978; Doyle and Pilkey, 1979). Such volumes illustrate the wide range of structural, morphological and sedimentological settings which are included under the general umbrella of the term "slope".

STRUCTURAL AND MORPHOLOGICAL SETTINGS

Emery (1977) distinguished six types of continental slope in the Atlantic Ocean (Fig. 1-1). Types A to E are associated with passive margins. The early rifting stage of a margin will produce a block-

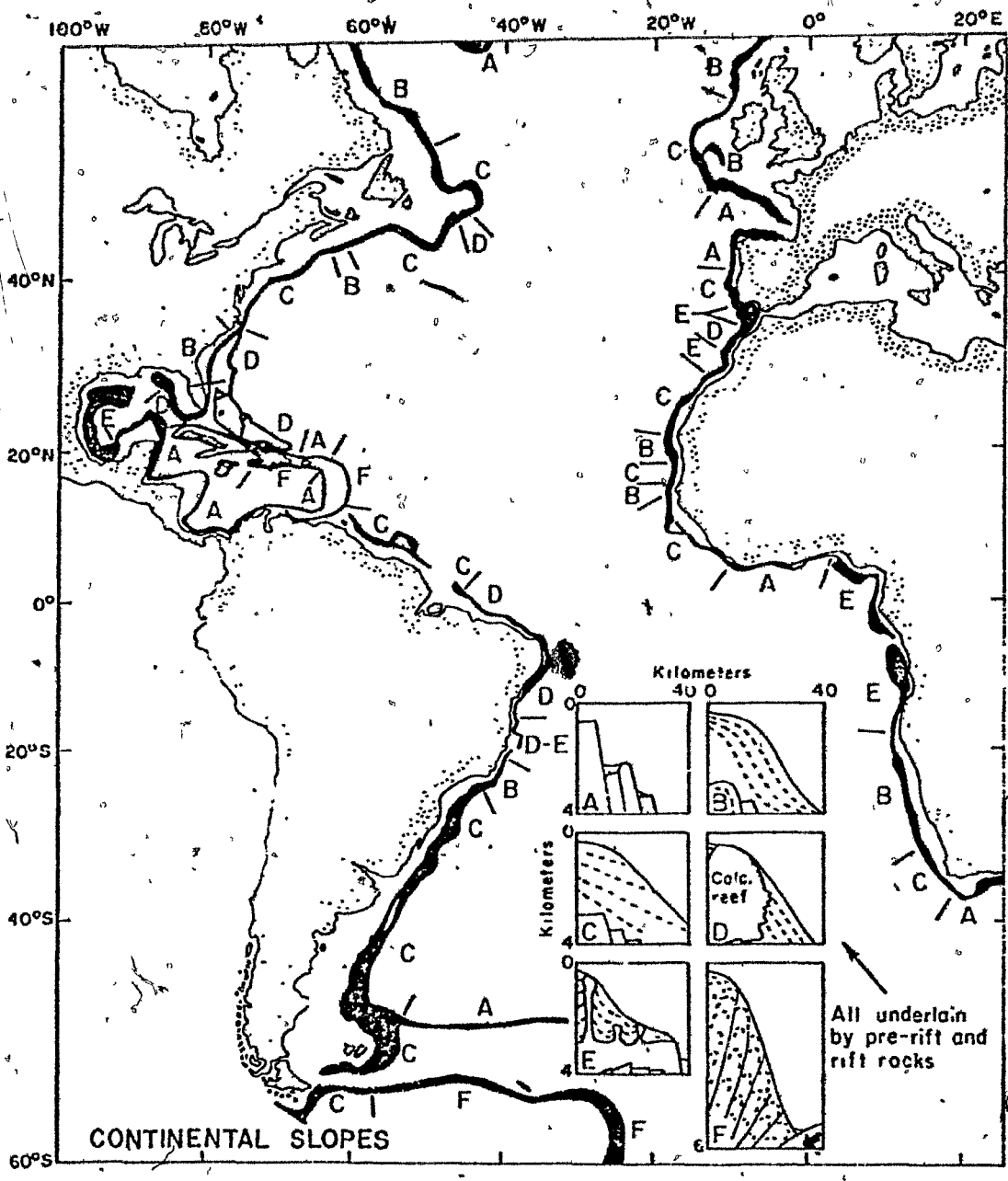


Figure 1-1. Structural settings of continental slopes of the Atlantic Ocean (from Emery, 1977). Types A to F explained in the text.

faulted margin which is mantled by sediment (type A). Progradation of the margin by deltaic or shelf sediments will result in a smoother slope with a characteristic sigmoidal geometry (type B). Erosion of the slope face by mass-wasting processes may truncate the progradational units (type C) and leave a steeper slope-face. Development of shelf-edge cemented calcareous reefs (type D) or intrusion by evaporite or mud diapirs (type E) can completely modify the generalised sequence of development from types A to C. Emery's type F slope (rather inadequately) incorporates convergent margin settings.

More detailed treatments of the development and structure of eastern US and eastern Canadian slopes are given by Schlee et al. (1979) and King and Young (1977) respectively. Both recognise that slopes undergo phases of (a) construction, where outbuilding of the continental margin progresses, and (b) destruction, where mass-wasting, canyon-cutting and other erosional processes truncate the basinward-dipping strata from a previous constructional phase.

From a glance at a bathymetric map, the slope off eastern Canada can be divided into dissected and non-dissected regions. For example, the Nova Scotian slope is dissected by numerous canyons at its northeastern and southwestern extremities, while a relatively narrow zone in the central section is largely undissected by large-scale morphological features (Fig. 1-2). This thesis is concerned with this central smoother area. After more detailed study, it becomes clear that the apparently undissected slope is by no means smooth and featureless. Rather, smaller-scale, but complex morphology may be present in some places.

4

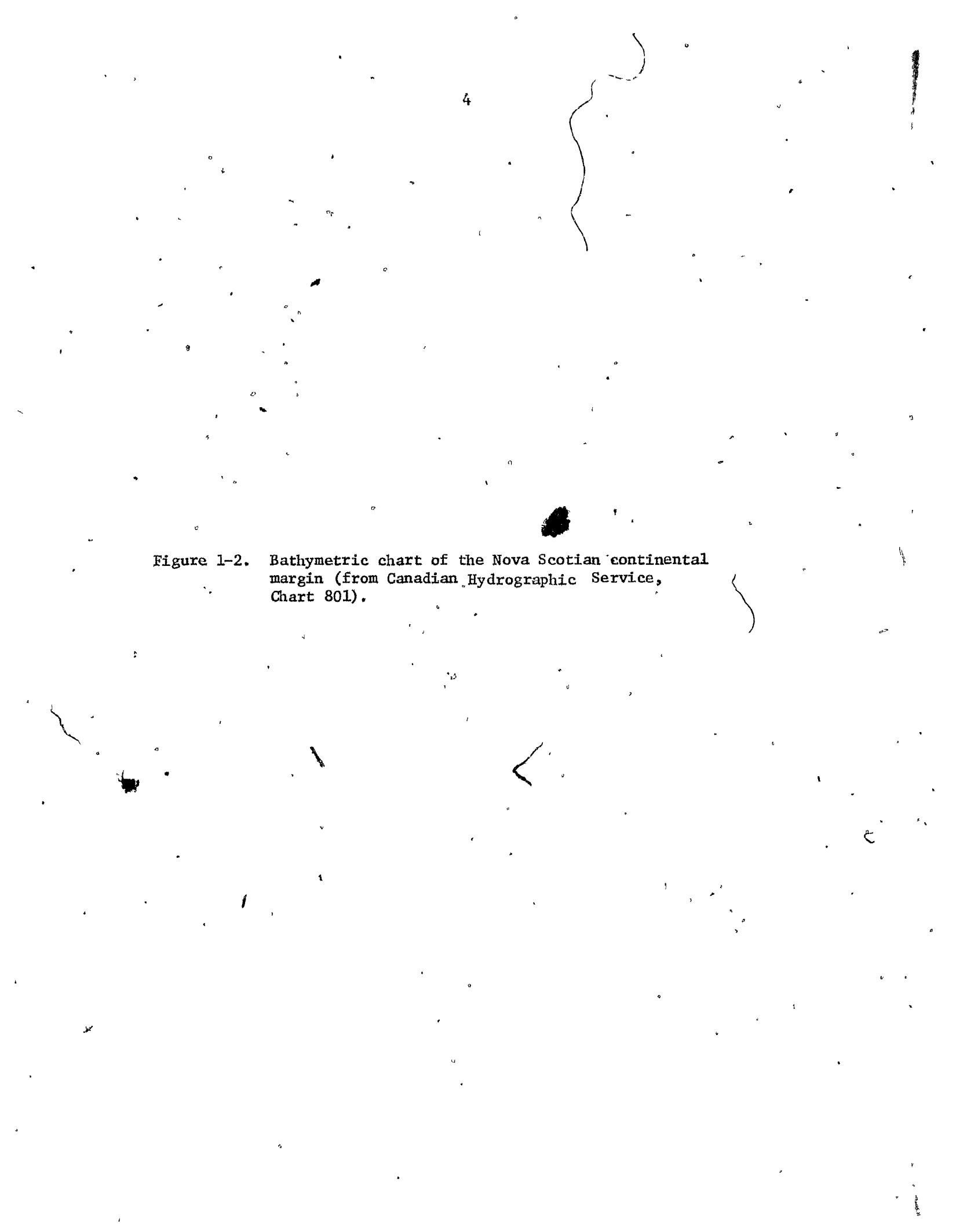
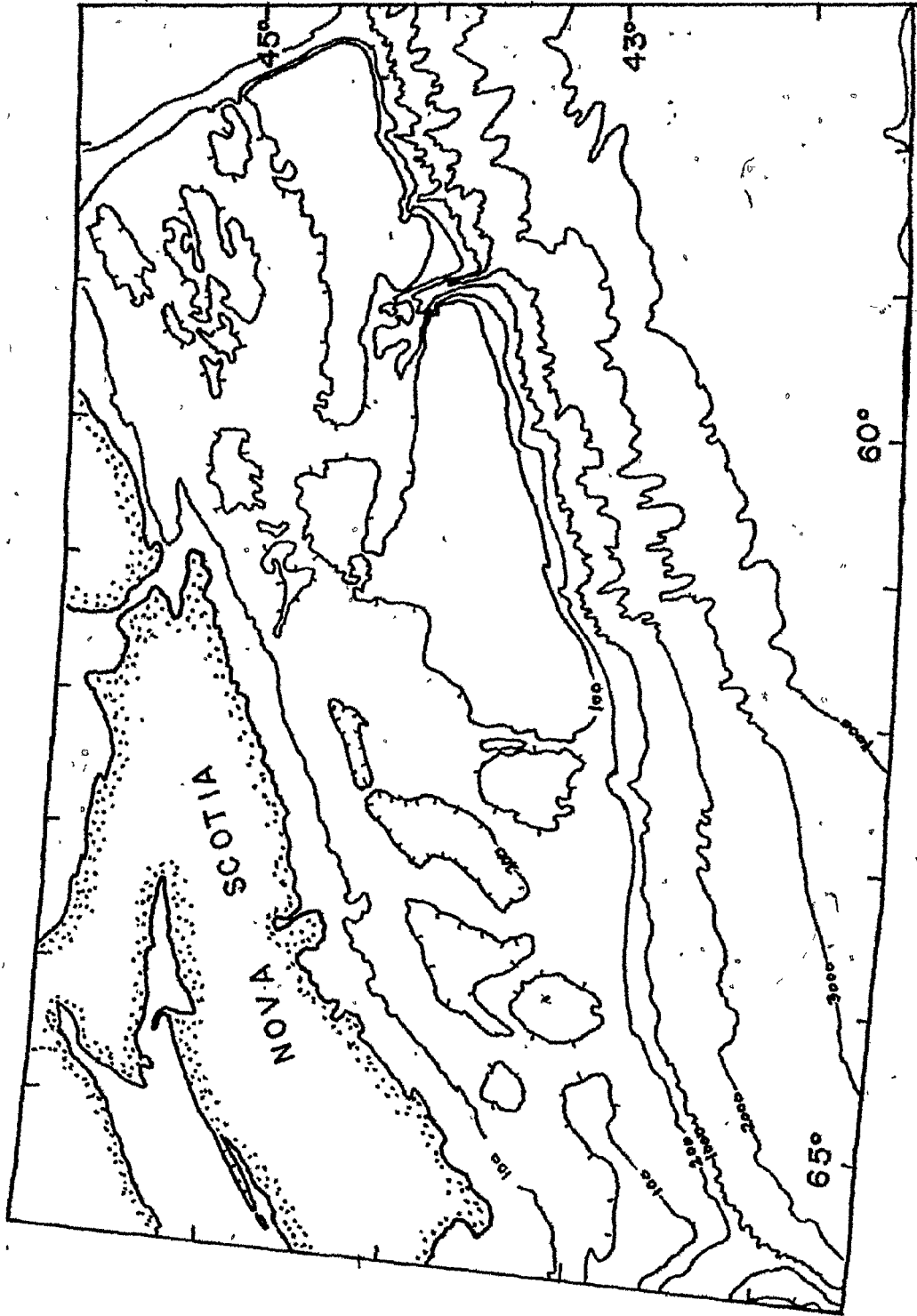


Figure 1-2. Bathymetric chart of the Nova Scotian continental margin (from Canadian Hydrographic Service, Chart 801).



## SEDIMENTARY PROCESSES

Sediment transport and deposition on slopes is poorly understood. Surficial sediments on most slopes are fine-grained, silt and clay being the dominant size-fractions (Kelling and Stanley, 1976). Most workers ascribe this characteristic to hemipelagic deposition (eg. Doyle et al., 1979) giving the impression that coarse sediment bypasses the slope via canyons. Thus turbidity currents are not generally thought to be important to continental slope deposition. Coarse sediment at the shelf edge may be transported short distances downslope by the (somewhat nebulous) process of "spillover" (Stanley et al., 1972). Stanley and Wear (1978) recognised a textural boundary on the upper-slope, which they termed the "mud line" and interpreted as a boundary between zones of mud erosion and mud deposition. The dynamic conditions causing such textural patterns have not been determined although numerous oceanographic processes have been cited as potential controls on sediment dynamics (Stanley and Wear, 1978; Southard and Stanley, 1976).

Mass movements in the form of slumps, slides and debris-flows are widely acknowledged as important slope processes (Nardin et al., 1979; Moore, 1977; Embley, 1980; Embley and Jacobi, 1977). These movements can range from very large scale (Jacobi, 1976) down to relatively small scale (Field and Clarke, 1979).

## THESIS OBJECTIVES

The initial approach to this thesis was exploratory, with a leaning towards stratigraphic and paleo-oceanographic problems. Two

study areas were selected from the undissected slope area (Fig. 1-3). No data was previously available from these study areas and the only previous work on the Nova Scotian slope was by Silverberg (1965) and Stanley et al. (1972) in the area off Sable Island Bank. Preliminary investigations (partly summarised in Hill, 1979) in the two study areas (Fig. 1-3) produced several results:

(a) Stratigraphically, the Holocene and latest Wisconsinan sedimentation was quite uniform, but older sediment was very difficult to correlate due to small-scale facies changes and sequence discontinuities.

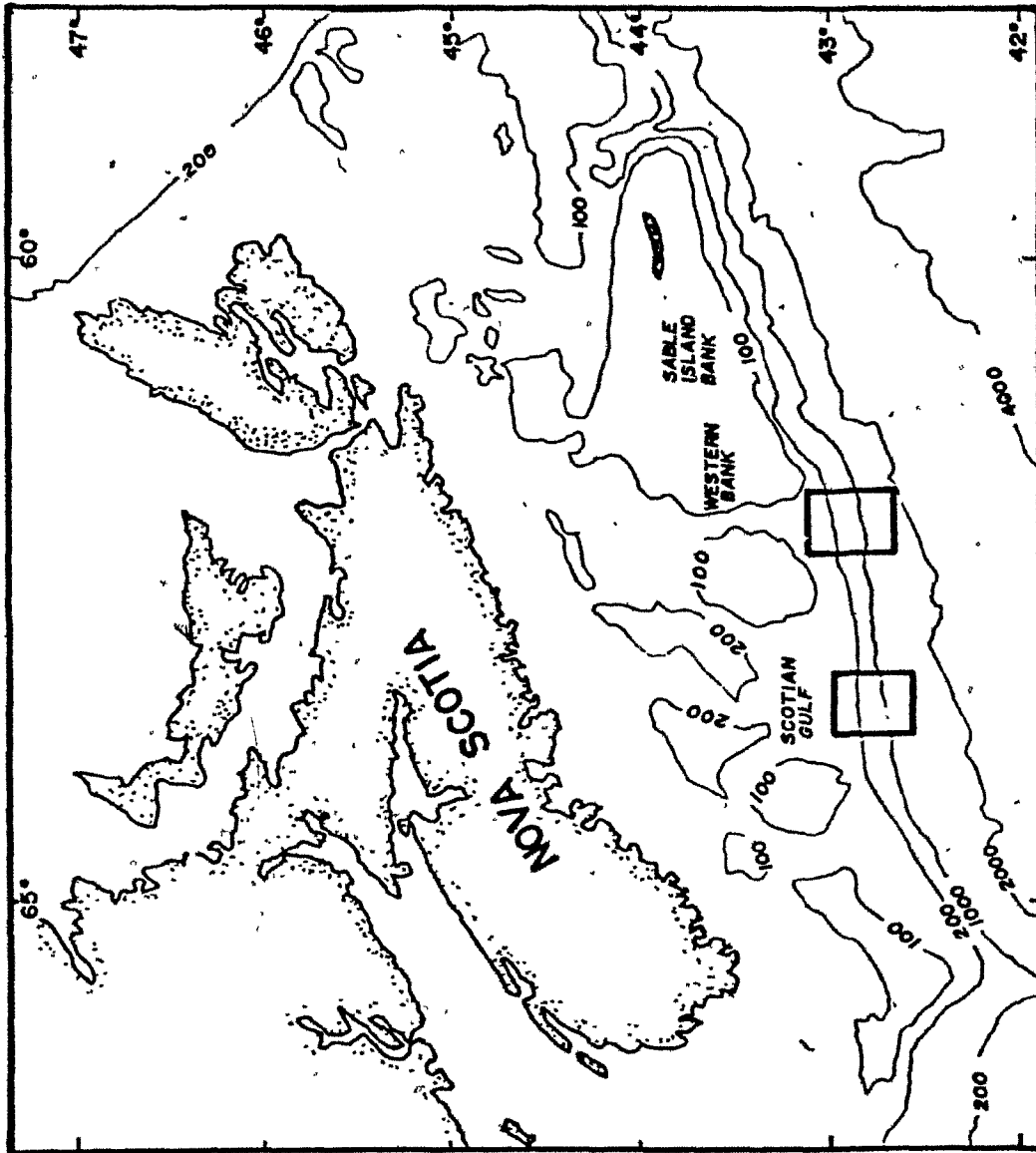
(b) Sedimentary processes were evidently more diverse in the Wisconsinan and involved coarse sediment transport.

(c) The Scotian Gulf study area (Fig. 1-3) was substantially more complex morphologically, than expected and contrasted in this respect with the lower relief Western Bank area.

These results indicated that the Scotian Slope did not fit into previously existing models of slope sedimentation. Detailed stratigraphic and paleo-oceanographic studies would clearly be impossible without better control on morphology and sedimentation. The subsequent study leading to this thesis therefore concentrated on the relationship between morphology and sedimentation. Three main projects were undertaken:

(i) To survey in detail the Scotian Gulf area in order to delimit major morphological features.

Figure 1-3. Bathymetric features of the Nova Scotian shelf and slope. Study areas outlined by boxes.



(ii) To determine the important sedimentary processes active on the slope at present and during the Holocene and late Wisconsinan.

(iii) To assess the factors controlling sedimentation, particularly morphology and glacial/postglacial conditions.

#### REGIONAL SETTING

Many good reviews of the geology of the southeastern Canadian continental margin are available (Stow, 1977; Alam, 1976, 1979), so this section will concentrate on the marine environment adjacent to the study area.

#### The Scotian Shelf

The Scotian Shelf (Fig. 1-3) is wide, varying in width between 125 km in the west to 230 km in the east. King and MacLean (1976) divide the shelf into three zones: an inner zone of rough topography, a central zone of isolated banks and intervening basins, and an outer zone of wide, flat banks. The surficial sediments on the shelf have been mapped in detail using echograms and bottom samples (King, 1970; Drapeau and King, 1972; MacLean and King, 1971). In all cases the bottom sediment types or "map units" informally defined by King (1970) were used.

The inner and central zones of the shelf are covered by varying amounts of till, some of which King (1970) interprets as Wisconsinan end moraines. Till deposited from earlier Pleistocene glaciation(s) extends below the surface to near the edge of the shelf. The bank areas and much of the inner shelf are covered with well-sorted sands

and gravels (Sable Island sand and gravel, Map Unit 8), which are interpreted as transgressive basal deposits. Surrounding the banks and in the Scotian Gulf (see Fig. 1-3), a second sandy unit outcrops, distinguished by its more skewed (fine-tail) grain-size distribution (Sambro Sand, Map Unit 6). The Sambro Sand also occurs in a bank seaward of the outermost banks, to the edge of the mapped area at the 100 m isobath. However, King (1970) states that the boundary between these two units is obscure and could not be defined on the basis of the criteria used for other areas covered by the map. Elsewhere, the Sambro Sand appears to grade into the till, suggesting that it is a reworked derivative of the latter. King (1970) implies that the Sambro Sand is relict.

It is difficult to assess the relationships between King's till, Sambro Sand and Sable Island Sand and Gravel units. They are similar in mineralogical composition and it is reasonable that both the Sambro Sand and Sable Island Sand and Gravel units are derived from the till during post-glacial transgression. However, the boundaries of the two reworked units appear to be distinctly depth-related which suggests either an adjustment to the present energy regime, or different histories of reworking during the transgression.

Currents with near-bottom velocities up to  $110 \text{ cms}^{-1}$  have been documented in the Scotian Gulf and correlate with strong offshore wind events. Reworking of till may therefore be an important contemporary process on the outermost shelf, even at depths greater than 100 m. King (1970), however, notes that at the edges of some basins, the Sambro sand is laterally equivalent to the Emerald Silt Unit which

clearly underlies modern LaHave Clay (Map Unit 7) in the basinal areas. Nevertheless, as the till source is likely to be similar in composition across the shelf, it is possible that similar sand units with similar composition and echogram properties would be produced at different stages of the transgression.

There is some evidence therefore, that sand transport and reworking is possible on both the shallow bank areas (Stanley et al., 1972), and the deeper areas e.g. Scotian Gulf, of the Scotian Shelf.

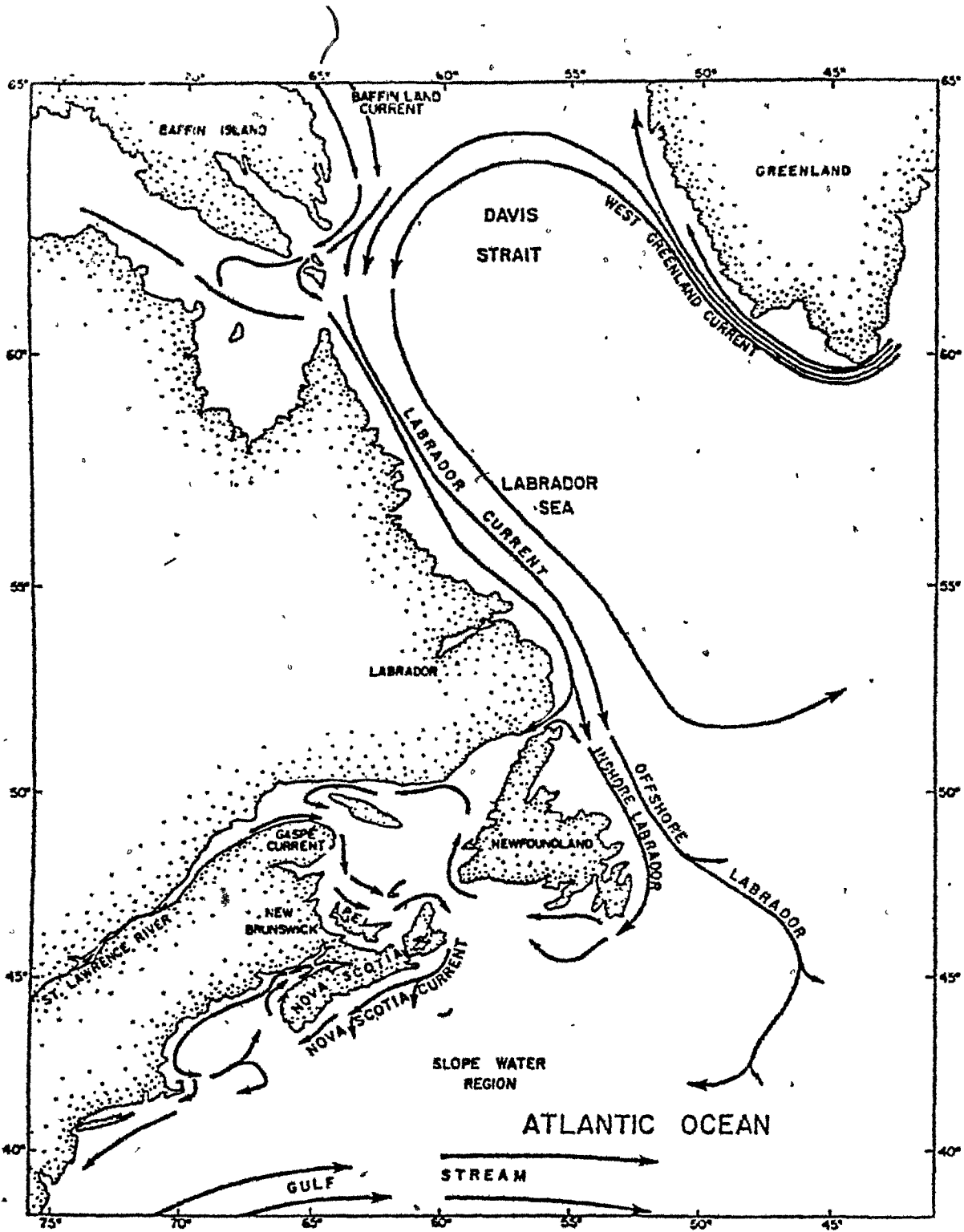
#### Physical Oceanography

The surface circulation (Fig. 1-4) along the southeastern Canadian margin is dominated by three main elements: the Gulf Stream Water, the Labrador Current Water and the Slope Water.

##### 1) The Gulf Stream Water

The Gulf Stream System is a major component of North Atlantic Ocean Circulation. According to Stommel (1965) most of the water which enters the system is water previously driven from the east by the trade winds, in the North Equatorial Current. Worthington (1976), who used a more complex five-layer model for the North Atlantic, disputes the importance of this current as a contribution to the Gulf Stream system. The surface circulation is seen by Worthington (1976) as an essentially closed (if eccentric) anticyclone, restricted to the southwest portion of the North Atlantic. A second, smaller gyre is postulated in the northern ocean which carries warm water further north.

Figure 1-4. Major elements of the surface circulation in the Northwest Atlantic Ocean (from Robe, 1971).



The Gulf Stream is a complex system, of variable temperature and salinity and of essentially geostrophic flow (McLellan, 1975, p. 71) with a velocity structure that is known to be highly complex. Important considerations are that it is warm ( $22^{\circ}$ - $24^{\circ}$  at its core) and occasional large-scale eddy-structures (rings) are known to transgress across shelf areas of the eastern U.S. (Fuglister and Worthington, 1951) and Nova Scotia (Gatien, 1975).

## 2) The Labrador Current Water

Robe (1971) identified two watermasses associated with the Labrador Current between Labrador and Newfoundland:

- (a) Labrador Current Water (LCW)
- (b) Labrador Current Core Water (LCCW).

Their relationships are shown in Figure 1-5, the LCW being all mixtures of LCCW and North Atlantic Deep Water. The core water consists of water derived from Hudson Bay and Baffin Bay which joins in the Davis Strait with the warmer West Greenland Current water. This join is more in the nature of a confluence than of mixing and at around the latitude of St. John's, Newfoundland, the current splits again into a colder inshore branch which flows across the Grand Banks and partly mixes with Gulf of St. Lawrence Water before crossing the Scotian Shelf, and a warmer offshore branch which follows the slope contours around the Tail of the Grand Banks to the Scotian Slope. The LCCW is very cold ( $-0.8^{\circ}\text{C}$  to  $-1.8^{\circ}\text{C}$ ) and relatively fresh (32.9 ‰ to 33.1 ‰) whereas the LCW in general can be as "warm" as  $4^{\circ}\text{C}$  and as saline

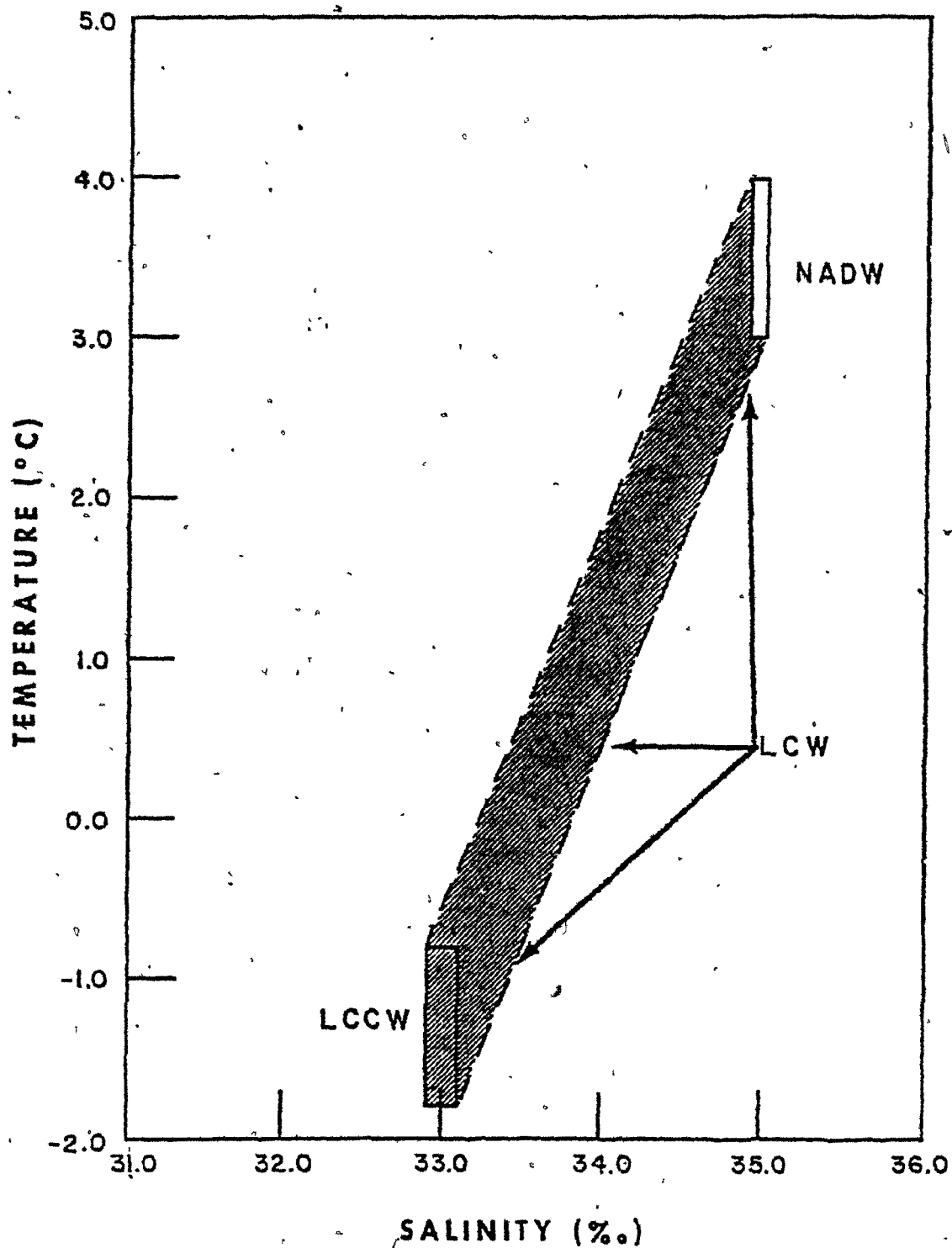


Figure 1-5. Salinity-temperature relationships between Labrador Current Core Water (LCCW), North Atlantic Deep Water (NADW) and Labrador Current Water (LCW). Labrador Current Water is defined to include LCCW but exclude NADW (from Rope, 1971).

as 34.8 ‰. Major seasonal fluctuations in volume transport are documented for the Labrador Current Water (Robe, 1971).

A notable characteristic of the Labrador Current Water is its relatively high dissolved oxygen content. In the Labrador Sea, values as high as 9.0 ml/l are recorded (Worthington and Wright, 1970).

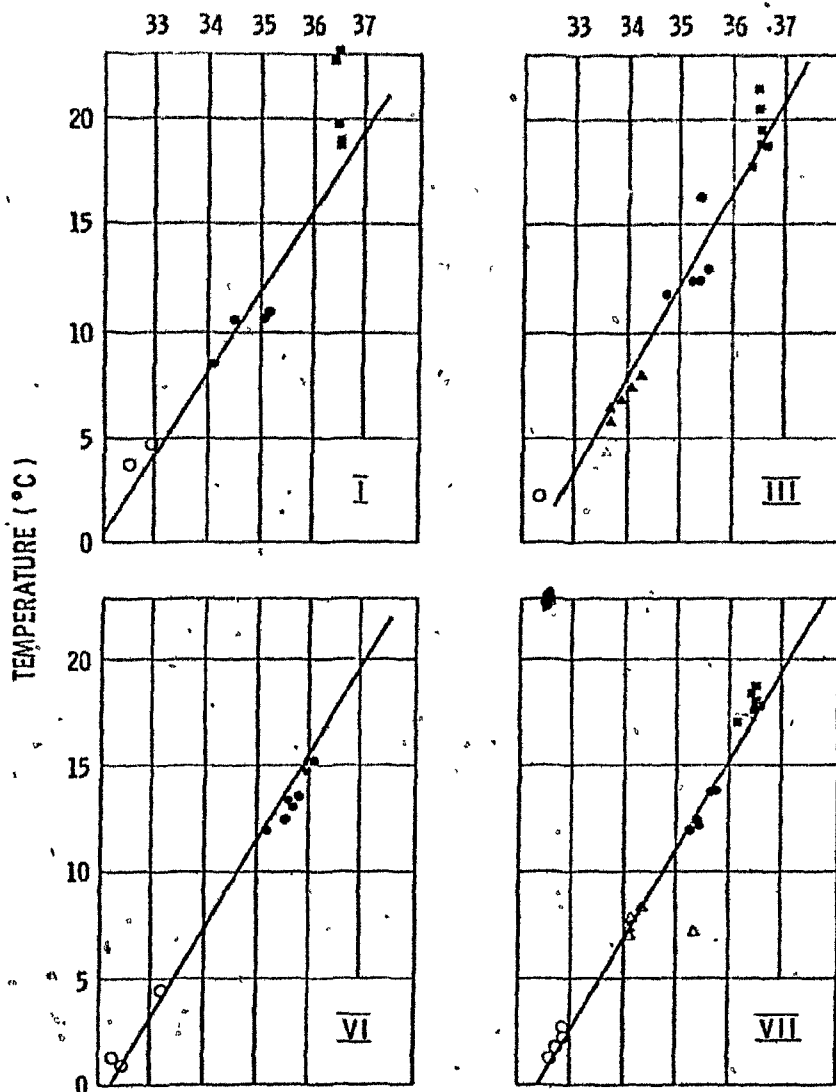
### 3) Slope Water

As it flows around Newfoundland to the Scotian Shelf area, surface warming and mixing with the Gulf Stream Water and deeper North Atlantic Central Water (NACW) modify the Labrador Current Water. The mixing product is known as the Slope Water (McLellan, 1957). Gatiien (1975) distinguished two parts of the Slope Water, based on detailed temperature and salinity data: Warm Slope Water and colder Labrador Slope Water (Fig. 1-6). The Warm Slope Water is a mixing product of LCW and Gulf Stream Water. It is well mixed (dissolved oxygen is reduced to 5-7 ml/l) and extends to 300 or 400 metres depth. The Labrador Slope Water is a mixture of LCW and NACW; it occurs at up to 100 metres depth on its western margin and it directly overlies the continental slope bottom down to at least 1200 metres (Fig. 1-7).

Flow in the Labrador Slope Water was observed by Foote et al. (1965) to be somewhat irregular, involving a generally westward drift with considerable fluctuations over time scales of several days. Using moored current meter arrays and meteorological data, Petrie and Smith (1977) studied these fluctuations in detail and concluded that

Figure 1-6. Salinity-temperature plots for four horizontal sections across the Scotian Slope at 50 metres depth. At this level, the Slope Waters are mixing products of coastal Water and Gulf Stream Water. At greater depth, the Labrador Slope Water is related to the North Atlantic Central Water.

SALINITY (‰)



- Coastal Water
- △ Labrador-Slope Water
- Warm Slope Water
- Gulf Stream Water

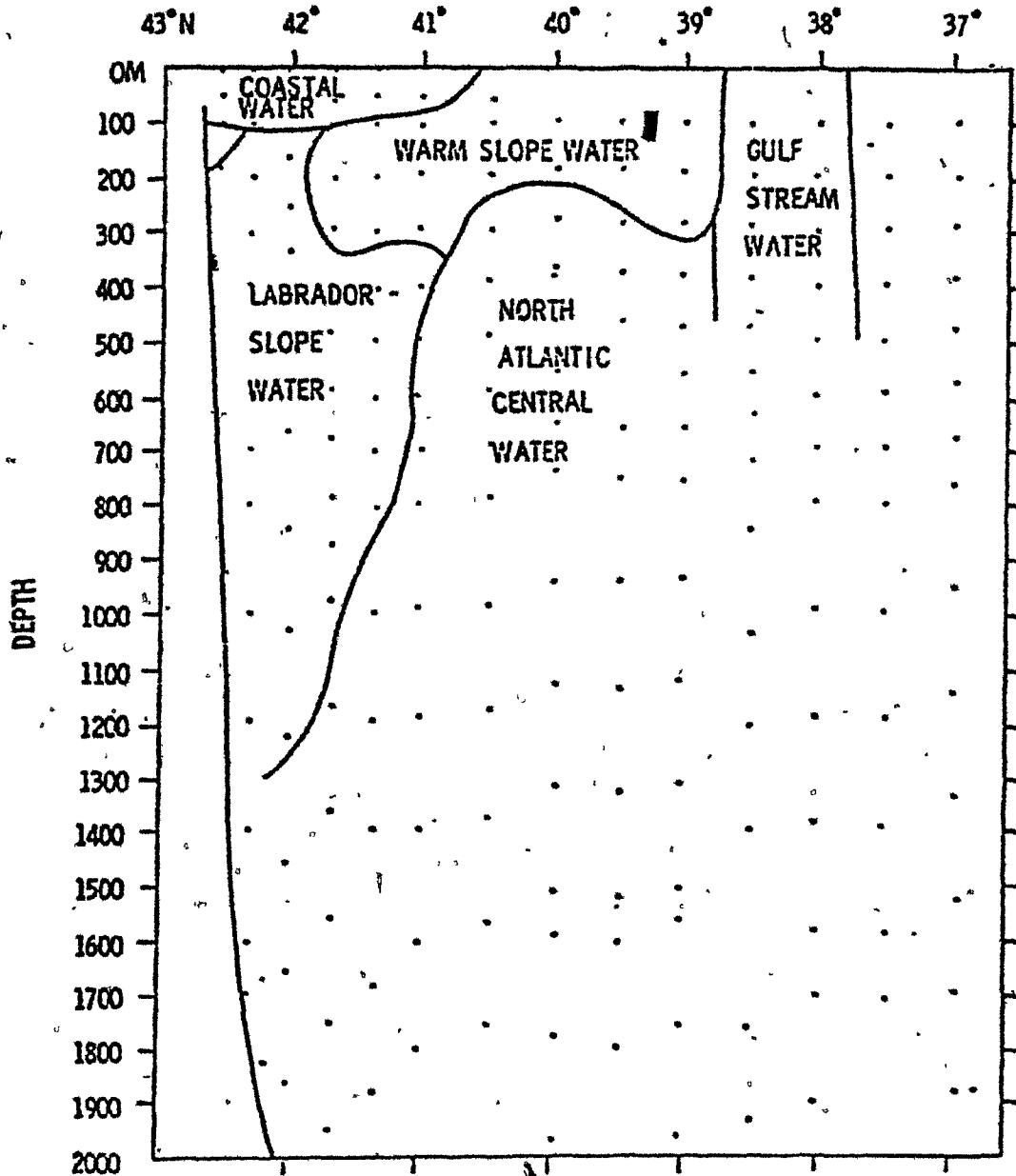


Figure 1-7. Cross-section through Slope Water Region (Gulf Stream 60, Section III) showing approximate positions of the two Slope Water zones (from Gatién, 1975).

meteorological forcing was an important energy source for such motions. Longer period motions were also investigated by Petrie and Smith (1977). Striking reversals in current flow direction were observed over a 33 day period (Fig. 1-8) along the azimuth of the local isobaths. In addition, marginally significant correlations between deep water off-shore (ie. southward) flow and westerly (blowing to the east) storm winds were observed.

#### Late Quaternary Events

Over recent years, important advances have been made in the Quaternary stratigraphic framework of the eastern Canadian margin. The cores used in this study are not thought to penetrate sediment older than late Wisconsinan, so that the following will summarise the present knowledge of the glacial, sea-level and watermass histories for this period of time.

##### (a) The Late Wisconsinan Glaciation

Through this century, two schools of thought have developed about the extent of the Wisconsinan glacial episode (Ives, 1978). These may be termed the "maximum" and "minimum" models of glaciation. Despite evidence to the contrary (Ives, 1957; Loken, 1966), the maximum model (Flint et al., 1942, 1945; CLIMAP, 1976) was generally accepted until recently. Grant (1977), summarising many years of work, called strongly for a reversion to a minimum glaciation for the Atlantic Provinces area. A number of terrestrial studies on Baffin Island (Miller and Dyke, 1974;

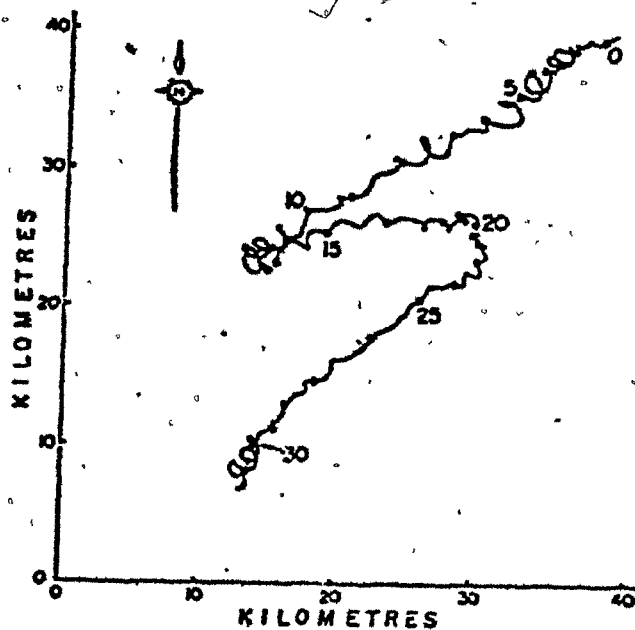


Figure 1-8. Continuous vector diagram for currents at 1500 metres depth (approximately 62°W) on the Scotian Slope, September/December 1968. Numerals indicate number of days from start of record. Note the current reversals between days 12 and 23. (From Petrie and Smith, 1977),

Miller, 1977; Andrews et al., 1976) and limited work in Labrador (Ives, 1957) and Newfoundland (Brookes, 1970) have documented the very limited extent of ice during the latter half of the Wisconsinan glaciation in the eastern Canadian arctic and subarctic. The most detailed work of Grant (1977) and evidence from the marine environment (Alam and Piper, 1977; Stow, 1977) also suggest the minimum model. Glaciological arguments for an extensive late Wisconsin ice sheet in this region (e.g. Hughes et al., 1977) have not been widely accepted.

The important points about Grant's interpretations are as follows:

1) Highland ice sheets existed over Nova Scotia, New Brunswick and Newfoundland, each separate from the other and from the main Laurentide ice-sheet, except for a probable connection with the Newfoundland ice-sheet across the Strait of Belle Isle.

2) The Gulf of St. Lawrence may have been free of ice for the late Wisconsinan event, although a glacier may have extended along the Laurentian channel as far as Cabot Strait during an earlier Wisconsinan stage.

3) The Scotian Shelf was free of grounded ice seaward of the nearshore moraine complex identified by King (1969).

4) The Grand Banks area was also essentially clear of grounded ice.

#### b). Sea Level

Traditionally, the maximum late Wisconsinan sea-level stand on the Scotian Shelf is considered to be about 110-120 m between 19,000

and 15,000 yrs. B.P. (Stanley et al., 1968; King, 1970; Stow, 1977). These values are largely based on the remarkably consistent position of prominent terraces and associated textural changes at this depth. Some doubt has been thrown upon this figure by the theoretical modeling of Quinlan (1981; Quinlan and Beaumont, 1981), based on minimum ice-thickness assumptions. Quinlan's models are largely supported back to 14,000 yrs B.P. by the accurate relative-sea level data of Scott and Medioli (1979, 1980) from Northumberland Strait, New Brunswick and the nearshore zone of mainland Nova Scotia. However, no data is yet available on the Scotian Shelf itself.

In trying to reconcile his model with the established 110-120 metre stand, Quinlan suggested that earlier melting, several thousand years prior to the 18,000 yr B.P. start of his model, and/or melting of more distant ice, either from Antarctica or globally, might explain the misfit. Ice sheet reconstructions (Hughes et al., 1981; Robin, 1977) and other geophysical models (Clark and Lingle, 1979) do not support the extra melting required so that Quinlan (1981) conceded that the land-based data of Scott and Medioli (1979, 1980) and thus his relative sea-level model were in disagreement with the 110-120 metre stand of King (1970) and others.

The problem has rather important implications to the slope as sea-level lowering would have resulted in significant shoaling and emergence of the outer-shelf banks (Fig. 1-9). A sea-level lowering of 120 metres (Fig. 1-9a) would cause the emergence of all the outer shelf banks leaving only the Scotian Gulf and the The Gully as narrow

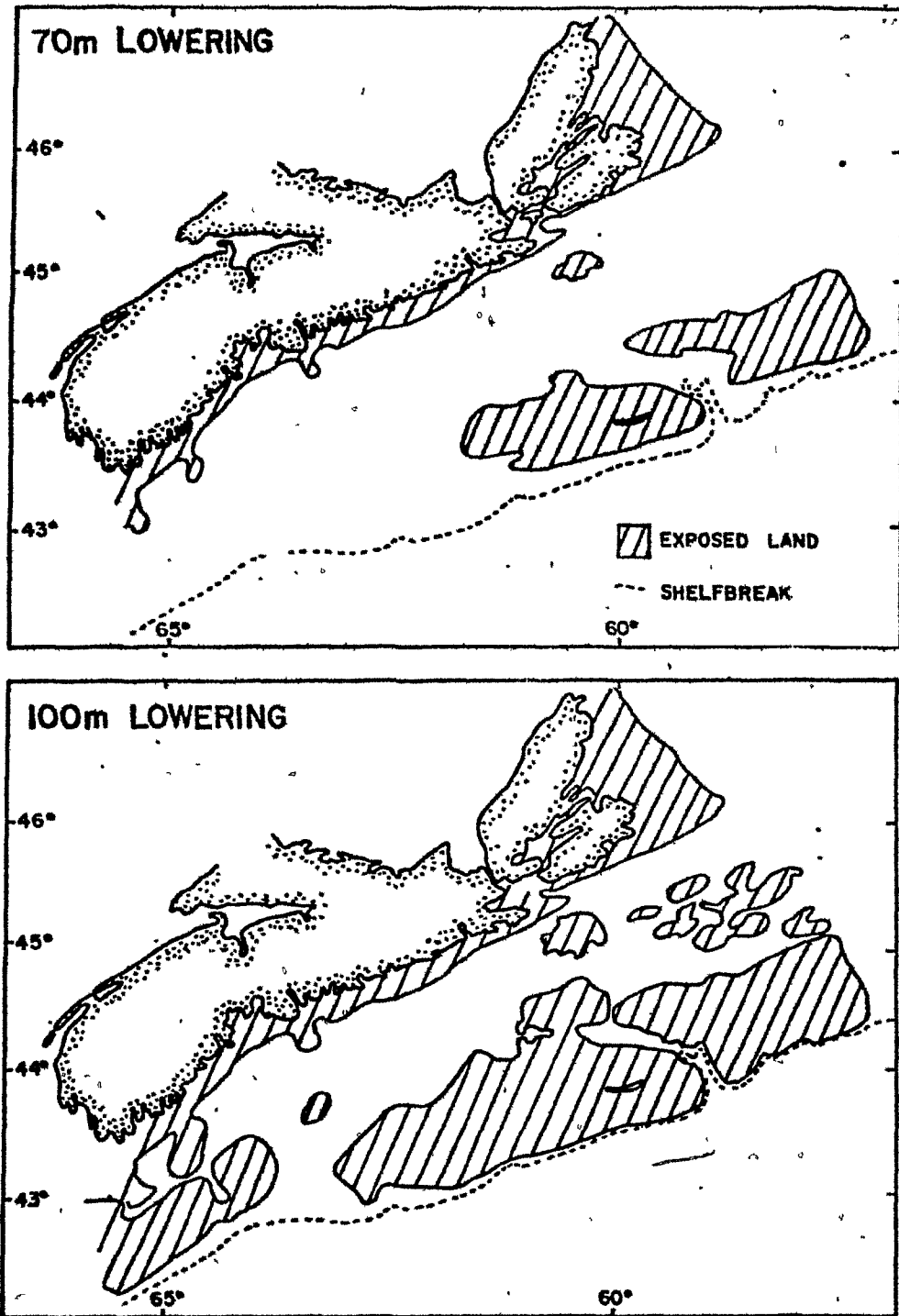


Figure 1-9. Effects of sea-level lowering on the continental margin of Nova Scotia. Top: 70 metre lowering, bottom: 100 metre lowering.

seaways. Quinlan's maximum lowering of 70 metres (Fig. 1-9b) would only leave Sable Island and Banquereau Banks exposed. Oceanographic processes involving cross-shelf mixing and fine sediment transport are clearly dependent on which scenario is closest to the truth.

### (c) Water Masses

There have been considerable recent advances in the interpretations of surface sea-temperature using oxygen isotopes and biological transfer function analysis of planktonic foraminiferal species and assemblages. These have led to increased sophistication in paleo-oceanographic reconstruction (e.g. see CLIMAP Project Members, 1976 for 18,000 yr B.P. map). The use of benthonic foraminifera for bottom-water reconstructions is less advanced, but recent work (Streeter, 1973; Lohmann, 1978) has demonstrated that certain benthonic assemblages seem to correlate well with certain watermasses. Streeter (1973), Schnitker (1974) and Streeter and Shackelton (1979) have used this relationship to interpret variations in North Atlantic bottom watermass distributions through the last 120,000 years.

The essential conclusion of these authors was that Atlantic deep circulation between 70,000 and 18,000 years ago was significantly different from the present circulation. This difference is explained by the restriction or disappearance of the North Atlantic Deep Water (Schnitker (1979)).

More locally, various forms of evidence (Fillon, 1976; Alam, 1979) point to a "cooling-event" around the eastern Canadian margin

beginning between 4,000 years B.P. and 6,000 years B.P. (Alam, 1979), or as late as 3,500 years B.P. (Fillon, 1976). Several authors have suggested that this event was the initiation of the cold Labrador Current over the Labrador Shelf (Fillon, 1976) which was absent during the previous glacial period. Alam (1979) suggests that only the cold component of the current was absent so that although the Labrador Current was flowing prior to 6,000 years B.P., it was in fact significantly warmer than at present.

#### EQUIPMENT, MATERIALS AND METHODS

##### 1) Acoustic Survey

The GLORIA II long range sidescan sonar system was made available for a short survey by D.G. Roberts of the UK's Institute of Oceanographic Sciences. The system operates on the same principles as conventional sidescan sonar, but has a total swath range of up to 50 km (Somers et al., 1978). Both transducer and receivers are housed in a neutrally buoyant tow-fish which was launched from a hydraulic platform. Technical details of GLORIA II are to be found in Somers et al. (1978). In the study area, the profiles were run with a 20 second sweep speed. The data is taped,, then replayed onto photographic paper in "a facsimile machine, of the sort found in newspaper offices for receiving pictures over the telephone lines" (Somers et al., 1978). These sheets are then rephotographed onto 35 mm film in a special purpose anamorphic camera to give an undistorted sonograph. The anamorphic ratio is determined by the ship-speed across the bottom. For the

purposes of this study, photographic prints were then developed on a scale of 1:50,000, for direct comparison with other data plotted on this scale.

Operating on a frequency of 7 KHz or less, the theoretical limit of resolution of GLORIA is of the order of 10-20 cm. This would indicate that bottom features in the scale of large bedforms would be detectable as differences in record texture. It is not at present possible to use this capability and experience tells that an actual resolution of tens of metres is more reasonable.

The identification of features on GLORIA records is very sensitive to the angle at which the beam illuminates the seafloor. Thus different profiles show up different features. It is imperative that GLORIA is used in conjunction with other systems so that features identified from GLORIA records can be groundtruthed.

During the GLORIA survey, a bottom-penetrating acoustic profile was obtained using a small capacity airgun.

Sparker seismic profiles were obtained in co-operation with the Nova Scotia Research Foundation Corporation, using its deep-towed bottom profiling system. The system uses a 300 to 7,000 KHz sparker sound source with a 200 joule output, firing at 250 to 500 milliseconds. The towfish, containing sparker, hydrophone and depth transducer is automatically depth compensated; it was towed at a depth of 100 metres and at a speed of 4-5 knots. Penetration of up to 100 m s was obtained.

Resolution of the system is in the order of 1 metre.

Echo-sounding profiles were run using a 12 KHz broad-beam profiler, with hull-mounted transducers and transceivers.

Navigation for the early cruises (1978-79) was by Decca and Satellite only. The Decca system is somewhat inadequate for the scale of survey undertaken (average line-spacing 1.5 to 2 km). Later cruises used the newly established Loran C 5930 Chain which provides good coverage for the whole Scotian Shelf and Slope. Positioning was much improved (theoretically repeatable to within 90 metres) and in good agreement with satellite fixes.

## 2) Sediment Sampling

Surface samples in sandy areas were collected using Van Veen (27 samples) and Shipek (27 samples) grab-samplers. Where the sand contained a substantial gravel fraction, neither corer performed well although, in general, the Shipek sampler recovered larger volumes of sediment.

A total of 41 gravity cores, 35 piston cores (with gravity trip-cores) and 6 box cores were obtained. A Benthos 3 inch I.D. gravity corer and an Alpine 2 1/2 inch I.D. piston corer were used. The box-corer was made at Bedford Institute of Oceanography. Long cores were cut into 1.5 metre lengths and stored until splitting. Details of the samples were presented in Table 1-1.

Table 1-1. List of core and grab-sample locations.

TABLE 1-1

## (a) CORES

CORE NO.	SAMPLE NO.	TYPE	LAT (*N)	LONG (*W)	WATER DEPTH (m)	CORE LENGTH (m)
1	78-005-3	G	42°45.55	63°30.59	700	1.07
2	78-005-7	F	42°46.48	63°30.10	500	5.50
3	78-005-8	G	42°45.50	53°30.04	600	0.53
4	78-005-9	G	42°44.00	63°30.10	800	1.09
5	78-005-10	G	42°42.30	63°30.00	900	1.36
6	78-005-11	G	42°39.46	62°15.09	1400	0.29
7	78-005-12	G	42°45.16	62°16.45	1200	0.24
8	78-005-13	P	42°47.94	62°15.12	1000	5.60
9	78-005-14	G	42°49.69	62°14.60	900	1.38
10	78-005-15	G	42°51.22	62°15.17	800	1.32
11	78-005-16	P	42°52.66	62°15.50	700	4.42
12	78-005-17	G	42°53.40	62°15.20	600	1.08
13	78-005-42	P	42°47.50	62°07.04	1000	4.52
14	78-005-43	G	42°50.00	62°06.50	900	1.10
15	78-005-44	G	42°52.50	62°06.90	800	1.03
16	78-005-45	G	42°53.40	62°06.80	700	1.00
17	78-005-46	G	42°55.70	62°06.50	595	1.00
18	78-005-47	G	42°55.40	62°06.50	500	0.92
19	78-005-54	G	42°54.8	62°12.4	495	1.02
20	78-005-55	G	42°54.8	62°10.4	500	1.20
21	78-005-56	G	42°55.0	62°09.0	502	1.26
22	78-005-57	G	42°54.3	62°08.9	550	1.25
23	78-005-58	G	42°54.4	62°10.8	550	1.21
24	78-005-59	G	42°54.1	62°12.2	550	1.15
25	78-005-75	G	42°55.0	62°06.4	550	1.35
26	78-005-76	G	42°53.9	62°08.9	600	1.05
27	78-005-77	G	42°53.75	62°10.5	593	1.26
28	78-005-78	G	42°53.4	62°12.1	605	0.96
29	78-005-79	G	42°54.0	62°14.6	550	1.29
30	78-005-80	G	42°41.5	62°23.0	1000	0.64
31	78-005-81	G	42°23.3	63°23.6	900	1.19
32	78-005-82	G	42°44.6	63°22.7	800	1.06
33	78-005-83	G	42°45.5	63°23.0	700	1.05
34	78-005-85	G	42°46.2	63°22.7	600	0.84
35	78-005-92	G	42°46.2	63°26.4	602	0.63
36	78-005-93	G	42°44.9	63°26.4	706	1.05
37	78-005-94	G	42°43.8	63°26.8	810	1.30
38	78-005-95					
39	78-005-96					
40	78-006-1	B	42°57.4	61°53.0	300	
41	78-006-2	B	42°57.4	61°53.0	300	
42	78-006-3	B	42°57.9	61°53.0	340	
43	78-006-4	B	42°54.99	61°49.48	700	
44	78-006-5	G	42°55.27	61°50.47	684	1.05
45	78-006-6	H	42°43.58	61°38.17	1698	
46	78-006-7	G	42°51.09	61°43.44	987	1.26
47	78-006-8	B	42°53.22	61°44.82	800	
48	78-006-9	G	42°52.99	61°44.10	794	1.16
49	79-002-2	P	42°46.5	63°25.0	602	5.02
50	79-002-4	P,G	42°44.3	63°24.5	798	5.69
51	79-002-5	P,G	42°42.5	63°25.0	920	3.59
52	79-002-6	P,G	42°41.4	63°24.5	1000	3.84
53	79-002-8	G	42°37.61	63°25.0	1400	0.45
54	80-004-15	P	42°43.0	63°29.3	622	3.72
55	80-004-16	P	42°42.5	63°28.8	950	3.37
56	80-004-19	P	42°43.0	63°27.1	866	4.16
57	80-004-20	P	42°43.0	63°26.0	856	5.46
58	80-004-21	P	42°43.3	63°25.2	886	5.56
59	80-004-22	P	42°43.6	63°30.2	820	4.02
60	80-004-23	P	42°40.7	63°30.0	1004	5.31
61	80-004-24	P	42°41.9	63°22.0	1020	6.12
62	80-004-28	P	42°46.0	63°27.0	600	5.24
63	80-004-29	P	42°44.6	63°22.0	800	4.74
64	80-004-60	P	43°12.3	60°59.5	492	4.35
65	80-004-61	P	43°10.8	61°00.4	648	5.01

<u>CORE NO.</u>	<u>SAMPLE NO.</u>	<u>TYPE</u>	<u>LAT (N°)</u>	<u>LONG (°W)</u>	<u>WATER DEPTH (m)</u>	<u>CORE LENGTH (m)</u>
66	80-004-62	F	43°09.9	61°00.5	775	4.63
67	80-004-63	F	43°07.6	61°00.9	990	5.03
68	80-004-64	F	43°04.2	61°06.7	1708	1.07
69	80-004-65	F	43°02.3	61°05.8	2120	.39
70	80-004-66	F	43°09.5	61°09.75	1350	.87
71	80-004-67	F	43°11.0	61°09.0	1030	.71
72	81-006-9	F			850	4.45
73	81-006-10	F	42°43.2	63°27.08	790	1.37
74	81-006-11	F	42°43.15	63°27.29	825	5.60
75	81-006-12	F			835	4.38
76	81-006-13	F			850	2.80
77	81-006-31	F			740	1.15
78	81-006-32	F			750	1.46
79	81-006-33	F			970	1.29
80	81-006-34	F			1245	2.68
81	81-006-44	F			830	5.20
82	81-006-45	F			628	3.00

G = Gravity Cores      F = Piston Cores

(b) GRAB SAMPLES

78-005-1	43°00.00	63°30.00	165
78-005-2	42°48.20	63°29.76	250
78-005-5	42°47.20	63°30.00	383
78-005-6	42°46.48	63°30.10	500
78-005-18	42°54.30	62°15.70	490
78-005-19	42°55.20	62°16.10	395
78-005-20	42°56.20	62°15.50	298
78-005-21	42°57.20	62°15.10	198
78-005-48	42°56.40	62°06.90	395
78-005-49	42°57.40	62°06.80	290
78-005-50	42°58.40	62°06.80	200
78-005-51	42°55.50	62°08.80	450
78-005-52	42°55.4	62°10.5	450
78-005-53	42°55.2	62°11.6	450
78-005-87	42°47.3	63°22.0	400
78-005-88	42°48.1	63°23.0	300
78-005-89	42°48.7	63°23.2	252
78-005-90	42°49.6	63°23.5	198
78-005-91	42°49.6	63°23.5	198

### 3) Laboratory Methods

Each core was split and x-rayed, then described using visual and x-ray criteria. Colour was determined using the Rock Colour Chart distributed by the Geological Society of America. For further analysis, sub-samples were removed from the cores and grab-samples.

Grain-size analysis was performed by standard dry sieve and pipette methods. Heavy minerals were separated by petrographic examination using tetrabromoethane (R.D. = 2.97 at 20°C). Clay minerals from the <math> < 1\mu </math> fraction were analysed by X-ray diffraction, using the method outlined in Piper (1976).

Foraminifera were separated from the sand fraction by flotation in carbon tetrachloride (RD = 1.58 at 25°C). Planktonic foraminifera were sieved out (using a 180 $\mu$  sieve) of the separated fraction. No size separation was used for benthonic foraminifera studies, but splitting of large samples, using a Soiltest sample splitter, was often necessary.

## CHAPTER 2

## SLOPE MORPHOLOGY

INTRODUCTION

For an adequate sedimentological model to be established for any particular sedimentary environment, it is vital to relate depositional processes to geomorphological features. Recent studies of continental slopes have begun to demonstrate a wide range of morphological types. A basic division between constructional and destructional types (Dietz, 1952; Rona, 1969) is useful (Fig. 2-1). Constructional slopes are characterised by continuity of reflectors between the shelf and slope, indicating progradation of the margin. Destructional slopes are generally steeper and show zones of chaotic reflectors and one or more large-scale discontinuity. King and Young (1977) give several examples from the eastern Canadian continental margin and demonstrate that a margin can undergo several phases of alternating construction and destruction.

Morphologically, constructional slopes appear relatively simple, although this may be mainly because of the lack of detailed studies on this type of slope. Much more interest has been taken on various aspects of destructional slopes, in particular, mass-movement and channel-features.

Mass movements (slumps and slides) similar to subaerial landslides and related features have been recognised at various scales

(a) CONSTRUCTIONAL



(b) DESTRUCTIONAL

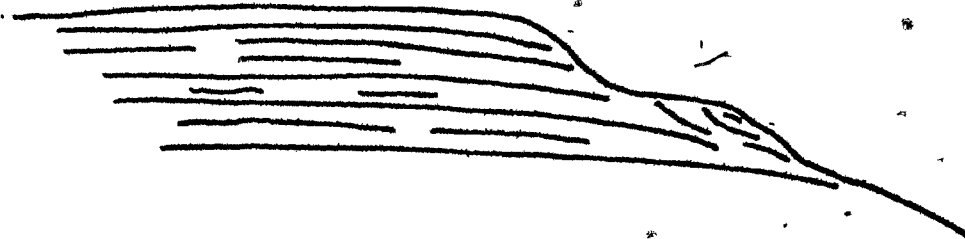


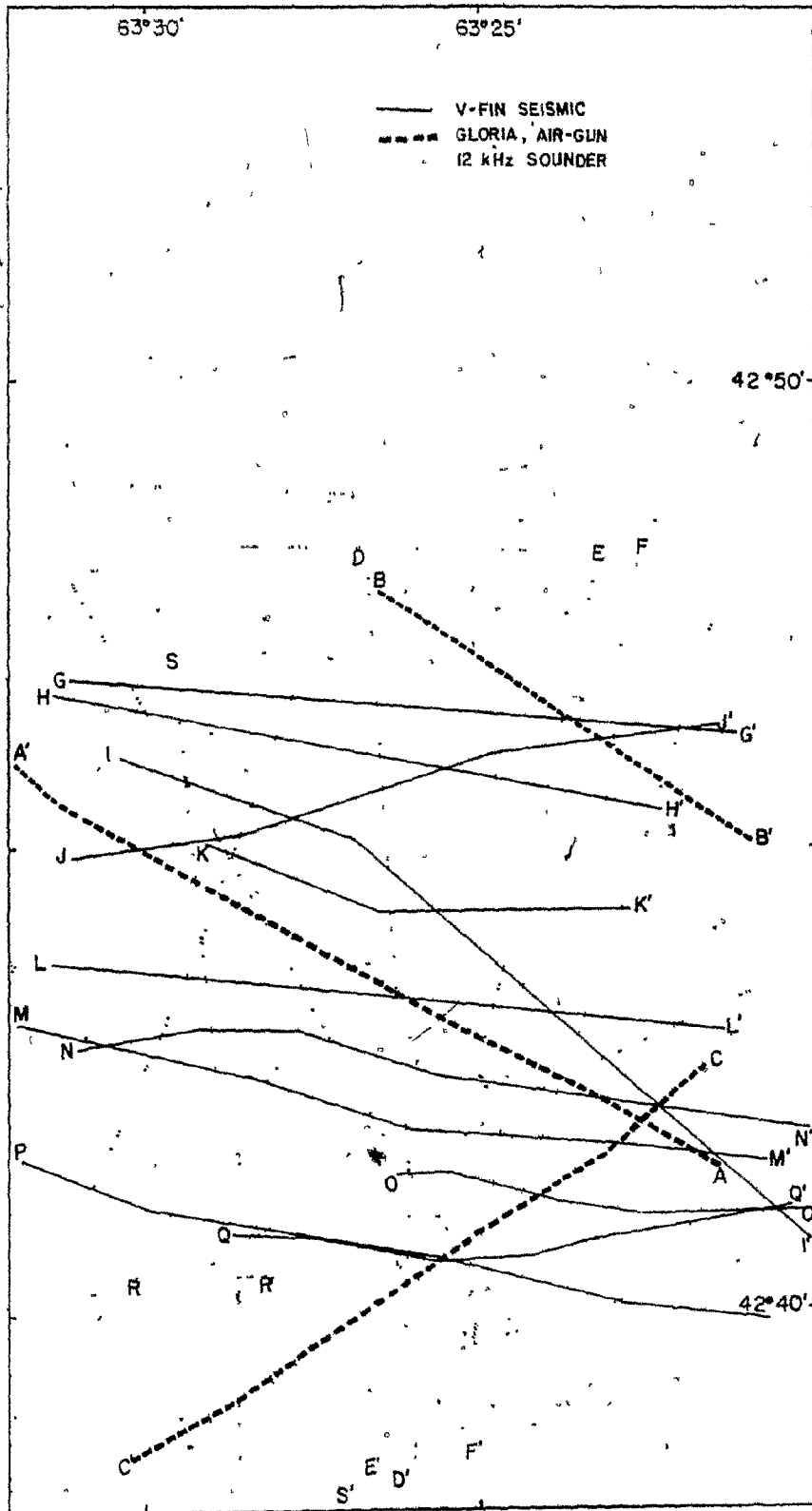
Figure 2-1. Schematic illustration of the characteristics shown by constructional and destructional slopes (after Rona, 1969; King and Young, 1977).

on continental slopes, from hundreds of kilometres (Gulf of Cadiz margin, D.G. Roberts, pers. comm.) to less than 500 metres (Field and Clarke, 1979). Evidence from the ancient record (Laird, 1968; Cook, 1979) suggests that smaller-scale slumps and slides, beyond the resolution of most acoustic systems, would be present. Slump slide features are largely responsible for the large-scale erosion of destructional slopes and their chaotic appearance on seismic profiles.

Erosion by canyons and turbidity-current channels is also an important process on continental slopes. McGregor et al. (1979) demonstrated that an apparently "scalloped" upper-slope morphology can be formed by tributary-channel erosion. Detailed correlation of reflectors is required to distinguish inter-channel ridges from slide-blocks of superficially similar appearance (McGregor and Bennett, 1977; 1979).

In this study, the morphologically complex Scotian Gulf area (Fig. 1-3) was investigated in detail, using 12 kHz echo-sounder, GLORIA long-range sidescan sonar, air-gun and high-resolution deep-towed sparker seismic records. Relatively little survey work was carried out on the Western Bank area, mainly for logistical reasons, but some high-resolution seismic profiles were obtained in the area. Survey lines are shown in Figures 2-2 and 2-3. Navigation prior to 1980 was by Satnav and Decca and since 1980 by Satnav and Loran C. The resolution of the Decca navigation is very poor and it was necessary to smooth the tracklines. The subsequent Loran C navigation is much better (accurate to within 200 metres or so) and indicates that the ship

Figure 2-2. Location of survey lines in the Scotian Gulf area. Solid line: V-fin seismic profiles; dashed line: GLORIA and air-gun profiles; dotted: 12 KHz echosounder profiles.



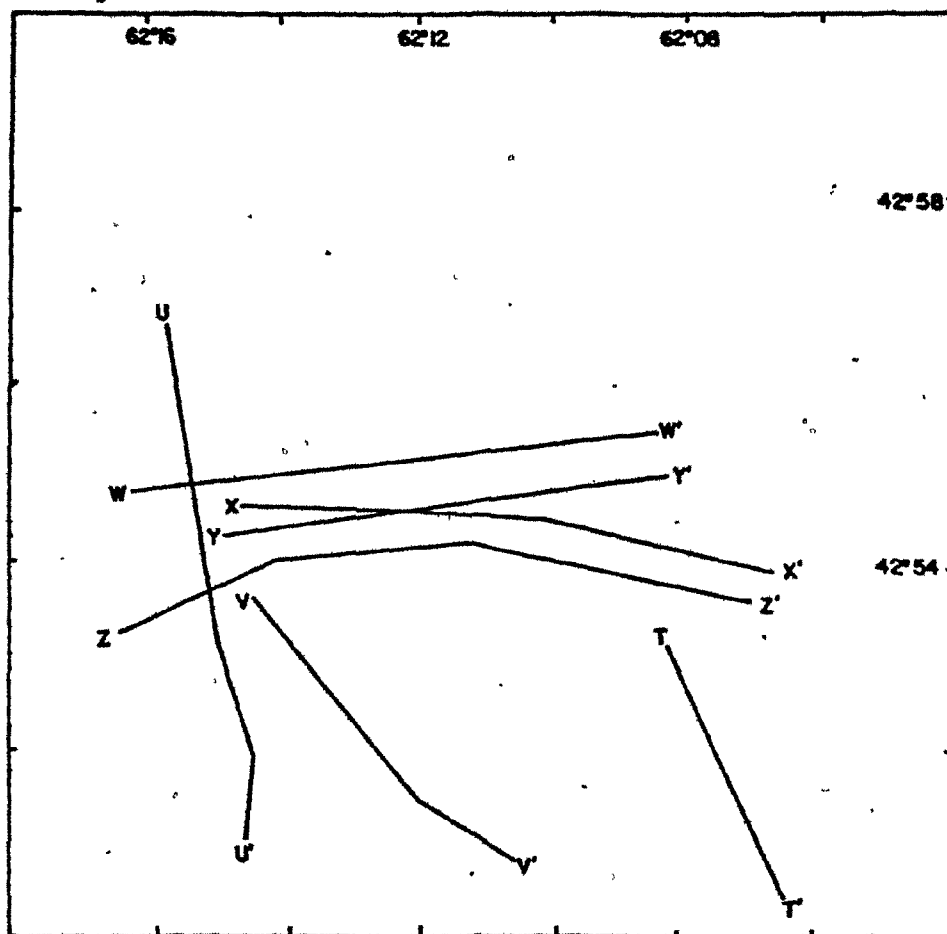


Figure 2-3. Location of V-fin seismic survey lines in the Western Bank area.

was generally able to maintain a steady course even in poor weather conditions. Where available, cross-overs were matched and the older lines were shifted. In the case of the deep-towed profiling system, the fish tow-length was assumed to be at a horizontal distance of 500 metres from the ship unless otherwise noted on the record.

### BACKGROUND

The deep structure of the continental margin off Nova Scotia has been the subject of extensive investigation by C.E. Keen and co-workers at Bedford Institute of Oceanography. The boundary between oceanic basement and continental basement occurs in a zone approximately 70 km wide near the slope-rise boundary (Keen et al., 1975). The sediment piles overlying basement vary in thickness from about 5 km, at the shelf edge to nearly 8 km below the base of the slope (Keen et al., 1975). The oldest sediments recovered from boreholes off Nova Scotia are Triassic and Early Jurassic in age (Jansa and Wade, 1975) and consist of red shales, limestones and evaporites. Overlying these are a thick sequence of Jurassic, Cretaceous and Tertiary clastics and limestones showing various phases of transgression and regression. The Quaternary is represented by a shelf-edge accumulation of glacially derived clastics, reaching up to 1500 metres thickness (Jansa and Wade, 1975) and representing extensive outbuilding of the margin as a result of high rates of glacially-derived sediment supply.

Although most of the post-Paleozoic sediment accumulation has a simple, flat-lying structure, King and MacLean (1970) and McIver (1972) recognised large-scale intrusion (piercement) features within the shelf

and rise sequences, which were interpreted as salt diapirs derived from Triassic and early Jurassic evaporites. The diapirs caused folding of overlying rocks in a distinctive zone beneath the continental rise from the Laurentian Channel in the north to Northeast Channel in the south, named the Sedimentary Ridge Province by Jansa and Wade (1975). The outer edge of this zone is very regular and corresponds approximately to the 4000 m bathymetric contour, while the inner edge is irregular and in places underlies the upper slope (Jansa and Wade, 1975).

#### THE SCOTIAN GULF AREA

##### Air Gun Record

Profiles A-A', B-B' and C-C' (Figs. 2-2 and 2-4) run obliquely down the slope. Up to 1.5 seconds of penetration was achieved, which probably includes most of the Quaternary section and perhaps the topmost Tertiary (Jansa and Wade, 1975). No good candidate for the strong Pliocene reflector of Jansa and Wade (1975) is seen. The section can be divided into four main units (Fig. 2-5).

##### UNIT A

The deepest reflectors (below 1 second penetration) dip gently southward and are either flat-lying or slightly undulating. They are apparently continuous across the whole area, although they cannot be traced individually across this distance.

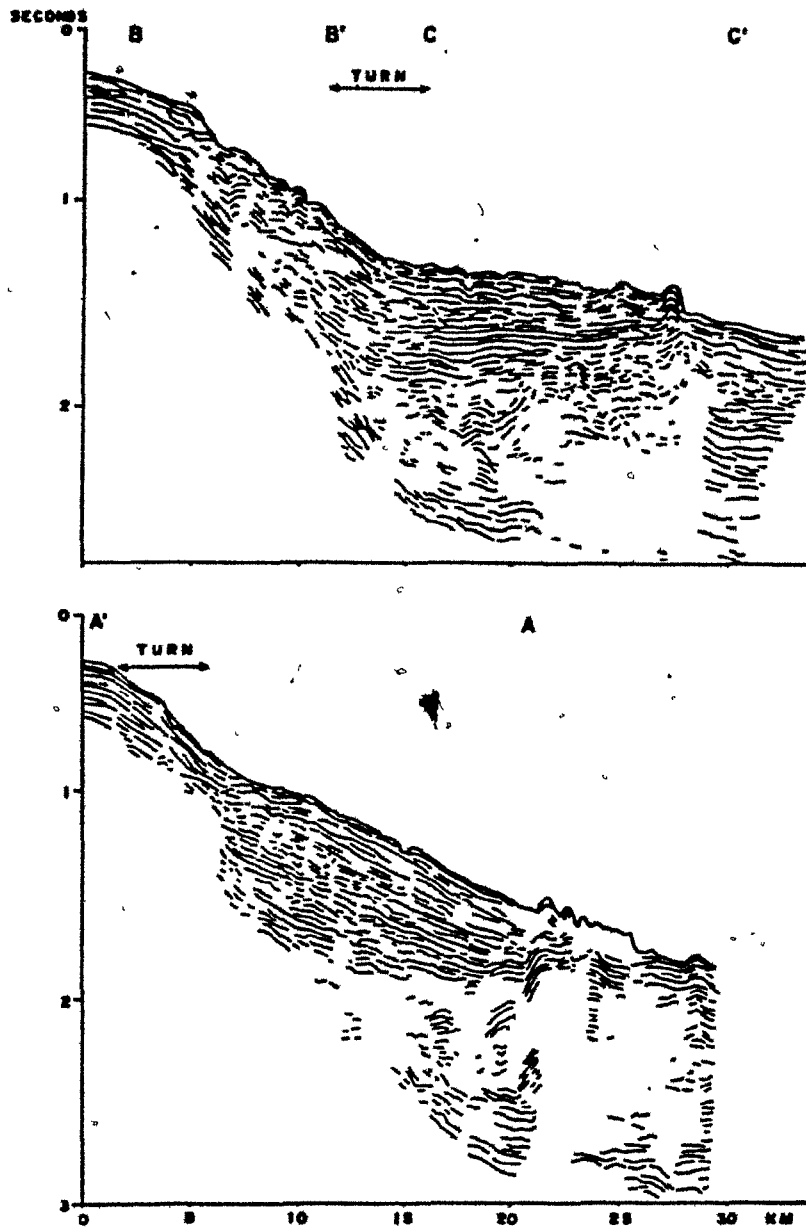


Figure 2-4. Line drawings of air-gun records from the Scotian Gulf area.

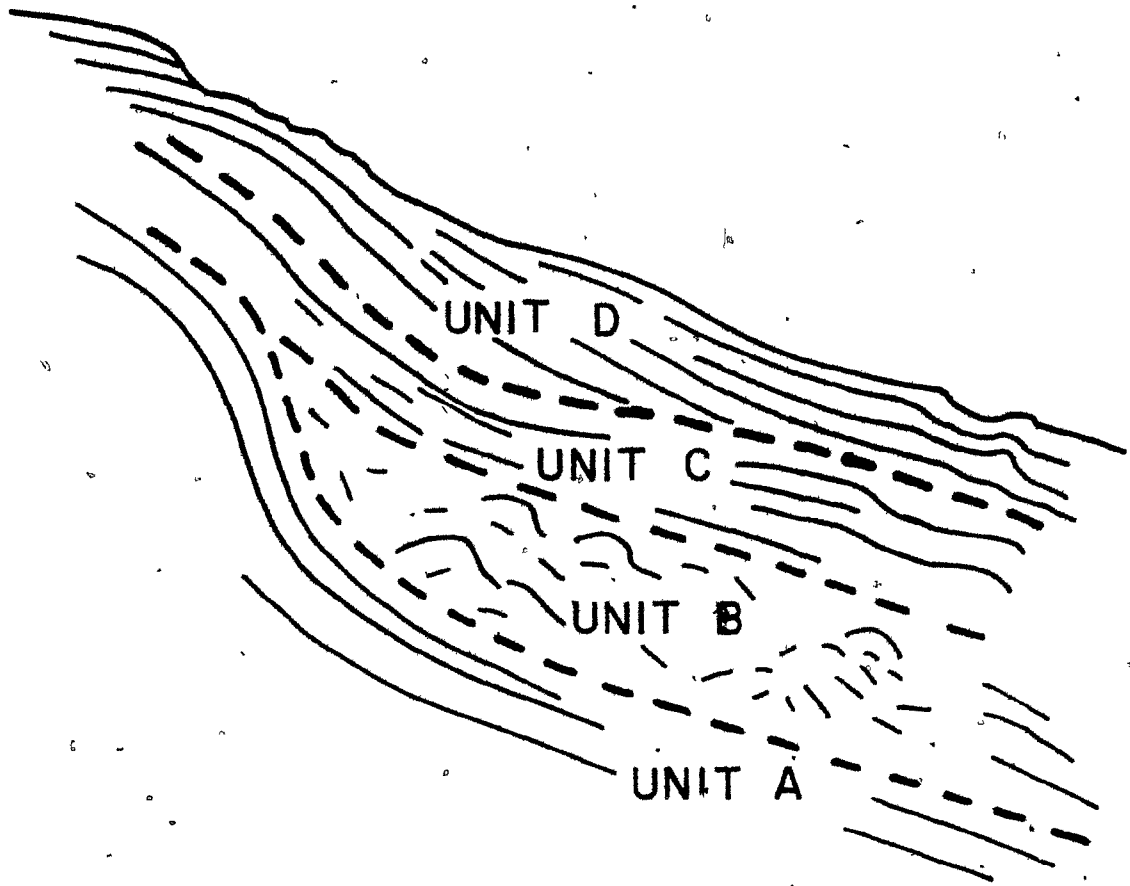


Figure 2-5. Schematic illustration of the four seismic units identified from the air-gun records shown in Figure 2-4.

## UNIT B

Directly overlying these deep reflectors is a unit of folded and distorted reflectors up to 0.6 seconds thick. In places, the folding appears coherent, but in general only discontinuous, steeply-dipping reflectors are seen. The unit pinches out in an upslope direction.

## UNIT C.

This unit consists of strong, continuous reflectors which appear horizontal or dipping upslope in profile C-C', suggesting a strike parallel to the ship's track and a true dip of the unit to the southeast. It apparently onlaps and partially drapes the rough surface of the underlying folded unit.

## UNIT D

The reflectors of Unit D are irregular and discontinuous in the upper-slope region, but become more coherent downslope. They appear to have a disconformable relationship with the underlying unit and there are suggestions of minor disconformities within Unit D itself. Just below 1000 metres water-depth in both profiles (Fig. 2-4), there is a region of elevated, irregular topography, with approximately 100 metres (maximum) relief.

There are two possible interpretations of the folded reflectors of Unit B and the elevated surface features of Unit D. In profile A-A', the nature of the disrupted reflectors, just below the surface

feature, suggests diapiric intrusion of salt or shale from below. The location of these structures is very close to the outer margin of the Sedimentary Ridge Province and some of the deformation may be associated with diapiric processes. However, the reflectors of Unit A beneath Unit B are not substantially deformed, so that intrusion from below is unlikely. Thus for a diapiric mechanism to be viable, either the salt or shale originated within Unit B or was intruded laterally. Shales make up a large part of the pre-Miocene Tertiary sequence (Hardy, 1975) and although little published information on the early Pleistocene sequence is available, it is likely that mud is a primary component of slope sediments at least in part. However, most diapiric features on the shelf and in the Sedimentary Ridge Province are from much deeper sources, and it seems unlikely that such young sediment would have been sufficiently loaded to cause diapirism.

The alternative explanation for these features is that Unit B represents a period of slumping which caused the deformation. The wedge-shape geometry of the Unit (Fig. 2-5) would be compatible with this explanation. Upslope-dipping reflectors are commonly seen and may be explained by subsequent infilling of small basins formed by slumped blocks. The elevated feature at the surface may itself be a slump- or slide-block. Apparent folding of reflectors beneath the features may be merely velocity effects as seen less markedly elsewhere in the profile. The locations of the slide-blocks may be related to the maximum thickness of Unit B. The southeastward dip of reflectors within Unit C suggests that Unit B thins in that direction and is a ridge-like feature, which partially controls the present-day bathymetry.

Thus, a slide originating on the upper slope may have been arrested by a decrease in slope-angle over one of these slump-controlled sub-bottom ridges.

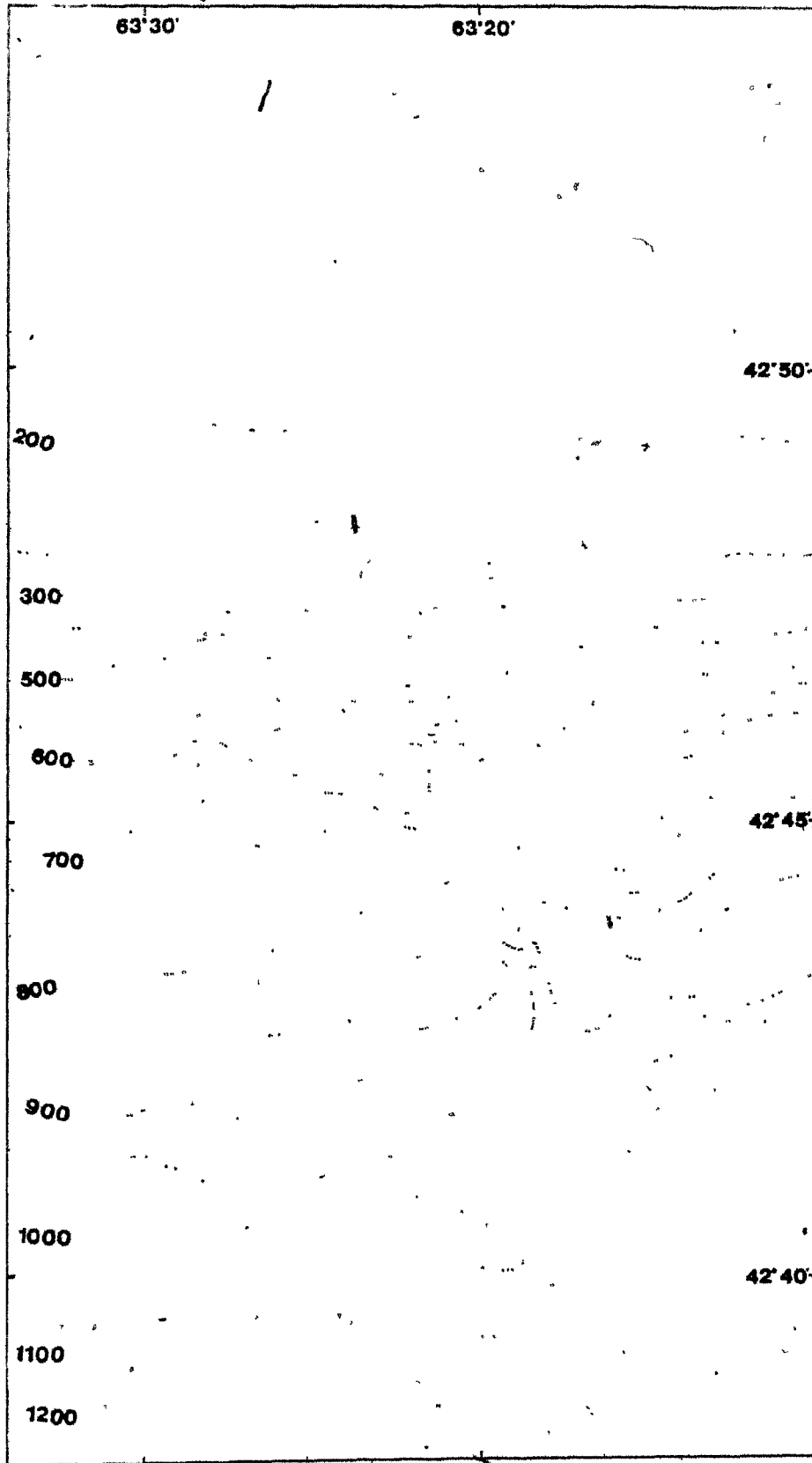
The present day regional morphology of the slope is clearly seen to be the result of substantial erosion of the upper slope with deposition (partly as slumps and slides) in downslope areas. Some of the upper-slope erosion may be concentrated in channels.

#### Bathymetry

The bathymetric map (Fig. 2-6) has been constructed from the echosounding and seismic-lines shown in Figure 2-2, and four sounding-lines completed by the Canadian Hydrographic Service. There is much bathymetric variation on the scale of 10-20 metres relief and 500 metres horizontally which is beyond the resolution of this map. However, the map shows the general features of the bathymetry quite well.

The shelfbreak is clearly defined at 250 metres depth and the uppermost slope is on average  $5.0^\circ$ . The average slope decreases in the downslope direction to  $2.7^\circ$  at 900 metres. At the base of the steepest part of the slope (500 metres) is an area of higher than average relief, which shows up on the map as an area of irregular contours. Two ridge-like areas of approximately  $0.5 \text{ km}^2$  are defined by the contours and a similar broader area to the east is apparent. A well-defined valley-like feature emanates from this area of high-relief, but from the contours, it does not apparently continue below 950 metres. However, careful examination of the 12 kHz profiler records suggest that it does continue

Figure 2-6. Bathymetric map of the Scotian Gulf area.



southward as a smaller-scale gully.

In the southern part of the area, the contours swing from a broadly W-E orientation in the west, to a more NE-SW direction in the east. Also in the south, there is evidence of other ridge-like features between 1000 and 1200 metres. One, in the southwest, is well-defined and corresponds to the elevated feature in air-gun profile C-C'. The more easterly ridge is not well-defined, but to the north of it is an area with a slope angle as low as  $2.2^\circ$ .

The 12 KHz echo-sounder profiles (Fig. 2-7) illustrate the changing character of the slope from west to east. Profile D-D', across the central part of the study area (Fig. 2-2) is steep and concave in the north, but becomes broadly convex to the south. Lines E-E' and F-F', on the other hand, have overall, more concave profiles. Both profiles E-E' and F-F' also cross the valley-feature which can be seen to be a well-defined incised channel.

It is interesting to note the relationship between bathymetry and the deeper structure. The broad bathymetric bulge in the southwest corresponds to the similar feature in sub-bottom unit C (Fig. 2-4). This itself is related to onlap of the slumped Unit B. It appears that the large-scale bathymetry of the slope is partially controlled by the locations of large early Pleistocene slumped masses.

#### Interpretation of Specific Morphological Features from GLORIA II Sidescan and High Resolution Seismic Profiles

Using all the data at hand, and in particular, the GLORIA II record

7

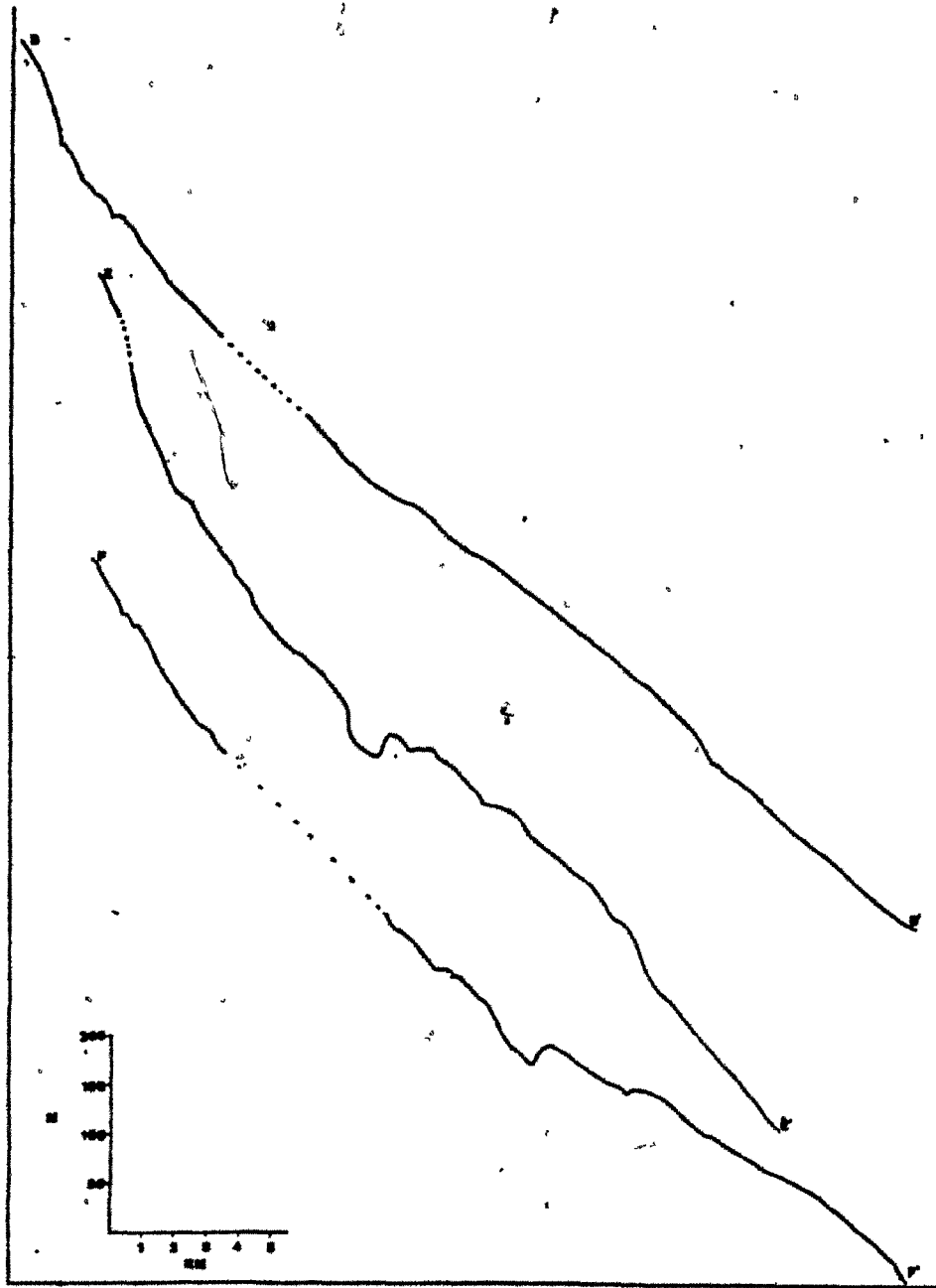


Figure 2-7. 12 KHz echo-sounder profiles run perpendicular to the slope contours, Scotian Gulf area.

and the deep-tow seismic profiles, a number of specific morphological features can be recognised. They are shown on Figure 2-8:

The GLORIA II survey was run along track-lines A-A', B-B' and C-C' (Fig. 2-2). A different aspect is presented by each of the records, which are shown in Figures 2-9, 2-10 and 2-11. The accompanying line-drawings are objective representations of features on the records. Occasionally, different features on separate records overlap which suggests either some system artifacts are present or that the navigation is inaccurate. The survey used Satnav navigation and a speed of 8 knots maintained, so that navigation problems should be at a minimum.

GLORIA records are best interpreted in conjunction with other data. In this study, good bathymetric control and high-resolution seismics are used as control. Several important morphological features have been recognised.

#### (1) UPPER SLOPE ESCARPMENT

On GLORIA profiles B-B' and C-C' (Figs. 2-10, 2-11), a straight to sinuous line (a) marks a boundary between a featureless part of the record to the north and a patterned area to the south. This feature is located just south of the shelfbreak and corresponds to the steepest part of the slope. The air-gun record (Line B-B', Fig. 2-4) shows it to be an escarpment-like feature; truncated reflectors indicate the erosive nature of the escarpment.

On profile B-B', the escarpment appears to curve round to the south (Fig. 2-10). This is confirmed by the presence of the dis-

Figure 2-8. Morphological features of the Scotian Gulf area.

- (a) Upper slope escarpment .
- (b) Zone of high relief hummocky topography
- (c) Upper slope slide blocks
- (d) Lower slope slide block(s)
- (e) Large debris flow
- (f) Constructional slope channel

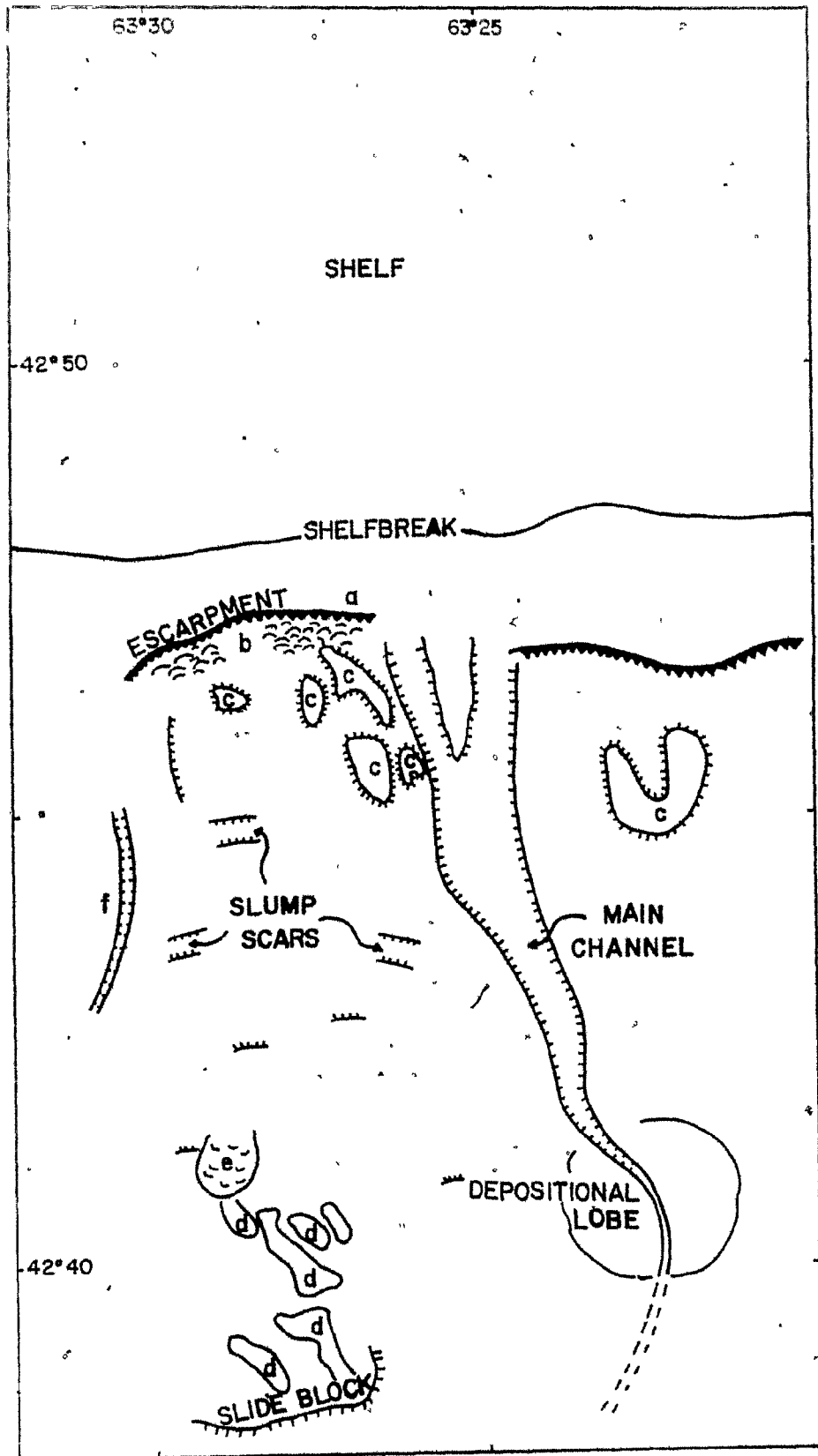


Figure 2-9. Features traced from GLORIA profile A-A'. 20 second sweep gives range of approximately 12 km each side of track-line (marked by arrow).



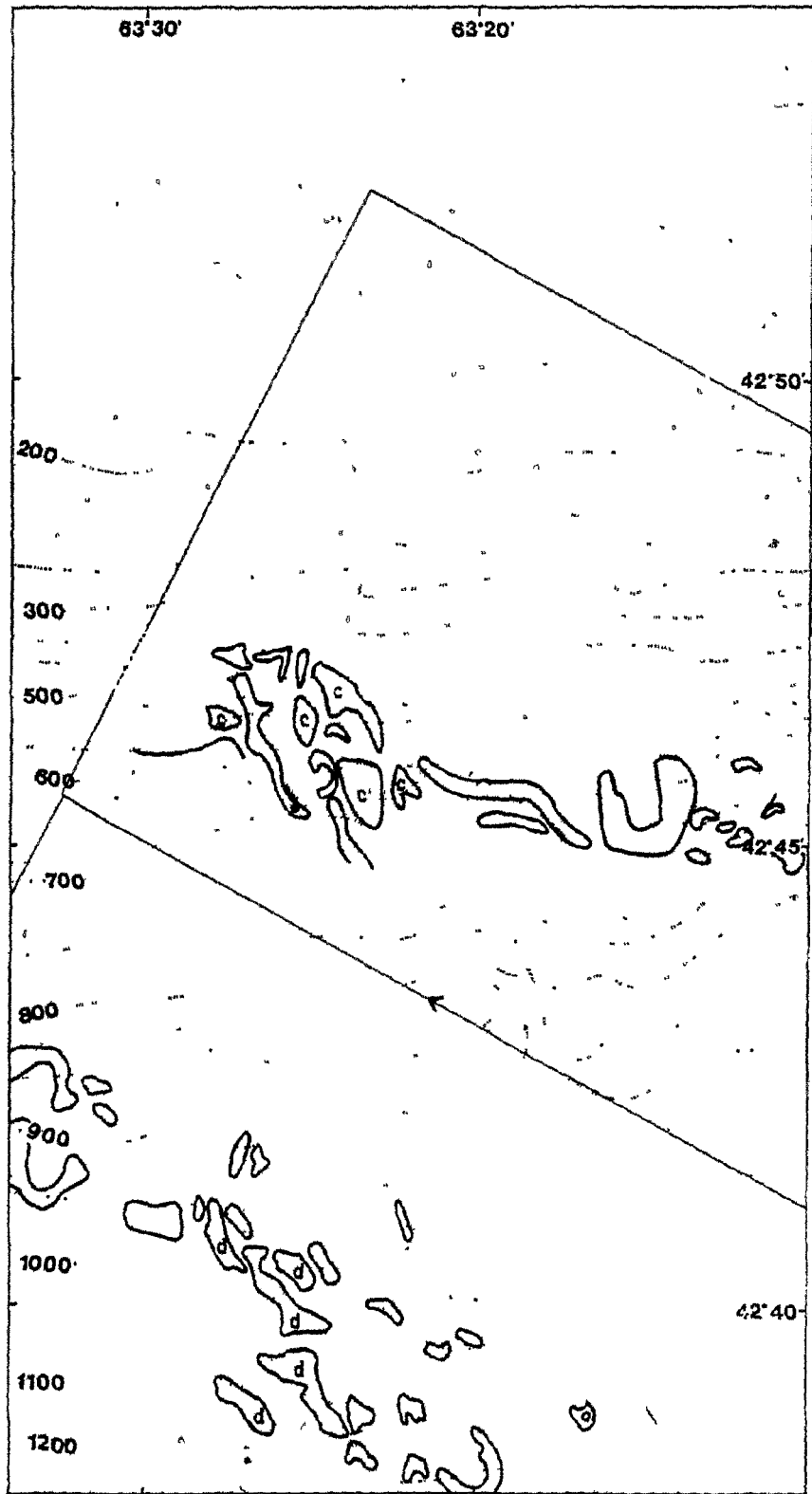


Figure 2-10. Features traced from GLORIA profile B-B'. 20 second sweep, starboard record only.

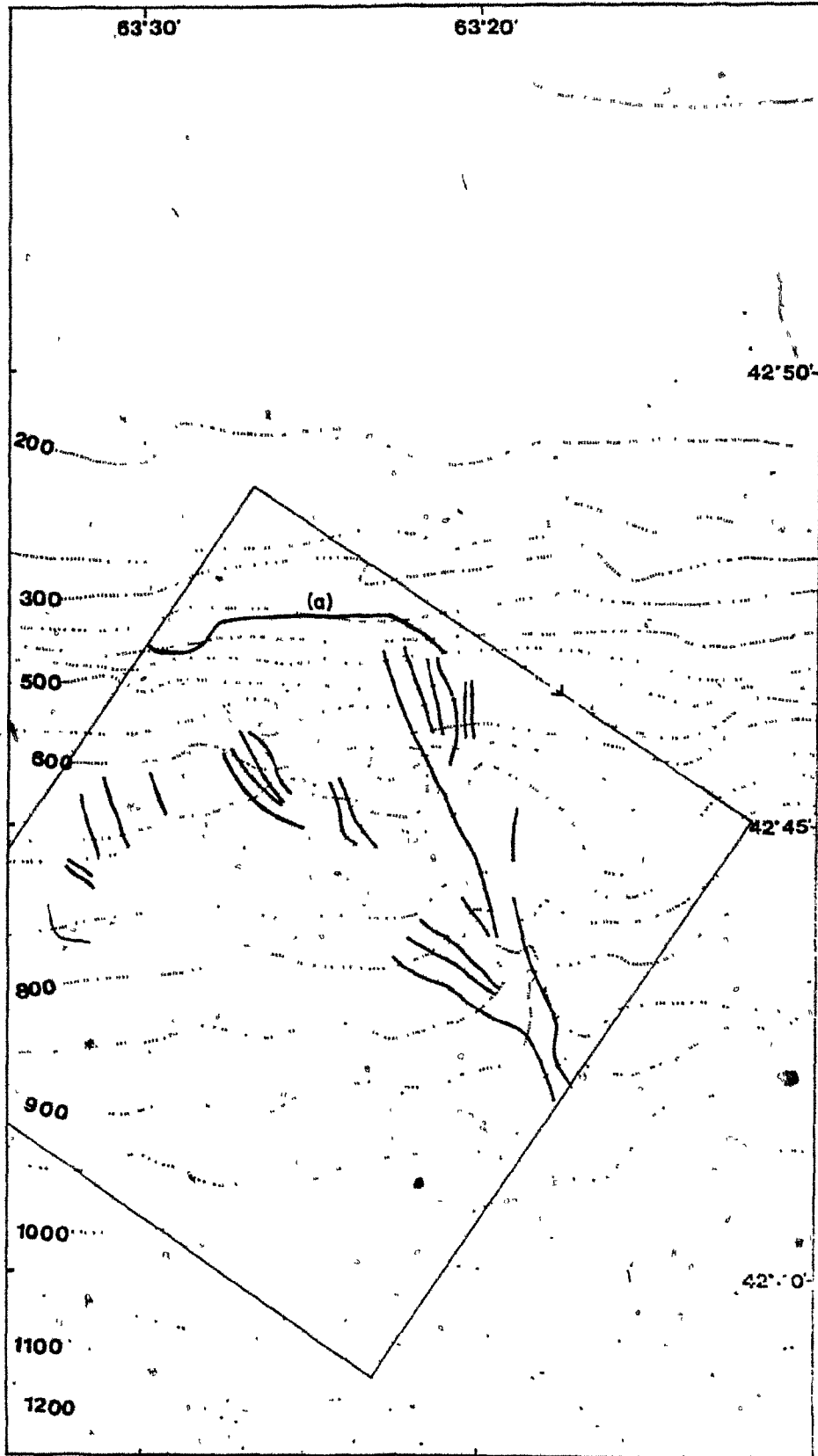
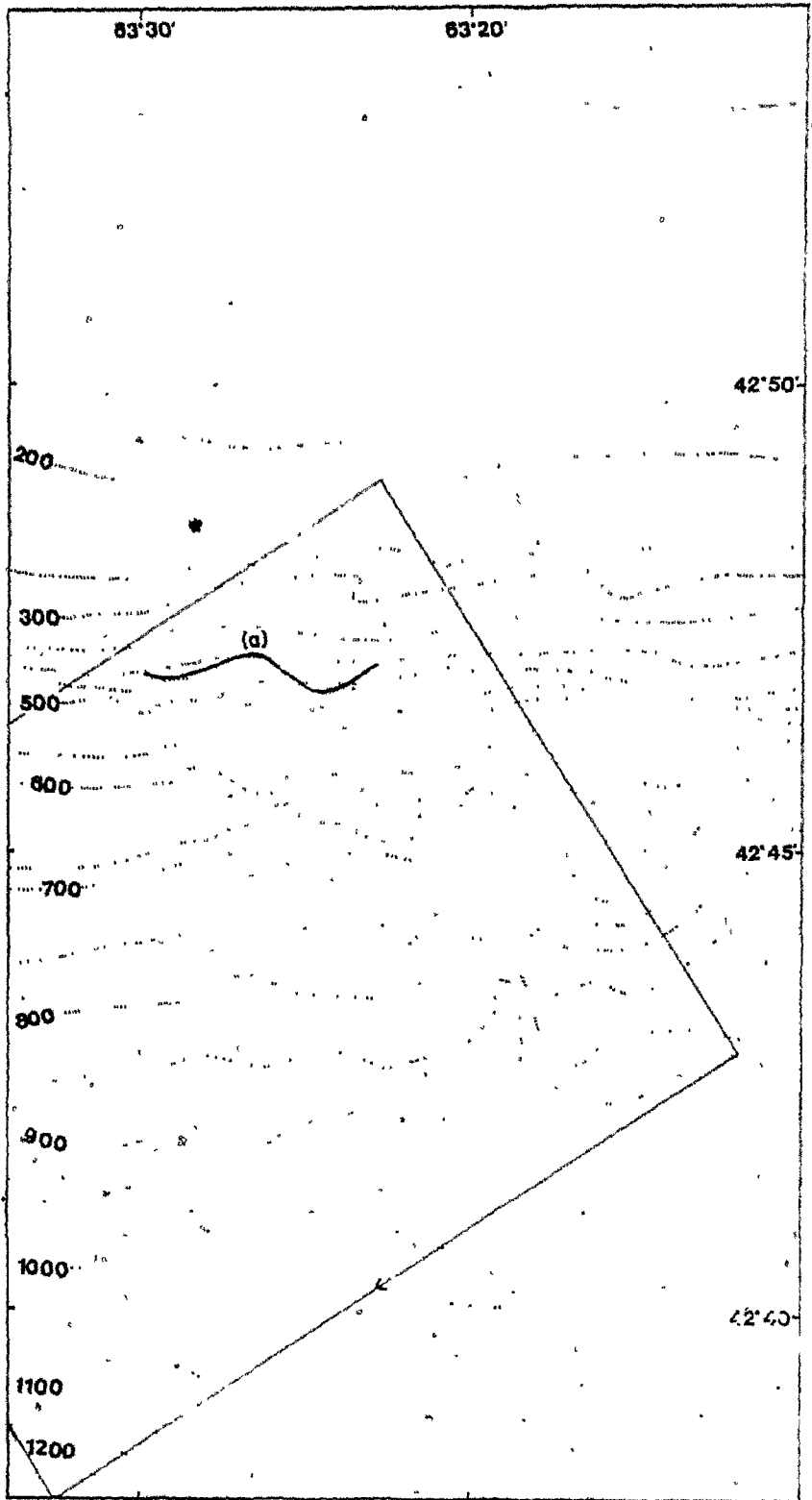


Figure 2-11. Escarpment feature traced from GLORIA profile C-C'.  
20 second sweep, starboard record only.



tinctive scarp on the seismic profiles I-I' and J-J' (Fig. 2-14). The same feature can be seen as far south as profile M-M' (Fig. 2-13). The nature of the seismic profile above and below the escarpment is very different. To the north and west, the bottom is smoother and the sub-bottom is characterised by continuous parallel reflectors, while below the escarpment, the bottom is hummocky on a scale of tens of metres or greater and reflectors are discontinuous (Figs. 2-13, 2-14). Prominent sub-bottom reflectors can be traced from upslope of the escarpment to beneath the scarp surface.

## (2) UPPER SLOPE AREA OF SLUMPS AND SLIDES

Just below the escarpment is an area of rough, hummocky relief characterised by a high density of hyperbolic returns (b, Fig. 2-8). It forms a narrow zone at the base of the escarpment and is crossed by profiles G-G', H-H' and J-J' (Figs. 2-12, 2-14). Similar chaotic bottom characteristics are generally interpreted as the products of slumping and mass-movement processes (eg. Damuth, 1980; Damuth and Embley, 1981). The location, just below the relatively steep escarpment adds weight to the argument for a slumped origin of this rough topography.

Within the slump mass and further downslope are a number of blocks with positive relief and greater acoustic penetration, showing regular, parallel sub-bottom reflectors (eg. c, Figs 2-8, 2-14) which are often tilted and/or slightly folded (Fig. 2-14). They have dimensions in the order of 20-50 metres thick and 500 metres wide. Some have well-defined

Figure 2-12. (in back pocket). Line drawings of seismic profiles G-G', K-K', Q-Q', R-R' from Scotian Gulf area. For locations, see Figure 2-3. Profiles arranged geographically with most northerly profile at top.

Figure 2-13. (in back pocket) Line drawings of seismic profiles L-L', M-M', O-O', P-P' from Scotian Gulf area. For locations, see Figure 2-3. Profiles arranged geographically with most northerly profile at top.

Figure 2-14. (in back pocket). Line drawings of seismic profiles H-H', I-I', J-J', N-N' from Scotian Gulf area. For locations, see Figure 2-2. Profiles arranged geographically with most northerly profile at top.

bases. On the GLORIA II records, a number of irregularly-shaped, strong-reflecting areas can be identified (see especially Fig. 2-9) which are likely related to the blocks identified on the seismic records. Where they correspond closely to positive features on the seismic records or to bathymetric features, they are shown in Figure 2-8 (c). It should be re-emphasised that these GLORIA reflections may not represent the true outlines of the actual blocks.

These features are interpreted as coherent slabs of consolidated sediment which have slid into or with the main slump mass. It is not clear whether the blocks slid independently or with the whole mass, but the narrowness of the slumped zone suggests that the complexity of features observed is best explained by a number of smaller slumping events rather than one large slump. The slumped zone represents the accumulation from these events at the base of the escarpment.

### (3) LOWER SLOPE SLIDE COMPLEX AND DEBRIS FLOW

Features similar to the blocks described above are also present on the GLORIA record to the south in water depths of 900 to 1200 metres, (d, Profile A-A', Fig. 2-9). Most of the features lie in a zone which is almost parallel to the ship's track and must therefore be regarded with suspicion as potential artifacts. However, the features themselves are irregularly-shaped and not oriented parallel to the track. Furthermore, some correspond very closely to bulges in the bathymetric contours in that area.

No seismic lines run through the southwest corner of the area, but a 12 KHz echo-sounder profile (S-S') across the features is shown in Figure 2-15. The GLORIA features can be seen to reflect the surface of a distinctive block some 7 km x 3 km size, with a stepped upper surface and a very steep downslope termination. The profile is typical of slide masses observed from other slopes (Embley and Jacobi, 1977; Field, 1979; Mullins and Neumann, 1979). The upper end of the feature is crossed by the seismic line R-R' (Fig. 2-12) in which the steep sides and flat top are very apparent. The record is poor, but undeformed reflectors can be made out within the block.

Just upslope of this large slide block on profile S-S' is a smaller, low-relief feature (E, Fig. 2-15). On the seismic profile P-P' (Fig. 2-13), this feature is seen to be lobate in cross-section, acoustically transparent and have very small-scale surface roughness, resulting in irregular hyperbolic returns. The feature has the appearance of a debris flow (Embley, 1980). It does not seem to be associated with the slide blocks along the line of profile S-S', being apparently separated by a small distance. However it seems likely that there is some relationship between the two features in terms of source and age.

#### (4) THE MAIN CHANNEL SYSTEM

Running through the central part of the study area is a well-defined channel (Fig. 2-8). It can be seen on one GLORIA profile (Fig. 2-10) and most seismic profiles (Figs. 2-12, 2-13). In its upper reaches, the channel is clearly incised, wide (~ 1 km) and deep

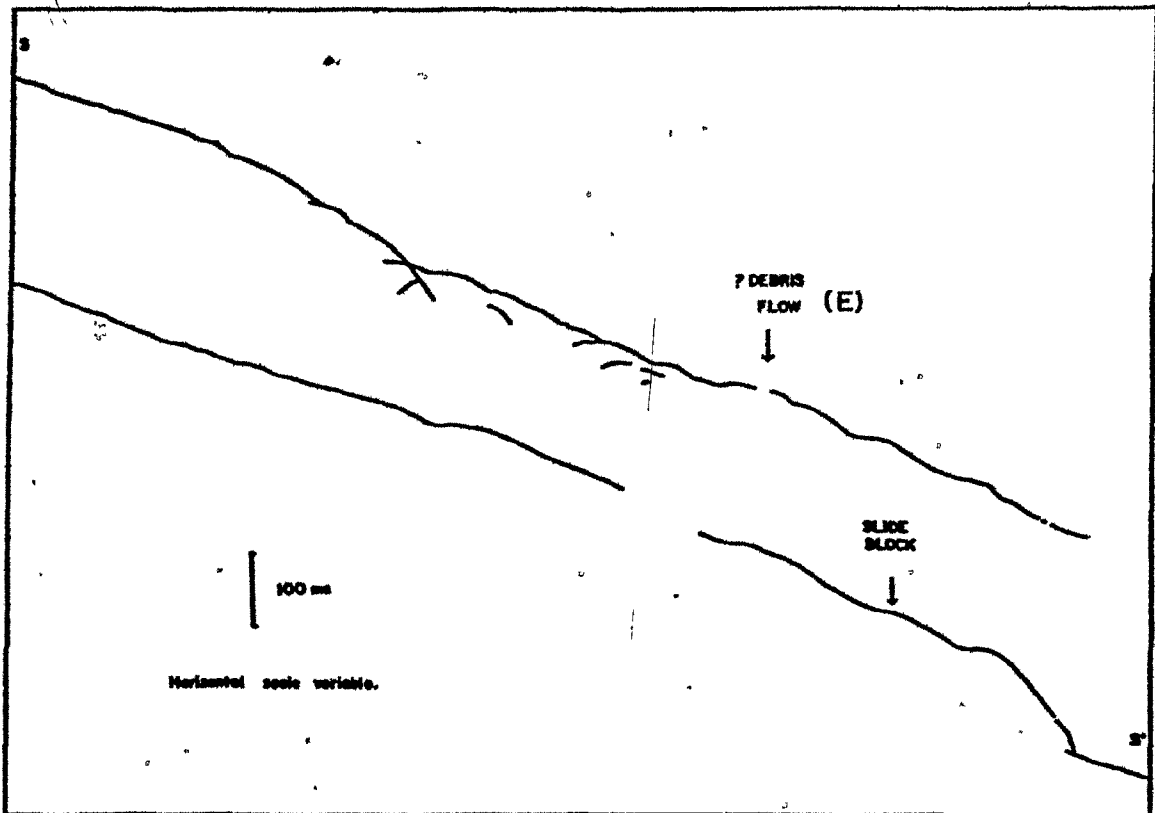


Figure 2-15. 12 KHz echo-sounder profile S-S' which crosses a large slide block near S'. Note the steep toe and undulating surface of the block. The convex-up profile of a large debris flow (E) is seen upslope of the slide block (see P-P', Figure 2-13).

(> 50 m) with a flat bottom and a distinct thalweg in mid-section (K-K', Fig. 2-12). As it progresses downslope, the channel decreases in both depth and width. In the midslope region, the channel margins are levee-like (L-L', N-N'), but these are difficult to distinguish unequivocally from uneroded slope or slide-blocks. Only in profile M-M' does the channel margin show the thickening of the reflectors that is characteristic of levees. In places, the internal organization of the channel margin is complex with several erosion surfaces being apparent (N-N', Fig. 2-14). Probably, the channel margins are as susceptible to slump-erosion as any other part of the slope, but depositional rates are high. True levees may never be formed, rather the channel margin maybe the site of alternating deposition and mass-wasting resulting in the complex structures observed.

Also in the midslope region, the channel is incised into a broad, flat or slightly hummocky area, characterised by strong surface reflectors and strong, discontinuous reflections in the immediate sub-bottom. In places, this broad surrounding area could be mistaken as part of the main channel as it has well-defined margins and a flat or very slightly hummocky bottom (Profile N-N', Fig. 2-14). Elsewhere the margins are less clear and the bottom more hummocky (Profile L-L', Fig. 2-13). This suggests that the surrounding area is not part of the actual channel, but is perhaps periodically an area of turbidity current activity. The margins of this "flood-plain"-like valley are controlled by slump and slide deposits.

In the southeast of the area, the channel decreases dramatically in size to around 15 m depth and less than 500 m in width (Fig. 2-16). The profile becomes V-shaped, (although this may be in part due to side-echoes) and the surrounding area is again characterised by strong discontinuous sub-bottom reflectors near the surface. At greater depth in the sub-bottom (within 20 msec) strong reflectors are common, some of which may be buried channels (Profiles O-O' and Q-Q', Figs. 2-13, 2-14). Echo sounder profiles show that a small channel continues southward out of the study area.

From the decrease in channel dimensions and nature of the bottom and sub-bottom reflectors, it appears that the southeast part of the study area is the site of substantial deposition. This corresponds to the area where the contours are deflected northeastward slightly (Fig. 2-6) so that the channel encounters a relatively steep drop followed by flattening of the slope below about 900 metres. Deposition resulted as the slope flattened out and both the seismic profiles (O-O' and Q-Q') and the contours suggest that as the channel size decreased, a small depositional lobe was built up.

The lobe has similar characteristics to the suprafan of a submarine fan (Normark, 1970), having a broadly convex upper surface with strong, irregular near surface reflectors and suggestions of buried channels in the subsurface (Fig. 2-17). The dimensions of the lobe, in terms of relief and area, are also similar to suprafans of small submarine fans, eg. Navy Fan (Normark, 1970). A small channel feature appears on an echo-sounder profile in the very south of the

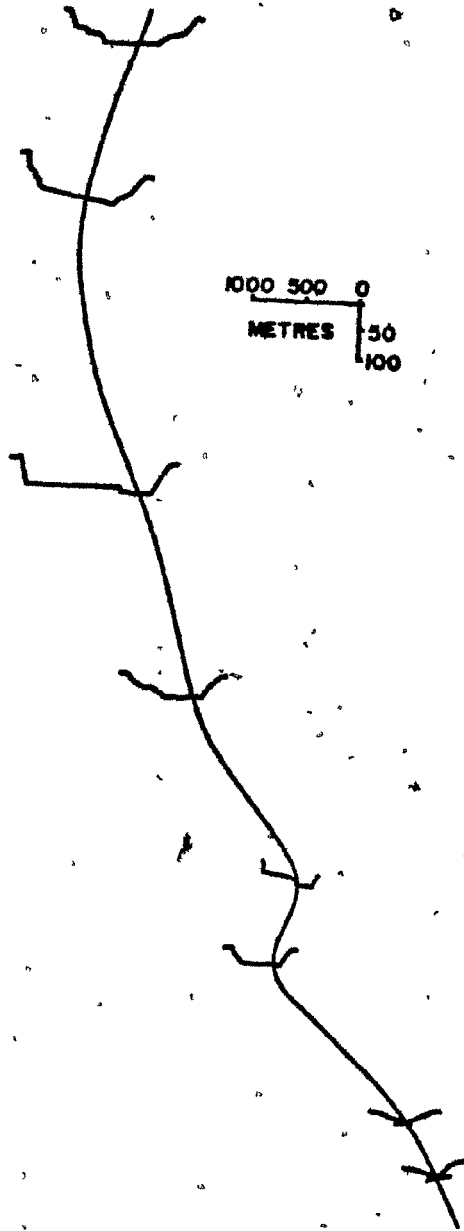
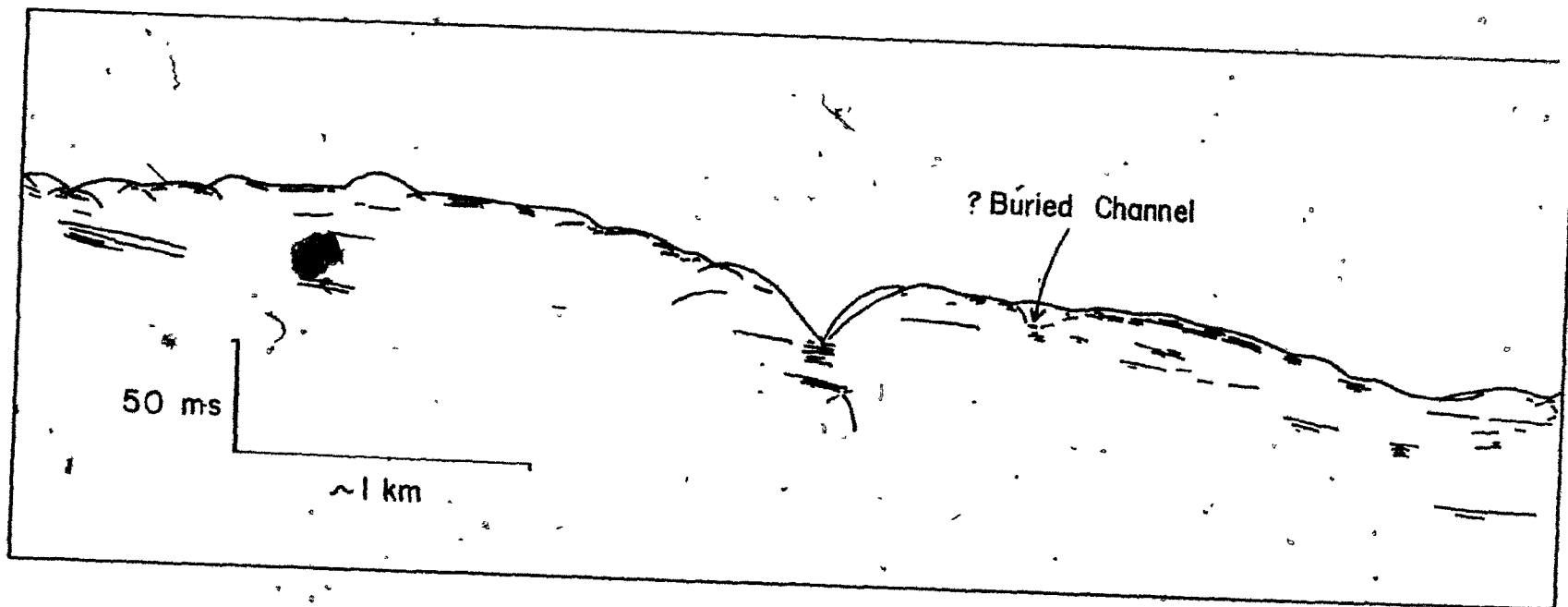


Figure 2-16. Variation in main channel dimensions (to scale) measured from seismic and 12 KHz profiles.

Figure 2-17. Line drawing showing detail of seismic line Q-Q' over the depositional lobe, Scotian Gulf area.



study area, suggesting that the channel now crosses the depositional lobe and carries on downslope.

As mentioned, the location of the depositional lobe is related to the local flattening of the slope in the southeast corner of the study area (Fig. 2-7). Although it is possible that this bathymetry is related to a local slump-scar, it is more likely the result of the undulating regional topography which itself is controlled by the early Pleistocene sub-bottom units A and B (Fig. 2-5).

The GLORIA record (Fig. 2-10) suggests that in its upper reaches, the channel is fed from the west by a number of tributaries. One major convergence is suggested between profiles L-L' and N-N' (Figs. 2-10, 2-13, 2-14) and several smaller ones further upslope. The nature of these tributaries is highly variable and a number of examples are shown in Figure 2-18.

On the upper slope, where the topography is very rugged as a result of slumping, small channels have developed between large slide-blocks and slump-masses (Fig. 2-18 (a)). They are recognised by the very strong returns from the valley-bottoms, which (allowing for side-echoes) have narrow, flat bottoms, probably filling an original v-shaped profile. Further downslope, the topography becomes gentler, but valleys are often flat-bottomed with strong bottom reflectors being characteristic of the floors (Fig. 2-18 b). These low-lying areas seem to have been filled with sediment. The large "tributary" seen on the GLORIA record between profiles L-L' and N-N' is shown in Figure 2-18 (c). The profile L-L' shows a definite, sharp, asymmetrical depression, bounded

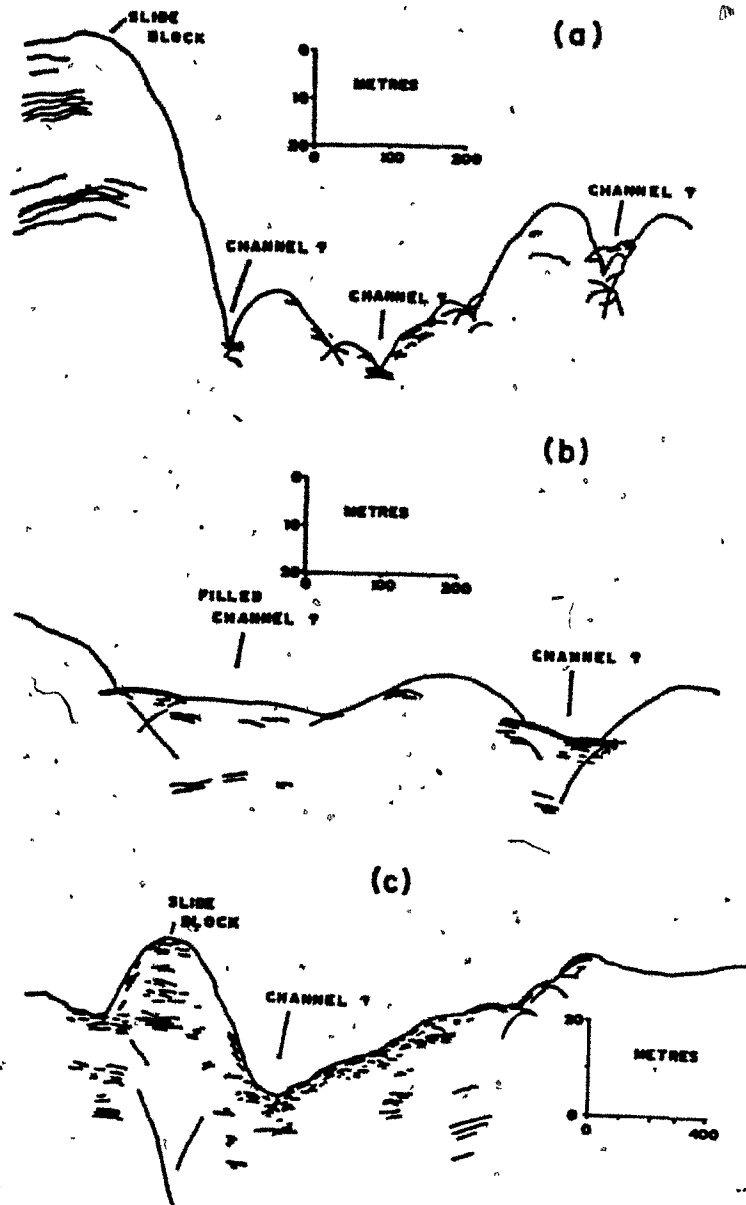


Figure 2-18. Line drawings from upper-slope seismic profiles, showing details of valleys between slide blocks, Scotian Gulf area.

on one side by a possible slide block and on the other by hummocky slumped material. The near-surface sub-bottom reflectors are discontinuous and relatively strong, especially in the deepest part.

This last-described feature is difficult to interpret. The GLORIA record does suggest that it is a large tributary which joins the main channel a little further downslope (Fig. 2-10). However, the valley is clearly related to the slide blocks which bound it and there is no seismic evidence which confirms that it is a continuous channel. The evidence presented above suggests that other tributary channel paths are controlled by slump masses and slide-blocks. This is probably also true in this last example. Although the channel may not now be active, it may have acted as a sediment conduit in the past.

#### (5) CONSTRUCTIONAL-SLOPE CHANNEL

In the west of the study area, where the slope has been unaffected by slumping (Profiles J-J', L-L', M-M', Figs. 2-13, 2-14), a small constructional channel (f) is present. The channel has built up substantially (50 msec) by levee accretion. Wedging of reflectors beneath the present channel suggest that it was constructed over a smaller, pre-existing leveed channel. The downslope continuation of the channel below profile M-M' is not known, although a small channel-like feature is seen on the west of profile P-P' (Fig. 2-13).

### The Nature of the Mid-Slope Area: Erosion vs Deposition

The mid-slope area (between 600 m and 1000 m) has a very irregular meso-scale topography which is the result of erosion and redeposition, mainly by mass-movements. The main channel divides the study area into two regions whose morphology are thought to have evolved separately.

West of the main channel, a distinction can generally be made between areas where erosion has dominated and areas of deposition. Profile L-L', for example, shows a distinct "zone of removal" (cf. Damuth and Embley, 1981) between two blocks with undisturbed parallel reflectors. It is difficult to trace reflectors across the eroded area but the erosion surface appears generally concave. Profile M-M' is similar in this respect, but the hummocky topography is less steep and more suggestive of deposition. Sub-bottom reflectors are more easily traced across this profile and suggest that substantial erosion has taken place, with the greatest removal from the central part of the profile. The hummocks, which have a relief of between 10 and 20 metres, have smooth surfaces and are generally transparent except for a thin region of strong reflectors at the surface (Fig. 2-19 a). It is suggested that the hummocky topography has been modified by subsequent deposition, which smoothed the irregular, eroded surface.

Profiles in deeper water, (N-N', P-P', Q-Q') suggest that deposition is the dominant control on the morphology. The general morphology is more convex than in upslope areas; the apparent concave profile of line Q-Q' is due to the crossing of the large slide-block in the west. The

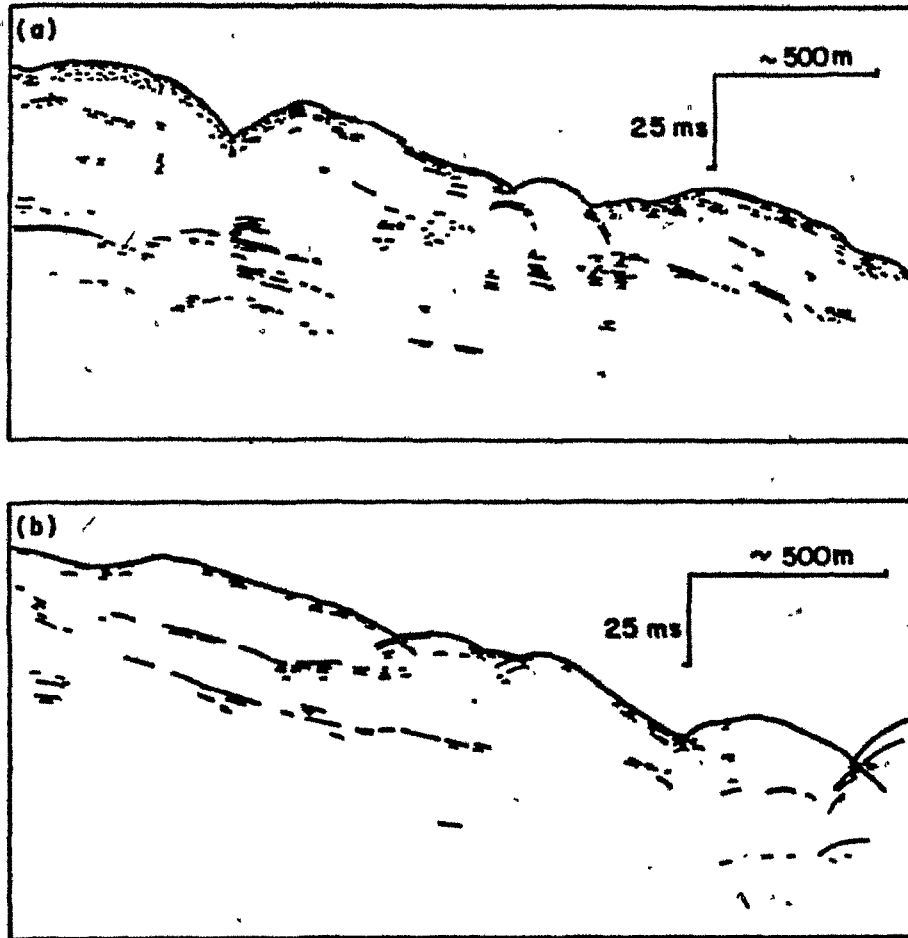


Figure 2-19. Line drawings of profiles from the mid-slope area  
(a) erosion dominant (b) deposition dominant.

hummocks appear to rest in places on a well-defined, near-planar surface (Fig. 2-19 b) and have smooth upper surfaces. Most are transparent, but some have parallel or hyperbolic internal reflectors. The hummocks in these profiles are interpreted as small slide-blocks and slumped masses, deposited after removal from the eroded upslope region. The large debris-flow/slump-mass described previously in this area is seen in profile P-P'.

Profiles along lines running almost perpendicular to the slope show evidence that large-scale slide-blocks may underlie much of the study area (Fig. 2-20). The seismic profiles shown in Figure 2-20 are located along the margins of the study area. However, similar features can be seen on echo-sounder profiles which run downslope in the west of the area (eg. D-D', Fig. 2-8). It is likely that much of the meso-topography is related to these larger slides and their slide scars.

East of the main channel, the slope shows mainly erosive characteristics (Profiles K-K', L-L'), except where the channel dies out and has built the small depositional lobe (Profiles O-O' and Q-Q; Fig. 2-12, 2-13). Even in these areas, small-scale slump erosion has taken place (Profile O-O').

#### Summary: Morphology of the Scotian Gulf Area

The regional bathymetry and erosion by mass-movements appear to exert first-order controls on the slope morphology in the Scotian Gulf area, which is summarised in a block diagram (Fig. 2-21). Slumping has

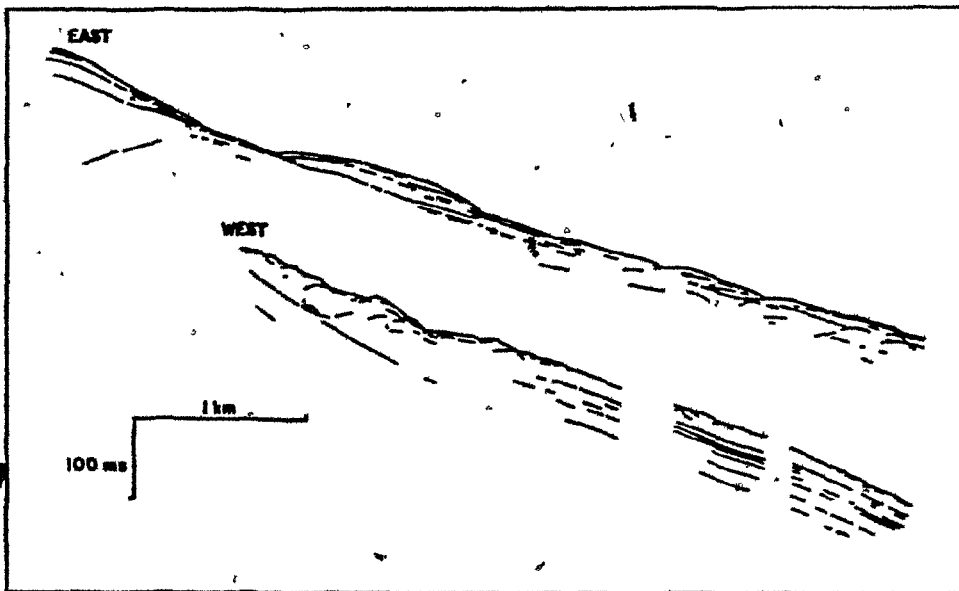


Figure 2-20. Line drawing of downslope profiles from just outside the Scotian Gulf study area as defined by Figure 2-2.

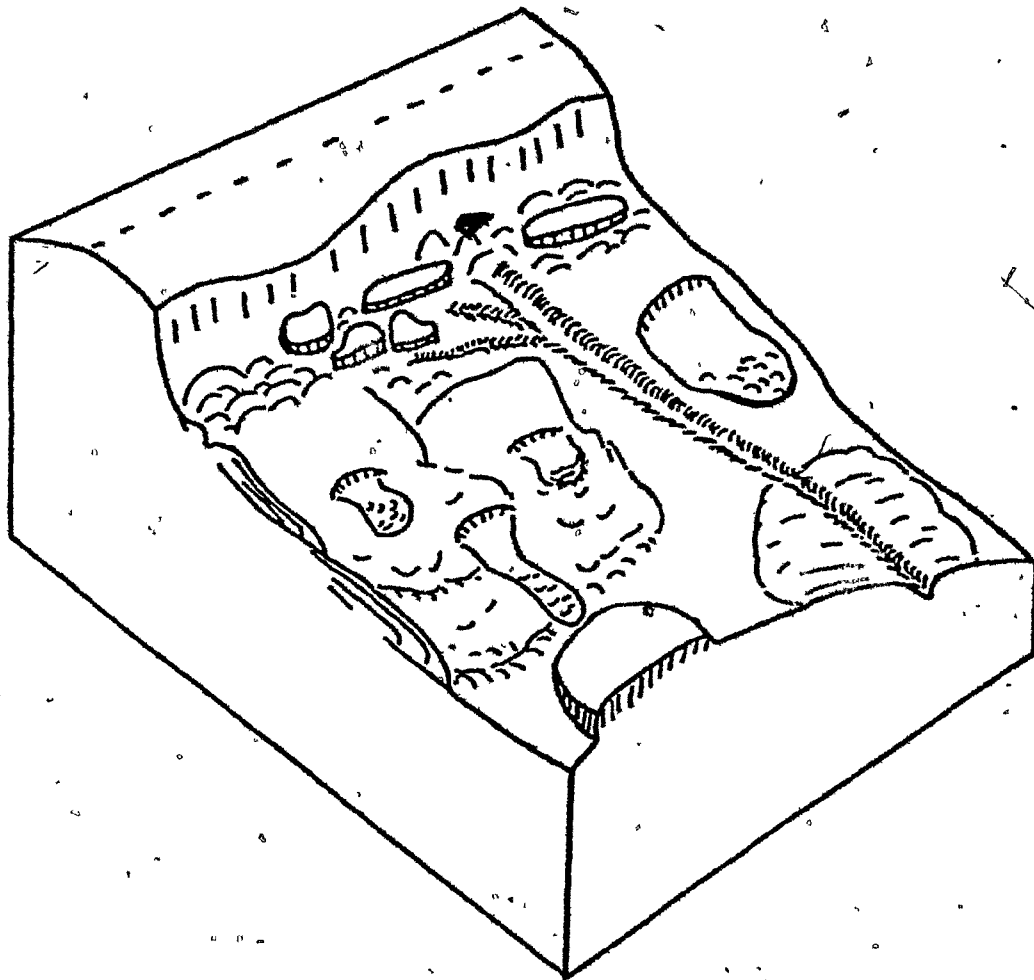


Figure 2-21. Schematic block diagram illustrating the main morphological features of the Scotian Gulf area. Vertical scale much exaggerated.

occurred on a range of scales below the steep escarpment located about 1 km below the shelfbreak. Individual slide blocks and slump-masses are irregular and variable in size. In one zone, just below the escarpment large, discrete blocks with considerable vertical relief ( $> 40$  metres) are identified. These contrast to the low relief, more tabular slide blocks in the mid-slope and lower slope areas.

Slump and slide-blocks control the meso-scale morphology. In cross-section, the surface of the slide-blocks are irregular. Some inter-block areas may have become active, continuous channels which supplied the main channel system in its upper reaches.

As the main-channel progresses downslope, its dimensions gradually decrease. This may be the result of the decrease in slope in the southeast corner of the area. There is strong evidence that the channel built a small depositional lobe in this area. This lobe may still be partly active, but the channel now crosses it and continues downslope.

#### THE WESTERN BANK AREA

The morphology of this area was not studied in great detail. The high resolution seismic profiles (Figs. 2-22 and 2-23) were run in 1978 using Decca Navigation. Figure 2-24 summarises the main morphological features of the area identified from these profiles.

The Western Bank area has a lower relief than most of the Scotian Gulf area, and the eastern part is characterised by a flat undisturbed bottom. To the west, a number of low-relief ( $> 20$  metre) erosion surfaces are apparent (Y-Y', Z-Z'). In cross-section (U-U'), these

Figure 2-22. (in back pocket). Line drawings of seismic profiles U-U', V-V', T-T' from Western Bank area. For locations, see Figure 2-3.

Figure 2-23. (in back pocket). Line drawings of seismic profiles W-W', X-X', Y-Y', Z-Z' from Western Bank area. For locations, see Figure 2-3.

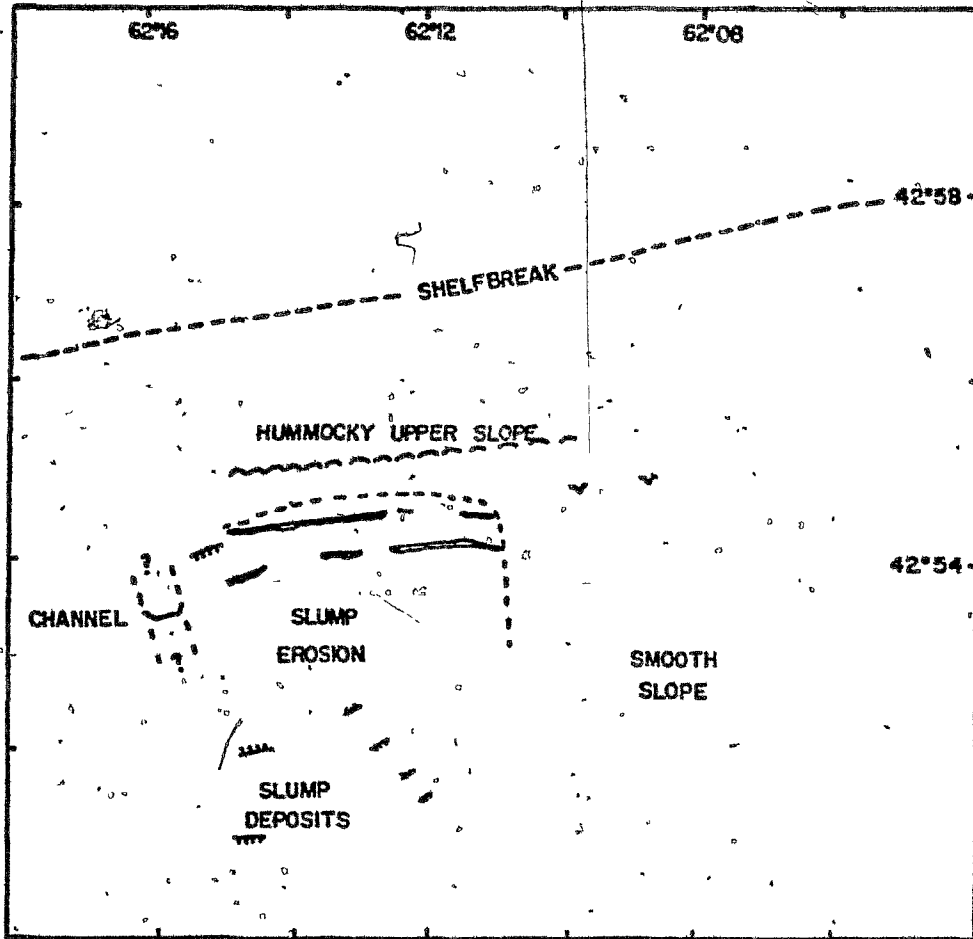


Figure 2-24. Sketch map of morphological features in the Western Bank area.

features have a distinct slump-scar morphology (=) and the slumped material (y) can be seen on the profiles further downslope (U-U', V-V'). No coherent slide-blocks are observed in any of the profiles. The upper slope shows a low, hummocky relief with low acoustic penetration. The hummocks are irregular and their origin is unknown.

In the west of the area, a 50-metre deep incised channel crosses profile Z-Z'. The up- or downslope continuation of the channel cannot be documented, but the dimensions of the channel suggest that it is probably a major feature. The channel-bottom is very flat (Z-Z'), and although the bottom return is strong, suggesting a coarse fill, flat sub-bottom reflectors are seen beneath it. The fill is probably no more than a thin lag layer overlying a near-surface erosion surface.

Unfortunately, not enough time was spent in the Western Bank area to allow more detailed interpretations. However, the survey does indicate that the Scotian Gulf area is not necessarily typical of the intercanyon areas of the Nova Scotian Slope. Areas of subdued and almost zero relief are also present.

## CHAPTER 3

CONTEMPORARY SEDIMENT DYNAMICS

Transport of sediment across the shelfbreak and on the slope is poorly understood on most continental margins. Qualitative models exist for slopewards transport of both fine-grained sediments (McCave 1972) and sand-sized material (Stanley et al., 1972), but there has been little success in developing quantitative models. Thus, it has been impossible to determine which of the many possible processes (eg. waves, currents, tides, internal waves; see review in Southard and Stanley, 1976) are important in this environment. This chapter attempts an analysis of quantitative hydrographic and textural data, to determine first order transport and depositional patterns and processes. The major aim was to decide if it is necessary to invoke catastrophic processes, such as turbidity currents generated at the shelfbreak, or catastrophic events, such as very large storms with geologically significant recurrence intervals, to explain the observed textures. Alternatively, are the textures consistent with transport by oceanographic events with a frequency of hours or months, which can be monitored by conventional current meters?

DATA

Since December 1975, a programme of continuous current monitoring has been in progress on the Nova Scotian shelf and slope by B. Petrie and P.C. Smith of the Bedford Institute of Oceanography. They have provided access to data covering the two year period, December-1975 to

January 1978. Current meter arrays were deployed at shelf, shelf-break and slope locations in the Scotian Gulf area (Fig. 3-1) with individual meters at near-surface, near-bottom and various intermediate positions (Lively, 1979). Temperature and conductivity (salinity) readings were taken concurrently and all data were averaged over one hourly periods. Only data from the bottom current meters are presented here as they pertain to bottom sediment movement. Basic mooring data for the three sites are shown in Table 3-1. The meters were deployed at approximately 20 metres above the seafloor, which in all cases was within the bottom mixed-layer (Table 3-1), as determined from CTD profiles.

Bottom sediment samples were taken with Van Veen and Shipek grabs from a ship located by Loran C and satellite navigation in the Scotian Gulf and Western Bank areas (Fig. 3-1). Below 500 metres water depth in both areas, gravity-core top samples were used. Recovery from the grab samples was variable. Samples containing substantial amounts of gravel were often relatively small in volume, indicating only shallow penetration. Very small samples and other samples where washout was suspected were rejected on a qualitative basis, so that only samples which could be reasonably assumed to be representative of the bottom surficial sediment were used in the subsequent analysis. Even so, statistically significant amounts of the gravel fraction were not obtained. Grain size analyses were conducted on the sand fraction using standard, calibrated sieves at  $1/4$  phi intervals, after wet sieving to remove silt and clay particles. The fine fractions of muddy samples were analysed by a pipette method.

Table 3-1. Mooring data for the three current meters used in the study. Thickness of bottom mixed-layers estimated from vertical salinity-temperature profiles only.

TABLE 3-1

STATION	LATITUDE	LONGITUDE	SOUNDING	INSTRUMENT DEPTH	THICKNESS OF BOTTOM MIXED-LAYER
81	42°48.0'N	63°30.0'W	250 M	230 M	60 M
83	42°45.0'N	63°30.0'W	710 M	690 M	250 M
86	43°00.0'N	63°30.0'W	170 M	150 M	30 M



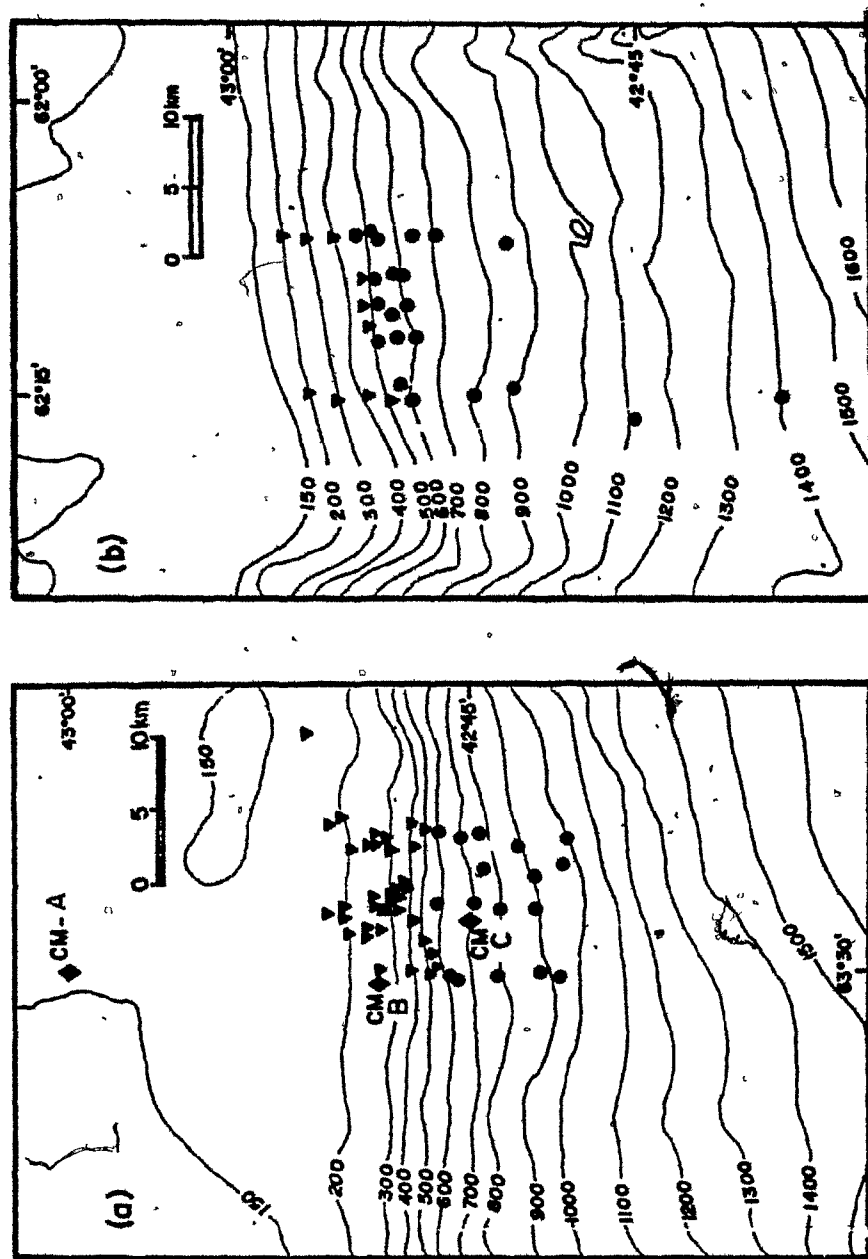


Figure 3-1. Location of surficial sediment samples (a) Scotian Gulf (b) Western Bank. Triangles: grab-samples; dots: gravity and piston-cores; CM: current meter. Bathymetry in metres.

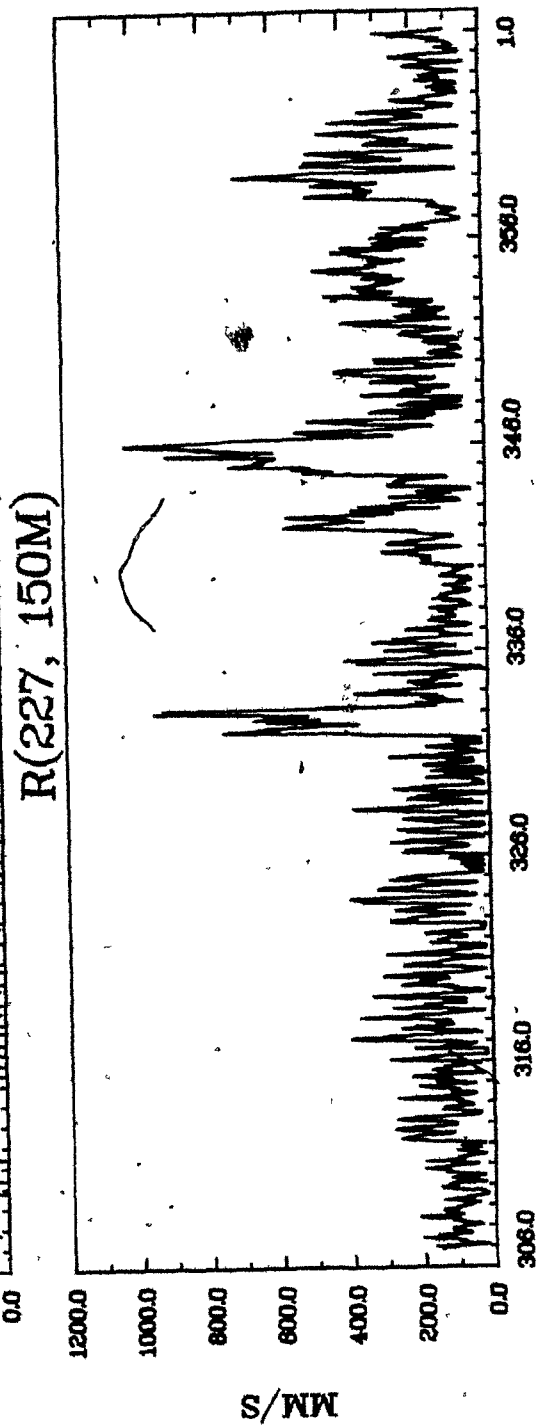
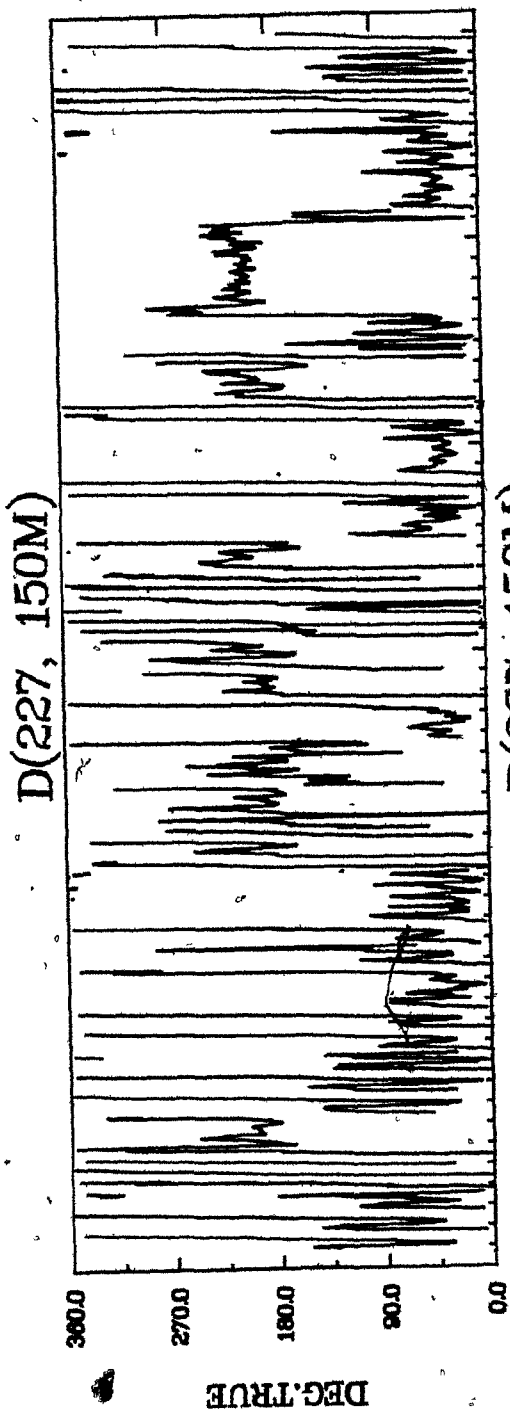
CURRENT METER OBSERVATIONS(a) Shelf.

The current meter located 20 metres above the bottom in 170 m water (CM-A in Fig. 3-1) shows a general eastward drift of bottom waters with a long period oscillation between northeastward and southerly daily motions. Petrie and Smith (1977) demonstrated that oscillations with a period of less than ten days correlate with wind stress variations measured on nearby Sable Island, and can be directly attributed to meteorological forcing. Longer period motions do not correlate with wind stress events; their origin is thought to be related to the propagation of topographic Rossby waves (Petrie and Smith, 1977; Louis et al., in press).

High current speeds are associated with wind forced events which occur predominantly in the winter months. Peak daily velocities reach values as high as  $60 \text{ cm s}^{-1}$  during the winter, but during summer, they rarely exceed  $30 \text{ cm s}^{-1}$  (Fig. 3-2). Some very large events appear on the record during the winters of 1976 and 1977 (Fig. 3-2) with current velocities exceeding  $100 \text{ cm s}^{-1}$  in a north to northeastward direction. The events are short-lived (generally 24 to 48 hours) but the high speed motions are maintained through at least 100 metres of water column. These motions do correlate with slightly higher wind stresses; the water at lower depths move onshore (northward) during westerly (eastwards) winds. They are probably the results of large-scale water-mass balancing imposed on the complex bathymetry of the Scotian Gulf area (B. Petrie, pers. comm.).

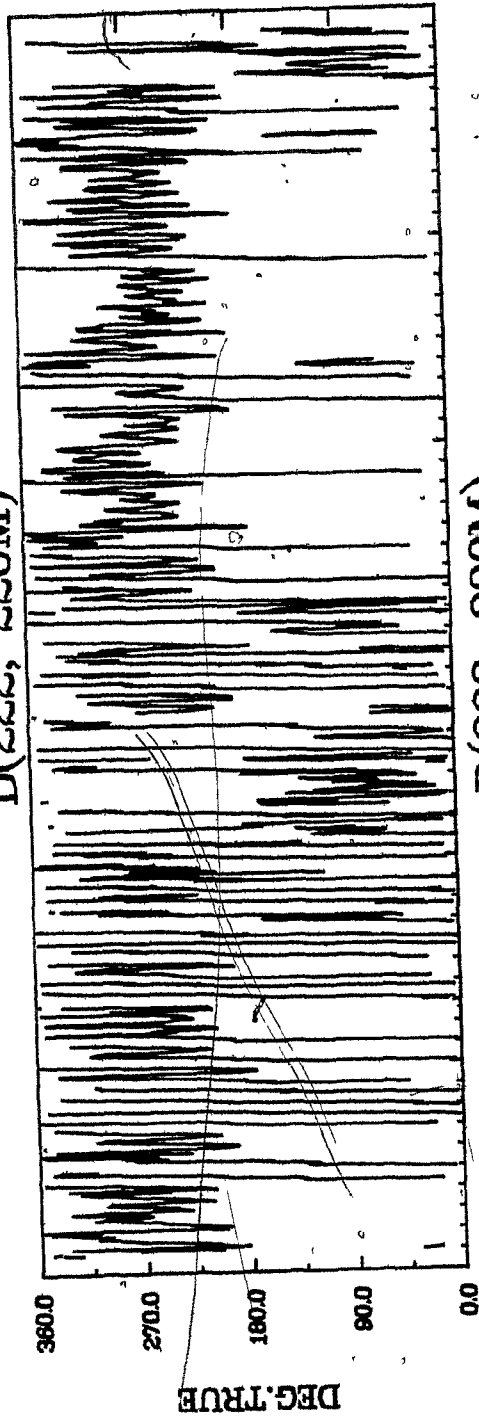
Figure 3-2. Current meter records for three stations shown in Figure 3-1(a). Readings were averaged at hourly intervals. (a) Shelf, (b) Shelfbreak, (c) Slope.

(a)

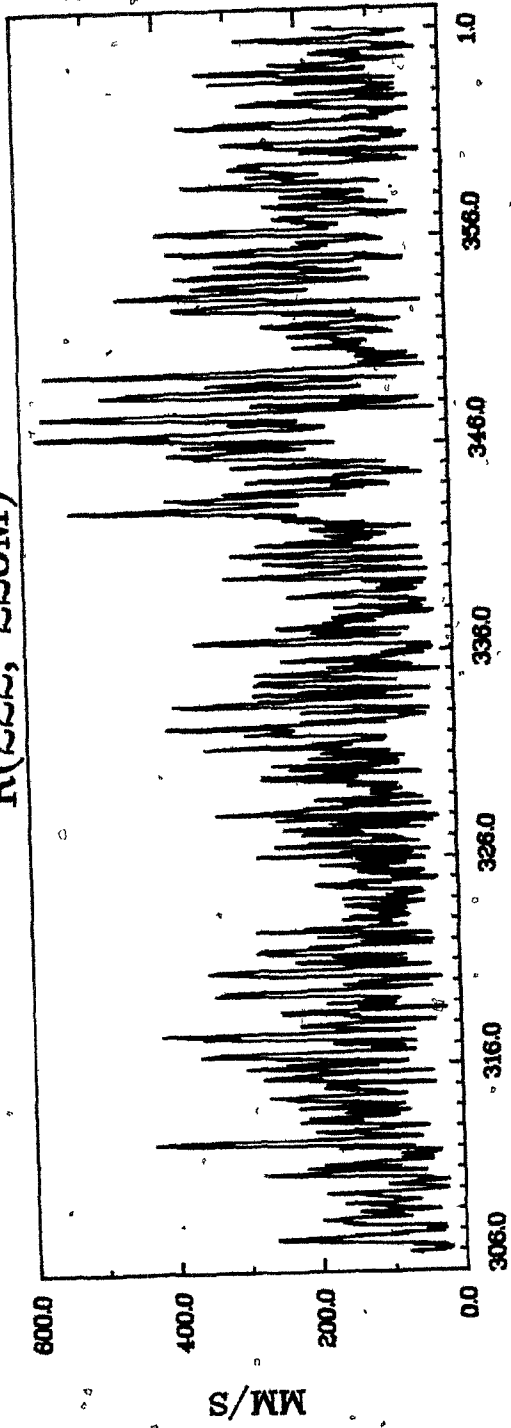


(b)

D(222, 220M)

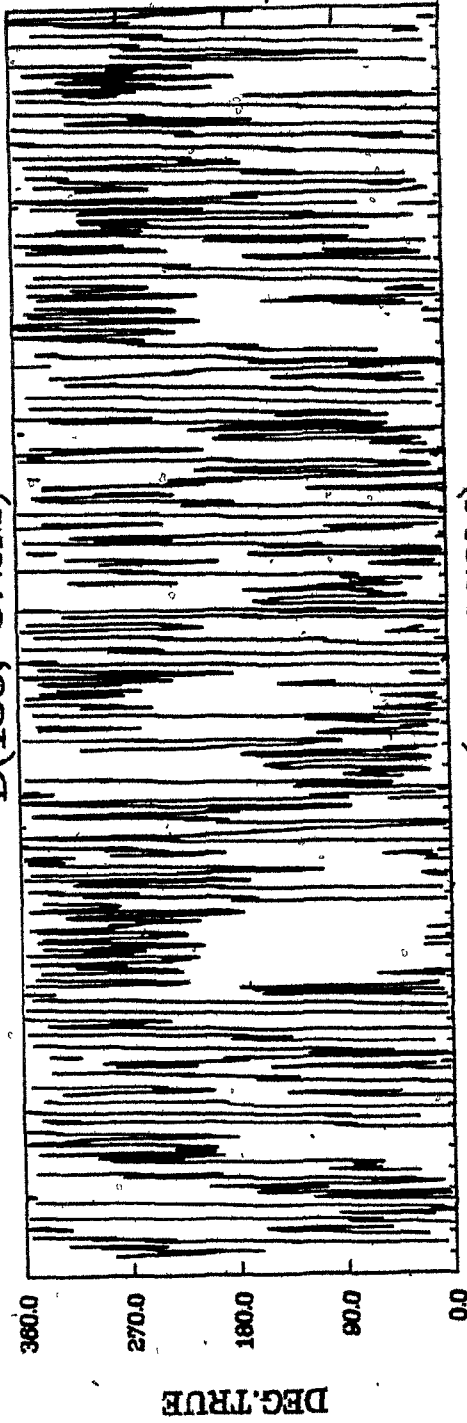


R(222, 220M)

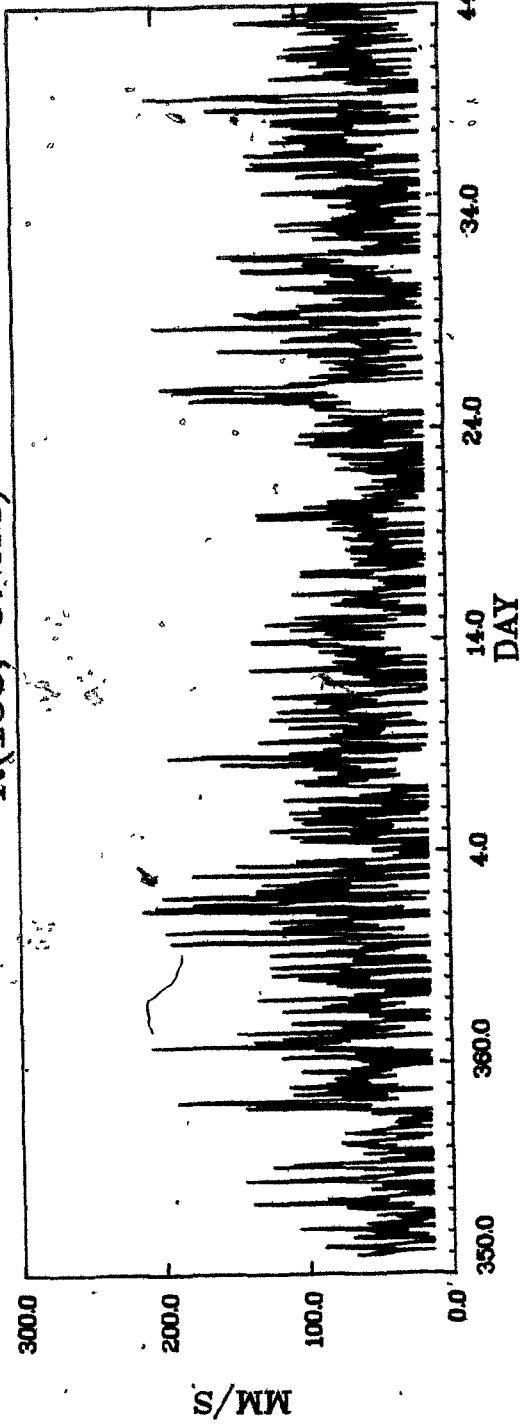


(c)

D(156, 672M)



R(156, 672M)



### (b) Shelfbreak and Slope

Motions at the shelfbreak (CM-B in Fig. 3-1) and on the slope (CM-C in Fig. 3-1) are dominated by strong currents parallel to the contours (Fig. 3-2). Long period reversals of the current are typical although net drift is to the west in the Scotian Gulf area as would be expected from the water mass distribution. Peak velocities of between 30 and 50  $\text{cm s}^{-1}$  are characteristic of these strong motions at the shelfbreak and 15 to 30  $\text{cm s}^{-1}$  on the slope at 700 metres water depth (Fig. 3-2). Superimposed on the current drift is the effect of the semi-diurnal (M2) tide. This causes most of the short period variability shown at all stations in Figure 3-2. During the long-period strong flows, the tide merely interferes to produce slight modulation of the current amplitude. When flow is minimal, the tide can dominate the water motions and current vectors follow an ellipsoidal pattern, similar to other tidally dominated seas (eg. North Sea, McCave, 1971). Current velocities during these periods are substantially lower, generally less than 20  $\text{cm s}^{-1}$  at both locations.

The very strong wind-forced motions, observed on the shelf, do not correlate with higher bottom-current velocities either at the shelfbreak or on the slope. However, strong near-surface currents flow to the south (offslope) at the shelfbreak during these events.

### GRAIN SIZE DISTRIBUTION

#### Methodology

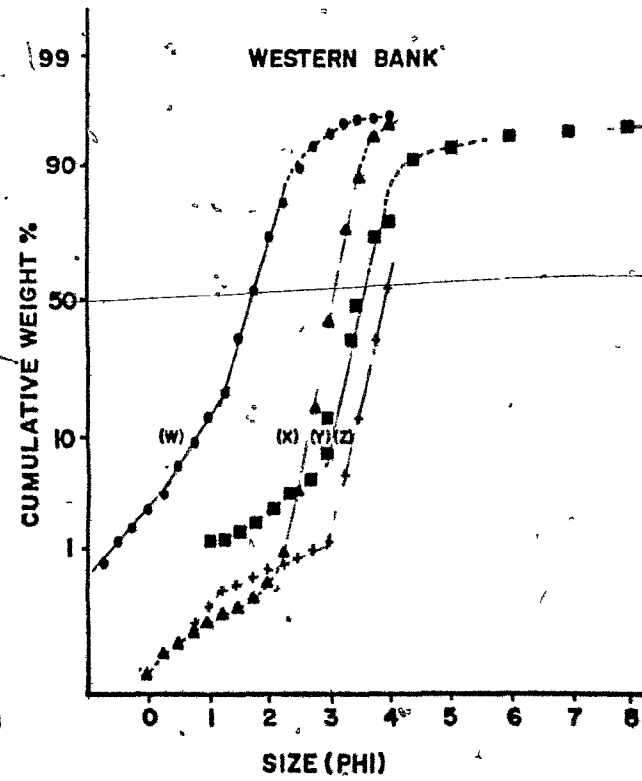
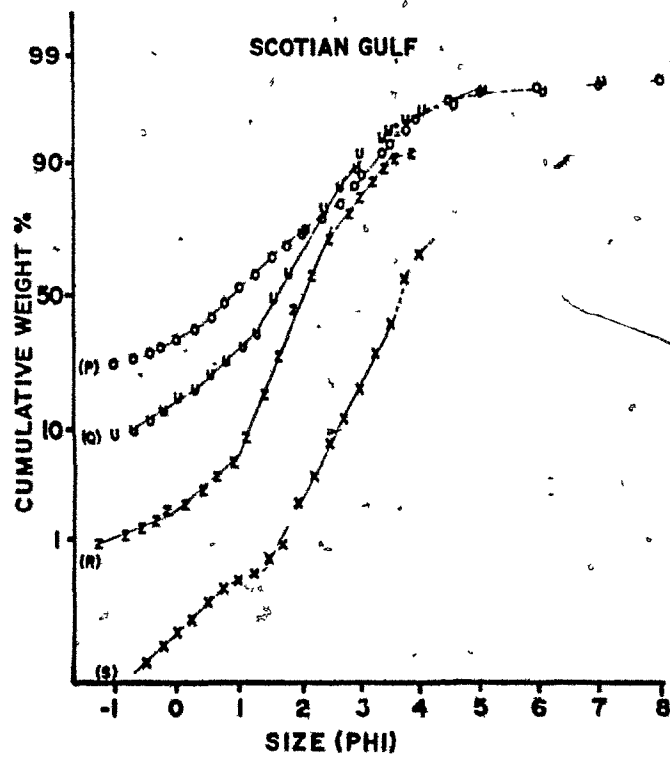
Various methods have been used to aid the interpretation of grain-

size distributions (Blatt et al., 1980, p. 43 ff). Most make the assumption that a size distribution closely approximates a Gaussian distribution when plotted on a logarithmic size scale. Several moment measures around the distribution have been used to measure deviation from the Gaussian model, to outline trends and to distinguish environments (Folk, 1966). Other workers have used probability graph paper to distinguish several lognormal sub-populations within a single sample (Visher, 1969; Middleton, 1976). Others again, however, have suggested that the distributions may be better described by combined logarithmic tails (Bagnold, 1937; Brandorff-Nielsen, 1977; Bagnold and Brandorff-Nielsen, 1980).

In the light of these differing opinions, great care is required when making quantitative comparisons between size distributions, as the parameters used may vary according to the assumptions made. The interpretations here are based on the following methods of analysis. The size distributions were first plotted on Gaussian probability paper as cumulative frequency curves (Fig. 3-3). Most curves consist of some straight line segments, suggesting approximation to Gaussian sub-populations. However, in the tail regions, significant deviations from the lognormal distribution are often observed, which suggests that the Gaussian assumption may not be valid for at least part of the distribution. This is no surprise as some depositional models do not predict Gaussian behaviour (eg. McCave and Swift 1976). Generally, the central regions show the best adherence to the Gaussian model.

Weight proportions for each size class were recalculated from the

Figure 3-3. Cumulative grain size distributions of selected samples from the N.S. Shelfbreak and Slope.



cumulative curves where the sieve calibration indicated intervals were non-standard. These values were used in graphical dissections of the curves following the method described by Dalrymple (1977). Reasonable fits could be obtained in the central regions (Fig. 3-4), but problems were encountered with many of the tails as expected from the probability plots. A second dissection method was therefore used. As the central subpopulation is almost always the best sorted and the most lognormal, it was extracted first, rather than start at the tails as in Dalrymple's method. The tails were subsequently replotted by simple subtraction from the lognormal models of the central subpopulation (Fig. 3-5).

The only assumptions of this second procedure, therefore, are the relative proportions of the subpopulations (the same proportions as the best-fit Gaussian dissections were used) and that the central subpopulation is near Gaussian. The straight-line plot of this subpopulation suggests that this is close to the truth, and when the subpopulation is very well sorted, the overlap with other populations is minimal. An advantage of this method is that it does not force a Gaussian model on either tail when there does not appear to be any justification for it in the probability plots. However, even forcing the Gaussian model onto the central part of the curve is probably partially in error. For one thing, there is no direct information on the nature of subpopulation overlap. Some of the odd shapes in the fine tail subpopulations (Fig. 3-5) may be artefacts of the method and suggest that the central subpopulation is in fact truncated at its fine end. The method is useful for indicating the tri-modality of the size

Figure 3-4. Size distribution of samples from the Scotian Gulf area, dissected according to the method of Dalrymple (1977), assuming Gaussian subpopulations. Broken lines indicate significant non-fit to Gaussian model.

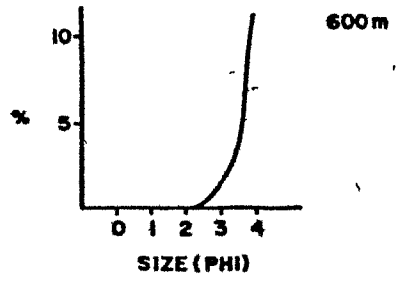
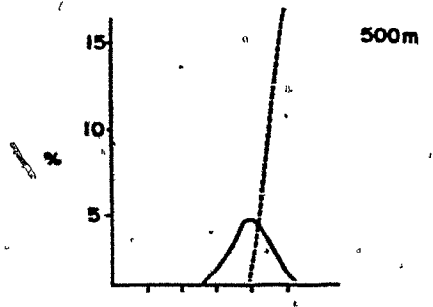
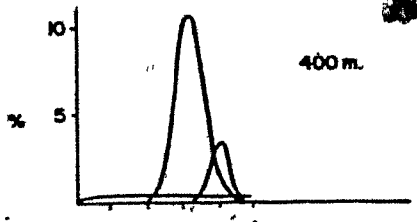
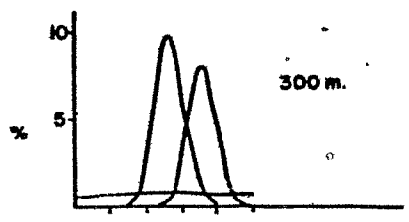
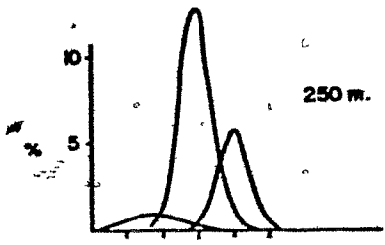
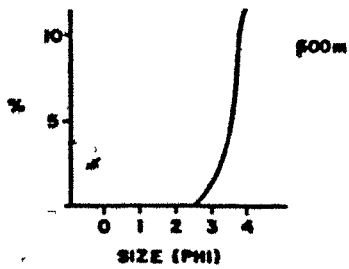
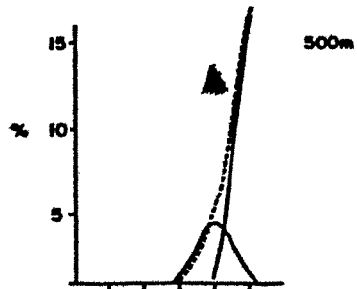
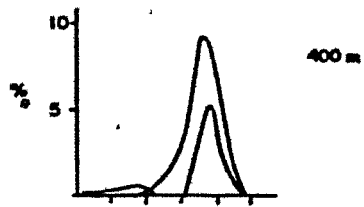
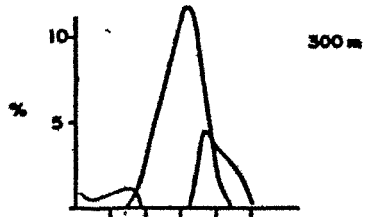
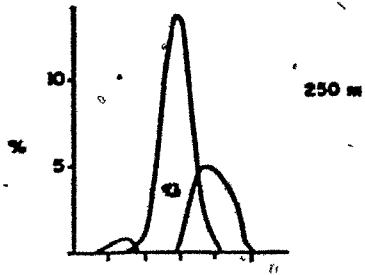


Figure 3-5. Size distributions of samples shown in Figure 3-4, dissected by removal of central subpopulation as explained in the text.



distributions using minimum assumptions, but the results should not be treated too literally.

### Interpretation of Size Distribution

Trimodality in sand samples from various environments has been recognised in several other studies (Visher, 1969; Möss, 1972; Middleton, 1976; Dalrymple, 1977) but agreement is not unanimous on the dynamic interpretation of the individual subpopulations. Perhaps the most widely accepted interpretation of trimodality is that of Middleton (1976), who felt that the subpopulations represented bedload (coarse tail), intermittent suspension (central subpopulation) and suspended load (fine tail). Essentially, our data support these contentions. The erosion and suspension criteria for sand size quartz particles have been well established experimentally (Fig. 3-6). At the Scotian Gulf shelfbreak (250 m) the central subpopulation has a distinct mode at close to 2 phi (Fig. 3-4). If this size was carried in suspension, a shear velocity would be capable of eroding and transporting, in bedload, particles a little larger than 0 phi, which is reasonably consistent with the size distribution of the coarse tail, although some coarser clasts are present and the gravel fraction is statistically unrepresentative.

A shear velocity of  $2.6 \text{ cm s}^{-1}$  is close to the values obtained directly from current meter velocities during maximum conditions, when a reasonable drag coefficient ( $C_D = 0.003$ ) is assumed (Table 3-2). Using the coarse tail of the central subpopulation to give a shear velocity estimate as suggested by Middleton (1976), requires higher values in the order of  $5.5 \text{ cm s}^{-1}$ . However, such a method is prone to considerable

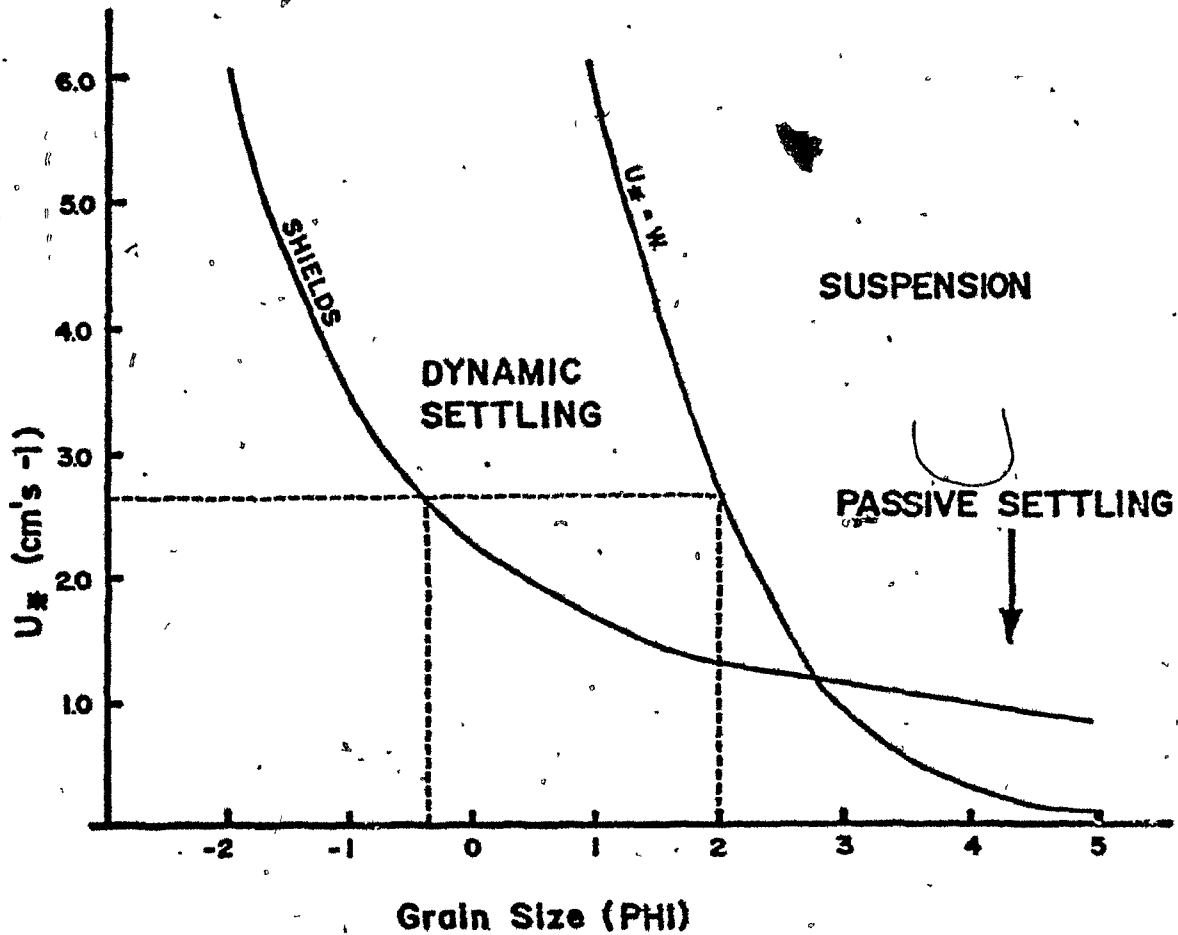


Figure 3-6. Criteria for initial movement (Shields) and suspension ( $U_* = w$ ) of quartz grains in water at  $20^\circ\text{C}$ , plotted on phi size scale, after Blatt et al. (1980), p. 103. Dynamic settling applies to grains coarser than approximately  $3\phi$  (where the two lines intersect), which must pass through a bedload transport phase before final deposition. Finer grains undergo passive settling, directly onto the bed, with no bedload phase.

Table 3-2. Estimates of shear velocity ( $u$ ) from observed currents and grain size distributions at the shelf break and slope. Current estimates: " $u_*(\text{max})$ " = from maximum observed currents; " $u_*(\text{Av. Max.})$ " = from estimated average of daily maxima. Grain size estimates: " $u_* = w(\text{mode})$ " = shear velocity obtained using suspension criteria (Figure 3-6) and the modal size of the central well-sorted population; " $U_*(a)$ " = shear velocity from Shields criterion (Figure 3-6) using maximum clast size (at 1% probability level).

TABLE 2-2

WATER DEPTH (Metres)	CURRENT ESTIMATES		GRAIN SIZE ESTIMATES	
	$u_*$ (Max)	$u_*$ (Av. Max)	$u_* = w$ (Mode)	Shields $u_*$ (a)
<u>Scotian Gulf</u>				
250	2.7	1.3	2.6	2.7
300	-	-	2.4	2.7
400	-	-	1.5	2.2
500	-	-	1.2	1.4
600	-	-	<1.0	1.2
700	1.6	0.7	<1.0	1.0
<u>Western Bank</u>				
200	-	-	3.2	3.0
300	-	-	1.1	1.3

error (Middleton, 1976; Dalrymple, 1977) being especially sensitive to the amount of subpopulation overlap and the assumed population proportions, not to mention the assumption of lognormal subpopulations. Furthermore, it seems more appropriate to use the mode of the subpopulation rather than the tail as it is a relatively well determined point whichever method is used.

The fine subpopulations appear to be strongly asymmetric (Fig. 3-5) as predicted by the McCave and Swift (1976) model. The tails fine from an apparent mode of between 2.5 and 3.0 phi in every sample above 500 metres water depth. This consistent value corresponds very closely to the size of particle that moves directly into suspension when eroded (Fig. 3-6) without a bedload stage, which suggests a depositional mechanism for the evolution of the separate subpopulations, from an original population moving as suspended load. Particles dropping out of suspension, with size greater than 2.75 phi, must pass through a phase of bedload transport before final deposition, whereas smaller sizes will settle almost passively, directly onto the bed. This can have two effects: (a) rates of transport decrease markedly in the bedload phase, (b) winnowing may sort size classes in the bedload. One or both of these effects may cause the apparent evolution of two subpopulations during the depositional stage of sediment transport. The decreased transport rate means that over any unit transport distance, bedload material becomes more concentrated as the suspended fines are more rapidly transported away. Over a longer period, winnowing of the fines deposited along with the bedload, would improve the sorting of the coarser population, making it more distinct from the fine population.

This interpretation of the fine tail subpopulation is supported by the downslope trends shown by the central populations. The central mode fines in a downslope direction until about 500 m water depth (Fig. 3-5). Below this depth only the fine tail subpopulation is significant. The undissected curve of the 500 m sample still shows a distinctive kink at 3  $\phi$ , where, as in coarser samples, passive settling takes over from "dynamic" settling. By 700 metres water depth, the mode is in the silt range, which suggests shear velocities of less than 1.0 cm s<sup>-1</sup>. This is compatible with observed current velocities at that depth (Table 3-2).

Samples from the Western Bank slope show a similar pattern (Fig. 3-7) with two main differences: (a) the subpopulations appear to be better sorted, and (b) the central subpopulation fines to 2.75 phi at a shallower depth (200 to 300 metres). The former may represent a difference in source material. King's (1970) map indicates that sand on Western Bank is better sorted than sand in the Scotian Gulf.

#### SEDIMENT TRANSPORT PATHS

##### Sources

Distinct downslope trends in the two coarsest populations (Figs. 3-5 and 3-7) suggest that coarse sand and gravel is derived quite locally from the outer shelf. In the Scotian Gulf, sediment textures are variable, poorly sorted and contain large gravel fractions (Fig. 3-8). Some textures appear to be only slightly modified from a very poorly sorted source material. One sample taken in this area contained a few gravel

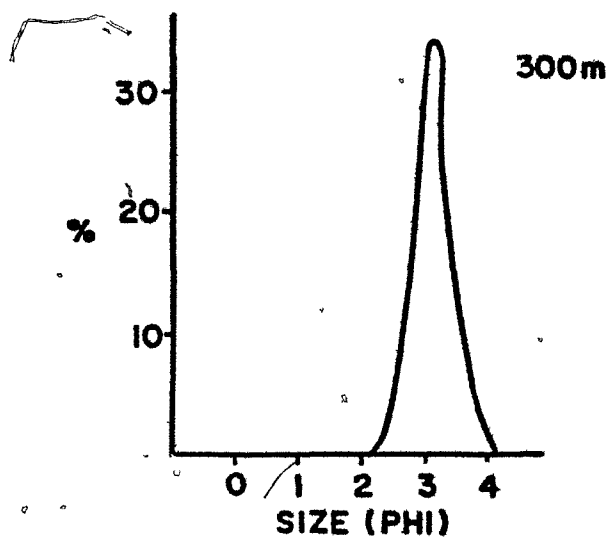
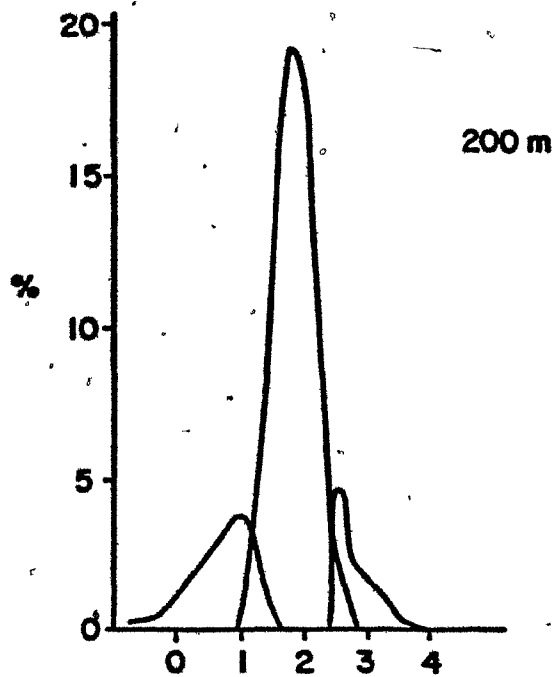


Figure 3-7. Size distributions of samples from the Western Bank area, dissected by removal of central subpopulations as explained in the text.

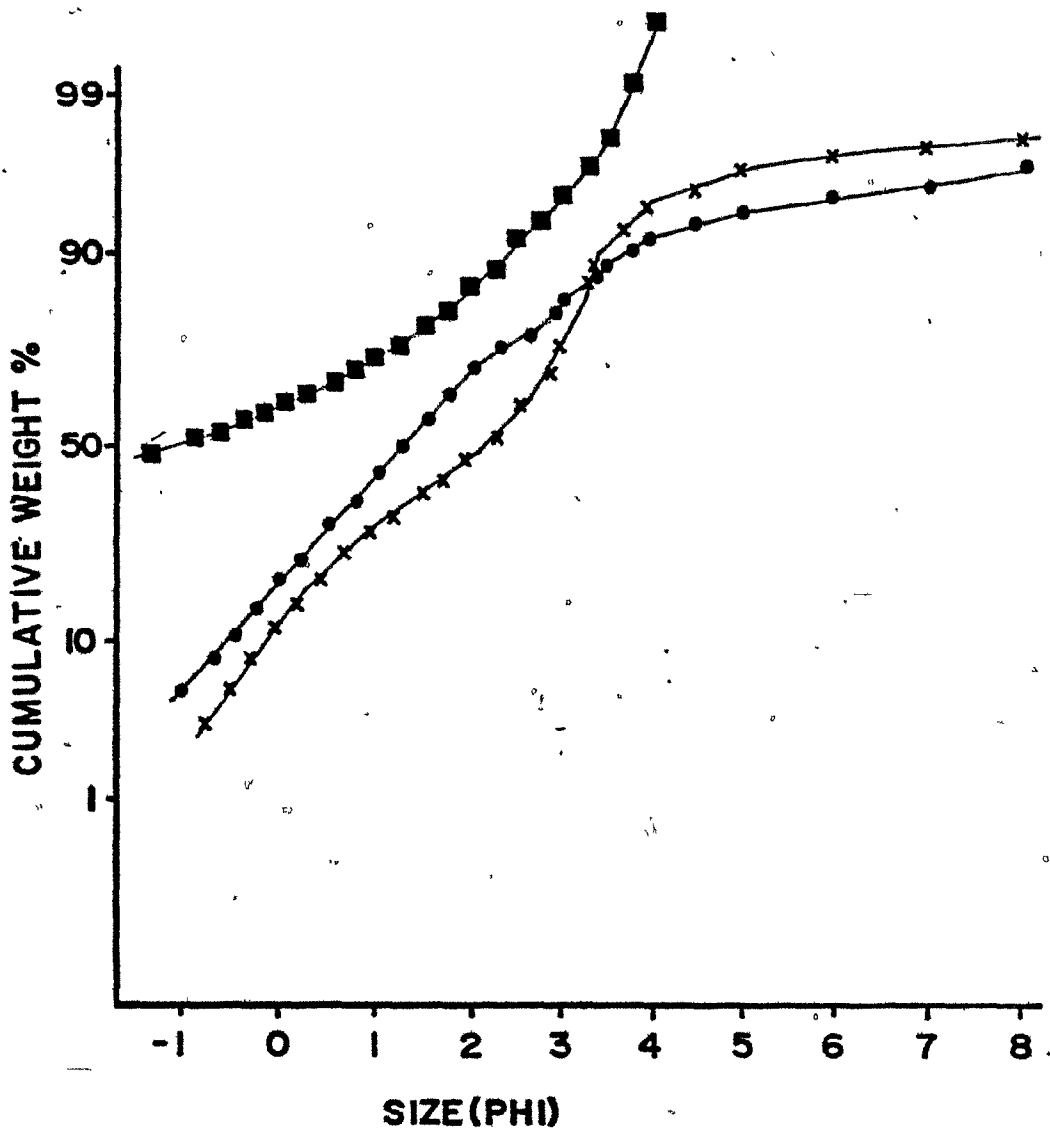


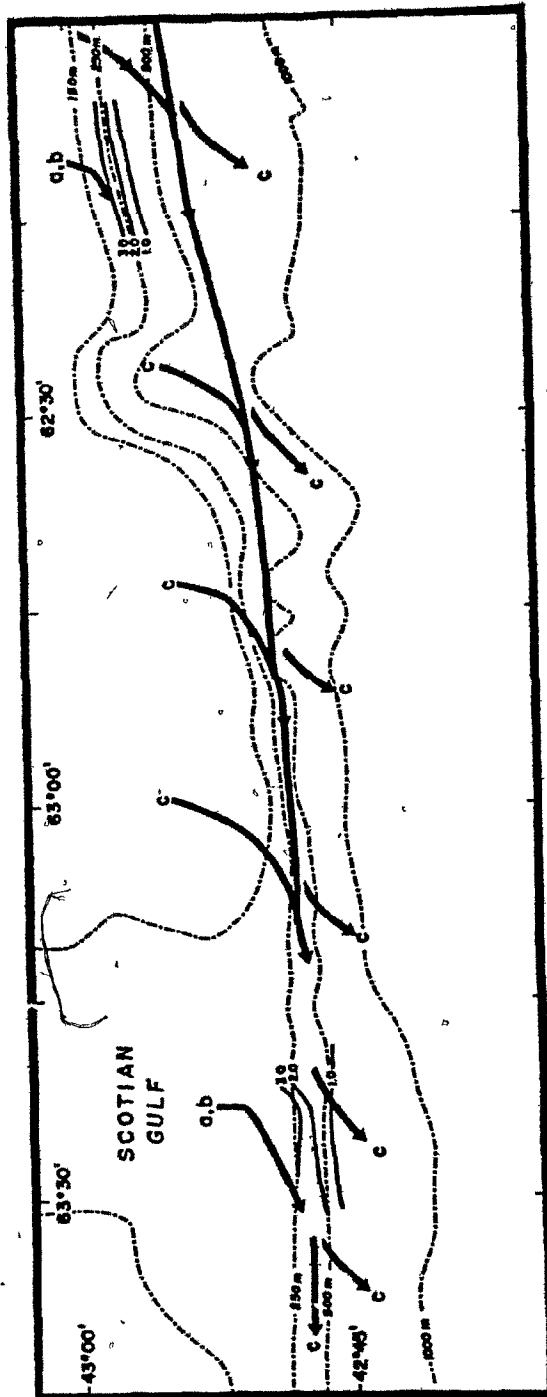
Figure 3-8. Cumulative grain-size distributions of three typical samples from the Scotian Gulf shelf. Note the variability and poorly-sorted nature of the sediments.

clasts in the grab jaws with stiff sandy, gravelly mud plastered on the outside of the sampler (personal observation). These textural properties and the hummocky nature of the sea bottom in the area suggest that glacial till is present in the Scotian Gulf. In places, it is very close to the sediment surface and probably covered with a thin gravel lag. The large bottom current velocities observed in the Scotian Gulf (up to  $100 \text{ cm s}^{-1}$ ) would be capable of erosion of the till, even with the protective gravel lag. However, these high velocities are always directed onto the shelf and probably result in transport of sediment into adjacent Emerald Basin rather than onto the slope. The currents may, however, expose and erode large areas of till and partially sorted sand near the shelf edge, which may eventually supply the slope.

Conditions on Western Bank are not well known. Most of the bottom is sandy (King, 1970) and relatively well sorted. Parts of the bank may be relict (King, 1970, 1979), but sand waves and ripples have been documented on other areas close-by (Stanley et al., 1972; King, 1970) indicating active sediment transport on some areas of the banks.

It is likely that the coarser sand is supplied to the slope from relatively local sources on the shelf (Fig. 3-9). Transport probably occurs across the shelfbreak only during the more severe conditions of strong flow (Fig. 3-2). Fine sand, on the other hand, is probably transported for a much larger proportion of the time, requiring relatively low shear velocities (Fig. 3-6). Thus, sources of fine sand are potentially much less local. Heavy mineral abundances in fine sands

Figure 3-9. Map of part of the Nova Scotian margin showing  $u_*$  contours derived from sediment texture in the two study areas, and schematic illustration of sediment transport routes. a = coarse tail subpopulation (bedload); b = central subpopulation ("intermittent" suspension); c = fine tail subpopulation ("continuous" suspension).



suggest a shelf source (Hill, 1979) but cannot be used more exactly due to the complex heavy mineral pattern on the Scotian Shelf (James, 1966). Fine sand and mud is probably supplied to the slope along the whole length of the Nova Scotian outer shelf (Fig. 3-9).

#### Transport and Deposition

The textural data suggests that sand transport is dominantly in suspension. However, the detailed interpretation of the separate subpopulations suggests that different rates of net transport apply to each subpopulation. From the current data (Fig. 3-2) and shear velocity calculations (Table 3-2), it can be seen that suspended transport of medium sand-sized material can occur only during short periods of high flow. As a result, medium sand transport is directed essentially along isobaths with the strong flows. The current direction during these periods are presumably variable over the short-term and would result in some net transport of sediment obliquely downslope. Deposition of the sand would be temporary in upslope areas where the current maxima consistently exceed the suspension criterion. For any particular grain-size, deposition would be greatest at the point where  $u_* = w$  (suspension criterion, Fig. 3-7), and less efficient bedload transport takes over from suspended transport as the primary transport mechanism so that the transport rate for that grain size is suddenly reduced. Thus, modal sizes should give a good indication of the local maximum shear velocity (Fig. 3-9).

The finer sediment, which essentially makes up the fine tail subpopulation, is suspended at lower velocities, and, consequently, transport is much more continuous and efficient. Fine sediment

transport would follow the mean flow direction more closely. This is variable over long periods and sediment dispersal is essentially both alongslope and downslope. Long-term averages of hourly current vectors (Table 3-3) suggest that there is a distinct downslope component to the average drift at the shelfbreak. Diffusive and density processes may also contribute significantly to the downslope transport. Settling of fines may occur ubiquitously during quiet periods, but can only be permanent at a point downslope where the environment is sufficiently quiet to allow accumulation of sediment.

#### Effects of Topographic Rossby Waves on the Slope

The correlation between texturally derived and current derived shear velocities is reasonable and suggests that the textural pattern is a response to the normal current regime in the Scotian Gulf area. The lack of current data makes it impossible to say whether exactly the same processes are important in the Western Bank area. In fact, there are interesting differences between the two areas. Figure 3-9 shows the position of shear velocity contours as derived from sediment textural data in the two areas. Contours of the same value are found at relatively shallower depth and the shear velocity gradient seems to be higher in the Western Bank area. Although the shelfbreak off Western Bank is also shallower, these are still unexpected results.

Recent data allow speculation on the problem. According to Louis et al. (in press), the Scotian Gulf regularly experiences the effects of Gulf Stream eddies. Most seem to form at around longitude 65°W and impinge locally on the slope. As a result, topographic Rossby waves are

Table 3-3. Long term averages of hourly current vectors, indicating net drift directions as average vectors (from Lively, 1979).

TABLE 3-3

STATION	DEPTH	NO. OF HOURLY SAMPLES	U (+ve. to E) cm s <sup>-1</sup> MEAN	STAND. DEV.	V (+ve to N) cm s <sup>-1</sup> MEAN	STAND. DEV.
8	230 M	4479	-2.7	12.4	-1.2	10.8
	230 M	9232	-2.7	13.7	-1.7	10.9
83	690 M	6283	-1.0	5.0	2	5.6

formed on the slope which have an average period of about 20 days and an amplitude in velocity terms of about  $10 \text{ cm s}^{-1}$ . The current meters at the shelfbreak and slope of the Scotian Gulf show the effects of these waves for approximately 65% of the total 1.5 years of record examined (B. Petrie, pers. comm.). Simple calculations (subtraction of  $10 \text{ cm s}^{-1}$  from current velocities in the Scotian Gulf) suggest that the shear velocity pattern would be very similar in the two areas if the topographic wave effect were removed. The Western Bank area is much further away from the map area of eddy generation so that the topographic wave effect would be considerably less important here.

This demonstrates that these results are only locally specific; however, the methods used would be usefully employed in other areas. More complex studies could be attempted if detailed information on bottom boundary layer dynamics and bedforms can be obtained. Sampling remains, however, a major problem, despite the fact that considerable efforts were made to use only representative samples. Not only are the samples often small and possibly non-representative of the areal distribution of sediment, but it is not known how much of the vertical sediment column is being sampled, or when that material was deposited. The sample could represent yesterday's event or an average of the last hundred years of events.

#### Deposition of Muds below 600 metres Depth

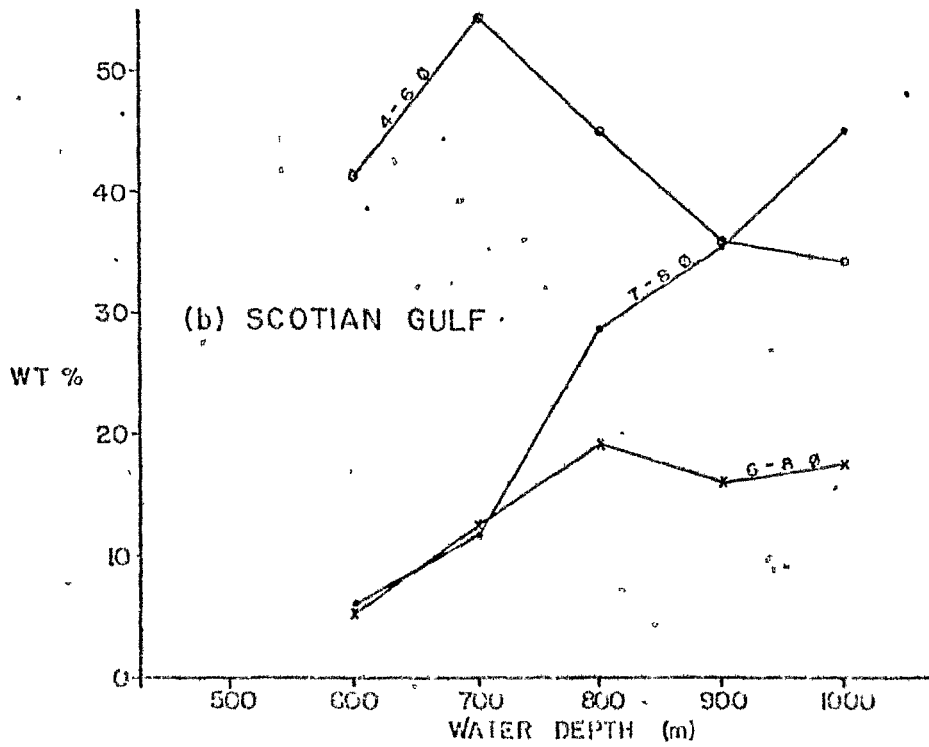
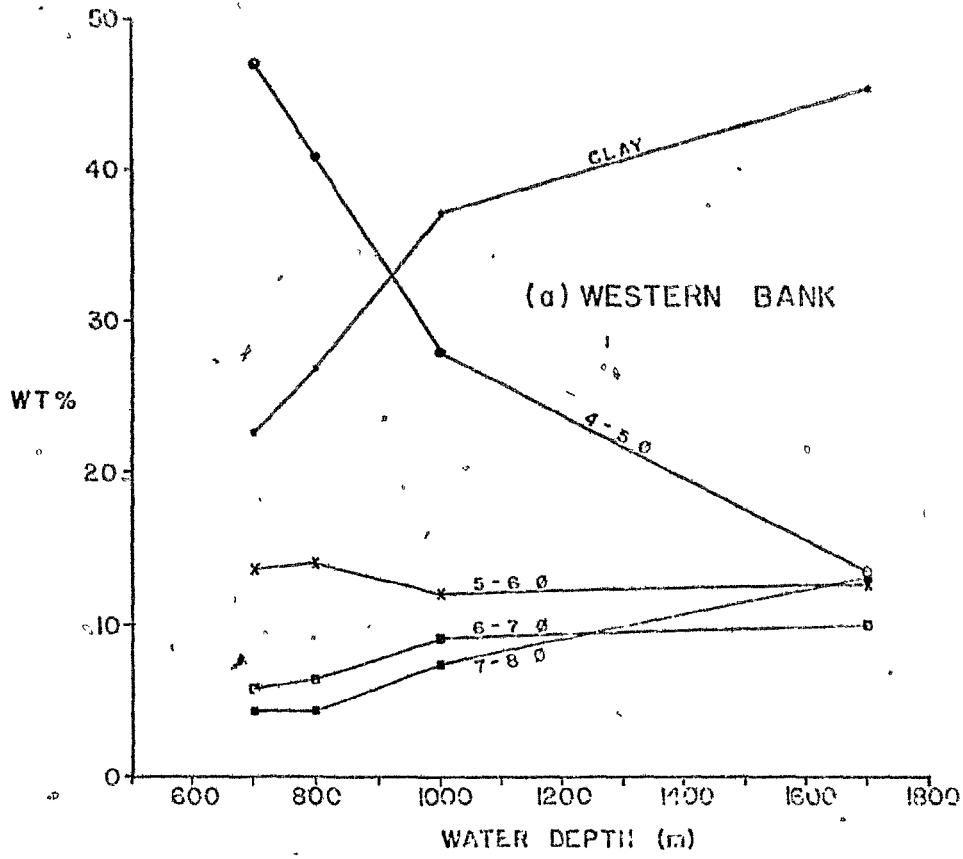
Most particles of silt and clay size eventually leave the energetic upper slope system and are deposited somewhere further downslope.

Exactly where depends on three important factors: (i) the dynamic conditions at the sediment/water interface and in the bottom boundary layer, (ii) the settling velocity of the particle, (iii) the flocculation state of the particle in the water column.

Maximum velocities decrease downslope, averaging  $10\text{-}15 \text{ cm s}^{-1}$  at 1000 metres depth and less than  $10 \text{ cm s}^{-1}$  at 1500 metres (Lively, 1979). With a drag coefficient of 0.003, a current speed of  $10 \text{ cm s}^{-1}$  should maintain particles finer than  $6 \phi$  in suspension (McCave and Swift, 1976), while coarser particles will be deposited. Size analyses, however, indicate that particles finer than  $6 \phi$  make up a substantial proportion of the total sediment at depths much shallower than 1000 metres (Figs. 3-10). In particular, the clay content increases rapidly with depth beyond 600 metres. This can be simply explained by particle flocculation. Small particles, particularly clay minerals, will form flocs with higher settling velocities which can thus settle and deposit under more energetic conditions.

McCave and Swift (1976) calculated rates of deposition for various particle sizes settling from a dilute suspension. They considered both the case of constant concentration (continuous replenishment of the bottom layer) and that of an initial concentration that moves away from the generating area without replenishment. They suggest that the latter may be applicable to shelf-edge suspension and slope deposition. The calculations show that for a bottom boundary layer thickness of 100 metres, the mean residence time of coarse silt ( $4\text{-}5 \phi$ ) particles

Figure 3-10. Proportions of various size intervals plotted against water depth for (a) the Western Bank area (b) the Scotian Gulf area. Note different horizontal scales.



is in the order of 20 days, even at very low current velocities.

This is important for two reasons. First, the dominant periods of velocity fluctuations at 1000 m are much lower than 20 days, although major changes in mean flow direction may occur at periods of 10 days or so (Petrie and Smith, 1977). Settling from a single suspension event can therefore never continue undisturbed. The process must occur in phases of resuspension and partial settling. Secondly, a suspended particle can be transported large distances even after it has reached a site of sufficiently low energy.

This last point explains why the proportion of particles larger than 6  $\phi$  drops off so gradually below 1000 metres (Fig. 3-10). At 1700 metres depth, the bottom sediment still contains 14 % particles of the 4-5  $\phi$  size range (although slightly less than 50% of this fraction is of biogenic origin). If the bottom shear stress was the only control on deposition, the size ranges should show more distinct bathymetric zones. However, McCave and Swift's (1976) model is based on supply to and concentration in the viscous sublayer. The settling properties of the particles thus play a major role in the overall depositional patterns.

Mud deposition on the slope is thus a complex problem. Predictive models based on McCave and Swift theory would be possible if the detailed structure of the bottom boundary layer could be modelled (in both space and time). Advances in our understanding of flocculation might also be incorporated into the model. Relationships have been discovered relating the natural and inorganic modal sizes with degree of flocculation and the modal size of the flocculation. (Kranck, 1975).

This would require detailed suspended sediment sampling from the bottom boundary layer.

Recent submersible dives on the Scotian Slope indicate ubiquitous biological activity at the sediment-water interface, including frequent signs of active resuspension of sediment by fish and mobile benthos. Not only this, but large burrow and mound structures are common and create a bottom roughness with tens of centimetres relief. On the larger scale of textural patterns, these effects are probably not significant. However, in terms of the dynamics of sediment deposition, the effects of high near-bottom concentrations of suspended sediment and increased bottom roughness may be much more significant. McCave and Swift's (1976) theory, for example, is based on low concentrations of suspended material in a thin viscous sub-layer. Extrapolation to high concentrations over a rough bottom would be very dangerous.

## CHAPTER 4

STRATIGRAPHY

Preliminary stratigraphic interpretations were made on Nova Scotian slope cores by Silverberg (1965) and Stanley et al. (1972). This chapter aims to expand these studies and include chronostratigraphic information in the form of radiocarbon dating. In accordance with the International Stratigraphic Guide (Hedberg, 1976), a type core (11) is designated for litho- and biostratigraphic purposes (Fig. 4-1). The chronologic control is given by radiocarbon dates from a number of cores, including the type core. No formal units are defined here.

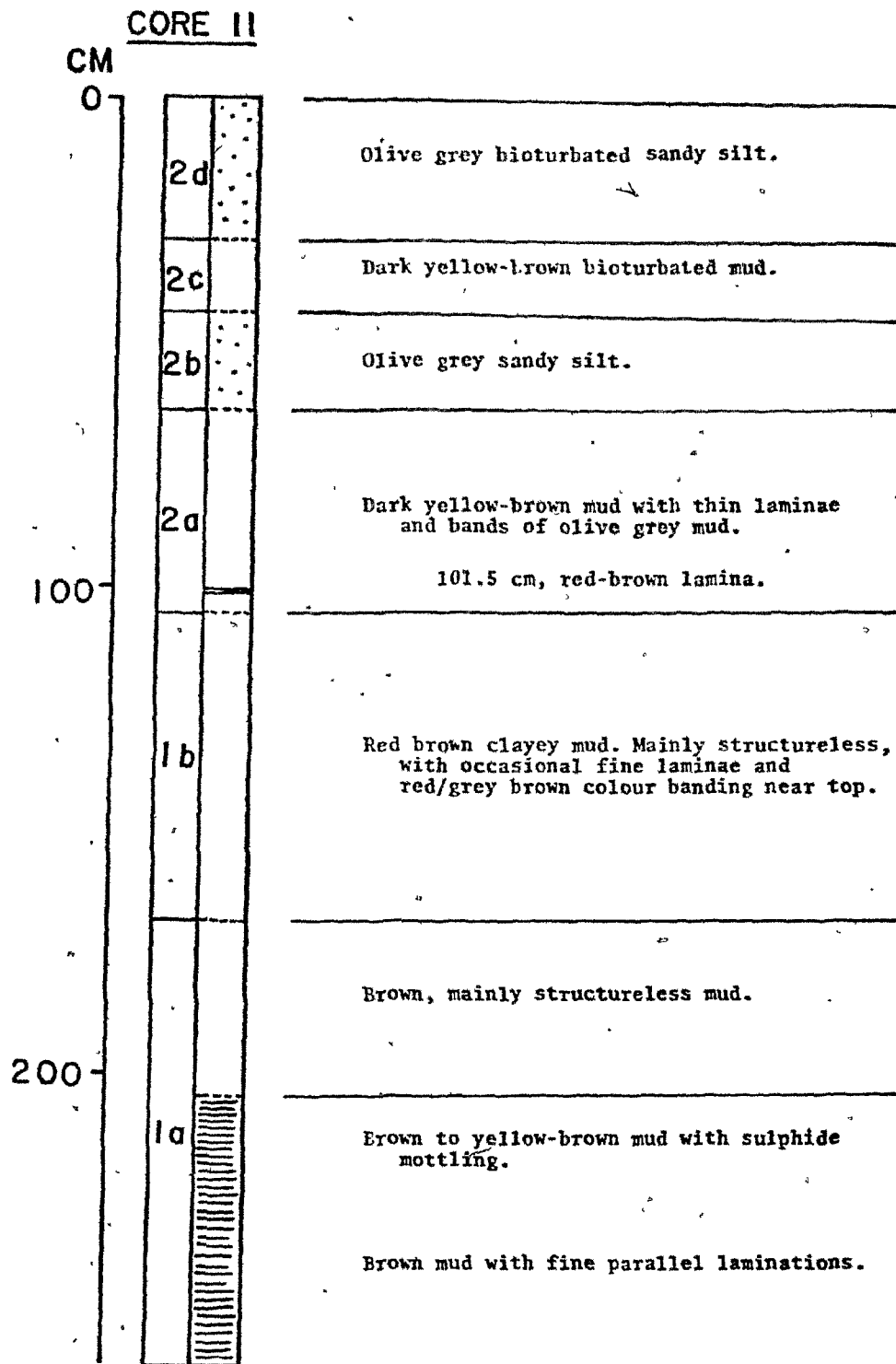
LITHOSTRATIGRAPHY

Core sequences can be divided into two distinctive units:

- 2) An upper, olive-grey and dark yellow-brown mottled mud sequence
- 1) A lower red-brown to brown mud with associated silt, sand and gravel beds.

These units can be traced along the length of the continental slope from the Scotian Gulf area of this study to Sable Island Bank (Fig. 1-3). The cores described by Silverberg (1965) from the latter area appears to show the two units, although they were not divided as such by him.

Figure 4-1. Type stratigraphic core (11) from the Western Bank area.



## UNIT 1

The dominant, distinguishing lithology of Unit 1 is red-brown to brown mud. Coarser beds are a common component, but these are very locally developed and cannot be correlated between cores.

The two end-member mud lithologies (red-brown mud and brown mud) often alternate. The red-brown mud appears to dominate at the top of the unit in most cores but it is completely absent from many cores in the Scotian Gulf area. Unit 1 is tentatively divided into two sub-units (Fig. 4-1):

(b) Upper dominantly red-brown mud sub-unit

(a) Lower dominantly brown mud sub-unit.

The boundary between the two sub-units is transitional but is arbitrarily taken as where red-brown mud first appears.

The apparent unit thickness is variable from core to core (Fig. 4-2) and the base is rarely penetrated. In core 66, the base is defined by a distinct erosion surface underlain by stiff, buff-coloured mud, but it is very doubtful that the whole sequence of Unit 1 is present in this core. Variability within the unit is considerable (eg. Fig. 4-2). Coarser beds are more abundant in the excavated Scotian Gulf area than on undisturbed parts of the slope, where continuous mud sequences predominate.

## UNIT 2

This unit consists of alternating intervals of olive-grey mud

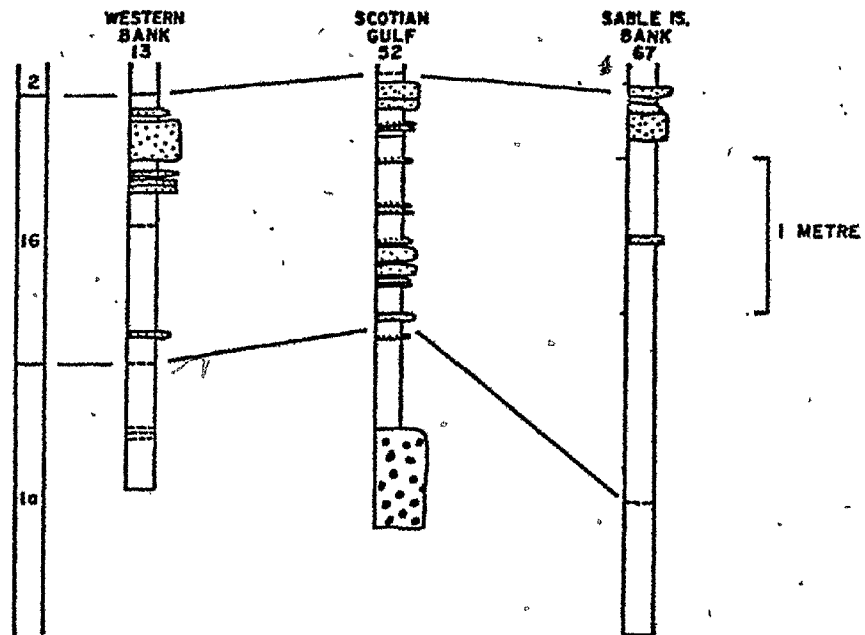


Figure 4-2. Variation in Unit 1 sequence along the Nova Scotian continental slope. See Figures 5-1 and 6-1 for key.

(subordinate sands) and dark yellow-brown mottled muds. The base is defined as the first occurrence of the characteristic dark yellow-brown mottled mud lithology. Bioturbation is pervasive throughout the unit except in a few coarser-grained beds where laminae are preserved. The unit can be divided into four sub-units:

- (d) Olive-grey sand and mud
- (c) (Thin) yellowish-brown mottled mud
- (b) (Thin) olive grey silt or mud
- (a) (Thick) yellowish-brown mottled mud

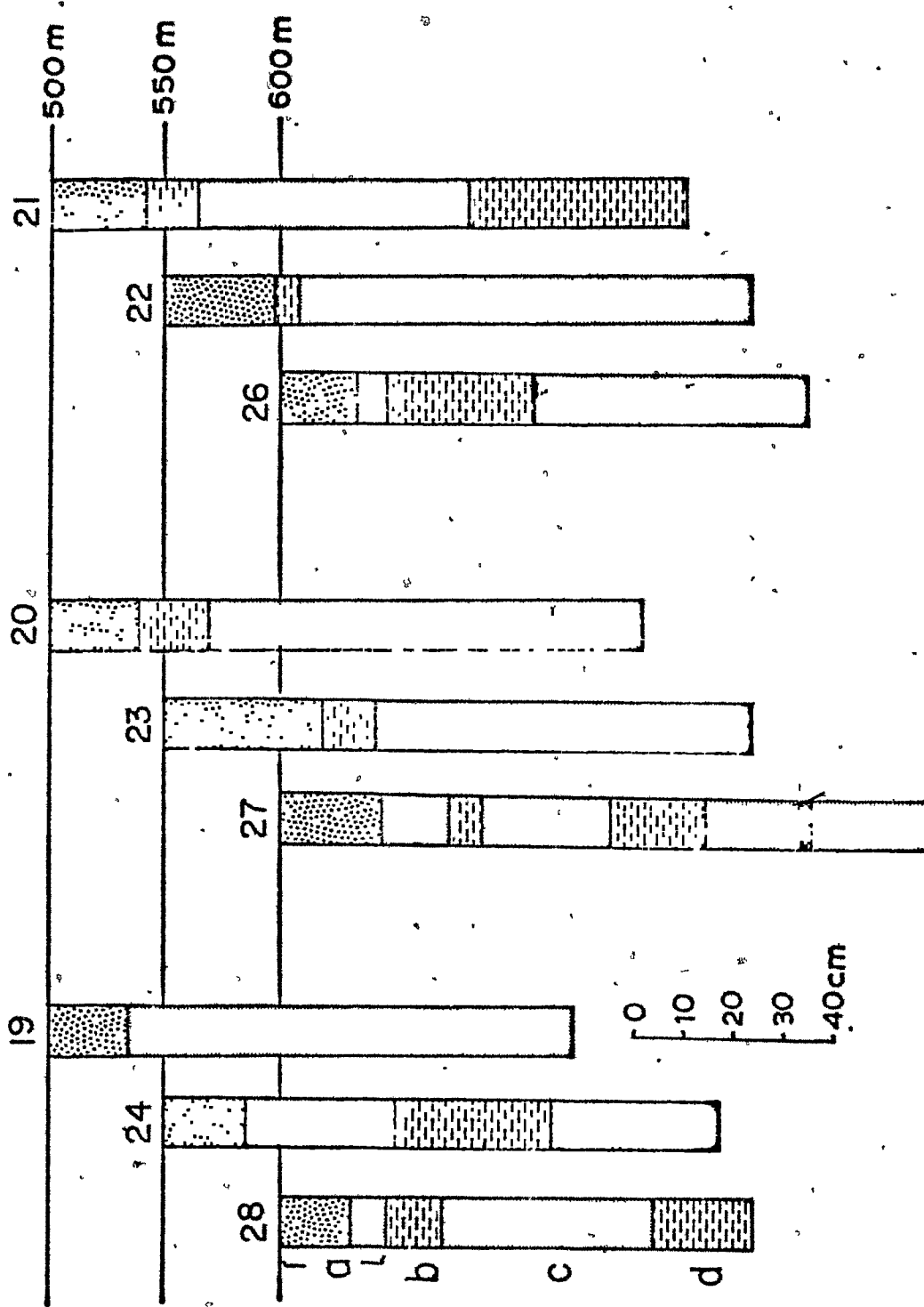
These units are correlatable over the Scotian Slope, from the Scotian Gulf to Dawson Canyon, although Silverberg (1965) did not recognize similar units off Sable Island Bank. Sub-unit (d) may consist of two beds, a surficial sandier bed and an underlying muddy olive-grey bed.

The maximum thickness of Unit 2 in the study areas is 200 cm. The unit as a whole and individual sub-units vary in thickness over short distances (Fig. 4-3). Unit 2 is often partially missing in piston-core tops, as a result of incorrect setting of the piston-corer, but it generally varies between 80 cm and 200 cm in total thickness.

In the standard core, the unit overlies a thin red-brown mud of Unit 1, but elsewhere it often overlies coarser-grained or slumped beds. This suggests that the base of the unit may be locally diachronous.

There is a distinct coarsening trend within the unit, in the up-slope direction, the sandy intervals of sub-units (b) and (d) being

Figure 4-3. Unit 2 members (a-d) in gravity cores from the Western Bank area. Heavy stipple: olive grey sandy silt; light stipple: olive grey mud; dashes dark yellow brown mud; horizontal lines: brown mud (Unit 1). The black band in core 27 represents red-brown gravelly mud.



best developed above 700 metres (Fig. 4-3). The olive-grey sand sub-units become more dominant and greater thickness variations are observed between cores in the upslope area.

#### BIOSTRATIGRAPHY

Biostratigraphic control is possible by the use of benthonic foraminifera to define assemblage zones. Five cores were subsampled for foraminifera, including the type-core (11). Some of the data were first presented in an unpublished report (Hill, 1979) where two distinct benthonic assemblages were identified in the slope cores. Recent detailed studies of Scotian Shelf fauna by M.A. Williamson and A.A.L. Miller have refined the taxonomy of some of the identified species. Nevertheless, the assemblages remain essentially the same:

Assemblage A: Trifarina occidentalis - Bulimina aculeata -  
Bulimina exilis assemblage

Assemblage B: Cassidulina crassa - Elphidium excavatum forma  
clavata assemblage

More complete faunal lists are shown in Table 4.1. Assemblage A contains a diverse range of benthonic foraminifera, but is usually dominated by Trifarina occidentalis. The assemblage is very similar to those obtained from surface samples below 700 metres (M.A. Williamson, pers. comm.). Assemblage B contains several species also present in Assemblage A, but Trifarina or Bulimina species are absent. It is generally less diverse than assemblage A and in places two species, Cassidulina crassa and Elphidium excavatum f. clavata, make up over

Table 4-1. List of main species comprising foraminiferan assemblages A and B.

TABLE 4-1ASSEMBLAGE A

Common species: *Trifarina occidentalis*  
*Bulimina aculeata*  
*Buccella frigida*  
*Cibicides pseudoungerianus*  
*Fursenkoina fusiformis*

Other species: *Elphidium excavatum* f. *clavata*  
*Cassidulina crassa*  
*Nonionella turgida*  
*Nonionellina labradorica*  
*Pullenia bulloides*  
*Saccammina atlantica*  
*Bulimina exilis*  
*Glandulina* sp.

ASSEMBLAGE B

Common species: *Cassidulina crassa*  
*Nonionellina labradorica*  
*Islandiella teretis*  
*Elphidium excavatum* f. *clavata*  
*Globobulimina auriculata*

Other species: *Nonionellina turgida*  
*Cibicides pseudoungerianus*  
*Bolivina* spp.  
*Fursenkoina fusiformis*

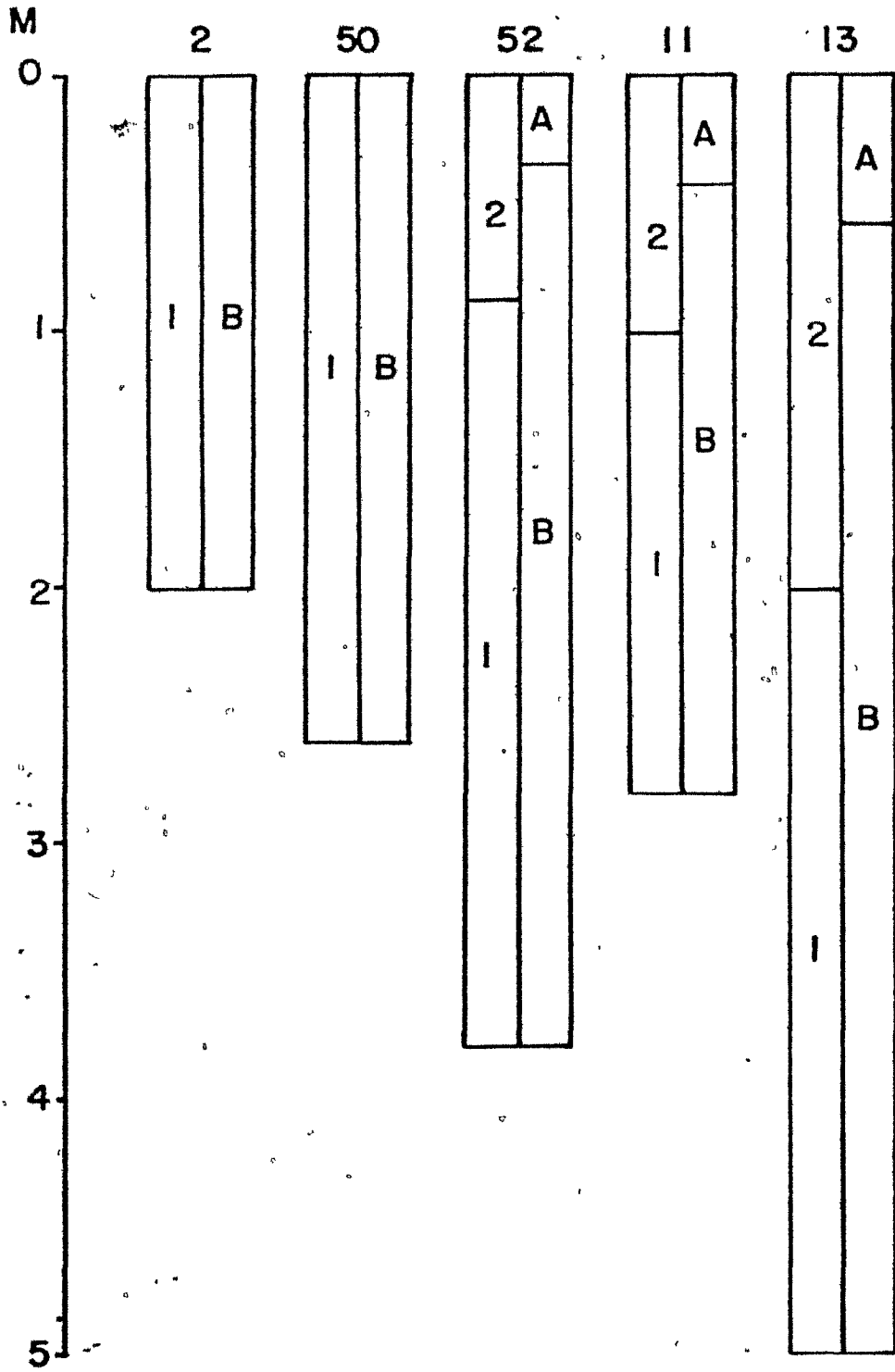
90% of the total population.

The distribution of these assemblages in the five cores studied is shown in Figure 4-4. Assemblage A is restricted to the top 20-50 cm of cores that show a complete Unit 2, while Assemblage B is present in the lower part of each core below that depth. The transition from assemblage B to assemblage A is quite rapid (within 10 cm), and seems to correspond to the lithological boundary between sub-units (c) and (b) of Unit 2 (Fig. 4-4). Silverberg (1965) and Stanley et al. (1972) recognised a similar faunal change at the northeastern end of the Scotian Slope.

Within assemblage B the proportions of certain species change significantly. The two dominant species, C. crassa and E. excavatum f. clavata, together make up over 70% of the fauna in the lower parts of the sequence, but upwards show a marked decrease in relative abundance (Fig. 4-5) as the assemblage becomes more diverse. Vilks (1981) has recently drawn attention to a similar transition which appears to be remarkably common on the continental shelves of eastern Canada, Denmark and Norway. In Vilks' cores, the initial abundance of E. excavatum f. clavata is usually as high as 60% and is more than 90% in one core. On the slope, E. excavatum f. clavata is usually less abundant, although the assemblage is dominated to a similar extent by the combined members of E. excavatum f. clavata and C. crassa.

This feature may prove to be a useful stratigraphic marker on the slope. Similar transitions are seen in both the Scotian Gulf and the Western Bank areas (Fig. 4-5). The dominance of E. excavatum f. clavata

Figure 4-4. Foraminifera assemblages in five cores from the Scotian Slope. Left column indicates lithostratigraphic unit, right column indicates foram assemblage (explained in text).



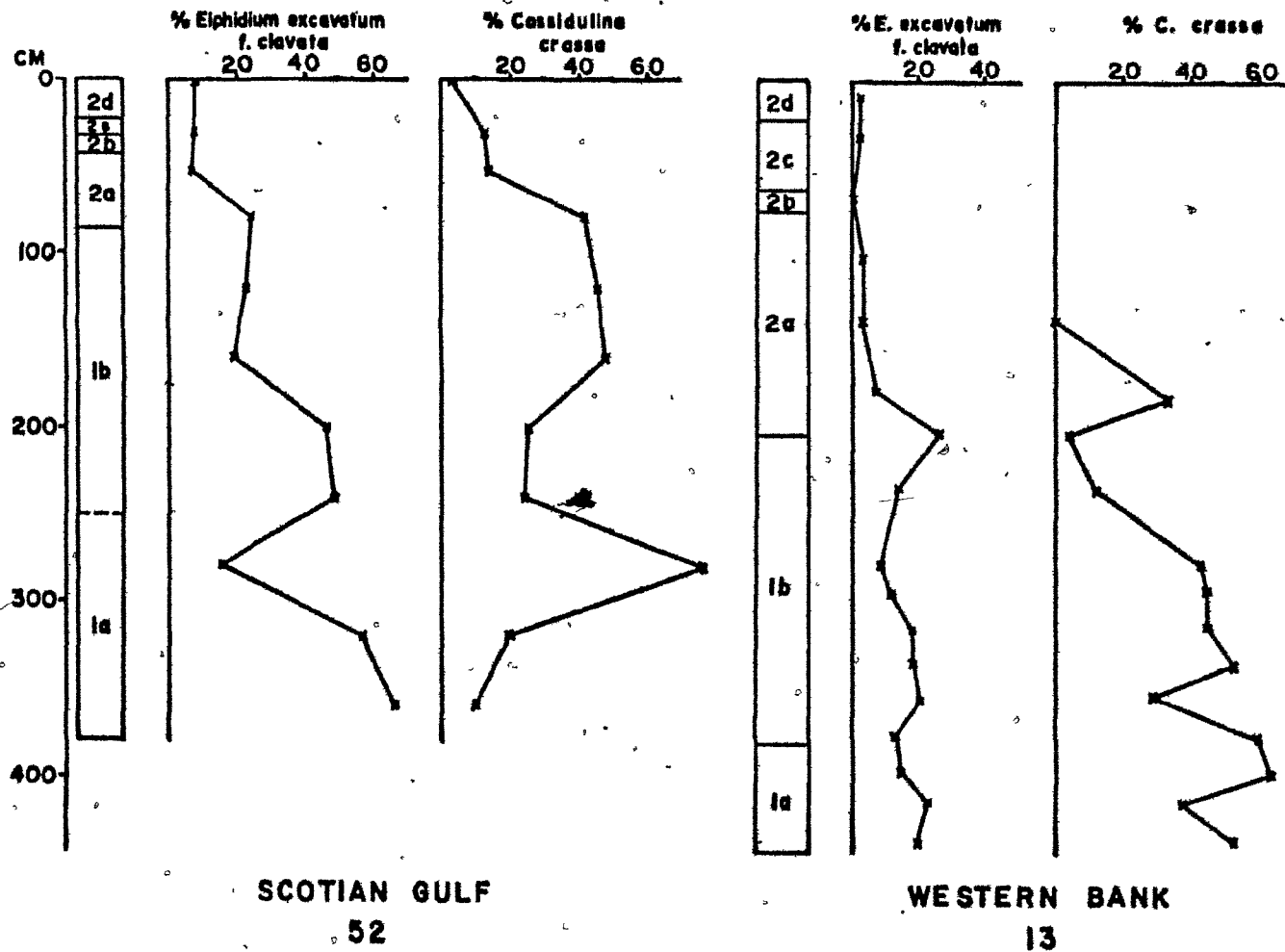


Figure 4-5. Downcore variation of the foraminiferan species *Elphidium excavatum* f. *clavata* and *Cassidulina crassa* in two cores from the Scotian Slope.

is greater in the Scotian Gulf area than off Western Bank where C. crassa is more dominant. However, the sudden reduction in the two species occurs close to the Unit 1/Unit 2 boundary in both areas and the size distribution of individuals in the samples indicates that the benthic faunas are in place, rather than redeposited.

As Vilks (1981) points out, a faunal change such as this can be a useful stratigraphic marker provided there is proper understanding of the cause of the change. Vilks accounts for the restricted Elphidium excavatum f. clavata-Cassidulina crassa assemblage by a cold, low-salinity coastal watermass generated at the ice-front/ocean boundary. A similar fauna on the slope would imply that this water extended to the shelf edge and then sank below warmer, less-dense ocean water and along the bottom down the slope. This, in turn, could have major implications to glacial paleoceanography in terms of bottom water generation. There is no supporting or conflicting evidence for this possibility, so that it cannot be said at present that the faunal change is understood. Both the intra-Assemblage B and the Assemblage B/Assemblage A horizons nevertheless appear to have potential biostratigraphical value.

#### CHRONOSTRATIGRAPHY

The core sequences can be placed in a time framework by the combined use of absolute dating and the correlation of biostratigraphic units with other studied areas.

Ten  $C^{14}$  dates were obtained from Scotian Slope cores and are summarised in Table 4-2. All but one were obtained from analyses of

7

Table 4-2. List of Carbon-14 dates on Scotian Shelf cores.

TABLE 4-2

Core	Interval (cm)	Age (y B.P.)	Type	Lab No.
27	58	5,050 ± 300	Carbonate	GX-5737
11	108 - 116	19,045 ± $\begin{matrix} 895 \\ 765 \end{matrix}$	Org. C	GX-6398
57	133 - 149	28,000	Org. C	GX-7273
55	80 - 100	18,860 ± 860	Org. C	GX-7452
54	150 - 190	18,790 ± 840	Org. C	GX-7453
57	80 - 100	21,355 ± 880	Org. C	GX-7451
58	262 - 291	28,000 ± $\begin{matrix} 2800 \\ 1800 \end{matrix}$	Org. C	GX-7769
55	18 - 39	8,280 ± 270	Org. C	GX-7767
55G	98 - 110	17,450 ± 650	Org. C	GX-7767
55G	35 - 57	9,920 ± 310	Org. C	GX-7766

total organic carbon. One shell sample was also dated, but the sample was small and its age must be treated with caution (Kreuger Geochron Lab Report, GX-5737). The dated cores are shown in Figure 4-6. Estimates of the proportion of reworked organic material in the dated samples, (from palynology preparations) are given in Table 4-3, courtesy of P.J. Mudie. This analysis suggests that some of the older dates may be up to 5,000 years too old. The technique is semiquantitative and in the process of development (P.J. Mudie, pers. comm.) but it is presently impossible to quantify the total error in the age of each sample. A sensible approach, in this light, is to treat the radiocarbon dates at face value, while keeping in mind the potential error.

The 21,355 yr date in core 57 may be seriously in error. The sample was taken across a lithological boundary which may represent a hiatus. Thus, the younger, overlying sediment may be up to 30% contaminated by sediment of infinite radiocarbon age.

Most of the piston cores appear to represent at least 20-30,000 years of sedimentation, thus extending back into the last glacial period. If viewed strictly, time planes appear to cross lithological and faunal boundaries (Fig. 4-6). This is probably largely due to the dating errors discussed above.

The boundary between Units 1 and 2 seems to fall between 17,000 and 20,000 years B.P. (Fig. 4-6). In core 54, the top of Unit 1 superficially appears to be much younger than 18,000 years. However, the sediment immediately overlying the dated section in this core

Table 4-3. Estimated contents of reworked ("dead") carbon in the dated samples, with potential error in absolute ages (courtesy of P.J. Mudie, Dalhousie University).

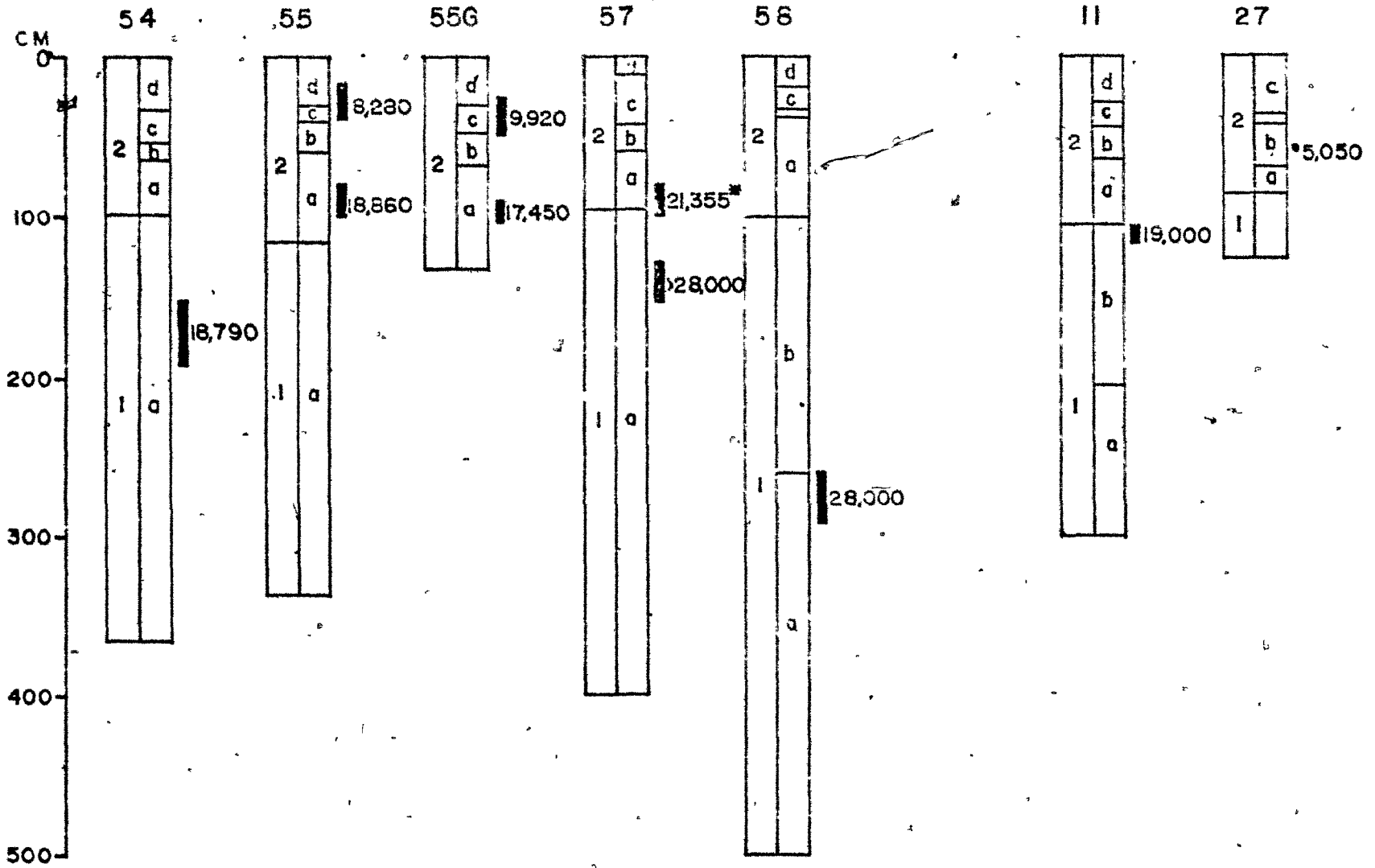
TABLE 4-3

CORE	INTERVAL	AGE (yr B.P.)	%REWORKED QUATERN- ARY PALYNO MORPHS	ERROR (yr B.P.)
55G	98-110	17,450	10	800
55G	35-57	9,920	20	1,500
55	17-39	8,280	20	1,500
55	80-100	18,860	50	5,500
54	150-190	18,790	80	>10,000
57	80-100	21,355	75	10,000
57	133-149	>28,000	90	-
58	262-291	28,000	80	>10,000

Figure 4-6. Carbon-14 dates (yrs B.P.) on cores from the Scotian Slope. Date with asterisk is unreliable as it was sampled across a possible discontinuity between Units 1 and 2.

SCOTIAN GULF

WESTERN BANK

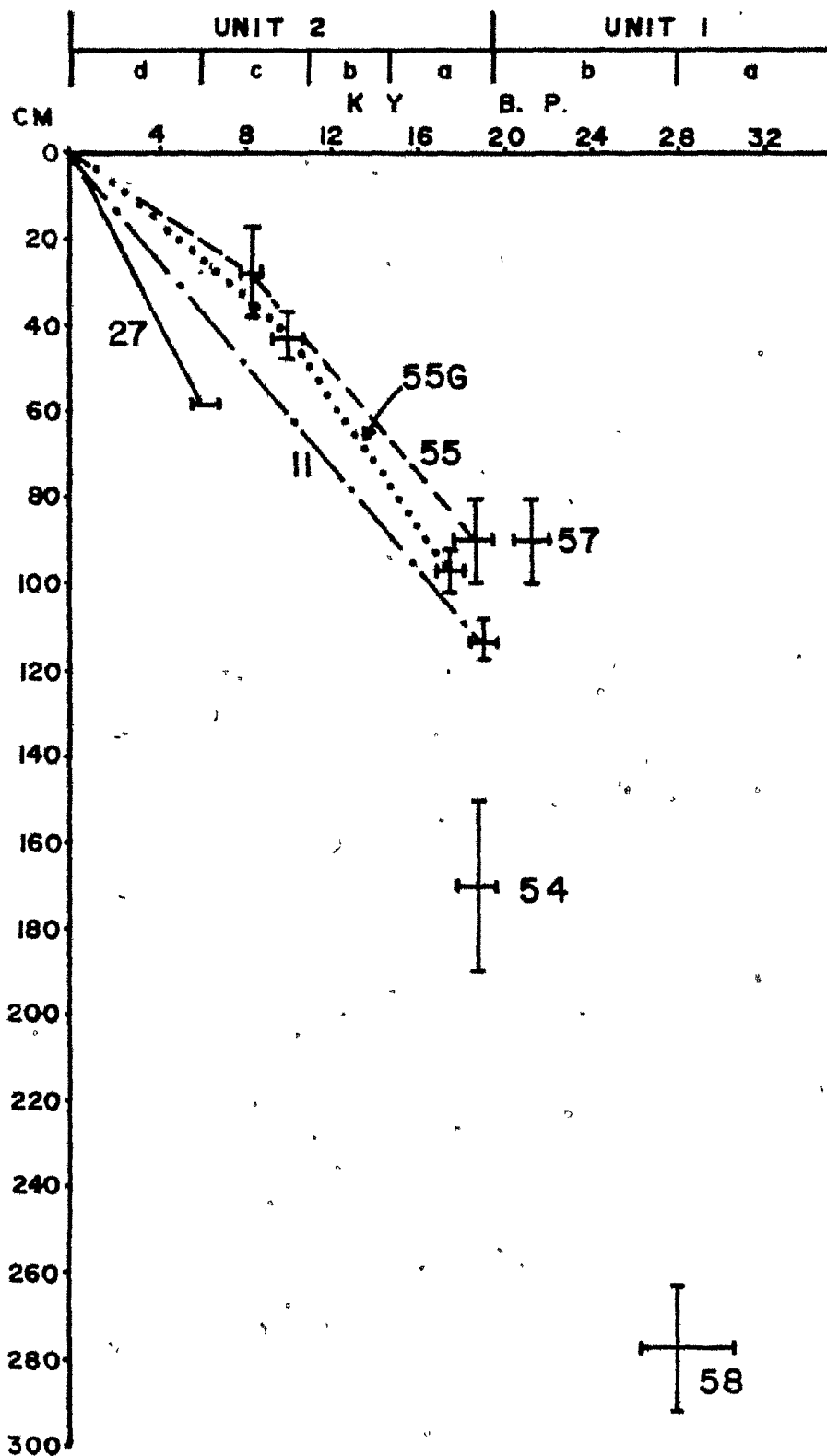


consists of sands, which were probably deposited relatively rapidly. Thus the age of the Unit 1/Unit 2 boundary may, in fact, be quite close to 18,000 years B.P. as in most other cores. If extrapolated strictly, the age of the boundary could be as old as 24,000 years B.P. in core 55, implying extreme local diachroneity. This is thought to be unlikely, especially in view of the large potential error. It is more reasonable to consider the boundary to be synchronous within the younger range of 18-20,000 years B.P.

Sedimentation rates in the core sequences are clearly not constant, especially in the Scotian Gulf area, as indicated by the numerous variations in lithology. The one finite date below the Unit 1/Unit 2 boundary suggests that the sedimentation rate was generally higher during deposition of Unit 1 than during Unit 2 (Fig. 4.7). This is supported by the less obvious signs of bioturbation and the more common preservation of primary sedimentary structures in Unit 1.

Sub-unit 1 (b) is often completely absent from cores taken in the Scotian Gulf area. In some cores (eg. core 57), there are obvious discontinuities close to the Unit 1/Unit 2 boundary, which may represent erosion of sub-unit 1 (b). However, in other cores (eg. 54 and 55), sedimentation of Unit 1 (a), seems to have been continuous until the major boundary. The base of sub-unit 1 (b) has been dated in core 58 at 28,000 years B.P.

Figure 4-7. Plot of distance downcore against time from  $C^{14}$  dated core sections. Numbers refer to cores (see table 1-1). Horizontal error bars refer to analytical error (see Table 4-2). Vertical error bars represent length of core removed for analysis.



#### COMPARISON WITH SHELF STRATIGRAPHY

Figure 4-8 illustrates the inferred stratigraphic relationships on the slope and compares them to core sequences studied by Mudie (1980) in nearby Emerald Basin. Mudie (1980) compared the sequences in two shelf cores (Fig. 4-9), one from the bottom of Emerald Basin (her core 20) and the other from the basin margin (her core 8). The basin-bottom core showed an apparently continuous sequence with little lithological variation except for a subtle colour change at depth. Part of the top was missing (Mudie, 1980), but the sedimentation rate decreased markedly after approximately 10,000 years B.P. Core 8 from the basin margin showed a more distinctive lithological change from brownish mud in the lower seven metres to grey mud in the upper four metres.

The cores both show distinctive foraminiferal assemblages which are quite similar to those found in slope cores. The surface layer in both cores contains a modern assemblage (FP) which is diverse and dominated by genera such as Bolivina, Bulimina, Cassidulina, Chilistomella, Globobulimina, Gyroldina, Hoglundia, Lenticulina, and Pullenia (Vilks and Rashid, 1976). This assemblage passes downwards into a more restricted assemblage (FN) characterised by Islandiella islandica (?Cassidulina crassa), I. teretis, I. norcrossi, Globobulimina auriculata and Nonionellina labradorica. In core 8, the brown lithology is characterised by the E. excavatum f. clavata-dominated assemblage.

Carbon-14 dates on core 8 suggest that there is a sedimentary discontinuity at the boundary between the brown and grey units. This

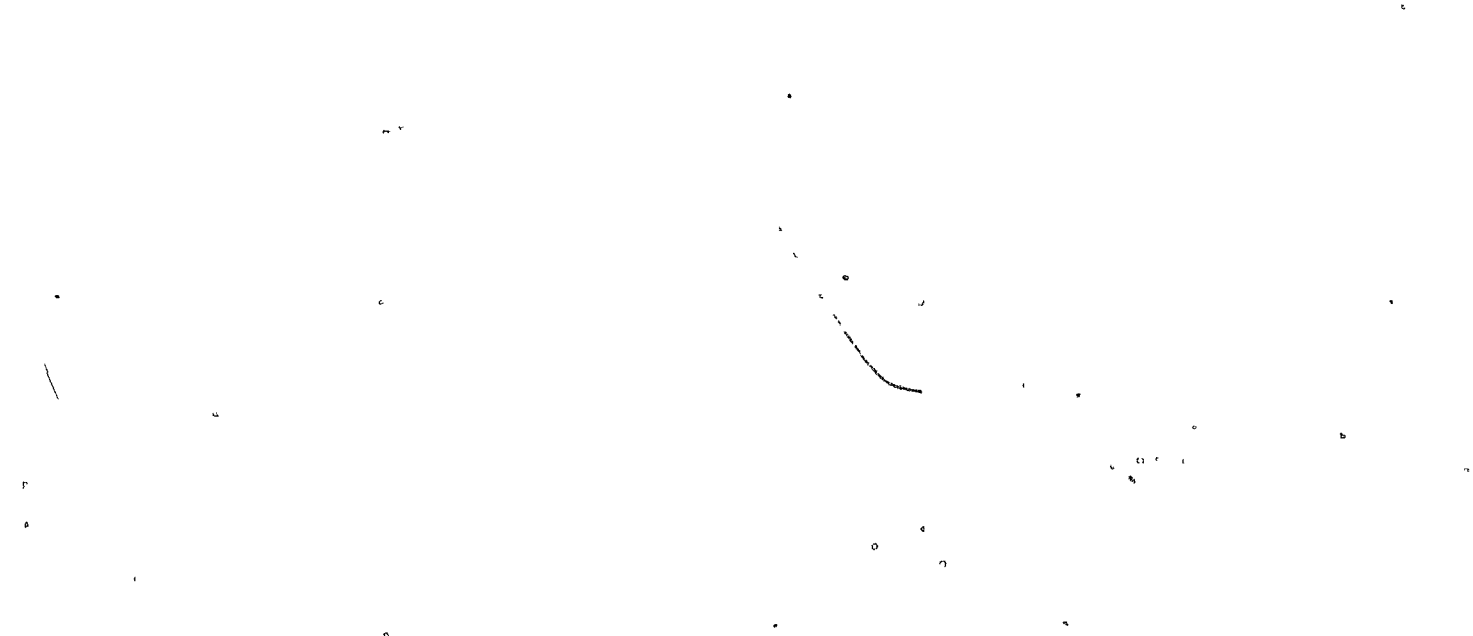
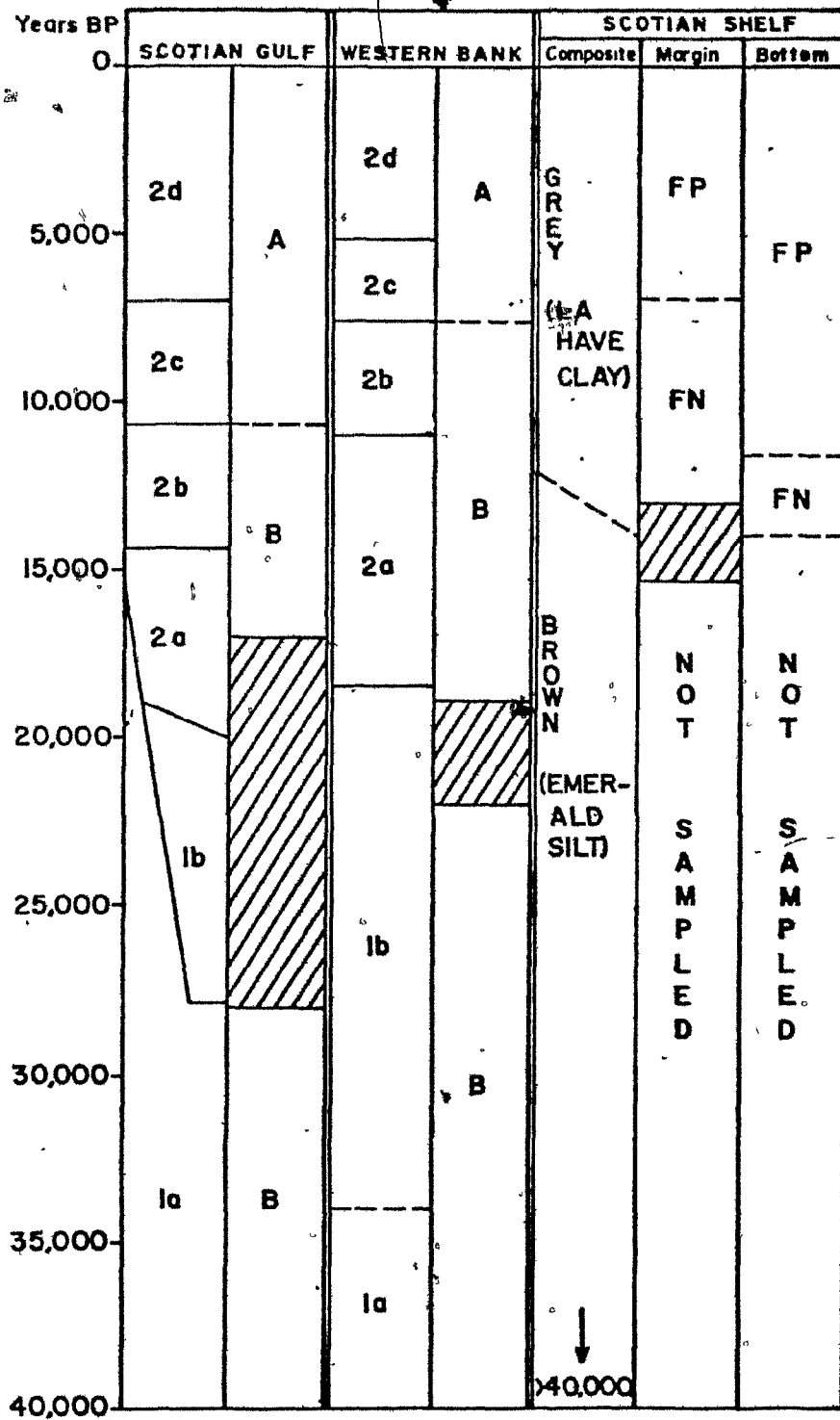


Figure 4-8. Stratigraphic summary of Scotian Slope cores and comparison to Scotian Shelf stratigraphy of Mudie (1980). Hachured areas represent zones where Elphidium excavatum f. clavata dominate the assemblage.



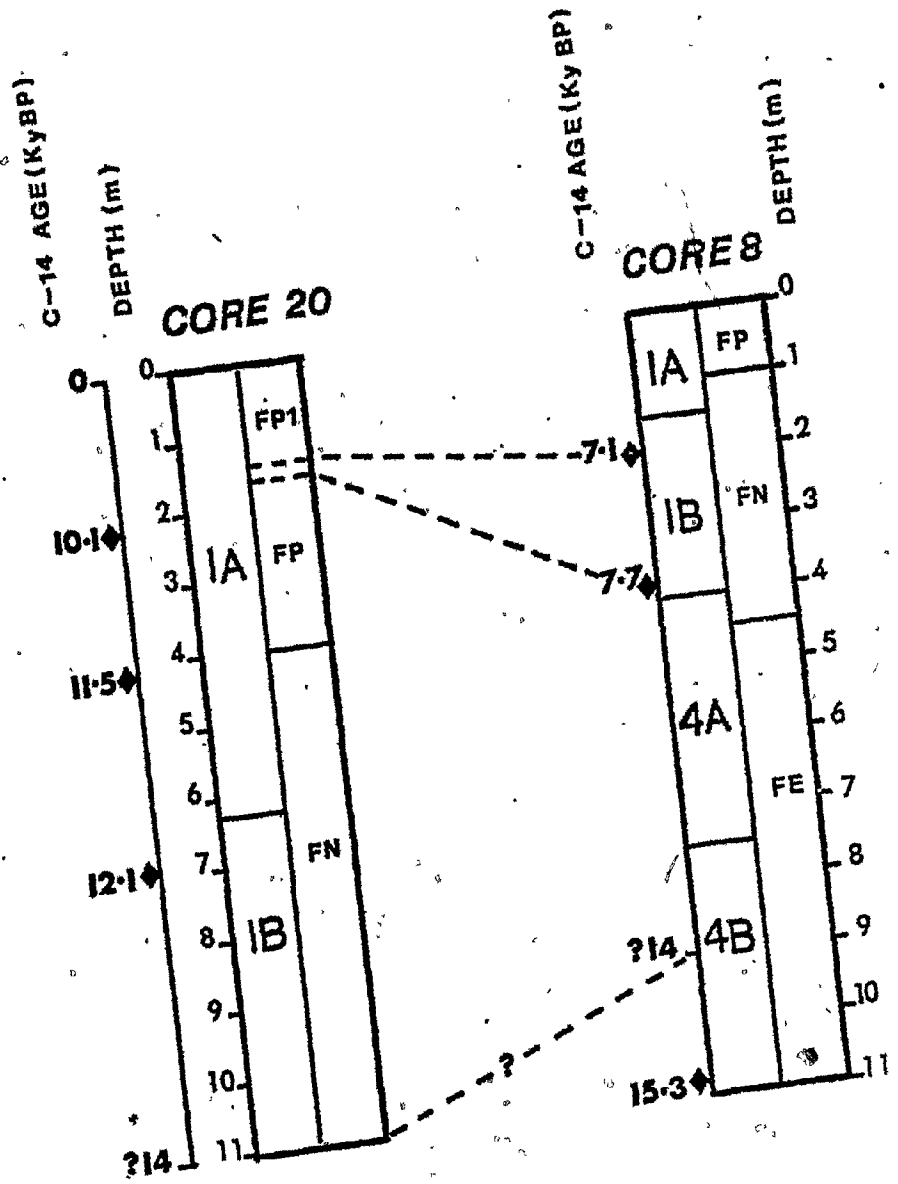


Figure 4-9. Correlation of Mudie's Emerald Basin core 20 (from the basin bottom) and 8 (from the basin margin) by carbon-14 dating. Note the diachronous foraminiferan assemblages (from Mudie, 1980).

is further supported by discontinuity of pollen and dinocyst assemblage zones in the core (Mudie, 1980). The missing section probably represents the period from 7,700 years B.P. to around 13,000 years B.P., thus placing a limit on the age of the brown unit. The base of core 20 is dated by extrapolation at approximately 14,000 years B.P. The brown-grey boundary may have been slightly time-transgressive, but its age can be estimated at approximately 12-14,000 years B.P. from these data. This corresponds closely to an independent estimate of the age for the Emerald Silt-LaHave Clay boundary (G.D. Fader, pers. comm.).

The FN/FP assemblage boundary does appear to be time transgressive between the basin-bottom and basin margin (Fig. 4-9). In core 20, it occurs at approximately 11,500 years B.P. while in core 8, it is dated at less than 7,100 years B.P. This boundary represents the establishment of modern conditions in Emerald Basin and it is not unreasonable to expect that these conditions were established earlier in the more stable, deeper parts of the basin than on the shallower margins during a marine transgression.

The slope sequence appears to correlate quite closely with the basin-bottom sequence (Fig. 4-8). The B/A faunal transition occurs at around 11,000 years B.P., very close the age of the FN/FP transition in core 20. The base of the basin-bottom sequence is dated at around 14,000 years B.P. and assemblage FN does not give way to the restricted Elphidium assemblage. It is possible that this assemblage change occurred as late as 20,000 years B.P., as on the slope, but in other Scotian Shelf cores, the boundary is generally closer to 15,000 years B.P. (Vilks,

1981). Both faunal changes apparently occurred considerably later, (by as much as 5,000 years), on the basin-margin than on the slope (Fig. 4-8).

#### PALEOCEANOGRAPHIC IMPLICATIONS

It was not the intention of this thesis to collect data that give direct paleoceanographic information. However, the faunal data does raise some interesting problems on paleoenvironmental conditions.

Vilks' (1981) explanation of the environmental conditions which resulted in the restricted E. excavatum f. clavata assemblage requires very cold, relatively fresh coastal water to dominate bottom waters on the shelf. This is feasible when an ice front is located on the inner shelf, melting directly into the ocean. For melting to occur, surface waters would necessarily be warmed, at least seasonally. Density considerations suggest that for cold, relatively fresh water to overlie the bottom, the shelf waters must either be essentially unstratified or have a much reduced surface salinity. This would be possible in an ice-margin situation, particularly if external water sources are reduced.

The occurrence of a restricted E. excavatum f. clavata assemblage on the slope suggests that this water may have extended to the shelf-edge and sunk down the slope beneath ocean waters. The S-T characteristics of present-day oceanic watermasses are shown in Figure 4-10. Both surface slope-water (C) and deeper slope water (E) have quite high densities ( $\sigma_t = 27-27.5$ ). The salinity required for very cold

water ( $-2^{\circ}\text{C}$ ) to have excess density relative to modern slope water is in the order of  $34\text{--}35$  ‰. It is possible that mixing of the coastal water with offshore watermasses quickly reduced the salinity across the shelf but mixing would also have raised the temperature of the more brackish water. Vilks' explanation for the restricted *N. excavatum* f. *clavata* assemblage requires substantially reduced salinity ( $<32$  ‰ is implied: Vilks 1981, Fig. 14). To allow water of this salinity to sink down the slope, the slope watermasses would need to be less saline and/or much warmer. It has been suggested, by Fillon (1976) and Alam (1979) that during glacial periods, the cold-core Labrador Current flow may have been substantially reduced by freezing in the Arctic source areas. This might allow encroachment of Gulf Stream water closer to the shelf-edge. However, there is no evidence from planktonic foraminiferal assemblages for warming of the surface water over the slope (Hill, 1979).

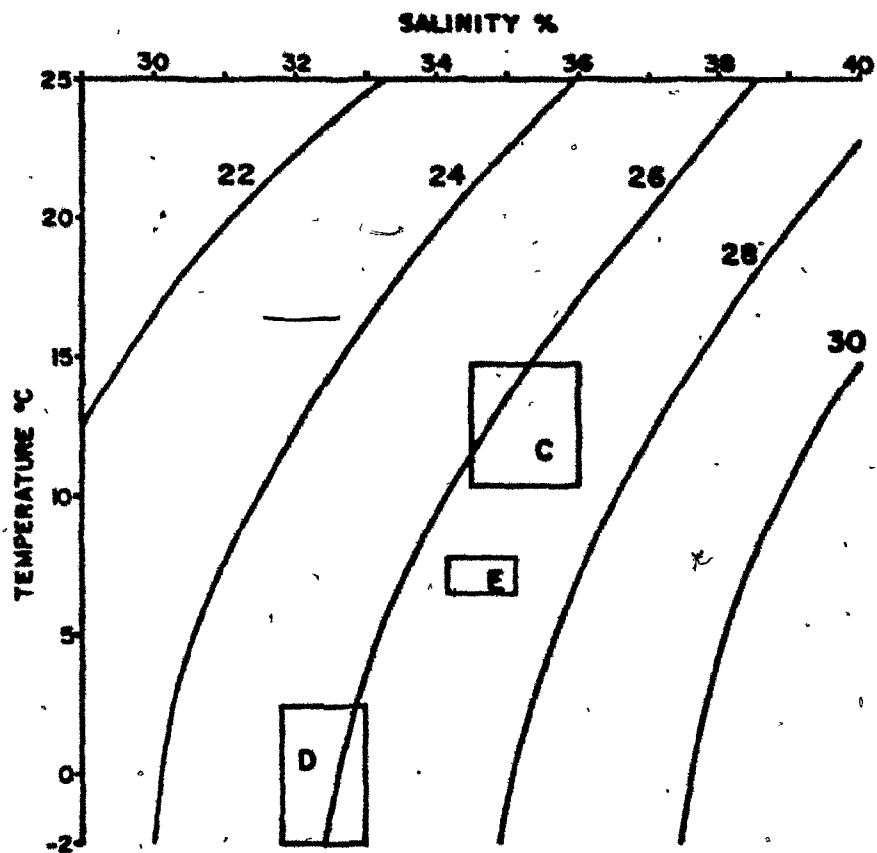
Another important factor in the paleoenvironmental interpretation is relative sea-level. Estimates of the last glacial reduction of sea-level in the Scotian Shelf area range from 110 metres (L.H. King and G.D. Fader, pers. comm.) to 50-70 metres (G. Quinlan, pers. comm.). One effect of a reduction of sea-level would be to expose large areas of the outer-shelf banks around Sable Island. The effects of 110 metres and 70 metres lowering of sea-level are shown in Figure 1-9. Even with 70 metres lowering, large areas of Sable Island Bank and Banquereau Bank would be exposed or less than 20 metres deep. This could have important oceanographic effects.

An important process governing the distribution of shelf watermasses is cross-shelf mixing between cold ( $-0.5$  to  $2^{\circ}\text{C}$ ) sub-surface water from the Cabot Strait and warmer ( $10$ - $14^{\circ}\text{C}$ ) slope water in the Sable Island and Banquereau Bank areas (Houghton, et al., 1978). If this mixing is prevented or greatly restricted, the cold Cabot Strait water would protrude further across the shelf. Only in the Scotian Gulf area might cross-shelf mixing be significant. The effect of this very cold (and relatively brackish (see Fig. 4-10)) water would be to reduce the amount of ice-margin melting and enhance the likelihood of sea-ice formation, especially in the northern part of the shelf where even surface water mixing would be drastically reduced.

Present day bottom-water in Emerald Basin has similar properties to slope-water at about 200 metres depth and is thought to be emplaced into the basin during winter storms when slope water intrudes onto the shelf (Houghton et al., 1978; Petrie and Smith, 1977). Modern conditions were established around 11,000 years B.P. and presumably, the reduced sea-level prevented the intrusion process before that time.

In summary, although reduced salinities can be used to explain the presence of a restricted E. excavatum f. clavata assemblage in Emerald Basin, it is very difficult to invoke the same hypothesis on the slope. Water of salinity less than 34 ‰ could not sink below the oceanic watermasses to form a bottom-water on the slope. It may be that other environmental parameters not considered here are more important controls on the fauna. High sedimentation rates during glacial

Figure 4-10. Salinity-temperature diagram with superimposed density ( $\sigma_t$ ) isolines. C = surface slope water, E = Labrador Slope Water, D = Maximum density of water suggested by Vilks (1981) for assemblage with Elphidium excavatum f. clavata predominant.



periods come to mind as one possibility. Cross-shelf mixing and slope water intrusions are important modern processes which may have been prevented by reduced sea-level. This would have led to considerably colder shelf waters and probably seasonal ice-cover on the Scotian Shelf.

## CHAPTER 5

ARGILLACEOUS FACIES

Fine grained sediments make up approximately 70% of the recovered core. Facies are distinguished on the basis of sedimentary structures and texture rather than colour. The main characteristics of each facies are summarised in Figure 5-1, and typical textures shown in Figure 5-2. Textures are classified according to Shepard's (1954) nomenclature.

FACIES 1: Mottled mud

This facies incorporates a range of mud textures from silty-clay to sandy silt. Its distinguishing characteristic is a patchy or mottled appearance. The facies often appears homogeneous on visual inspection, but the mottling is clearly seen on X-radiographs. In places, distinct burrow structures can be seen (Fig. 5-3). One common biogenic trace is identified as Zoophycos (c.f. Chamberlain, 1978). It consists of parallel-sided, subhorizontal burrows, often with crescent-shaped back-filling structures. The individual traces are part of a larger network of burrows, so that burrows are usually encountered in groups.

FACIES 2: Parallel laminated mud

This facies consists of muds with even, horizontal laminations which reflect a distinct grain size contrast between laminae (Fig. 5-4). The individual laminae vary in thickness from thin to very thin (nomenclature

Figure 5-1. Important characteristics of the argillaceous facies (1 to 5). Left column gives symbols for each facies as used on core diagrams (Figs. 7-4 to 7-8). Ice-rafted debris is common in muds (Facies 1-4) of unit 1, either as scattered clasts or more concentrated clusters. Clast sizes rarely exceed 2 cm diameter.

FACIES	DESCRIPTION	INTERPRETATION
1.	Mottled or patchy muddy silt to clay. Burrow structures and bioturbation common.	Hemipelagic mud deposited from non-catastrophic processes.
2.	Mud with very thin to thin parallel laminae.	Turbidite mud, E <sub>1</sub> division of Piper (1978).
3.	Wispy laminated mud with indications of ripple-drift cross lamination.	Hemipelagic mud deposited from slow but heavily loaded current.
4.	Homogeneous mud, no visible structures even in X-radiograph.	Turbidite mud, E <sub>3</sub> division of Piper (1978).
5.	Graded sandy silt to mud couplets.	Turbidite deposit. Bouma D and E divisions.

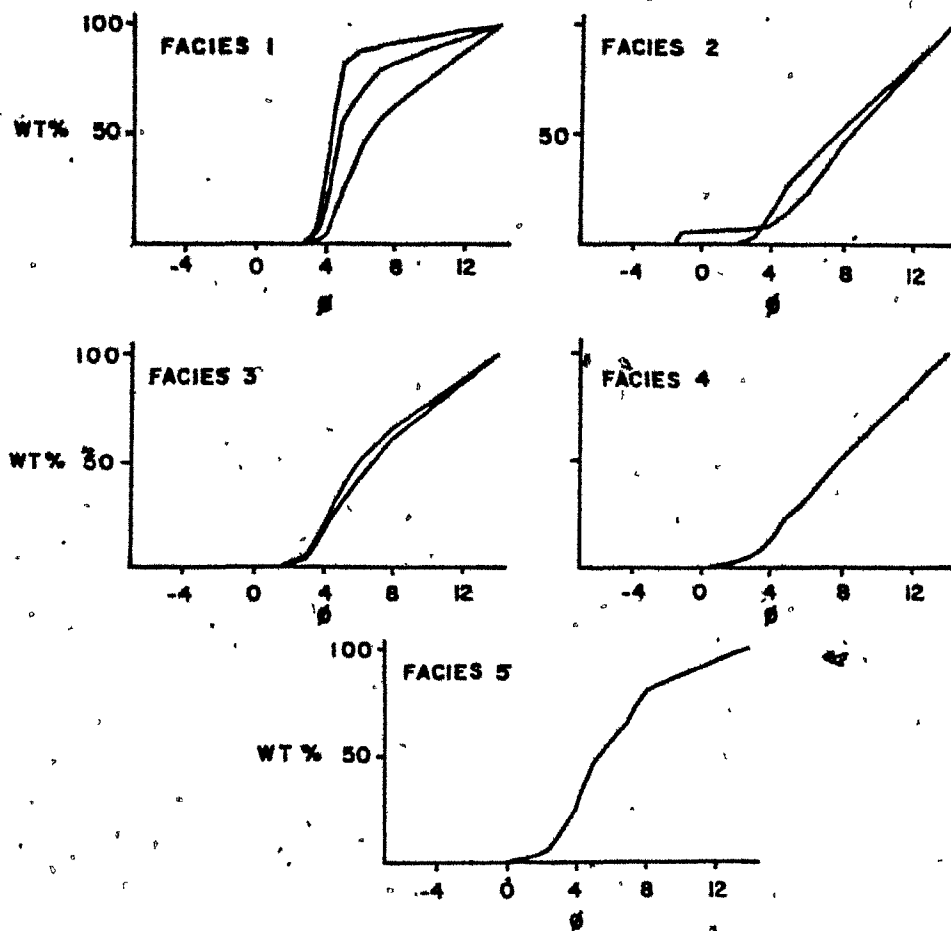


Figure 5-2. Representative cumulative grain size distributions for the fine-grained facies (1 to 5).

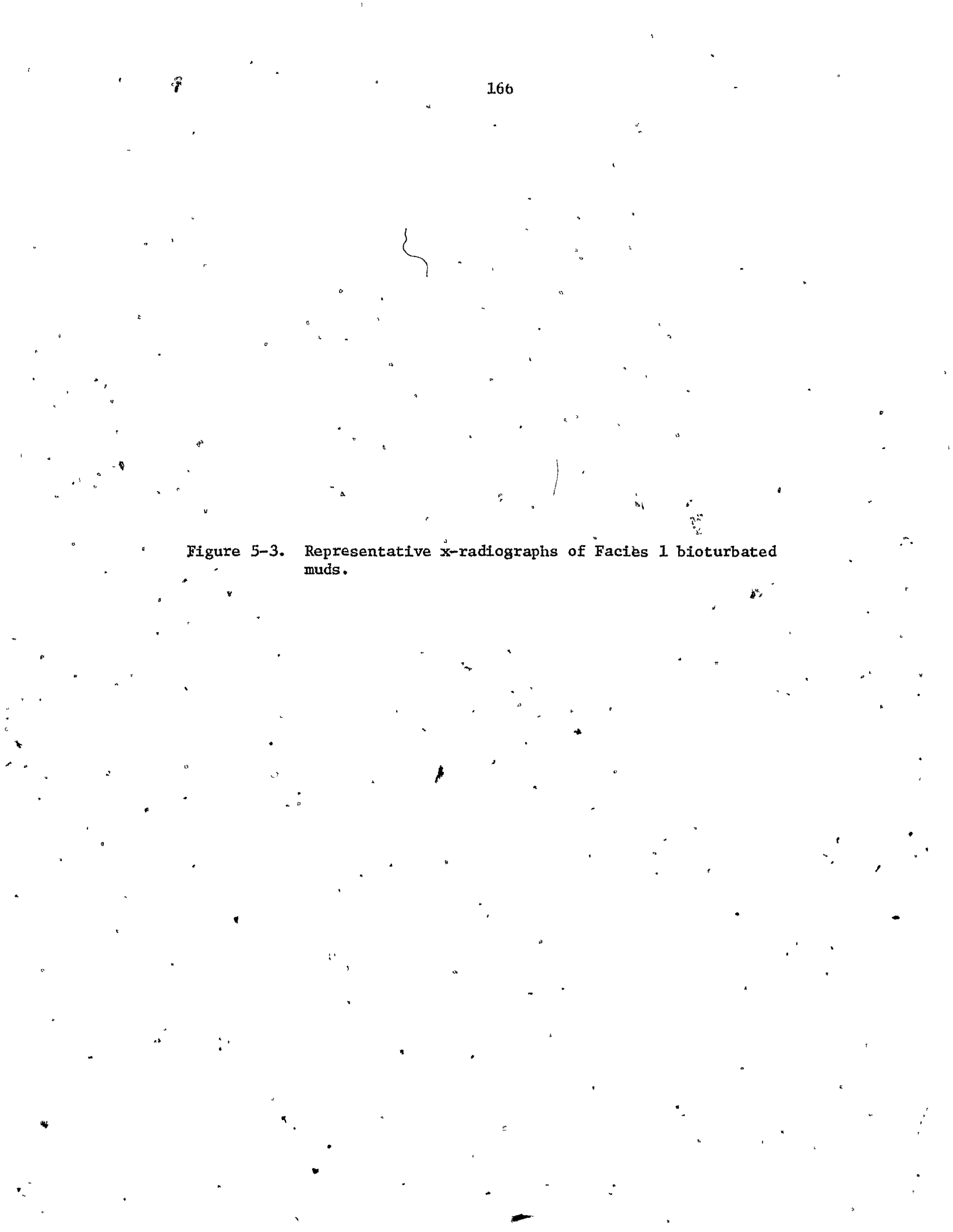


Figure 5-3. Representative x-radiographs of Facies 1 bioturbated muds.

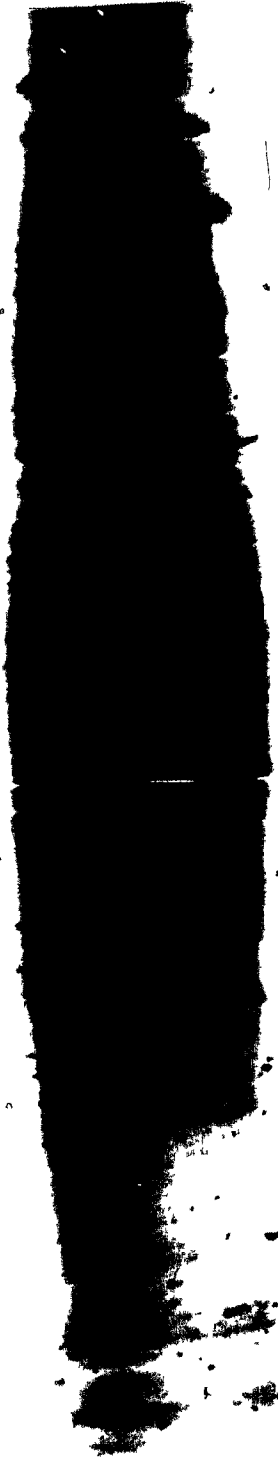


CM.

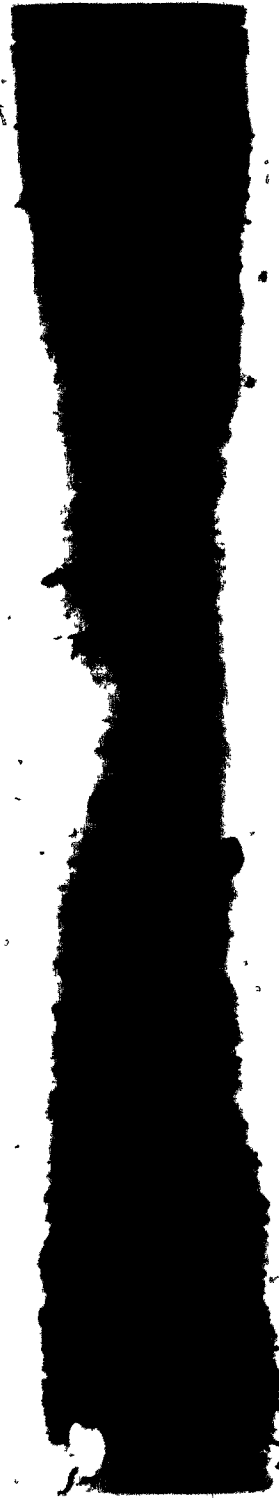


Figure 5-4. Representative x-radiographs of Facies 2 parallel laminated muds.

(a)



(b)



CM



of Ingram, 1954) and coarser laminae may be closely or widely separated by finer mud (Fig. 5-4). Laminae of the first type are generally sharper while those of the second are less clearly defined on X-radiographs (Fig. 5-4). In some cases, Facies 2 muds form fining upwards units (Fig. 5-4), although the same laminated lithology occurs in ungraded beds of varying thickness. Bed boundaries may be poorly defined; the facies often grades into other facies at both upper and lower boundaries.

#### FACIES 3: Wispy-laminated mud

Muds with very fine, often wavy lamination are assigned to this facies. Individual laminae are non-parallel, often showing micro-cross lamination, giving the mud a general wispy appearance in X-radiographs (Fig. 5-5). These structures are best seen in X-radiographs of thin slabs, although they are detectable in thicker sections. The facies may show distinct colour banding but is more usually made up of a single mud colour. Gradational contacts with adjacent lithologies are typical and individual units may be many centimetres thick.

#### FACIES 4: Homogeneous mud

Muds which show no internal structures, even in X-radiographs, are placed in this facies (Fig. 5-6). Individual units are variable in thickness, but generally less than 10 cm. Boundaries are usually gradational and there is no sign that primary sedimentary structures have been destroyed.

Figure 5-5. Representative x-radiographs of Facies 3 wispy-laminated muds.

(a)



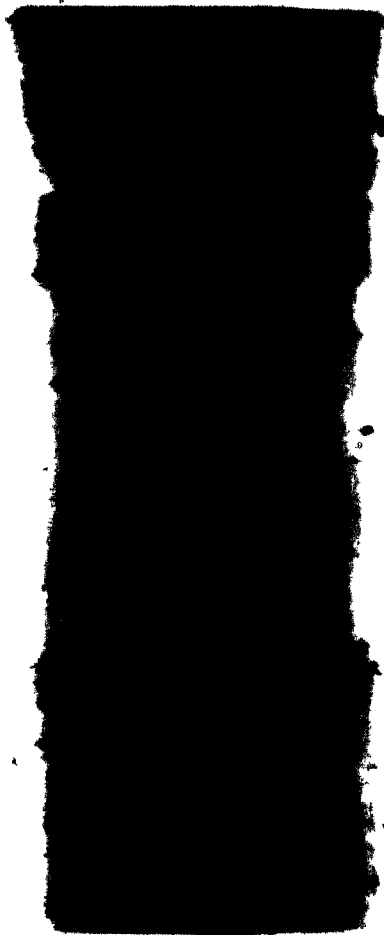
(b)



CM



Figure 5-6. Representative x-radiographs of Facies 4 homogeneous muds.



CM



### FACIES 5: Graded sandy-silt and mud couplets

This very distinctive facies consists of basal sandy or silty units which fine upwards into muds (Fig. 5-7). Individual couplets range from 0.2 to 5.0 cm in thickness and have sharp, often erosional bases (Fig. 5-7). The sandy-silt beds are generally poorly sorted and may be lensoid or discontinuous. Single, isolated couplets are sometimes partly destroyed by bioturbation. The brown/grey graded units are sometimes overlain by red mud to form distinctive bed triplets. The red mud is generally homogeneous or mottled.

### MUD TYPES, SOURCES AND TRANSPORT PATHS

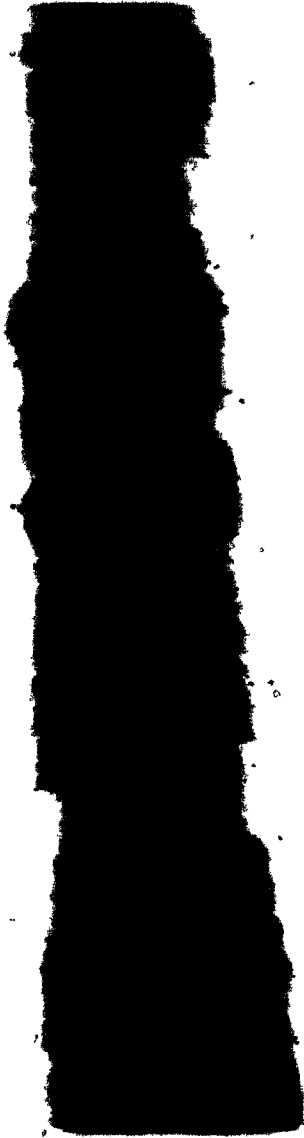
Mud on the Scotian Slope also shows quite distinctive colour variations by which the main stratigraphic units (see Chapter 4) are distinguished. There is a continuum of mud colours, from olive-grey to red-brown, but four lithotypes have been distinguished:

- (a) olive-grey (5Y 3/2)
- (b) dark yellow-brown (10YR 4/2)
- (c) brown (5YR 3/4)
- (d) red-brown (10R 4/6)

The compositional range of these muds is small (Fig. 5-8) and individual mud-types have gradational, overlapping fields. The sand fraction of olive-grey muds is characteristically rich in amphiboles and pyroxenes with respect to opaque minerals. X-ray diffraction shows that these muds have relatively high (> 10%) montmorillonite content

Figure 5-7. Representative x-radiographs of Facies 5 silt/mud couplets.

(a)



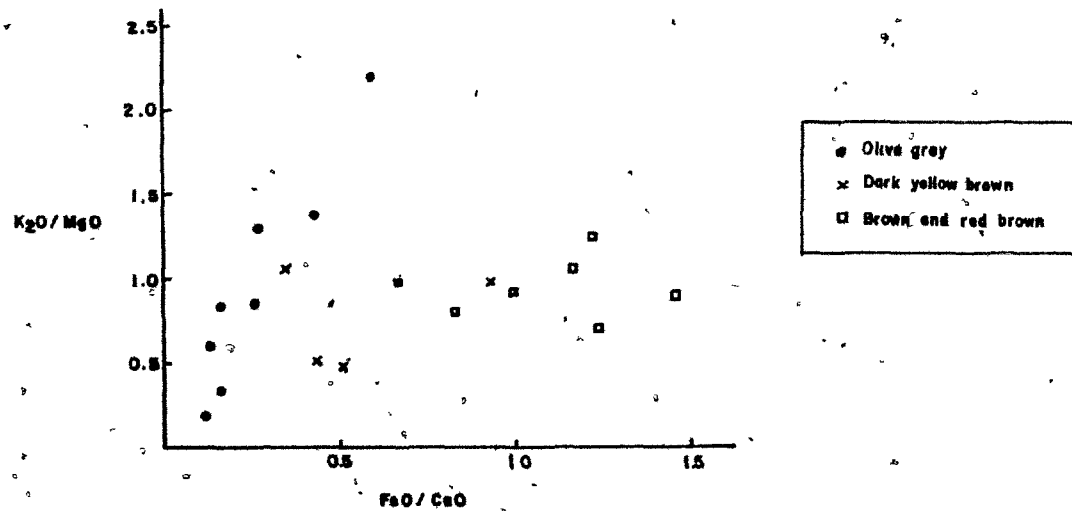
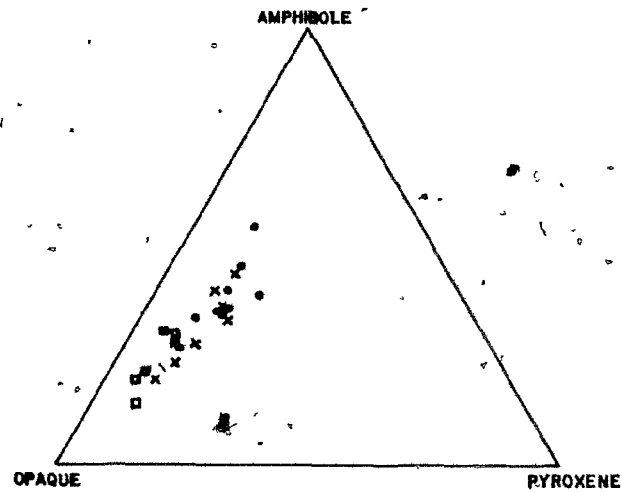
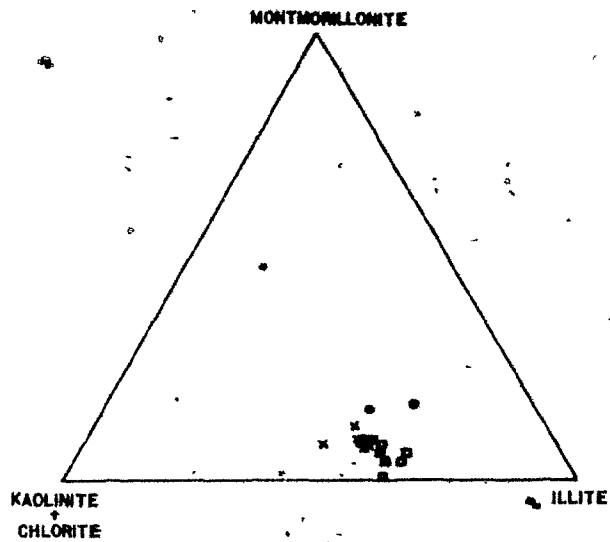
(b)



CM



Figure 5-8. Heavy mineral, clay mineral and chemical compositions of olive-grey, dark yellow-brown, brown and red-brown mud types. Clay mineral proportions calculated from area of peaks on X-ray diffraction pattern multiplied by an intensity factor (see Carver, R.E. (1971) Procedures in Sedimentary Petrology, Wiley-Interscience, New York, p. 548-551).



(in the  $< 2 \mu$  fraction) and are low in total iron. Red-brown and brown muds are petrologically indistinguishable from each other, but compared to olive grey muds, are relatively rich in opaque minerals with respect to other heavy minerals. They contain less than 10% montmorillonite and have high total iron contents. Dark yellow-brown muds have heavy mineral, clay mineral and chemical compositions intermediate between olive grey and red-brown/brown muds. The correlation of total iron with red colouration suggests that the latter is not merely a reflection of oxidation state, but of primary iron content.

Stow (1977) recognised similar compositional differences in mud lithologies on the Laurentian Fan and adjacent continental rise. Particularly, he noticed a relatively high montmorillonite content in his olive-grey facies, and following Biscaye (1964), suggested a northern source for the mineral. Recent data on the clay mineralogy of Nova Scotian tills (G. Camp, pers. comm.) include samples with up to 25% montmorillonite in the  $< 2 \mu$  fraction. The distribution of montmorillonite-rich tills on the Nova Scotian mainland is scattered, but these data suggest that local sources of montmorillonite do exist. Older shelf till deposits may also contain relatively high amounts of montmorillonite derived from Mesozoic or Cenozoic coastal plain strata.

Heavy mineral data shows a broad similarity between outer shelf sediments and olive-grey slope sediments. The heavy mineral provinces on the shelf are complex (James, 1966) and the shelf mineralogy southwest of Sable Island Bank has not been studied in detail. However, Stow (1977) recognised heavy mineral provinces within the olive-grey

sediment on the eastern slope, similar to those on the adjacent shelf. In view of this evidence and the textural continuity of olive-grey surface muds with the surficial bank sands (see Chapter 3), it is likely that the olive-grey muds are in large part derived from the adjacent outer banks.

Olive-grey mud, however, is a rather ubiquitous surface lithology over the shelf area including inshore areas (Piper et al., in prep.) and mid-shelf basins (Mudie, 1980). Piper et al. estimate that approximately 50% of mud-sized sediment is lost from the nearshore zone. Much of this probably accumulates in the mid-shelf basins but the net cross-shelf flux of suspended sediment is not known. However, it is possible that a proportion of the total modern supply of sediment to the deeper slope is derived from inshore, shelf and on-land sources.

The brown and red-brown muds are similar to muds described by many workers in the eastern Canadian offshore region. Red muds are seen as far north as the Northeast Newfoundland Shelf (Dale, 1979), on the Grand Banks Margin (Alam, 1979), on the Laurentian Fan and the adjacent rise (Stow, 1977), in the Gulf of St. Lawrence (Loring and Nota, 1973), on the northeastern Scotian Slope (Silverberg, 1965; Stanley et al., 1972), in Emerald Basin (Mudie, 1980; G. Fader, pers. comm.) and in nearshore basins (Piper et al., in prep.). A similar lithology was reported by Heezen et al. (1966) and Schneider and Heezen (1966) on the continental rise as far south as the Bahamas. The source of the

"red" sediment south of the Grand Banks is generally agreed to be the Gulf of St. Lawrence where Triassic and Carboniferous red-beds outcrop. Detailed mineralogy and chemical analyses also suggest a partial Canadian Shield source (Loring and Nota, 1973).

On the Scotian Slope, the brown and red-brown muds are broadly similar to Gulf of St. Lawrence red muds. High opaque mineral and total iron contents are characteristic of muds in both areas. Needham et al. (1969) have suggested that the presence of reworked Carboniferous palynomorphs can be used as a Gulf of St. Lawrence source indicator. Carboniferous palynomorphs are found in brown, red-brown and dark yellow-brown muds of the Scotian Slope, but rarely in olive-grey muds (P.J. Mudie, pers. comm.).

However, the Carboniferous basins of northern mainland Nova Scotia are also potential sources of red sediment. Much of the red till found along the eastern and southern shore are largely derived from these sources (Nielsen, 1976). The Gulf of St. Lawrence and mainland Nova Scotia sources of red mud are probably indistinguishable mineralogically or chemically, but the two are significant because substantially different transport routes to the slope are implied.

Undoubtedly, large volumes of red sediment were carried out of the Gulf through the Laurentian Channel to the outer margin in the Laurentian Fan area (Stow, 1977; Alam, 1979). Transport along the slope by the paleo-Labrador Current could then have acted to supply the more southerly parts of the slope, either in a surface plume as

suggested by Alam (1979) or in the bottom turbid layer.

A second route involves glacial transport of red sediment across mainland Nova Scotia, followed by cross-shelf transport and supply to the slope. The red coastal tills of Nova Scotia characteristically overlie greyer tills which contain dominantly locally-derived debris. The grey tills were interpreted by Nielsen (1976) as lodgement till while the red tills were more likely the result of melt-out processes. The bulk of the debris carried in the ice was derived from Carboniferous basins of Nova Scotia and the Gulf, then transported across Nova Scotia before being deposited by melt out at the edge of the ice sheet. King (1969) has recognised an end-moraine complex on the inner Scotian Shelf and recent work (L.H. King and G.B. Fader, pers. comm.) confirms his original interpretation that the moraines represent the edge of the late Wisconsinan ice sheet. Certain nearshore basins contain several metres of red mud overlying glacial outwash or till deposits (Piper et al., in prep.) which suggest high rates of sedimentation just seaward of a retreating ice-front (D.J.W. Piper, pers. comm.)

Most of this sediment was probably supplied to the ocean in surface water suspension. Mudie (1980) presents some data which supports surface-water transport of brown sediment across the shelf. Two cores (mentioned in Chapter 4) were collected from Emerald Basin, one from the deepest part (Mudie's Core 20) and the other from the basin margin (Mudie's Core 8). A major difference between the two cores is that the marginal core contains brown mud below a grey surface layer, whereas at the same stratigraphic level (prior to 18,000 yrs. B.P.),

the basinal core contains only grey mud. Marine palynomorph and foraminiferan assemblages indicate somewhat different paleo-oceanographic conditions at the two sites during the same late deglacial period (Mudie 1980). Basin margin assemblages indicate a relatively stressful bottom environment with turbid and relatively low salinity surface waters. In contrast, the benthic assemblage of the deep basin indicates that more normal marine water formed a deep bottom layer in the basin.

Although these cores do not penetrate below about 15,000 yrs. B.P., there is some evidence that a low-salinity surface-water mass existed over the shelf at that time, which transported brown coloured sediment from nearshore areas. High concentrations of littoral diatom indicators were also associated with this layer (Mudie, 1980) suggesting that reworking of nearshore sediments contributed some sediment, in addition to direct melting at the ice front.

With evidence for surface water transport of brown sediment across the shelf, it seems likely that a proportion would cross the shelf-break and be supplied to the slope. Lowered sea-level and emergence of the outer banks means that supply may have been restricted to the slope south of Sable Island Bank. However supply from the mouth of the Laurentian Channel was probably substantial (Alam, 1979) and sufficient to contribute sediment to the slope for some distance south. The Gully may also have acted as a local supply conduit to the slope. Whichever route was most important, the sediment must have been transported a considerable distance (in the order of 250 km) from the ice-front source before reaching the slope. This may explain the relatively

fine-grained nature of the mud compared to the more proximally derived olive-grey mud (Fig. 5-2).

The dark yellow brown mud was probably derived from both outer shelf and ice front/nearshore sources as it shows an intermediate composition in all the characterising parameters (Fig. 5-8). In several cores, the brown and olive-grey lithologies are seen interbedded on a fine scale. It is not clear whether the sediment from the two sources are mixed during transport in suspension, or by bioturbation after deposition.

#### RATES OF SEDIMENT SUPPLY AND DEPOSITION

##### (a) Olive-grey sediment

The surficial olive-grey mud unit has accumulated at an average rate of 5 cm ky<sup>-1</sup> (Fig. 4-7), or by weight, 11 g cm<sup>-2</sup> ky<sup>-1</sup>. Using a slope area of 3 x 10<sup>4</sup> km<sup>2</sup>, the required supply of mud to the slope is approximately 3.3 x 10<sup>15</sup> g ky<sup>-1</sup>. This value can be compared to rates of supply from coastal and outer bank sources.

Piper et al. (in prep.) estimate the loss of clay from the coastal zone of Nova Scotia from Lockeport to Peggy's Cove to be 10<sup>9</sup> g y<sup>-1</sup> (which extrapolates to 10<sup>12</sup> g ky<sup>-1</sup>). The supply from the whole coastal zone would be 3 to 4 times higher, say 4 x 10<sup>12</sup> g ky<sup>-1</sup>. Much of this load would be lost in transport across the shelf anyway, but it can be seen that the contribution of coastally derived sediment is probably not significant.

Supply from the outer banks (an area of  $6 \times 10^4 \text{ km}^2$ ) can be calculated by assuming winnowing of sediment containing 1% silt and clay. A cubic metre of sediment eroded would thus supply  $2 \times 10^4 \text{ g}$  of mud, so erosion of one metre over the whole bank area would supply  $1.2 \times 10^{15} \text{ g}$  of mud. An erosion rate of  $1 \text{ m ky}^{-1}$  on the outer banks would therefore approximately meet the supply requirements for the slope. As an order of magnitude estimate, this calculation demonstrates that supply from the outer shelf could account for all the slope mud in the olive-grey surface unit. The 1% mud value used for the outer banks is probably conservative as several areas of the outer shelf (eg: the Scotian Gulf) appear to have till (with mud content perhaps as high as 50%) outcropping at the surface and being actively eroded (submersible observation). An erosion rate of  $1 \text{ m ky}^{-1}$  is at least at a reasonable order of magnitude, although no estimates of Holocene erosion rates have been published for the outer banks.

(b) Red-brown sediment

Estimates of ice-margin sediment supply are very poorly constrained. Several factors control the sediment supply rate from ice sheets (Piper, 1976):

(i) the rate of continental erosion, itself dependent on relief, rock-type, climate, glacier temperature and the overland extent of the ice sheet.

(ii) thermal structure of glaciers and ice-shelves; whether wet or dry based.

(iii) the size of ice shelves which limits basal melting or freezing as well as surface ablation or accumulation.

(iv) sea and associated air temperatures at the ice margin

Direct methods of estimating Wisconsinan supply rates are obviously not available and reasonable analogies are not available in the modern. The melting of a temperate latitude ice margin during the Wisconsinan would be very different from that of the modern day polar ice sheets.

From the average slope sedimentation rate of  $10 \text{ cm ky}^{-1}$  (Fig. 4-7) for the Wisconsinan, the supply rate to the slope would be  $6.6 \times 10^{15} \text{ g ky}^{-1}$ . If a Nova Scotian ice-sheet were to supply all of this sediment, the actual ice margin discharge would be expected to be at least an order of magnitude higher, due to sediment deposited on the shelf and beyond the slope. Thus a value approaching  $10^{16} \text{ g ky}^{-1}$  might be expected. This rate is comparable to the discharge of moderately large rivers such as the Eel of the western United States (Holeman, 1968). The Eel has an upland drainage area of approximately  $8000 \text{ km}^2$  compared to the lower relief  $40,000 \text{ km}^2$  of Nova Scotia. Thus, the supply value does not require inordinate rates of erosion.

It seems likely, therefore, that a Nova Scotian ice-sheet could supply a sufficient volume of sediment to account for the observed rates of deposition on the Scotian Slope. However many factors are involved in the erosion, transport and supply of sediment to the ice-margin, even before marine transport processes are involved. The calculations suggest that supply from other sources (eg. Laurentian

Channel) need not be involved to explain sediment supply to the slope, but as has already been discussed, some supply from other sources is to be expected.

#### FACIES ASSOCIATIONS

In order to assess the significance of fine-grained facies associations and to aid interpretation of the individual facies, a Markov sequence analysis has been applied to the slope core sequences. The method is described in Appendix 1 with the various intermediate matrices generated during the analysis. The final difference matrix (Table 5-1) highlights the statistically significant transitions between facies as positive values. Those lower than 0.05 cannot be considered significant (Cant and Walker, 1976).

Figure 5-9 shows the original, observed facies relationships in the form of a flow diagram and is compared to the preferred relationships derived from the Markov chain analysis. The latter suggests that two facies associations can be separately identified, one consisting of Facies 2, 4 and 5 and the second of Facies 1 and 3.

#### Facies 2, 4, 5: Turbidite Association

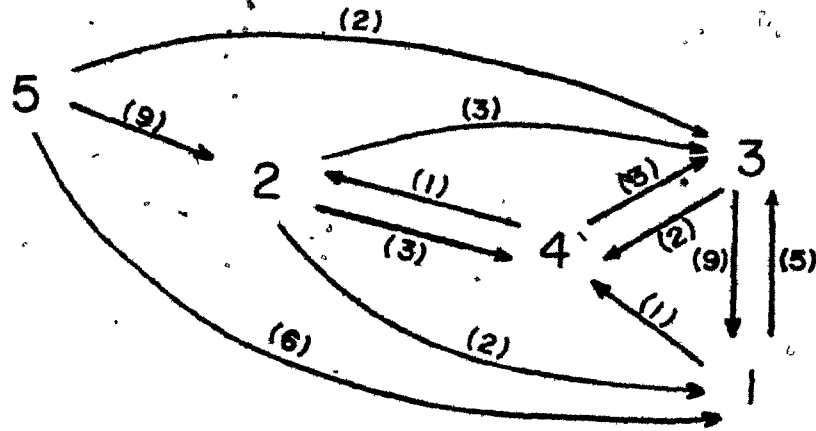
The analysis shows the close association between silt/mud couplets of Facies 5 and muds of Facies 2 and 4 (Fig. 5-9). The dominant sequence is a fining upward sequence from the silt mud couplets (Facies

Table 5-1. Difference matrix, Markov sequence analysis of fine-grained sediments.

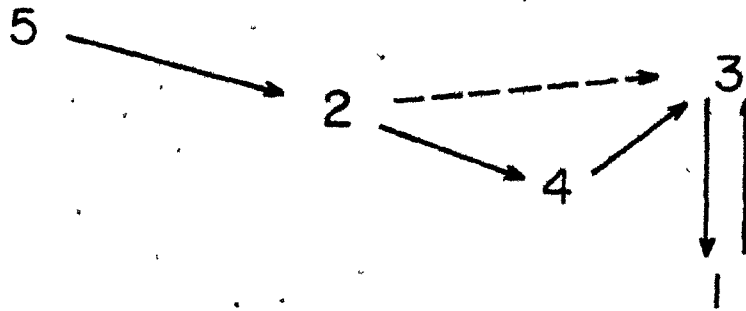
TABLE 5-1

DIFFERENCE MATRIX

	1	2	3	4	5
1		-0.34	0.32	-0.11	
2	-0.22		0.01	0.20	
3	0.31	-6.30			
4	-0.42		0.43		
5		0.31	-0.17	-0.13	



ORIGINAL



PREFERRED

Figure 5-9. Facies sequence analysis. Top: original observed facies transition (numbers in brackets indicate number of observed transitions); bottom: preferred facies transitions from Markov analysis.

5), through parallel laminated mud (Facies 2) to homogeneous mud (Facies 4). This is a generalisation and this complete sequence is not always present. Three typical sequences are recognised from visual examination of cores (Fig. 5-10).

- (a) Multiple silt/mud couplets.
- (b) Complete sequences of silt/mud couplets, parallel laminated mud and homogeneous mud.
- (c) Parallel laminated mud with slightly coarser basal silt laminae and homogeneous mud.

Type (a) sequences are not recognised in the Markov analysis because only gradual transitions were included. Type (c) sequences often consist only of Facies 2 units, with the slightly coarser base allowing identification of individual units. Such distinctions can sometimes be made only in X-radiographs.

The general sequence recognised here is very similar to the standard sequence proposed by Piper (1978) for turbidite muds and silts (Fig. 5-10). The basal part of Facies 5 is equivalent to a Bouma D division. Piper's model includes three subdivisions of the Bouma E division: E1 laminated mud, E2 graded mud and E3 ungraded mud. Subdivisions E1 and E2 are equivalent to Facies 2 of this study and E3 is equivalent to Facies 4.

In general, then, this association of facies is interpreted as of turbidite origin. The different types of structure represent "proximal" to "distal" changes in turbidity current deposition. There



are no distinct downslope trends in the distribution of facies, so the sequence-types are more likely related to proximity to a turbidity-current channel. They are similar to turbidites interpreted as over-bank or levee deposits (Walker and Mutti, 1973).

Although the graded sequences strongly favour a turbidite origin for these facies, many individual units cannot be unequivocally interpreted as such. "Muddy contourites" as described by Stow and Lovell (1979) and Piper (1978) have very similar characteristics and it is possible that some thin sequences of Facies 2 and 4 may be deposited from ordinary bottom currents. Present day current velocities (Chapter 3) are certainly sufficient to transport the fine sediment and dynamically sort the silt and mud laminae by either Stow and Bowen (1980) or Hesse and Chough (1980) mechanisms. Sediment supply was sufficiently high during the Wisconsinan and textural trends do not run demonstrably downslope. Definitive criteria are still not available for distinguishing muddy turbidites and contourites.

The sequence analysis suggests that the wispy-laminated mud (Facies 3) might make up a fourth member of the association (Fig. 5-9). This facies shows a strong Markov dependence on the massive mud (Facies 4) and an insignificant dependence on the laminated mud (Facies 2). Stow (1977) in a detailed analysis of muddy turbidites, suggests that a wispy-laminated division can occur between divisions E1 and E2 of Piper (1978).

There have been very few studies concerning the dynamics of fine sediment movement and the resultant bedforms. One study of interest to

this problem (Banerjee, 1977) includes data on relative current speeds (absolute values were considered only rough approximations by Banerjee) and rates of deceleration. In this flume experiment, Banerjee (1977) generated two ripple forms. At moderate to slow decelerations of the flow, asymmetrical, climbing ripples formed, resulting in ripple cross-lamination with preservation of steep foreset laminae. At lower speeds during very slow decelerations, lower amplitude sinusoidal ripples or "silt-waves" of finer (clayey-silt) were generated. Jopling and Walker (1968) observed and classified examples of ripple-drift cross-lamination in coarser sediments. They interpreted a transition from sinusoidal to climbing ripple lamination as the result of a decrease in the rates of suspended to traction load.

It is difficult to classify the wispy laminae of Facies 3 from narrow core samples, into any specific category. However, there are indications of ripple-drift in the form of upbuilding of the ripple forms by consecutive laminae (Fig. 5-11). The structures are very likely the result of relatively high sediment supply (from suspension) in a relatively slowly decelerating current.

In Banerjee's (1977) experiments, even slower flow speeds resulted in deposition of a structureless mud blanket. The homogeneous mud facies represents this low-flow speed condition. Stow (1977) and Piper (1978) also have structureless mud as their uppermost turbidite division. Thus the sequence of homogeneous mud to wispy-laminated mud indicated by the Markov analysis represents an increase in flow conditions. In view of this fact, the thickness of wispy-laminated units and the

Figure 5-11. Wispy laminae of Facies 3 with line drawings to illustrate possible ripple-drift cross-lamination.

CM 0 5



interdependence of Facies 1 and 3, it is thought that most occurrences of Facies 3 in the slope cores are not part of turbidite sequences.

#### Facies 1 and 3: Hemipelagic Association

The transition analysis indicates a close relationship between the mottled muds of Facies 1 and the wispy laminated muds of Facies 3. Transitions from one facies to the other are common in both directions. There are generally no textural changes across these transitions; the main change is in the preservation of sedimentary structures. Facies 1 muds are clearly bioturbated to the extent that all primary structures have been destroyed, whereas patches of undisturbed sediment usually reveal the characteristic wispy lamination of Facies 3 (Fig. 5-3).

Bioturbated muds on continental slopes are generally interpreted to result from hemipelagic sedimentation (Doyle and Pilkey, 1979) as they reflect relatively low rates of sedimentation and contain much planktonic biogenic sediment. The close two-way association of these bioturbated muds with wispy laminated muds suggest that their respective depositional processes are also related. The preservation of sedimentary structure is the only discernible difference between the two facies, suggesting that the rate of deposition may be the only difference in process. The indications of ripple-drift in the wispy-laminated facies supports the idea of a high sedimentation rate. Thick units of wispy-laminated muds are restricted to Unit 1, when generally higher sedimentation rates are observed (Fig. 4-7) and predicted from sediment supply estimates (this chapter).

Differences in textural trends between olive-grey and brown muds (Hill, 1979) suggest some change in fine-sediment dispersal between Unit 1 and Unit 2 times. Olive-grey sediments show a well-defined downslope fining trend from sandy silt at 500 m depth to silty clay below 1000 metres. Dispersal of fine sediment into deep water is not well understood. Pierce (1976) summarised the various mechanisms that have been proposed (Fig. 5-12).

Apart from Moore's (1969) density-flow model, which is largely discredited by Pierce (1976), all the models use some combination of lateral transport in a mid-depth or bottom turbid layer and settling into the bottom turbid layer (or nepheloid layer). Variations in oceanographic conditions dictate that a sedimentation model of this type should be locally specific. On the Scotian Slope, mid-water turbid-layers are not likely to be present below 100 metres, as the density interfaces are not available. This situation would not have been radically different in the late Wisconsinan, at least above 1000 m. Thus lateral transport across the Scotian shelfbreak must be in either surface or near bottom turbid layers.

Surficial olive-grey muds have been interpreted in detail in Chapter 3. Sediment is suspended at the shelf-edge, transported mainly in the bottom boundary layer and deposited at a distance from the shelf edge which is determined by the settling rate and initial concentration of the particle size and by the dynamic conditions at the depositional site. Transport in the bottom boundary layer is likely as the initial suspension occurs at the bottom and distinct high-turbidity zones (at

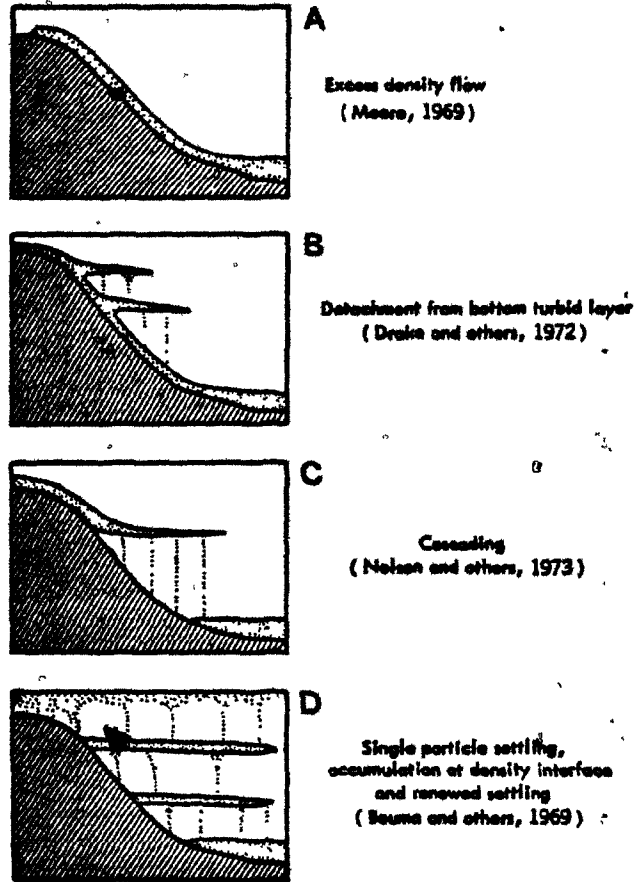


Figure 5-12. Mechanisms of fine sediment transport across the shelfbreak and slope (from Pierce, 1976).

density interfaces) are probably absent. The possible role of slope channels in this process is discussed in Chapter 7.

Red-brown and brown muds of Facies 1 and 3 are finer-grained and do not show a distinct downslope fining. These muds were introduced to the slope from more distal sources on the inner-shelf or along slope. Because much of the sediment transported in the bottom layer would have been trapped in mid-shelf basins (or in the Laurentian Channel), larger volumes of suspended sediment were probably transported to the slope in the surface turbid layer.

## CHAPTER 6

ARENACEOUS AND MUDACEOUS FACIES

Although coarser-grained sediments make up only 30% of the recovered core, it is quite likely that they are under-represented by the sampling. Several cores (see Fig. 7-3, next chapter), bottom in sand or stiff gravelly, sandy mud which probably prevented further penetration. Several core barrels were bent during coring operations indicating hard bottoms, either of eroded, indurated mud or of sand, and on the upper slope, above 500 metres water depth, coring was impossible. The main characteristics of each facies are summarised in Figure 6-1. Surficial sandy facies are not described here as no information on bedding or primary structures is available.

FACIES 6: Thick-bedded medium sand.

The dominant characteristic of this facies is that it occurs in thick beds which are apparently massive (Fig. 6-2). Textural analyses, however, indicate that there is significant variation in grain-size through the thick beds (Fig. 6-3). This suggests normal grading and that the thick beds may be composites of more than one sedimentation unit. Most of the sands are well-sorted (Fig. 6-3) and have an olive-grey colour similar to surficial sands. The exception to this latter characteristic is the bed at the base of core 2, which is distinctly browner. This bed is overlain by brown mud, indicating a low strati-

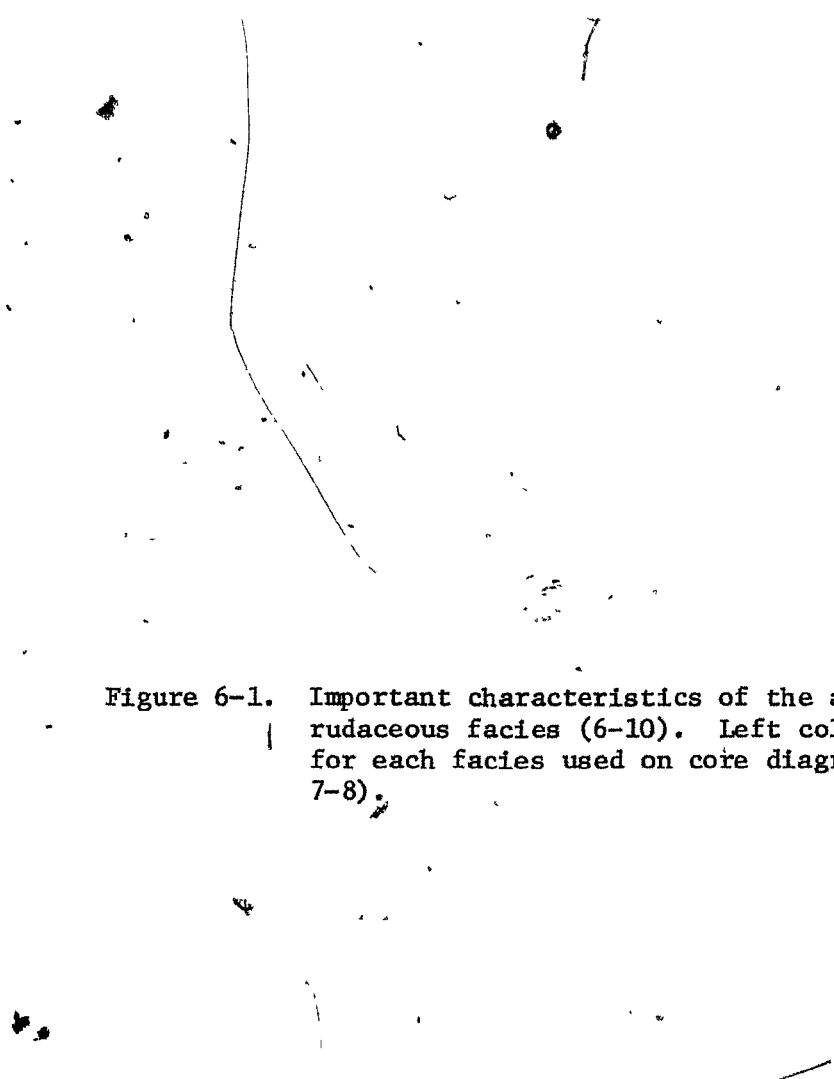
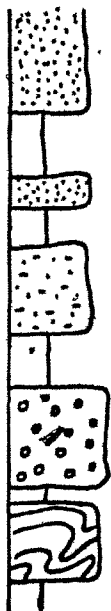


Figure 6-1. Important characteristics of the arenaceous and rudaceous facies (6-10). Left column gives symbol for each facies used on core diagrams (Fig. 7-4 to 7-8).

<u>FACIES</u>	<u>DESCRIPTION</u>	<u>INTERPRETATION</u>
6.	Thick-bedded, well-sorted medium sand with sharp bases. Beds may be amalgamated.	Channel-fill turbidite. Bouma A divisions.
7.	Thin-bedded, well-sorted medium to fine sand with sharp bases and sharp or gradational tops.	Turbidite, ?head-overspill. Bouma A and B divisions.
8.	Medium-bedded, muddy, fine sand. Massive, graded, laminated, bioturbated or convoluted.	Turbidite, ?small local flows. Bouma C and D divisions.
9.	Massive, gravelly sandy mud with sharp tops and bases.	Debris flow deposit.
10.	Deformed beds, mainly muddy, but often with discrete sandy patches.	Slump deposit.



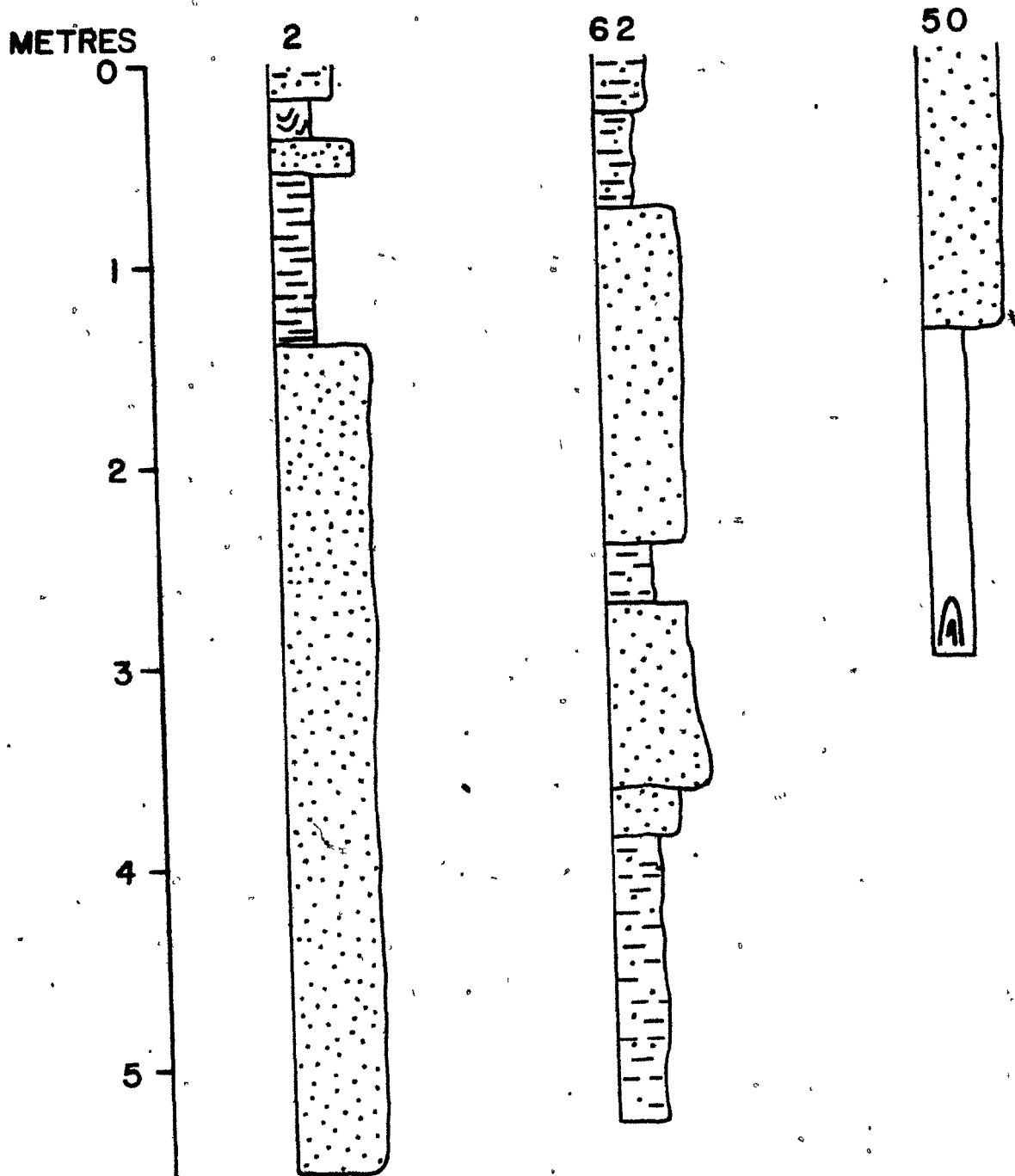


Figure 6-2. Occurrence of Facies 6 thick bedded, sand units in three piston cores; cores 2 and 62 from the upper slope, core 50 from the main channel.

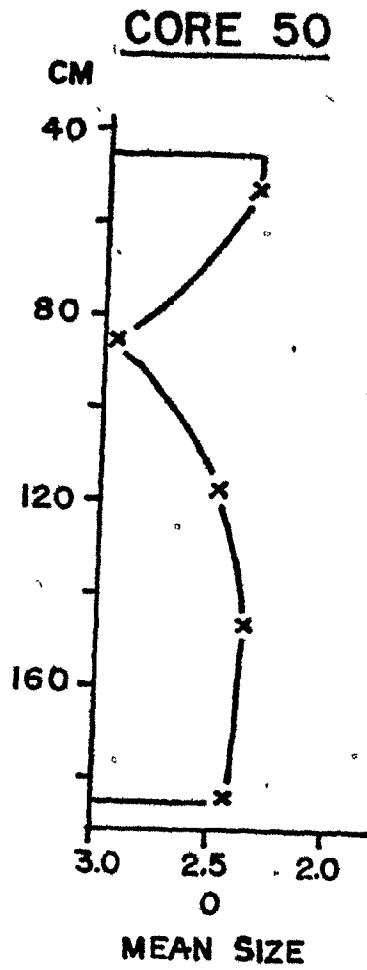


Figure 6-3. Grain size variation through Facies 6 thick sand bed. Note size scale fines to the left.

graphic position within Unit 1. The thick sand beds in cores 50 and 62 which are directly overlain by Unit 2 muds are probably younger.

FACIES 7: Thin-bedded sand

This facies consists of thin (2 to 20 cm thick) beds of well-sorted sand with sharp bases and tops. Grain-size ranges from fine to medium sand (Fig. 6-4) with mud making up less than 10% of the sediment. Most beds do not show significant size-grading except in two instances in core 54. Sedimentary structures are generally absent, but some beds show distinct parallel laminations (Fig. 6-5). Size analyses through these laminated units suggest that the modal size varies by 0.5  $\phi$  at the most between laminae (Fig. 6-4).

The sands are exclusively olive-grey and closely resemble shelf and upper-slope sands of the same size. The heavy mineral composition of a single sample from this facies is compatible with a local shelf source.

FACIES 8: Thin- to medium-bedded muddy sand

A rather variable range of beds comprise this facies whose dominant characteristic is the poorly-sorted sandy lithology. Facies 8 has a broad sandy mode and may contain up to 50% silt and clay (Fig. 6-6). Bed thicknesses are generally in the 15-20 cm range and bed boundaries may be sharp or gradational with indications of bioturbation (Fig. 6-7). Internally, the beds may be massive, graded, crudely laminated or disrupted (Fig. 6-7) and in some cases it appears that the

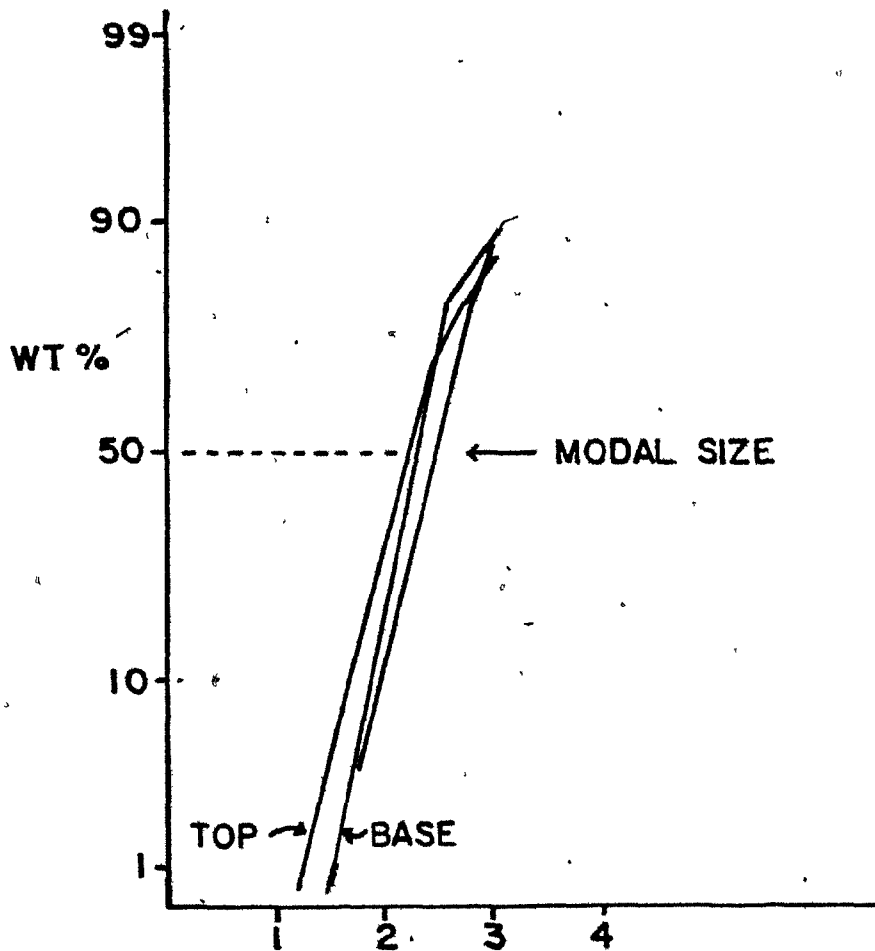


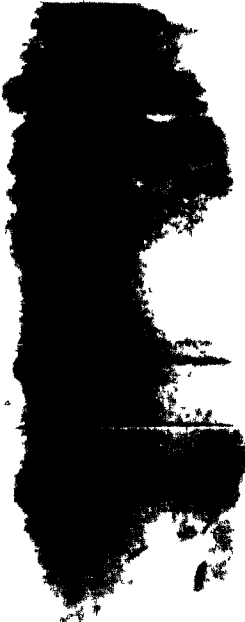
Figure 6-4. Grain size variation through Facies 7, well-sorted thin sand bed.

Figure 6-5. Representative x-radiographs of Facies 7 well-sorted, thin sand beds.

(a)



(b)



CM

0

5

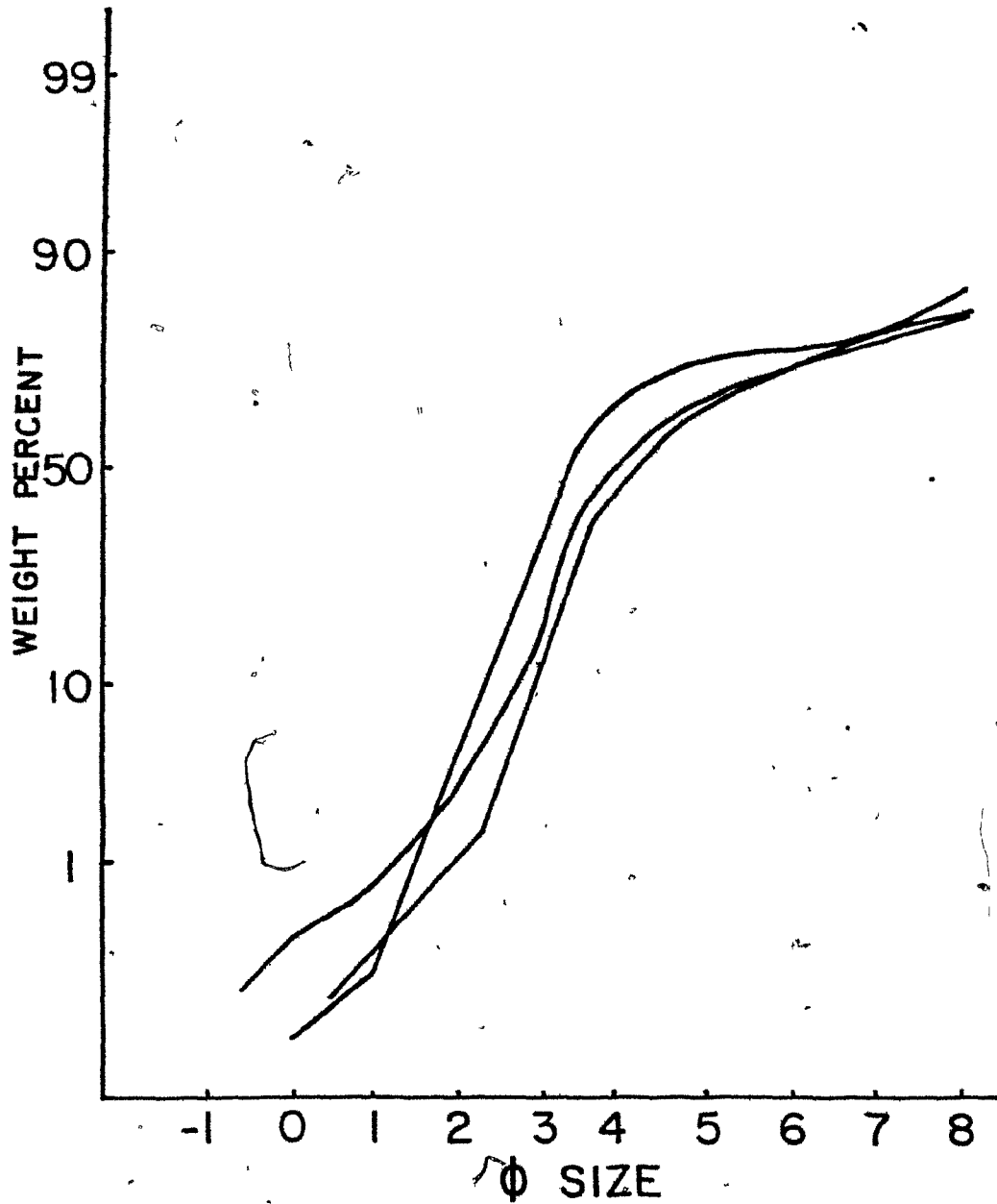
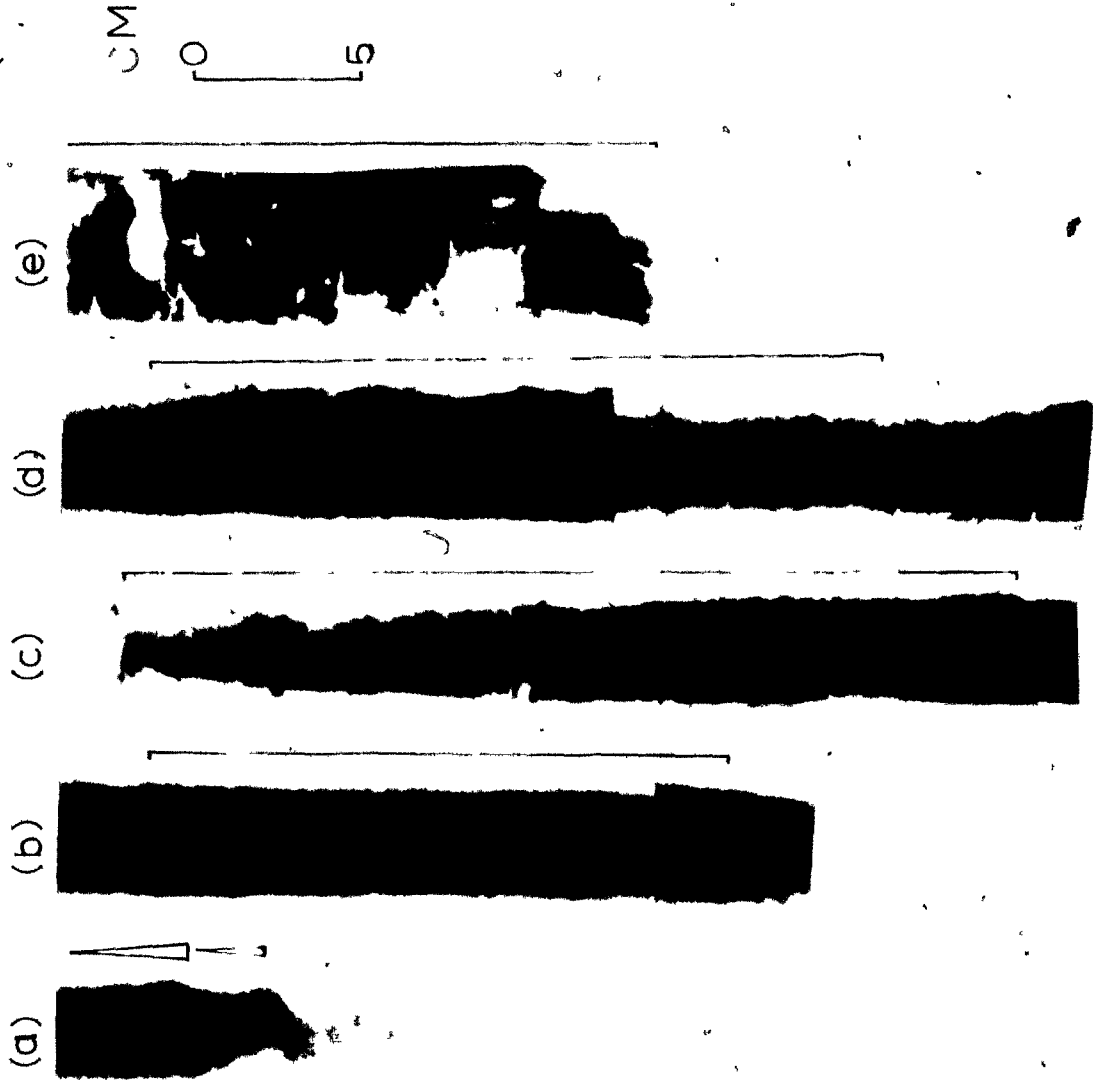


Figure 6-6. Representative grain-size distributions of Facies 8 muddy sand.

Figure 6-7. Representative x-radiographs of Facies 8 muddy sand beds.

- (a) Graded bed
- (b) Homogeneous bed
- (c) Laminated bed
- (d) Bioturbated bed
- (e) Deformed bed.

Tops and bottoms of beds indicated by ticks.



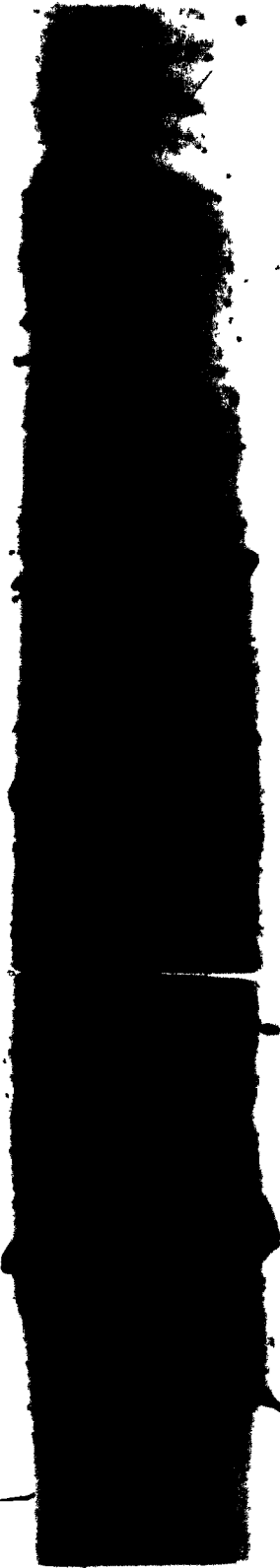
beds may be amalgamations of thinner depositional units, which closely resemble the finer sandy silt couplets of Facies 5.

Several examples of the facies are shown in Fig. 6-7 to illustrate the range of structures. One bed (Fig. 6-7a) clearly grade from a relatively well-sorted, coarse sand with a sharp (? scoured) base into mud. In the same core, overlying this unit is a thick, muddy sand which has a sharp base and top but appears to be completely homogeneous (Fig. 6-7b). The broad "laminations" shown by the bed in Fig. 6-7c may represent a set of amalgamated and partly bioturbated beds or an internal primary structure. Bioturbation has reworked the sand bed in Figure 6- d so that its boundaries are totally gradational. The bed shown in Figure 6-7e includes mud clasts which are enclosed in the sandy matrix. The mud clasts are generally rounded and show signs of internal deformation, whereas the matrix appears granular. In the centre of the bed, tilted laminations of mud and sand suggest that the whole bed is deformed. A similar lithology occurs not far below in the core, separated by a sorted sand similar to Facies 7. One cannot be sure that the described bed is not part of a larger deformed bed.

FACIES 9: Massive, gravelly, sandy muds

The very distinctive gravelly sandy mud lithology occurs in beds from less than twenty centimetres to several metres thick. The beds generally lack any sedimentary structures and have a massive appearance in x-radiography (Fig. 6-8). Two cores contain gravelly sandy mud units with finer, muddy intervals within them. It is not clear

Figure 6-8. Representative x-radiograph of Facies 9 gravelly sandy mud bed.



CM



whether these units were formed by a single or separate depositional events. Facies 9 has a multimodal size distribution (Fig. 6-9), but on a probability plot, the distribution appears to be a single population, with no sorting of particular size intervals. An important characteristic of the facies is its relatively indurated nature and its apparently low pore-water content.

#### FACIES 10: Deformed Beds

Units with signs of internal deformations are assigned to Facies 10. Several structures are characteristic of deformation, namely inclined and contorted bedding, isoclinal folds and eyelet structures, rounded sand patches and sharp colour boundaries between muddy sections (Fig. 6-10). Deformed beds vary in thickness from a few centimetres to several metres and where they are bounded by mud, their bedding surfaces may not be well-defined. Dominantly fine-grained deformed beds can often only be recognised in x-radiograph.

#### INTERPRETATION OF COARSE-GRAINED FACIES

##### (a) TURBIDITE DEPOSITS

Classical turbidites are characterised by sharp bases, normal grading (fining-upward) and the model sequence of structures distilled by Bouma (1962). On the Scotian Slope, there are very few beds with such classical characteristics. Nevertheless, there are a number of reasons for interpreting the sediments of Facies 6, 7 and 8 as turbidites.

Figure 6-9. Grain size distribution in some gravelly sandy mud beds.

- A: Seven analyses from one bed in core 63
- B: Single analysis from same bed.

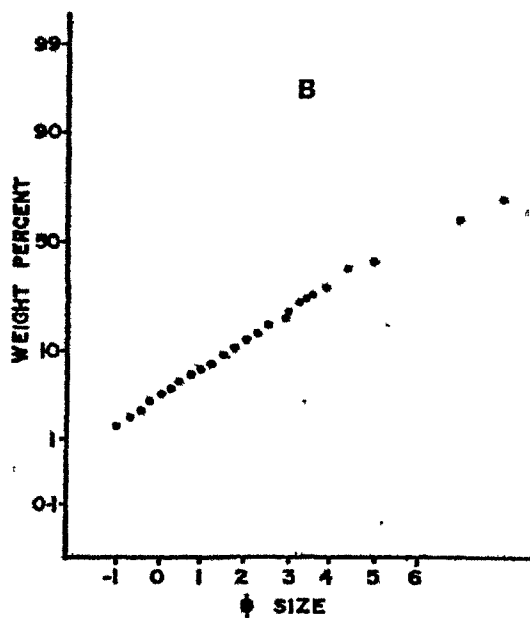
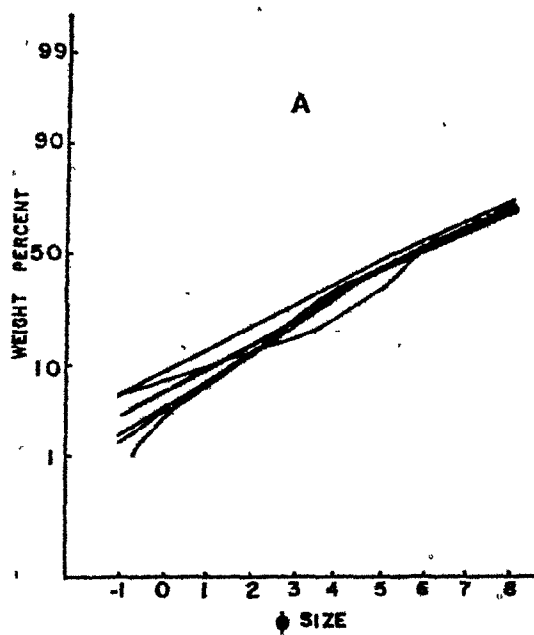
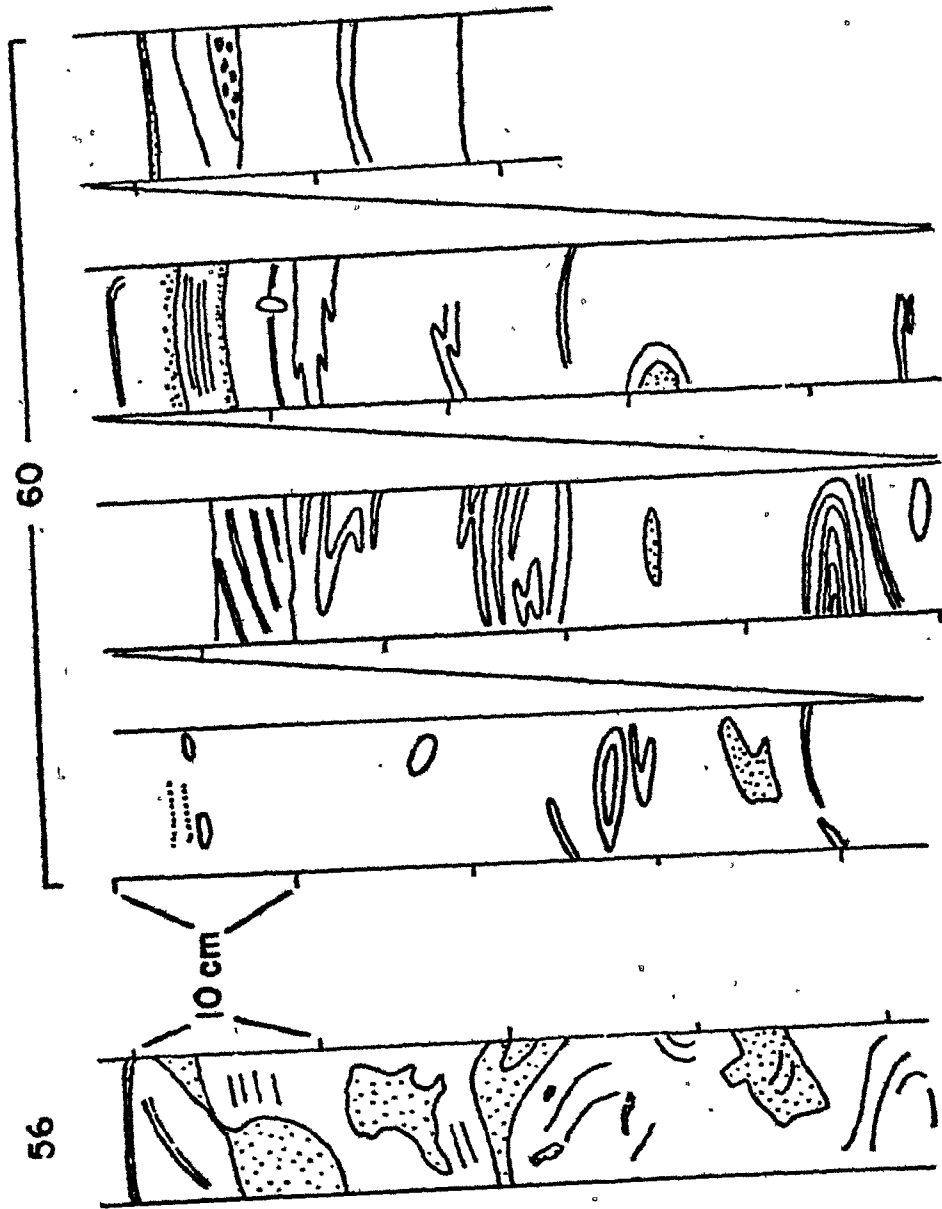


Figure 6-10. Sketches of deformed structures from visual inspection and X-radiographs of Facies 10 slumped beds.



The thick-bedded sands of Facies 6 were recovered from water-depths exceeding 500 metres. The modal sizes, ranging from 2.5 to 3.0  $\phi$  are clearly out of equilibrium with present-day current velocities at this depth (Chapter 3). There is no reason to believe that stronger geostrophic currents flowed on the slope during the last 50,000 years. If anything, the finer-grained texture of Wisconsinan muds suggests that local dynamic conditions were generally less energetic at that time than at present.

Bottom conditions at the shelf-break could have been more vigorous at a time of lowered sea-level as a result of storm-wave impingement. Storm-induced bottom currents may have resulted in greater spillover (Stanley et al., 1972) in the Scotian Gulf area. However spillover deposits would still be controlled by the local bottom current regime and would produce a more sheet-like deposit.

A strong argument in favour of a turbidite origin for the thick-bedded sands is the association with channels (see Fig. 7-2). Core 50 is located on the margin of the main channel and core 62 in a well-developed channel between two large slide blocks. This strongly suggests that the sand was transported through the channels. Core 2 is not well-located, but was recovered from below the steep upper-slope escarpment in an area of rough topography.

The facies is similar to the massive sandstone facies of Walker (1979), characterised by thick beds, which may amalgamate to form multiple beds and poorly-developed grading. In Walker's deep-sea fan

model, this facies is placed in the channels of suprafan lobes. Upper fan channels are more characteristically conglomeratic. The lack of gravel in these cores may be partly a sampling problem. The Scotian Gulf shelf and slope certainly provide a gravel-rich source. On the other hand, the cores are located at the channel margins rather than in the channel axes. The fact that the sand is well-sorted does require that considerable sorting of sediment occurs in the early stage of turbidity-current flow.

Facies 7 and 8 are more problematical as they cannot be directly related to the channel. Their size distributions suggest that they were each deposited under rather different dynamic conditions.

In core 54, Facies 7 sand underlies Facies 8 sand at two horizons, to form single graded beds. In core 57, the thin basal unit of a Facies 8 sand is relatively well-sorted and coarse-grained (Fig. 6-7a). These examples strongly suggest the turbidite origin of the two sandy facies, but for the most part, the two facies are not directly associated. They are therefore considered separately and in more detail.

Facies 7 is well-sorted and was deposited from strong currents maintained over the period of deposition, which did not allow fines to settle out. The inevitable turbidite or contourite question must be asked. Stow and Lovell (1979) have summarised the criteria used to distinguish thin-bedded turbidites and contourites by many authors. They point out that almost all the textural and lithological criteria

are ambiguous. For example, contourites are in general better-sorted than turbidites, yet well-sorted turbidites have been described by many authors (eg. Piper and Brisco, 1975). Even paleocurrent determinations can be confusing because overbank turbidites would give similar current directions to contourites. On the slope with such complex topography, paleocurrent directions from turbidites would be very complex.

Two other arguments can be made to support a turbidity current origin for Facies 7.

(i) Facies 7 sands show very similar textural characteristics to the thicker-bedded sands of Facies 6. The modal size of 2.0 to 3.0  $\phi$  (Fig. 6-5) is similarly out of equilibrium with reasonable current regimes for both the present day and the late Wisconsinan.

(ii) Bed thicknesses are variable and are as great as 25 cm. Most contourites from dominantly muddy environments are thin (Stow and Lovell, 1979) and represent winnowing of finer sediments.

It seems likely that the sand of Facies 7 was introduced by turbidity currents. Later reworking by bottom currents is of course possible, but no other facies (eg. Facies 9) have undergone this process, and it is more reasonable to conclude that the facies is a primary turbidite deposit.

The muddy texture of Facies 8 sands almost excludes them from the possibility of being contourites. The massive and graded beds together with the textural similarity to the graded silts of Facies 5,

strongly suggest that most Facies 8 beds are turbidites. Some have been bioturbated, a feature not usually associated with turbidites. However, some clear examples of bioturbated turbidites have been documented (eg. Piper and Marshall, 1969) so that it is not an objection to the turbidite interpretation.

The internal deformation shown by some beds (Fig. 6-7e) may be syndepositional (convolute bedding) or post-depositional (slumped). Reineck and Singh (1975) note that convolute bedding is most often observed in a fine sand or silty sand sediment. Many flysch sequences show abundant examples of it (eg. the Meguma rocks of Nova Scotia) (Harris and Schenk, 1975). In the case of the bed shown in Figure 6-7e, syndepositional convolution is probably the correct interpretation. The deformation is only seen in the central part of the bed between apparently undeformed sediment.

In conclusion, Facies 6, 7 and 8 are all interpreted as turbidite deposits. In the nomenclature of Bouma (1952) and Walker (1979), Facies 6 consists of A.A.A. sequences, Facies 7 of A,B and AB sequences and Facies 7 of ?C,D and DE sequences. In addition, fine-grained Facies 5 couplets consist of DE sequences. Only rarely are Facies 7 and 8 combined to give more complete Bouma sequences.

#### (b) DEBRIS FLOW DEPOSITS

Facies 9 has the poorly sorted gravelly sandy mud texture which is characteristic of subaerial and submarine debris flows (Johnson,

1970; Hampton, 1970; Crowell, 1957). However in northern latitudes, similar lithologies can be produced at the base of a grounded ice-sheet (marine tills), or offshore, by the combination of normal marine sedimentation and deposition from floating ice and icebergs (paratills; Harland et al., 1966; Kurtz and Anderson, 1979). Marine tills can be discounted in the deep-water slope environment, but it is necessary to determine whether the gravelly sandy muds of Facies 9 are debris flow deposits or paratills. Several criteria have been established as being useful for this purpose (Table 6-1).

Facies 9 beds are massive, have sharp boundaries (Fig. 6-8) and "single-population" grain-size distributions (Fig. 6-9) with few indications of current-sorting. The largest pebbles are generally oriented with their long axes subhorizontal (Fig. 6-11). The facies contains significantly fewer foraminifera per unit weight than the surrounding muds and almost completely lacks planktonic species or juvenile benthic tests (M.A. Williamson, pers. comm.). In addition, the facies is characteristically indurated, suggesting early (? syndepositional) expulsion of interstitial water. Facies 9 can thus be confidently interpreted as a debris flow deposit. Dispersed ice rafted debris is common within some mud sequences and is easily distinguishable as such.

The sandy laminae observed within two beds (see Fig. 7-4, Cores 73 and 75) are of interest. Subaerial debris-flows have been observed to flow in a series of surges (Johnson, 1970; Pierson, 1980). Between viscous, laminae flows, turbulent slurry flows may occur along the same

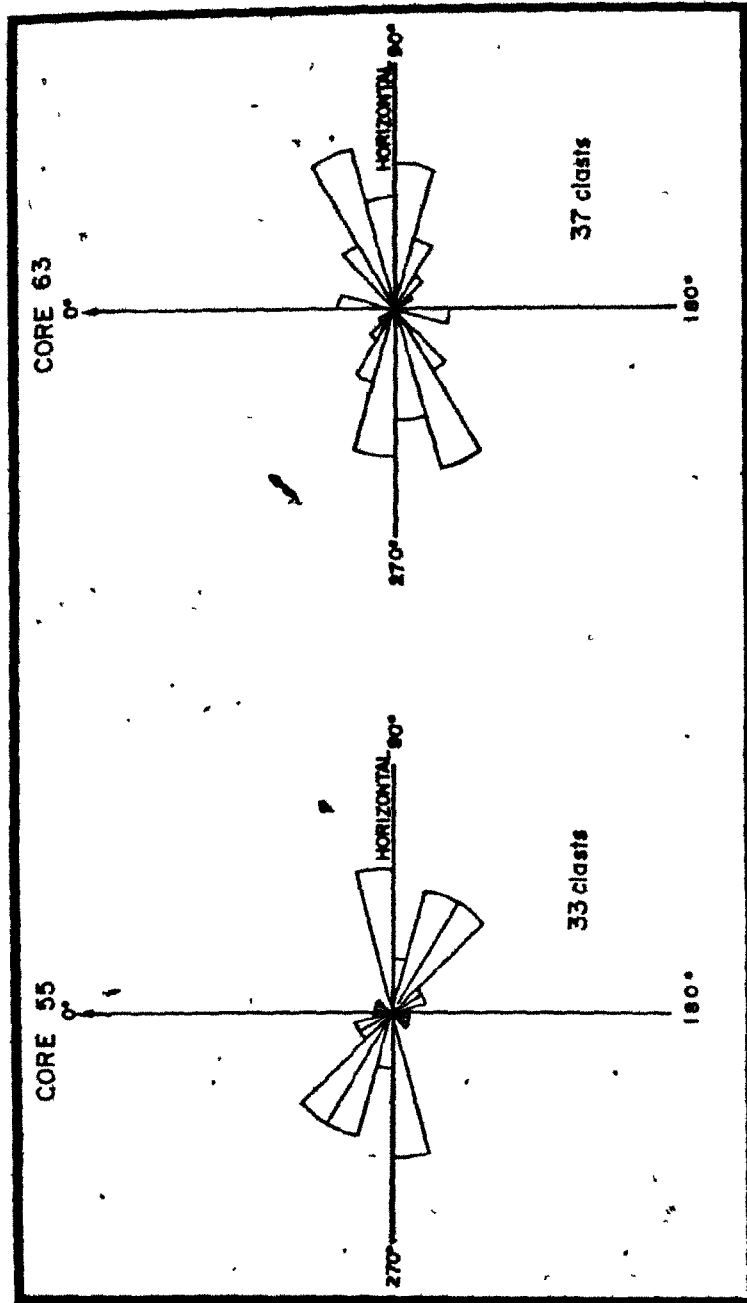


Table 6-1. Criteria for distinguishing paratills and debris flows (modified after Kurty and Anderson, 1979; and Aksu, 1980).

TABLE 6-1

CRITERION	DEBRIS FLOWS	PARATILLS
1. Contacts	Sharp	Gradational
2. Faunal content	Rare, or if present, displaced fauna.	Normal in situ assem- blage.
3. Fabric	Imbricated or sub- horizontally ori- ented clasts.	Randomly to horizontally oriented clasts.
4. Texture	Single population.	Multiple populations.

Figure 6-11. Orientation of elongate clasts  $> -1 \phi$  in vertical section of thin gravelly sandy mud beds from cores 55 and 63.



channel with velocities as high as  $5 \text{ m s}^{-1}$ . These flows are capable of sorting and leaving lag deposits (Pierson, 1980). A similar mechanism could be envisaged to explain the sorted laminae within single debris-flow beds on the Scotian Slope. However, the submarine environment provides somewhat different controls on these processes. For example, shear at the upper surface of such a flow would be much higher, tending to suspend the slurry. Also the generation of submarine debris flows is poorly understood; the likelihood of turbulent surges of this type cannot be well estimated.

#### (c) SLUMP DEPOSITS

The deformed beds of Facies 10 are probably produced by relatively small-scale slumping. Damuth and Embley (1981) have illustrated similar deposits in deep-sea cores and there are numerous examples in the ancient record (Cook, 1979, Enos, 1969; Stanley and Unrug, 1972). It is interesting that many of the deformed beds contain lenses of clean sand which has not been mixed during the slumping. This indicates that either the transport distance of the slump was very small, or that the sand has a brittle resistance to shearing processes within the slump. Well-packed, wet sand enclosed in a muddy slump-mass and sheared, would exhibit dilatancy when repacking of the grains occurs. As the pore volume increases, the inter-granular forces also increase and the sand behaves in a more brittle fashion. Thus discrete patches of sand as seen in Figure 6-10 can be maintained.

## CHAPTER 7

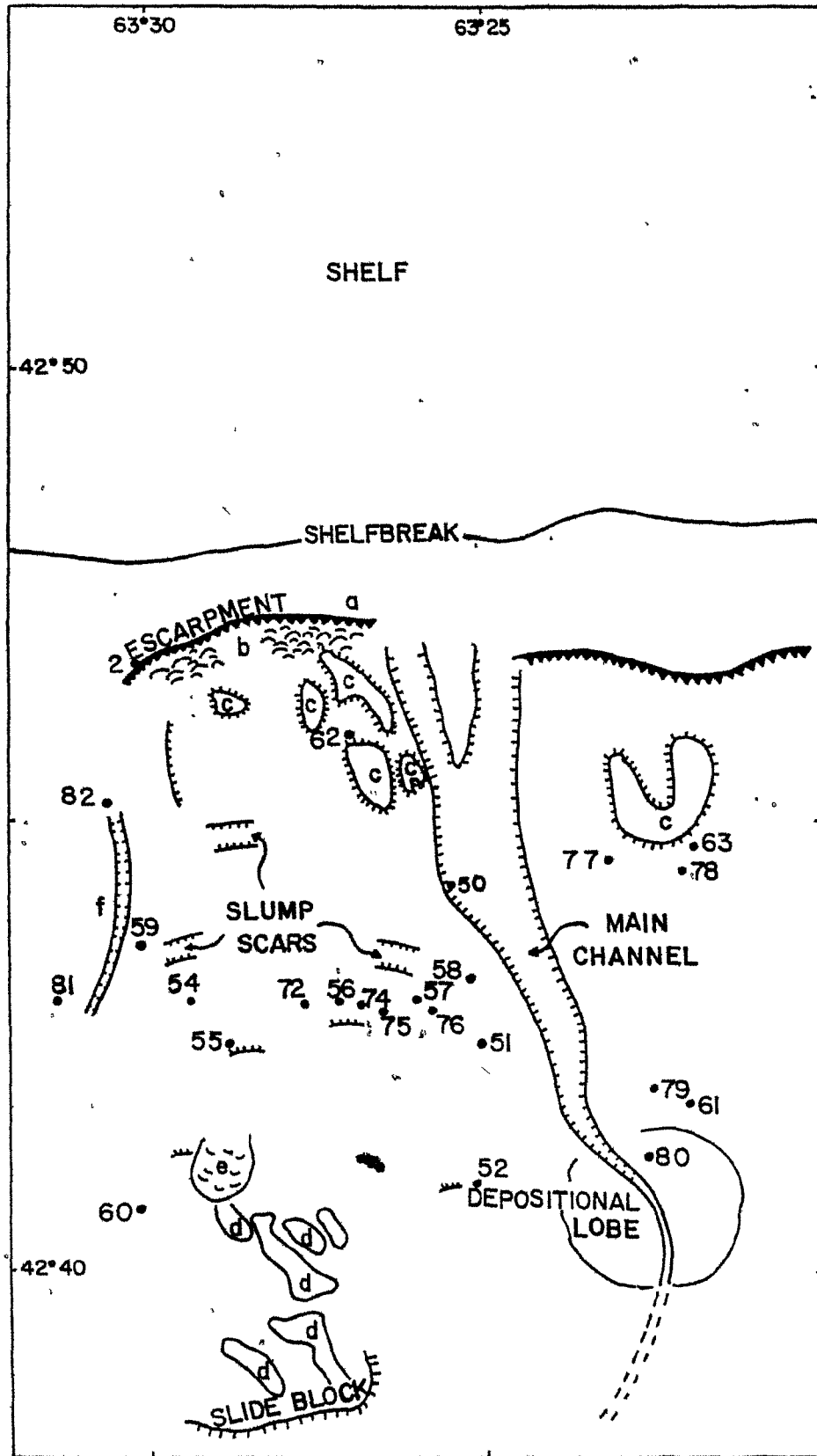
DISTRIBUTION OF FACIES IN THE SCOTIAN GULF AREA

The Holocene (Unit 2) sequence on the Scotian Slope is very uniform, even in areas of complex mesotopography. This chapter concentrates on the pre-Holocene (Unit 1) sequence in which a great variety of facies is found. Correlation of individual beds in Unit 1, between even the most closely-spaced cores in the study area, is impossible and the facies distribution initially seems random. Detailed study, attempting to relate individual core sequences to their morphological situation suggests that some patterns are present.

Figure 7-1 shows the location of piston-cores with respect to the major morphological features and figures 7-3 to 7-8 illustrate core logs from the Scotian Gulf area. Seismic profiles or 12 KHz echo-sounder records are provided to locate each core as closely as possible to the local mesotopography. Few cores are longer than 5 metres, so it should be emphasised that they cannot be related to sub-bottom features illustrated in the seismic profiles.

The accuracy of core locations on the profiles is controlled by several factors. The ship and core positions, for the most part were determined using Loran C and Satnav and are believed accurate to  $\pm 100$  m, but prior to 1980, Loran C was unavailable and much less accurate Decca navigation was used. The deep-tow profiles required adjustment for the fish position, which was a significant distance behind

Figure 7-1. Location of piston cores in the Scotian Gulf area with respect to major morphological features.



the ship. The actual fish position is not exactly known, but can be estimated and the potential error is not greater than 300 metres. Where coincident echo-sounder profiles were taken, the tow-fish position and morphological features on the profile can be located without this error. Finally, some cores were not always taken exactly on the profile lines, and because of the complex morphology, they cannot be clearly related to morphological features on the profiles.

On each diagram, an indication of the confidence with which a core is located on a profile is given. Figure 7-2 provides a key to the symbols used.

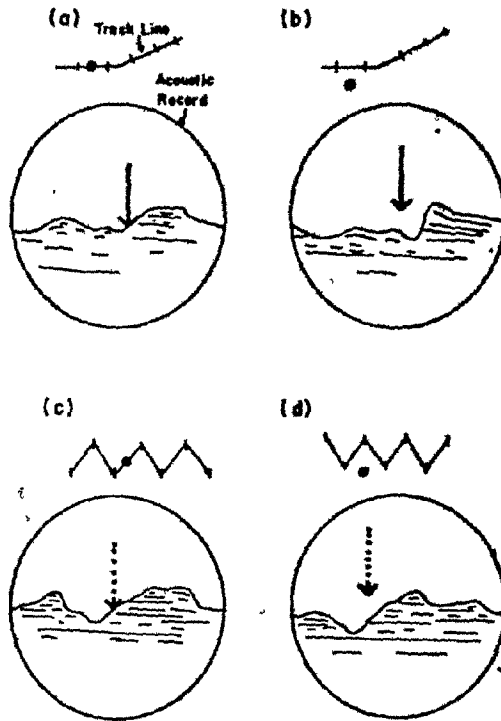
#### UPPER SLOPE AND CHANNEL ASSOCIATION

Cores from the upper slope, high relief area (2, 62, Fig. 7-1) and from the main channel margin (50, Fig. 7-1) contain a similar association of thick sand beds and intervening thick mud units (Fig. 7-3). The mud facies between thick sand beds is variable. In cores 2 and 50 laminated mud and graded silt beds are found, while in core 62, the mud is mainly bioturbated.

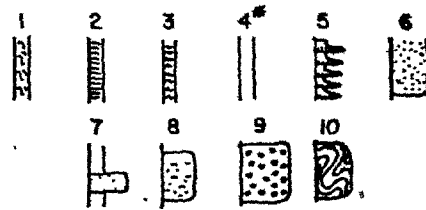
The three cores are not accurately located with respect to meso-topography. However, core 62 appears to be located between major slump-blocks, both on the GLORIA profiles (Fig. 7-1) and the seismic profiles (Fig. 7-1). Core 2 is apparently located very close to the main escarpment (Fig. 7-1), its water-depth of 500 metres suggesting a position just at the base, within the area of hummocky relief, rather than its apparent position at the top of the escarpment. Core 50 is located within the main channel, probably just on the channel margin.

Figure 7-2. Key to Figures 7-3 to 7-8, indicating reliability of survey navigation and core positioning:

- (a) Solid arrows in contact with bottom trace: accurately located core and profile, with core positioned very close to the profile line.
- (b) Solid arrows not in contact with bottom trace: accurately located core and profile, but position of core is a significant distance from the actual profile line.
- (c) Dotted arrows in contact with bottom trace: inaccurately located core and/or profile, position of core apparently close to profile line.
- (d) Dotted arrow not in contact with bottom trace: inaccurately located core and/or profile, position of core apparently distant from actual profile line.



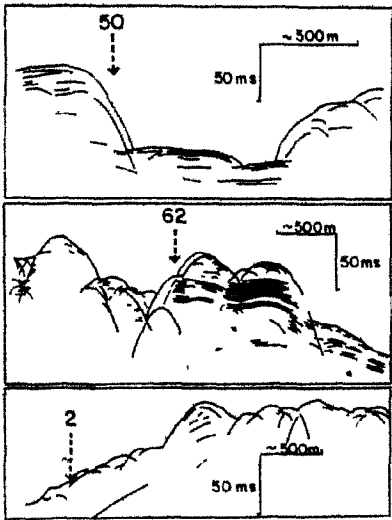
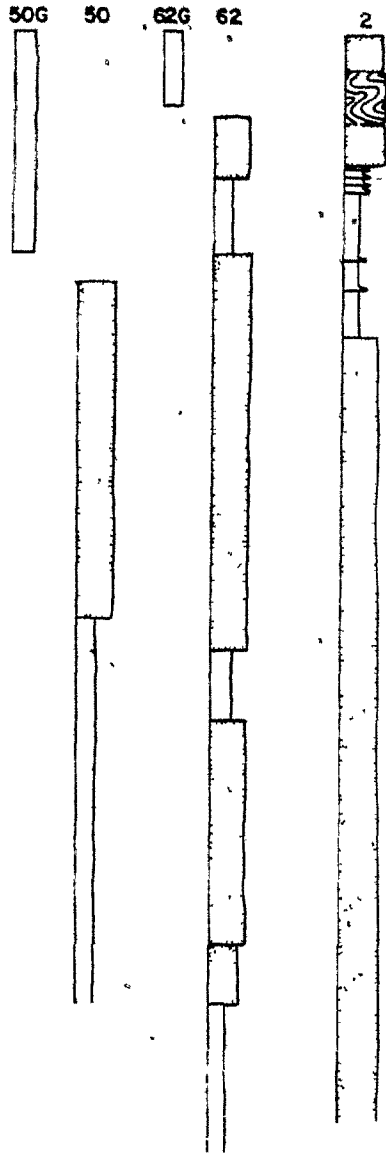
FACIES



\* Includes undifferentiated mud.

7

Figure 7-3. Facies sequences and locations of cores from the upper slope and main channel. G = gravity trip core. Key in Figure 7-2.



MID-SLOPE FACIES ASSOCIATIONS

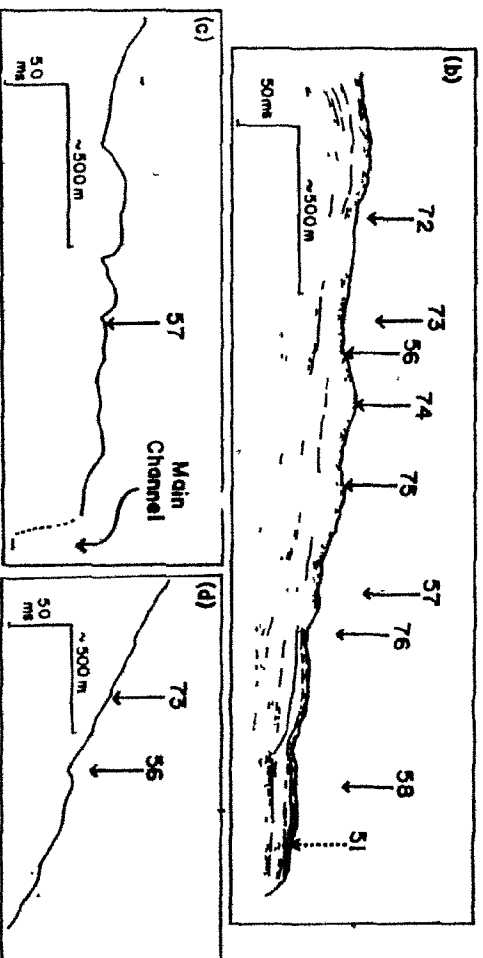
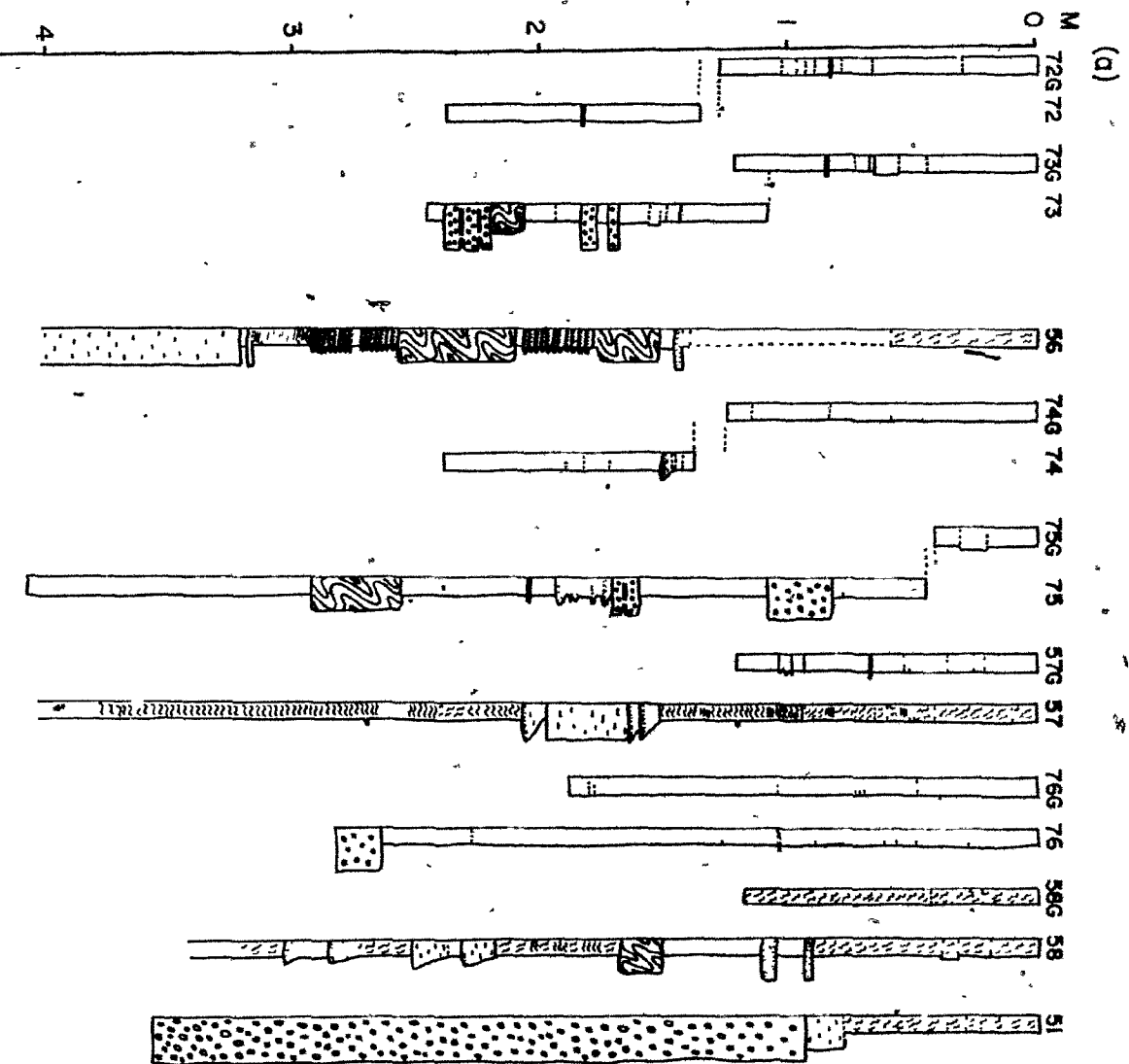
Mid-slope core sequences are characterised by the association of Facies 5 graded silt beds, with thin sand beds of Facies 7 and 8 (Figs. 7-4 to 7-7). Facies 1 to 4 muds are all present in places, making up anything from 20% to 90% of individual sequences. Thin units of Facies 9 and 10 are also present in the sequences, and three cores bottom out in the gravelly, sandy mud of Facies 9.

Figure 7-4 shows a detailed suite of cores clustered around profile N-N'. Both the seismic line and the cores are accurately positioned and the cores have an average spacing of between 0.5 and 1.0 km. Three cores are located almost exactly on the seismic line and coincident 12 KHz profile; core 56 is located in the deepest part of a broad depression, while cores 74 and 75 were taken on two adjacent low hummocks (Fig. 7-4b). The three cores show distinctly different facies compositions.

Figure 7-4(d) also shows the position of core 56 on a downslope profile. Although the core is not accurately located on this profile, the nature of the depression can be more clearly seen. It is located just upslope from a well-defined slide sheet and either represents the zone of detachment for that slide or lies between the slide sheet and smaller slump/slide-related hummocks upslope of it.

Core 56 from the depression contains only thin muddy intervals, but is dominated by three bundles of Facies 5 graded silt to mud couplets (and triplets). Two slumped units (Facies 10) and a single thin bed of Facies 7 sand are also present. The bottom of the core penetrates

Figure 7-4. Facies sequences and locations of cores from the mid-slope area, along seismic profile N-N'. (a) Core logs, (b) line drawing of part of seismic profile N-N', (c) and (d) 12 KHz echo sounder profiles.



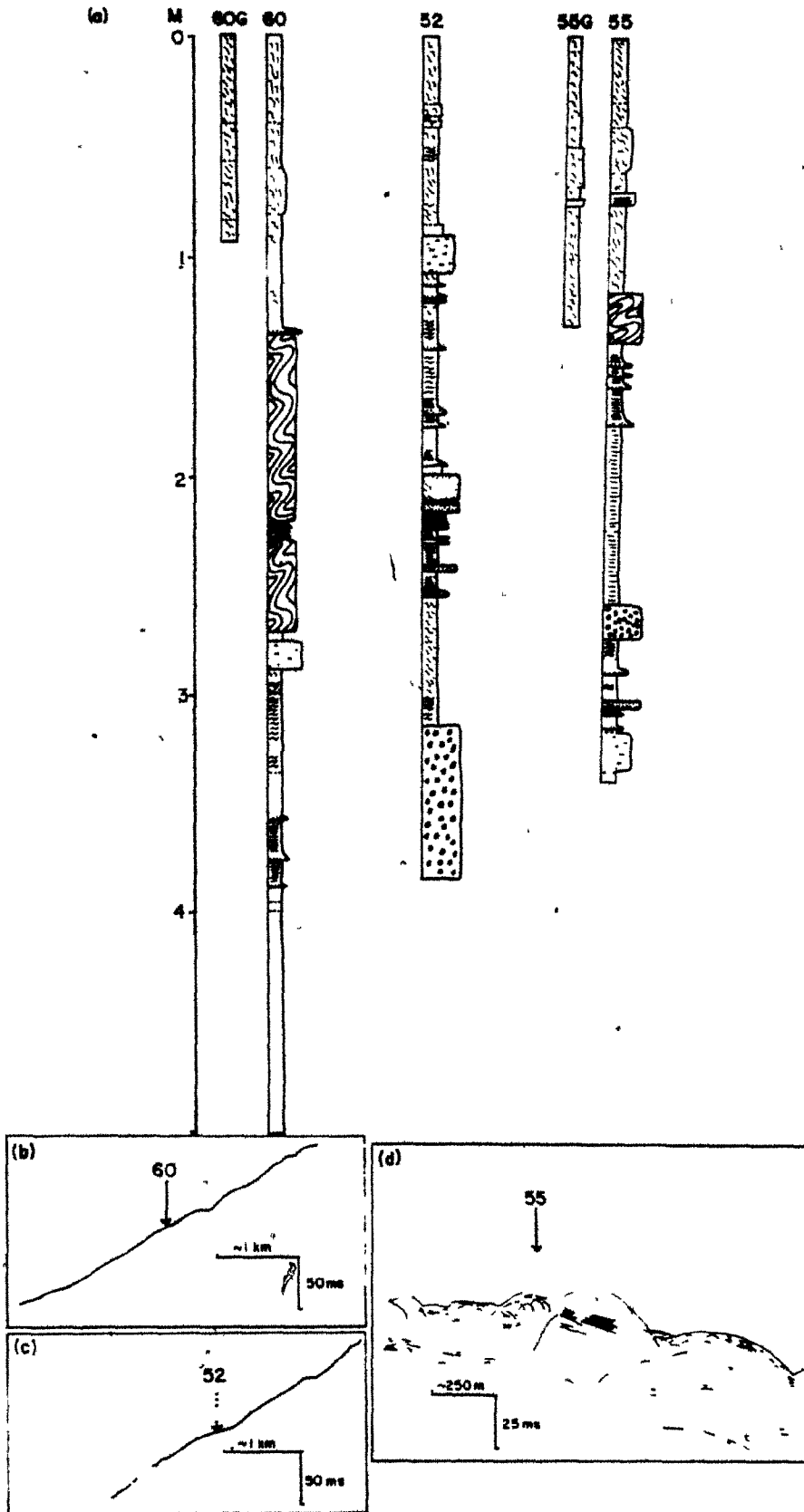
a thick unit of Facies 8 muddy sand.

Cores 74 and 75 from the hummocks contain a higher proportion of mud than core 56 (Fig. 7-4a). Isolated units of Facies 7 and 8 sands, Facies 5 silts, slumped beds (Facies 10) and/or gravelly sandy mud beds (Facies 9) are also present in these cores, but occur between thick mud intervals.

Cores 57 and 73 lie very close to 12 KHz profiles (Fig. 7-4c and d). The former is located on the low-relief, broadly hummocky area adjacent to the main channel (Fig. 7-4c) and contains a thick mud sequence dominated in the lower part of the core by Facies 7 laminated mud. Three thin, distinctly graded units of Facies 8 sand and Facies 5 silt to mud couplets and a thicker ungraded bed of Facies 8 form a bundle of beds in the middle of the core. Core 73 is located in the hummocky area just upslope of core 56 (Fig. 7-4d). Although dominantly muddy, it contains three thin beds of Facies 9 and a single bed of Facies 10. The core is unique in the respect of containing several beds of Facies 9, which is otherwise found in isolation within single core-sequences.

Cores 52 and 60 (Fig. 7-5) are located a short distance downslope of the suite of cores just described. They show very similar types of disorganised sequence. Two relatively thick slump beds are prominent in core 60 which is located on a low relief hummocky area (Fig. 7-5b). Core 52 is located close to a between-slump depression (Fig. 7-5c) and contains a relatively large proportion of coarse beds. Particularly abundant are graded sequences of Facies 2 and 5, but perhaps more significantly, the core contains three well-sorted sand beds of Facies

Figure 7-5. Facies sequences and locations of cores 52, 55 and 60 from south of profile N-N'. (a) core logs, (b) and (c) 12 KHz echo-sounder profiles, (d) part of seismic profile M-M'.



7 and a single bed of Facies 8 muddy sand. It is interesting that Facies 8 occurs only in cores from the deeper depressions (52, 56) and close to the main channel (58).

Three cores from east of the main channel are shown in Figure 7-6. Two of these contain single thin beds of Facies 7. The relief in this area is quite pronounced and the cores are not located close to seismic profiles so little can be said concerning the facies distribution in the three cores.

#### DEGRADED CHANNEL-MARGIN OR LOBE FACIES ASSOCIATION

The depositional lobe (fig. 7-1) was probably largely constructed by rapid deposition of thick sand units, in a fashion similar to deposition on suprafans (Normark and Piper, 1972). However, at present, the main channel is thought to completely cross the lobe. For this reason, sediments recovered from the lobe area (Fig. 7-7) are not representative of the main lobe-building phase; rather they represent deposition in an environment close to a degraded and probably unequilibrated channel.

Cores 79 and 61 are located on the outer fringes of the lobe (Fig. 7-1), 79 in a broad erosive depression (Fig. 7-7c) and 61 on a large hummock close by. They show strikingly different facies contents. Core 79 contains abundant Facies 5 silt/mud couplets with a thicker graded unit (Facies 8) and a thin Facies 7 sand bed near the base. Core 61, however, is almost 100% mud with a single coarser (Facies 5) lamina near the base. This demonstrates a similar relationship between facies and morphology as in mid-slope cores.

Figure 7-6. Facies sequences of cores 63, 77 and 78 from east of the main channel. The cores cannot be related to any survey lines.

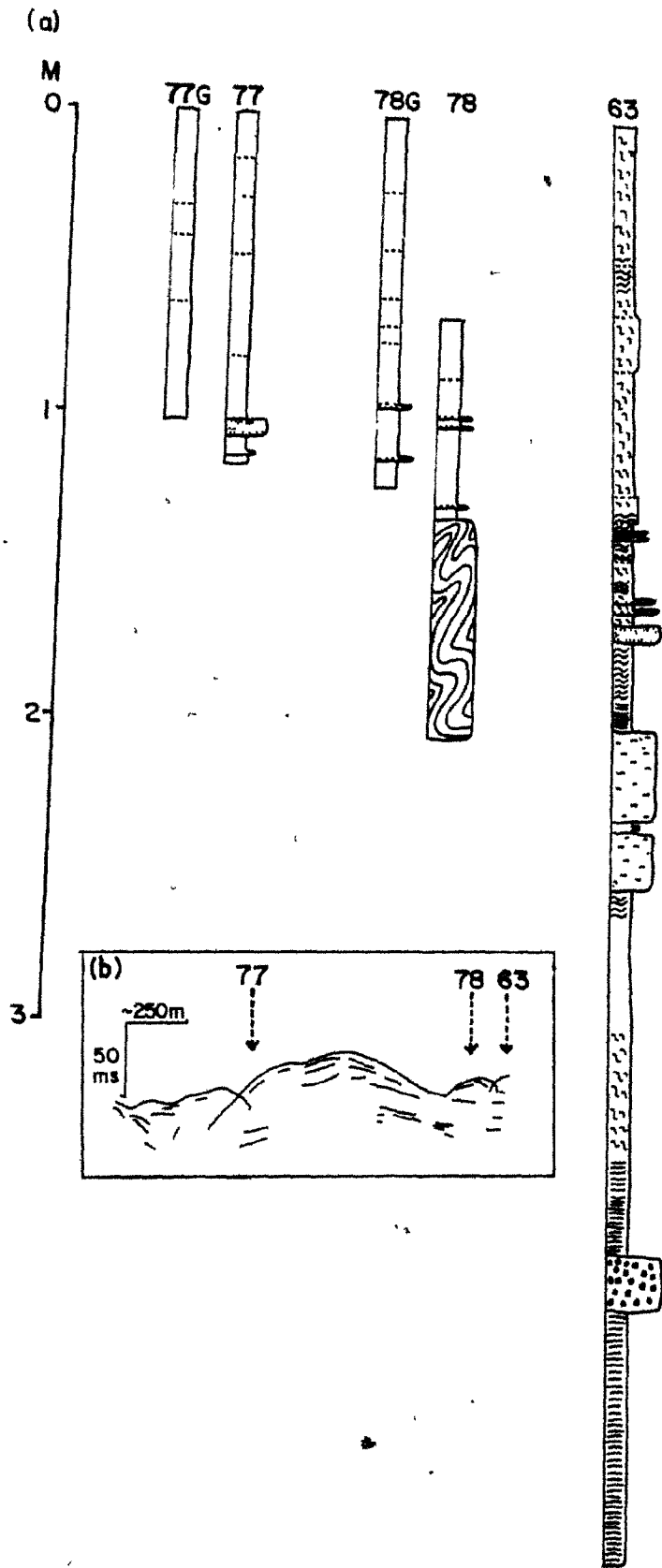
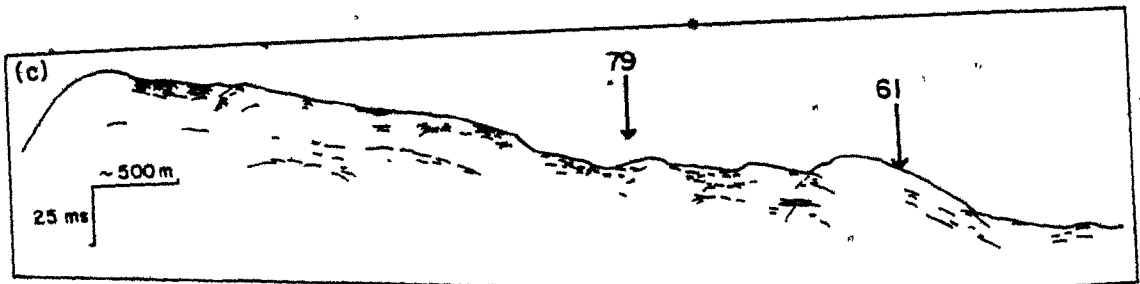
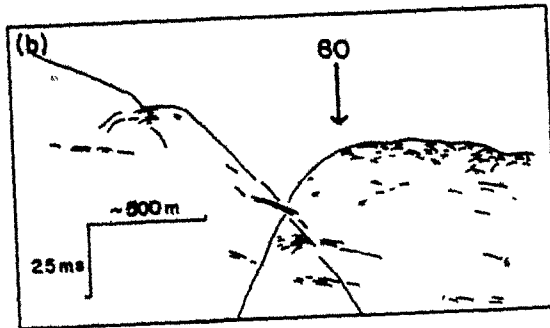
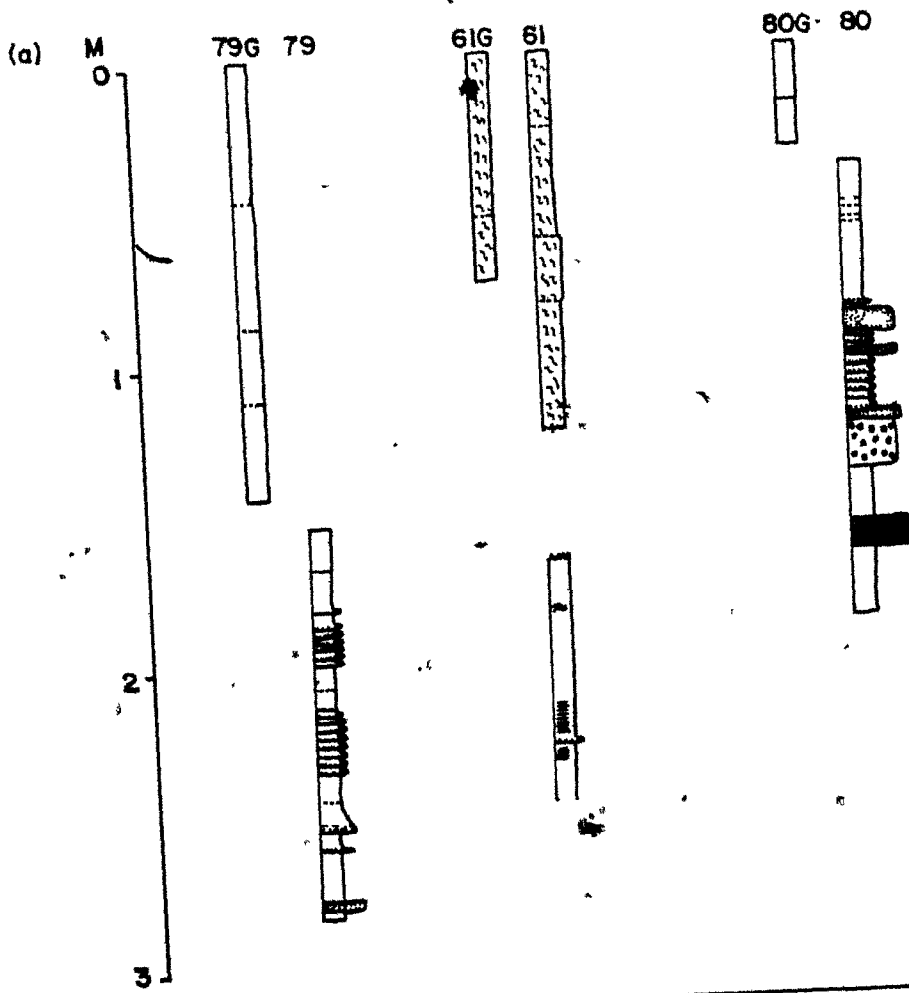


Figure 7-7. Facies sequences and locations of core 61, 79 and 80 from the depositional lobe area (a) core logs, (b) part of seismic profile 0-0', (c) part of seismic profile M-M'.



Core 80 (Fig. 7-7a) is situated very close to the degraded main channel (Fig. 7-7b) and contains a high proportion of coarse grained beds. Prominent among these are three well-sorted sand beds and a very coarse sand/gravel bed. Also within the sequence is a bundle of Facies 5 units and a single gravelly, sandy mud unit. This core clearly demonstrates that rapid sedimentation of coarse-grained sediments is associated with the channel in the area of the depositional lobe.

#### CONSTRUCTIONAL SLOPE ASSOCIATION

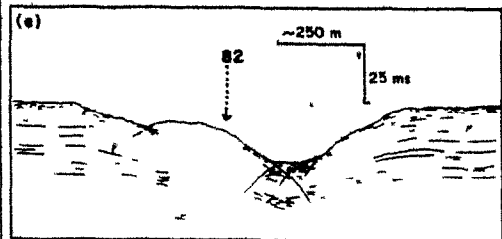
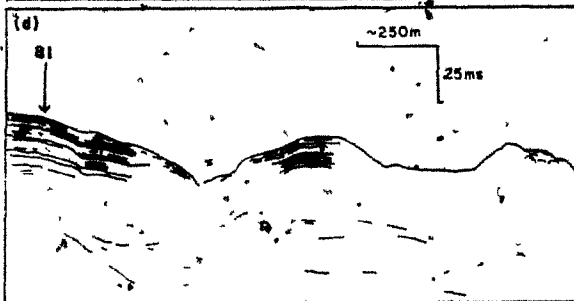
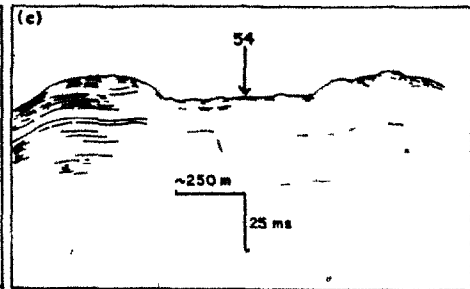
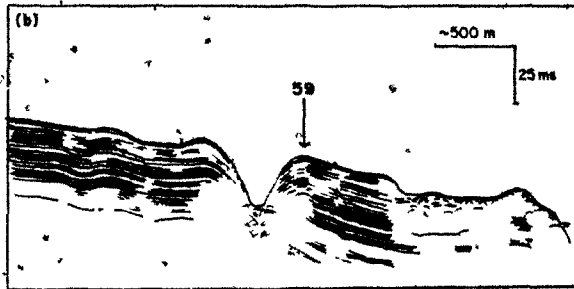
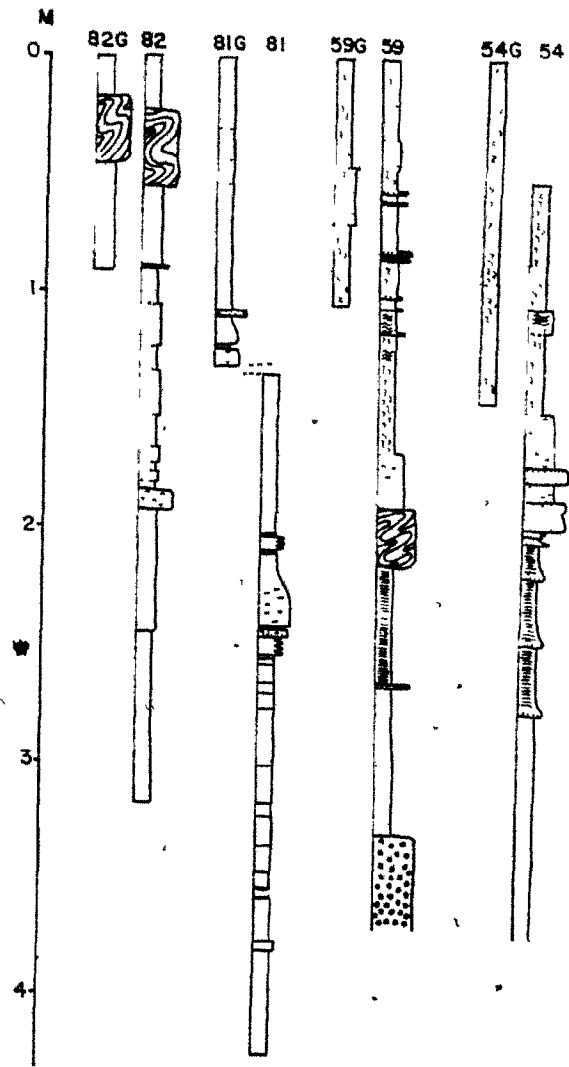
Core sequences in the vicinity of the area of smooth topography, in the west of the Scotian Gulf area (Fig. 7-1) are predominantly made up of bioturbated mud (Fig. 7-8). All three cores (59, 81, 82) are located close to the constructional channel and contain muddy sands of facies 8 and/or graded silt to mud couplets of Facies 5.

Cores 81 and 82 show broadly similar sequences of alternating olive-grey, red-brown and brown muds. The brown muds in the shallower core (82) are sandier and occasional sand and coarse silt laminae are preserved. Core 59 from the channel margin does not show the same alternation but contains a greater proportion of sandy beds or laminae and bottoms in stiff gravelly sandy mud of Facies 9.

#### SUMMARY AND INTERPRETATIONS

Figure 7-9 summarises the morphology-related distribution of facies in the Scotian Gulf area.

Figure 7-8. Facies sequences and locations of cores from the constructional slope area. (a) core logs, (b) part of seismic profile L-L', (c) part of seismic profile N-N', (d) part of seismic profile M-M', (e) part of seismic profile J-J'.



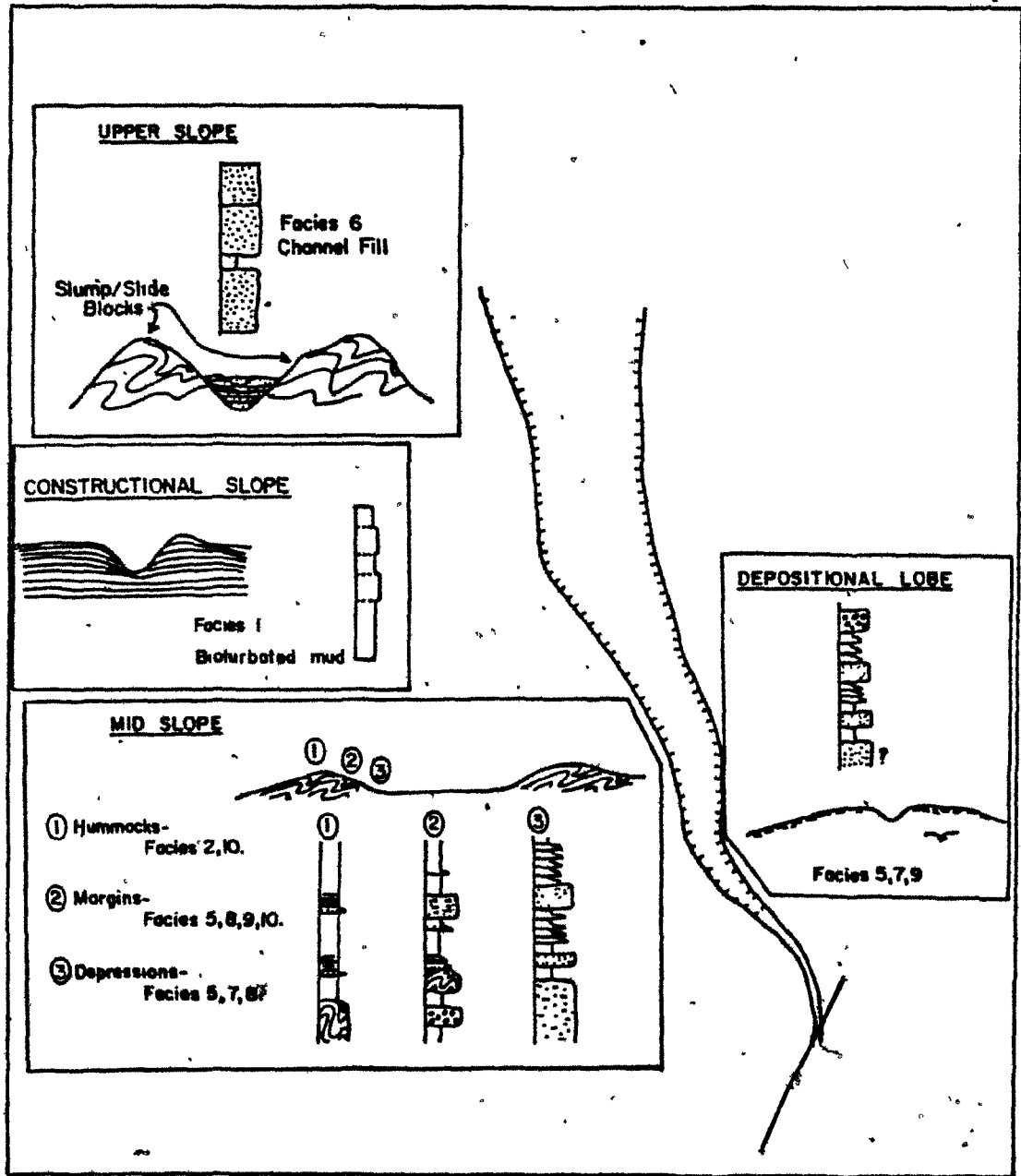


Figure 7-9. Summary of morphological regions and their characteristic facies association, Scotian Gulf area.

On the upper slope, the association of thick sands and various muds are characteristic of the valleys between large slump or slide blocks. The thick sands have been interpreted as Bouma turbidite units (Chapter 6) and are evidence that turbidity currents flowed down these upper-slope valleys. Individual flows were separated by periods of time when mud accumulated, suggesting that flows through these valleys were intermittent. The valleys may have acted as tributaries to the main channel as suggested by a GLORIA profile (Fig. 2-10), but there is also evidence that turbidity currents flowed onto the midslope area.

Sequences on the destructional midslope area are very variable, but where it is possible to locate cores in relation to morphological highs and lows, it can be said that coarser beds are more common in the depressions, while the hummocky areas are draped with finer sediment. The coarser beds are interpreted as turbidite deposits. The topography probably controlled the paths of turbidity currents which flowed either from upslope or from overspill of the main channel, and deposition of coarser sediments at the base of the flow occurred preferentially in the depression.

Coarse sand was also transported down the main channel, and is deposited on the channel margins. Thick sand beds probably also accumulated where the channel narrowed to form a depositional lobe which the channel now crosses. Overspill of this shallower channel resulted in coarse sand and gravel beds on the margins. More distal parts of the lobe contain sequences similar to other midslope areas as a result

of subsequent slumping and generation of an irregular topography.

On the undisturbed slope, bioturbated muds dominate except very near to the constructional channel. Coarser beds in this area are turbidites and probably related to the local channel. It is not clear, however, whether this area is completely immune from flows in the adjacent destructional area and main channel.

CHAPTER 8DISCUSSION: CONSTRUCTIONAL SLOPE PROCESSES

In the two study areas of the Scotian Slope, constructional morphologies are present (a) at the western margin of the Scotian Gulf area and (b) in the eastern half of the Western Bank area. They are acoustically uniform areas, showing smooth sediment surfaces and continuous sub-bottom reflectors (Fig. 2-23). Only three piston cores are available in the Scotian Gulf constructional area, but they show strikingly different sequences below the Unit 2 cover from cores in the destructional parts. The sequences comprise alternations of red-brown and brown lithologies (Fig. 7-8) on a scale of 10-20 cms. The patchy or mottled mud facies predominates, suggesting hemipelagic processes are most important. Core 82 from 500 metres water depth contains sandier brown and olive grey units (Fig. 7-8), which although bioturbated may be related to turbidity currents. However, the equivalent browner and greyer beds downslope (core 81) have no clear turbidite characteristics, although this core from close to the constructional slope channel (Fig. 7-8) does contain other sandy beds which are interpreted as turbidites. The sandier beds of core 82 are thus thought to be more related to hemipelagic processes rather than turbidity currents.

The processes involved in constructional slope sedimentation are not restricted to these areas of the slope which have not been disturbed by slumping or other destructional processes. By and large, hemipelagic

type sedimentation is independent of slope morphology. Thus, this discussion can be made broader to include that part of destructional sedimentation which is not related specifically to the morphology. Thus, the Holocene mud drape over the slope and intervals of non-turbidite mud sedimentation within the Wisconsinan sequence can be considered as constructional phases and the following discussion pertains to these intervals as well as constructional slope sequences per se.

The processes involved in hemipelagic sedimentation are not very well understood beyond the conceptual models illustrated in Pierce (1976, see Fig. 5-12). Systematic textural variations in the very uniform modern sedimentation, discussed in Chapter 3, can be related mainly to dynamic conditions, but the downcore variations in cores 81 and 82 particularly, indicate that other factors are important. Sediment supply rates, transport paths and transport mechanisms are identified as controls on "hemipelagic" deposition in addition to the local dynamic conditions.

#### (a) Sediment Supply Rate

The rate of sediment supply from individual sources determines the dominant compositional characteristics of the sediment. Cores show a stratigraphic division between a late Wisconsinan unit, dominated by red-brown and brown muds, and a latest Wisconsinan/Holocene unit characterised by olive-grey and dark yellow-brown muds. Although gradations are common, it is simplest to consider the controls on the end-member red-brown and olive-grey lithologies and the broad

differences between Holocene and Wisconsinan conditions.

The inferred ice-sheet supply of red-brown mud is restricted to the Wisconsinan glacial period, although reworking of coastal and inner-shelf tills may have contributed some red-brown mud since deglaciation. However, the lack of olive-grey sediment in the Wisconsinan should be accounted for. The shelf-edge supply of olive-grey sediment would be largely controlled by relative sea-level. A maximum sea-level lowering of 110 metres (King, 1970) would leave large areas of the outer-shelf banks subaerially exposed (Fig. 1-9). The area then available for reworking and supply of mud would be substantially reduced, resulting in a large decrease in supply of olive-grey sediment during the Wisconsinan.

Less extreme sea-level lowering would allow greater supply of olive-grey mud to the slope at least along the southern half of the continental margin. The sedimentation rate (and presumably supply rate) of Wisconsinan red-brown sediment was approximately twice that of Holocene olive-grey mud so that the outer-shelf bank supply may be masked by the ice-sheet supply. However, the data argues more strongly for a substantial decrease of olive-grey sediment supply during the Wisconsinan. This argues also for the more maximal sea-level lowering of 110 metres. Other factors such as storm regime and the effect of a floating ice shelf during the Wisconsinan may also play an important role in restricting olive-grey sediment supply.

(b) Sediment Transport Paths

Supply of olive grey sediments from the outer shelf banks to the slope is controlled by the net current regime on the shelf and slope. Periods of strong downslope flow are not common in the modern current regime (Fig. 3-2), but downslope transport of sediment is achieved by currents with essentially alongslope flow and small downslope vectors. Thus downslope transport is oblique and considerable alongslope transport is likely. Stanley et al. (1972) concluded that the shelf circulation patterns around Sable Island resulted in local zones of high sediment supply at certain points along the shelf-edge. However, alongslope transport as described above would largely smear out any local supply effects.

Wisconsinan supply of red-brown mud to the slope would have been controlled by sea-level and paleo-oceanographic condition. Transport across the shelf was largely by surface layer suspension (see Chapter 5), but exposure of large areas of the outer banks as a result of 110 metre sea-level lowering would restrict the supply from the ice-sheet to the narrow conduits of the Gully and the Scotian Gulf (Fig. 8-1). More moderate sea-level lowering would allow supply along a broader front with only Sable Island and Banqueréau Banks preventing sediment supply to the slope (Fig. 8-1). The effects of seasonal ice-cover over the shelf (Mudie, 1980) would be to restrict sediment transport to summer months, a feature one could not hope to detect in the slope record.

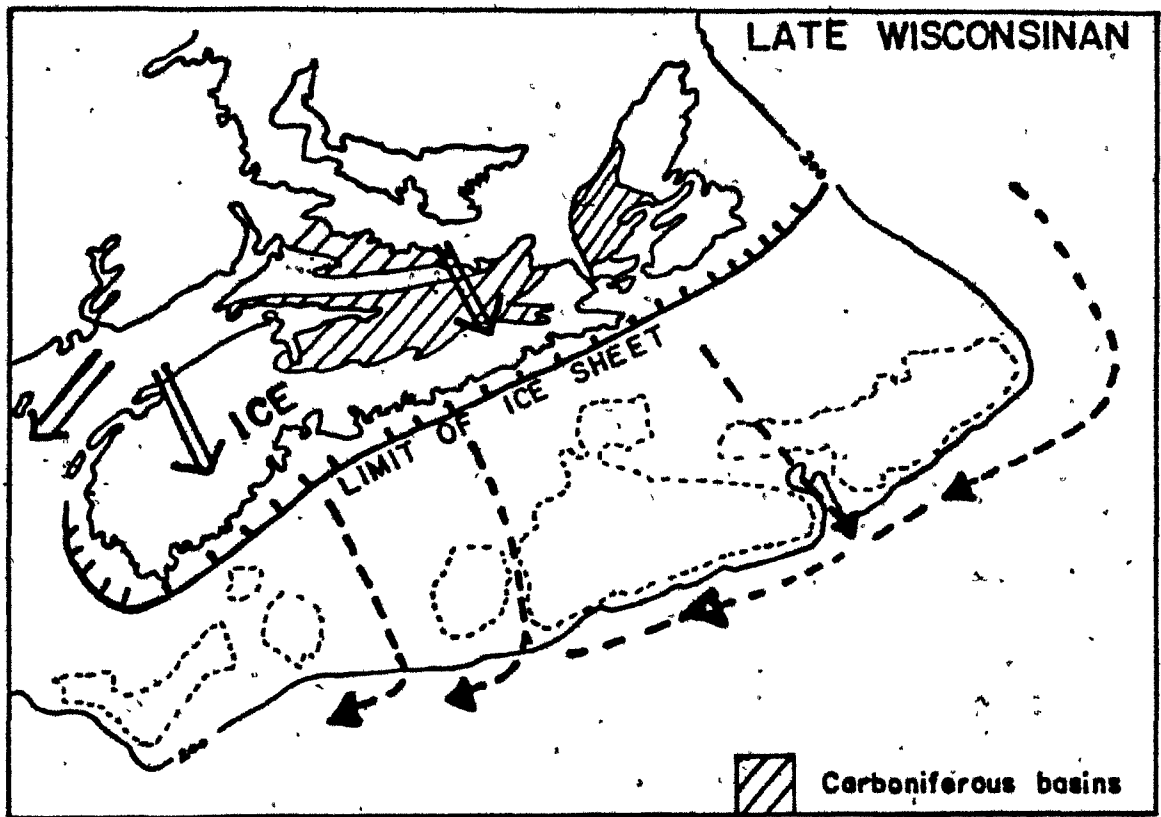


Figure 8-1. Wisconsinan transport paths of red-brown mud

(c) Slope Transport Mechanisms

It has been suggested in Chapter 5 that olive-grey and red-brown mud are transported from the shelfbreak by different mechanisms. Olive-grey mud, eroded from the outer shelf banks is transported in the bottom boundary layer, while red-brown mud, supplied mainly in the surface layer, is transported over the slope also in the surface layer and eventually settles through the entire water column (Fig. 8-2). In both cases, sediment must settle through the bottom boundary layer prior to deposition so that the net result should be similar. The finer-grained character of the red-brown mud may be related mainly to the long transport distance before reaching the slope. However, the red-brown mud is deposited in upslope areas (eg. cores 2 and 82) where the modern current regime would prohibit substantial mud deposition. This suggests that a less powerful current regime may have existed during Wisconsinan times.

Low salinity water covering the shelf during Wisconsinan times as implied by Mudie's (1980) data (see Chapter 5), and sea-level lowering near the maximum 110 metres of King (1970) would mean that sediment laden surface water moving offshore would not encounter open ocean conditions until it crossed the shelfbreak. An analogous situation exists at the mouths of many rivers where fresh water encounters saline marine water (Wright, 1977). In most cases, a stable fresh water layer is maintained at the surface because turbulent vertical mixing is not significant (Bates, 1953). However, tide and wave action can rapidly

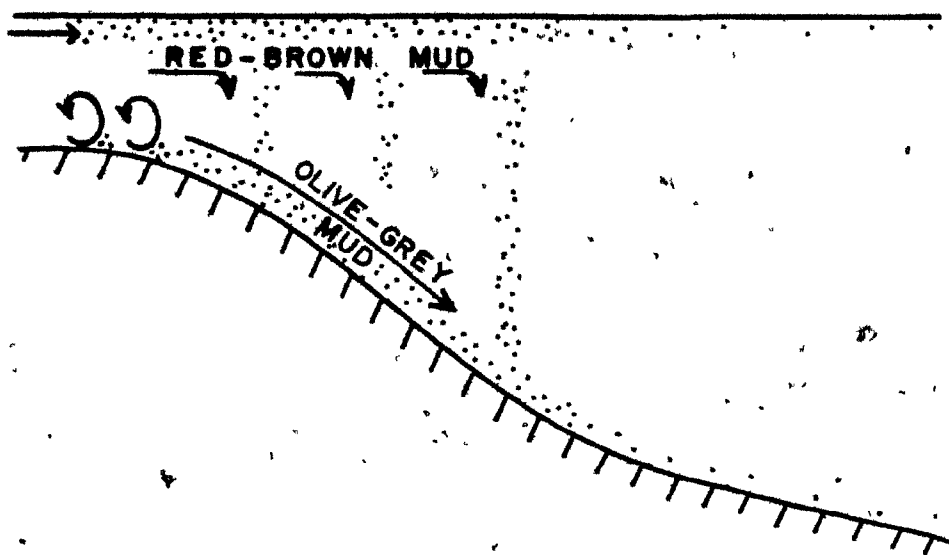


Figure 8-2. Slope transport mechanisms for red-brown and olive-grey sediment. Based on models in Pierce (1976).

mix the surface layer and prevent further offshore transport.

Kranck (1981), working in an estuarine environment, found that flocculation of suspended particles has a stronger relationship to concentration and turbulence than to salinity. Thus, by analogy, the increase in turbulence as the low-salinity surface layer encountered open ocean conditions at the shelf-edge may have resulted in increased flocculation and rapid deposition of red-brown mud on the slope, during the Wisconsinan. With maximum sea-level lowering, this may have been particularly important in the vicinities of the Scotian Gulf and the Gully.

#### THE ROLE OF CONSTRUCTIONAL SLOPE CHANNELS

The Scotian Gulf constructional area contains a 30 metre deep depositional channel (Fig. 2-8). Very few detailed surveys have been made of other constructional slope areas so it is not known whether such channels are common features of constructional slopes. The up- or down-slope continuity of the channel has not been established and, in fact, seismic line P-P' (Fig. 2-2) indicates that, if present, it must take a large westward deflection. Perhaps more likely is that the channel is discontinuous. Discontinuous gullies have been documented on delta-front slopes (Shepard and Dill, 1966) and they are thought to be of slump origin (Shepard, 1973; Coleman et al., 1974).

The clearly leveed nature of the western Scotian Gulf channel (Fig. 7-4) suggests that it is a stable feature and nearby cores contain turbidite units (Fig. 7-4). These features suggest that if the valley originally had a slump origin, it has more recently acted as a conduit along which turbidity currents have passed. The morphology

may have been modified in the process by channel-floor erosion and levee construction.

One particularly interesting aspect of the channel is the continuity of reflectors from the leveed channel margin to the adjacent slope (Fig. 7-4). The usual conclusion from this evidence would be that the adjacent slope has been largely built up by overbank turbidite deposition. Although nearby cores contain a few identifiable turbidite beds, the dominant lithology is bioturbated mud, even during late glacial times when turbidity-current activity was high in the adjacent excavated part of the Scotian Gulf area. It is generally assumed that hemipelagic processes construct continental slopes, while turbidity currents bypass them (Kelling and Stanley, 1976). Recently, however, attention has been drawn to the likely importance of dilute, low-velocity turbidity currents in canyons (Shepard et al., 1979) and on submarine fans (Stow, 1977). The theory for dilute turbidity currents, put forward by Stow and Bowen (1980), is based on the suspension settling model of McCave and Swift (1976). That model predicts a downslope decrease in modal grain-size, much as is observed in "hemipelagic" muds of the slope.

The begged question therefore, is what contribution do dilute turbidity-currents make to the construction of continental slopes? The evidence for dilute turbidity currents lies in current-meter records from submarine canyons (Shepard et al., 1979), which show periods of strong downcurrent flow disrupting the normal oscillatory current patterns. These velocities may reach over  $100 \text{ cm s}^{-1}$  and are sometimes

X

followed by a loss of record indicating even higher velocities. The likeliest explanation for these events is that low-velocity turbidity currents have flowed through the canyons, but the lack of contiguous measurement of suspended sediment concentrations precludes confirmation of this hypothesis.

In the examples studied by Shepard et al. (1979), the possible turbidity currents were generally preceded by strong upcanyon flow resulting in a unusual buildup of water at the canyon head. It is possible that a similar mechanism could exist in the smaller scale channels such as those on the Nova Scotian Slope. Although currents at the shelfbreak are predominantly alongslope, tidal oscillations sometimes dominate and periods of up- and down-slope flow are observed (Fig. 3-2). Although those flows generally have relatively low-velocities ( $20-30 \text{ cms}^{-1}$ ), they are of the same magnitude as Shepard observed before the strong downcanyon flows. It is not clear whether a 30-meter deep valley can channelise flows to the same extent as the much deeper canyons of Shepard et al. (1979). Nevertheless, the possibility that fine-grained, dilute turbidity currents may be generated in these channels, cannot be ruled out.

Many of the flows described by Shepard et al. (1979) did not appear to continue for long distances downslope. Events recorded by canyon head meters were not observed in other meters less than 2 km downslope. The implication is that the flows are short-lived, intermittent phenomena and that downslope transport may be by the integration of these events rather than by single catastrophic flows. However each

flow would considerably resuspend sediment which could then be supplied to the adjacent slope in a series of relatively short-lived pulses.

This discussion raises the possibility that dilute turbidity currents may play an important role in "hemipelagic" sedimentation. Occasional preserved laminae in bioturbated muds (Fig. 5-3) argue that relatively strong events do occur at least occasionally. Beyond this, however, there is little direct evidence for the process. Several things need to be established before such a process might be accepted. Most important are that slope channels are common features even on smooth constructional slopes, and that currents similar to those observed by Shepard et al. (1979) flow in them.

#### AN ANCIENT ANALOGUE: THE RIO DELL FORMATION

An ancient example of a constructional slope sequence is found in the Plio-Pleistocene Rio Dell Formation of northern California (Piper et al., 1976). The formation outcrops in cliffs along Centreville Beach, south of Eureka, California (Fig. 8-3) and consists of a progradational sequence from basin to shelf environments. The slope sequence makes up the lower half of the upper member (Fig. 8-4) as defined by Piper et al. (1976) and was independently established by them using well-defined foraminiferal depth assemblages.

From the work of Piper et al. (1976) and my own observations, three slope facies can be recognised in the sequence:

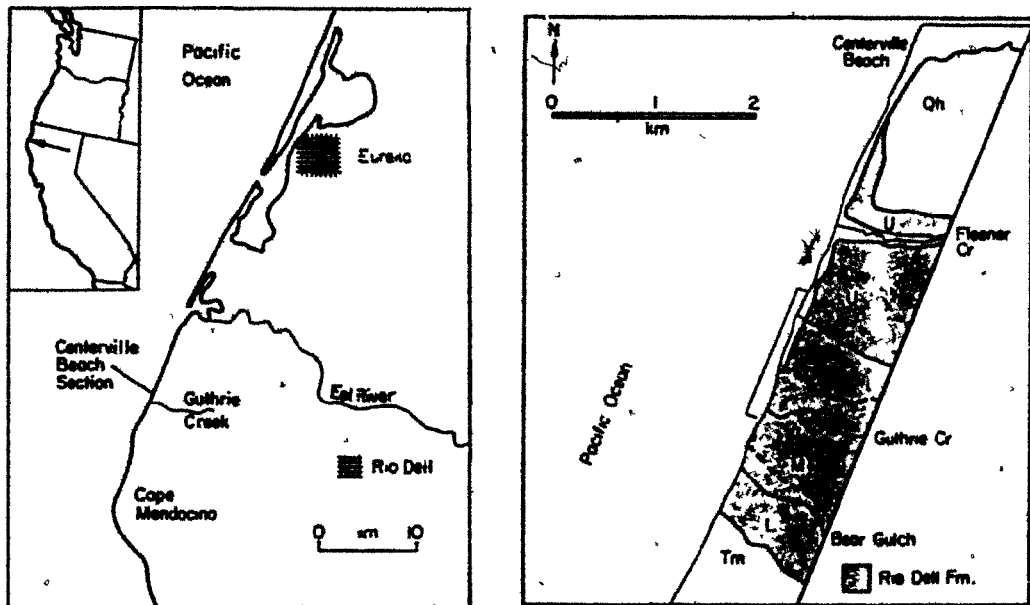


Figure 8-3. Location map for Rio Dell Formation in northern California (from Piper et al., 1976).

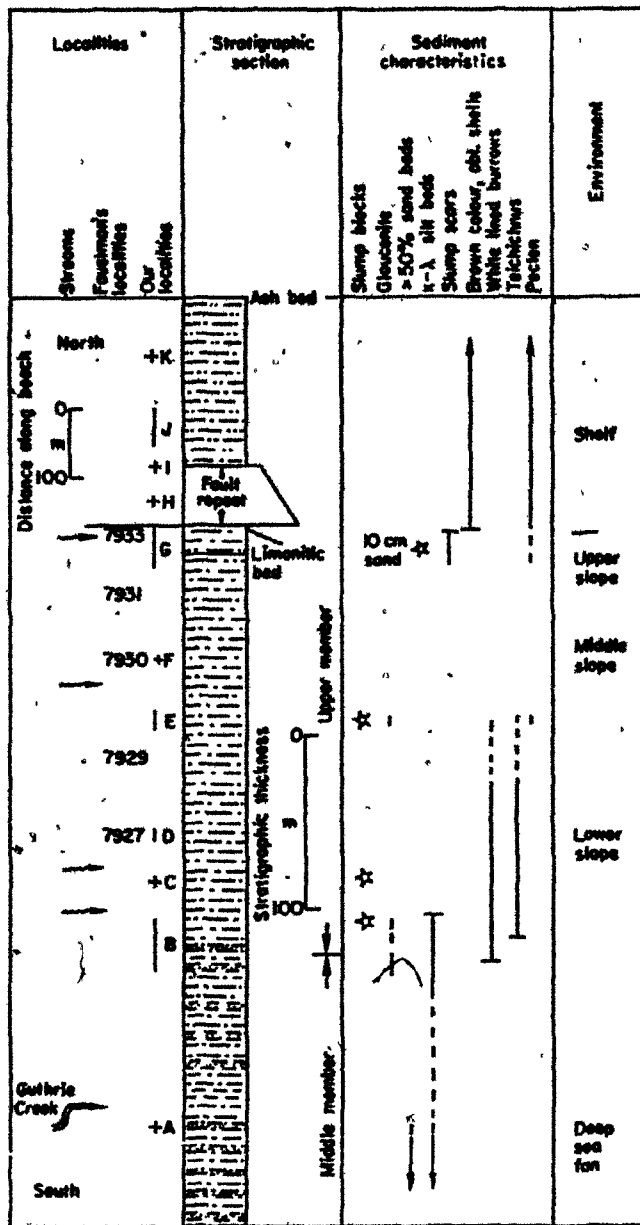


Figure 8-4. Generalised stratigraphic section for the Rio Dell Formation (after Piper et al., 1976).

- (a) dark-grey mudstone
- (b) light-grey silty mudstone
- (c) brown-weathering siltstone and sandstone.

The dark mudstone and light silty mudstone facies are end members and gradations between the two lithologies are commonly observed. Both facies are irregularly bedded, although laterally extensive over several metres. The brown-weathering siltstone and sandstone facies makes up only a very minor proportion of the sequence. The brown weathering is due to iron concretion, which occurs preferentially in the slightly coarser beds.

The lower part of the slope sequence (equivalent to Section B of Piper et al., 1976, Fig. 6-4) is dominated by the finer dark mudstone facies (Fig. 8-5 Sections 1 and 2) with subordinate interbeds of light silt mudstone and very occasional thin brown sandstone. Generally, individual bed thicknesses do not exceed 10 cm although the upper part of both Sections 1 and 2 contain dark mudstone layers up to 40 cm thick. The light silty mudstones become more dominant up-section and can make-up units over a metre thick (Section 3, Fig. 8-5). Coarser units of brown siltstone or sandstone are still very rare, but dark mudstone interbeds are still important (Section 4, Fig. 8-5).

The overlying shelf sequence (above Section G of Piper et al., 1976; Fig. 8-4) consists of light coloured silty mudstone, similar to the slope facies (b), and more frequent sandstone beds. The dark mudstone is very rare in the shelf sequence except at the very top of the exposed section. In a small exposure north of Fleener Gulch,

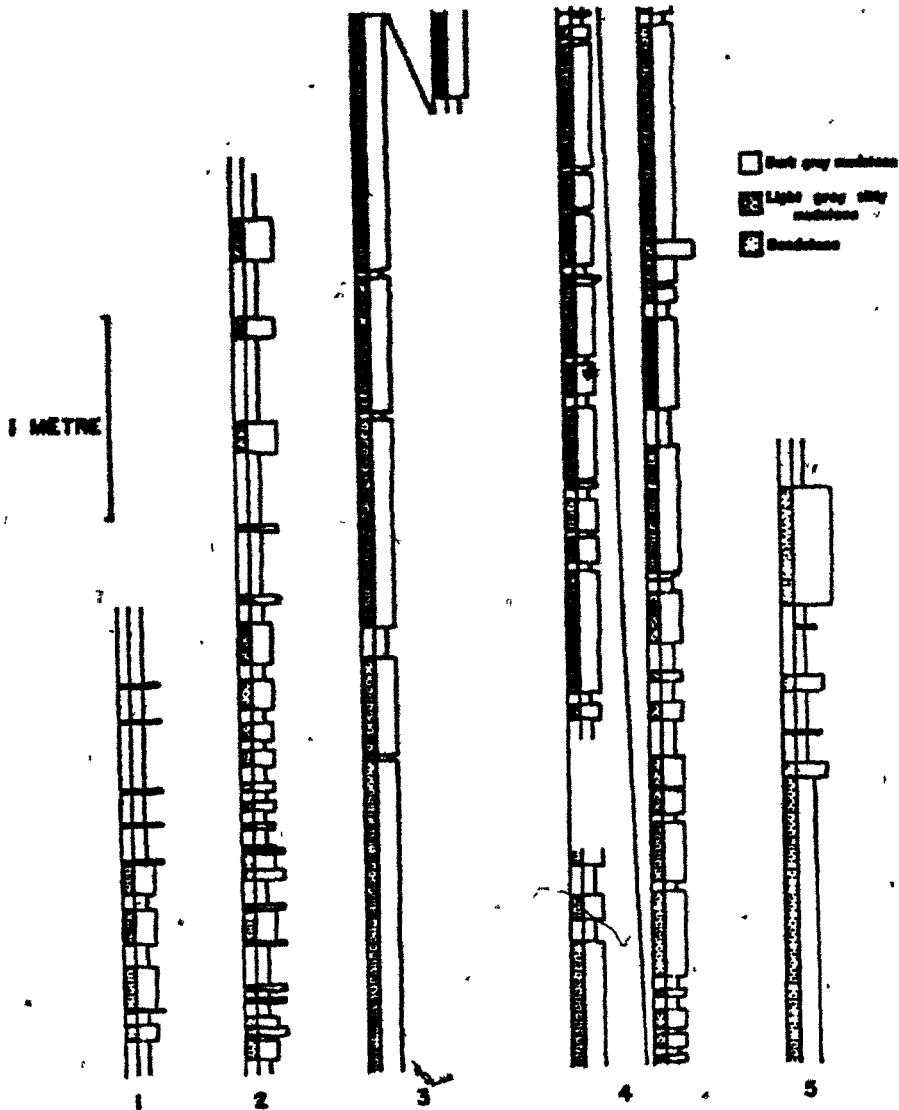


Figure 8-5. Detailed measured sections in the Rio Dell Formation. Location of sections are shown in Figure 8-4.

(Fig. 8-3) dark mudstone is associated with thick medium to coarse sandstone beds (Section 5, Fig. 8-5). The sandstones often exhibit trough-shaped scour surfaces which may represent channel margins (Fig. 8-6). The troughs are sometimes draped with dark mudstone and filled with sandstone (Fig. 8-6). The example in Figure 8-6 shows several scour surfaces within a single trough.

This exposure is hard to interpret in isolation. The sequence as a whole reflects shallowing according to Piper et al. (1976) with no evidence for later transgression. Thus the exposure at the top of the section may represent an inner-shelf or nearshore environment. The re-appearance of the dark mudstone lithology at this point in the section suggests a nearshore source of the mud. The lack of dark mudstone in the remaining shelf sequence indicates either a temporary halt in the supply of mud or bypass of the shelf by the transport process which supplies the mud to the slope.

#### COMPARISON OF SCOTIAN SLOPE AND RIO DELL FORMATION SEQUENCES

The Rio Dell Formation slope sequence seems to be a good example of a constructional slope sequence. The processes observed on the Nova Scotian Slope are useful for understanding this ancient sequence. An important feature in the Rio Dell Formation is the "two-tone" nature of mud lithologies. Just as on the Nova Scotian Slope, siltier olive-grey and more clayey red-brown end-member muds are identified, so too, in the Rio Dell Formation, there are dark grey mudstone and light-grey silty mudstone end-members. Gradations between end-member lithologies is common in both examples. The Rio Dell dark mudstones

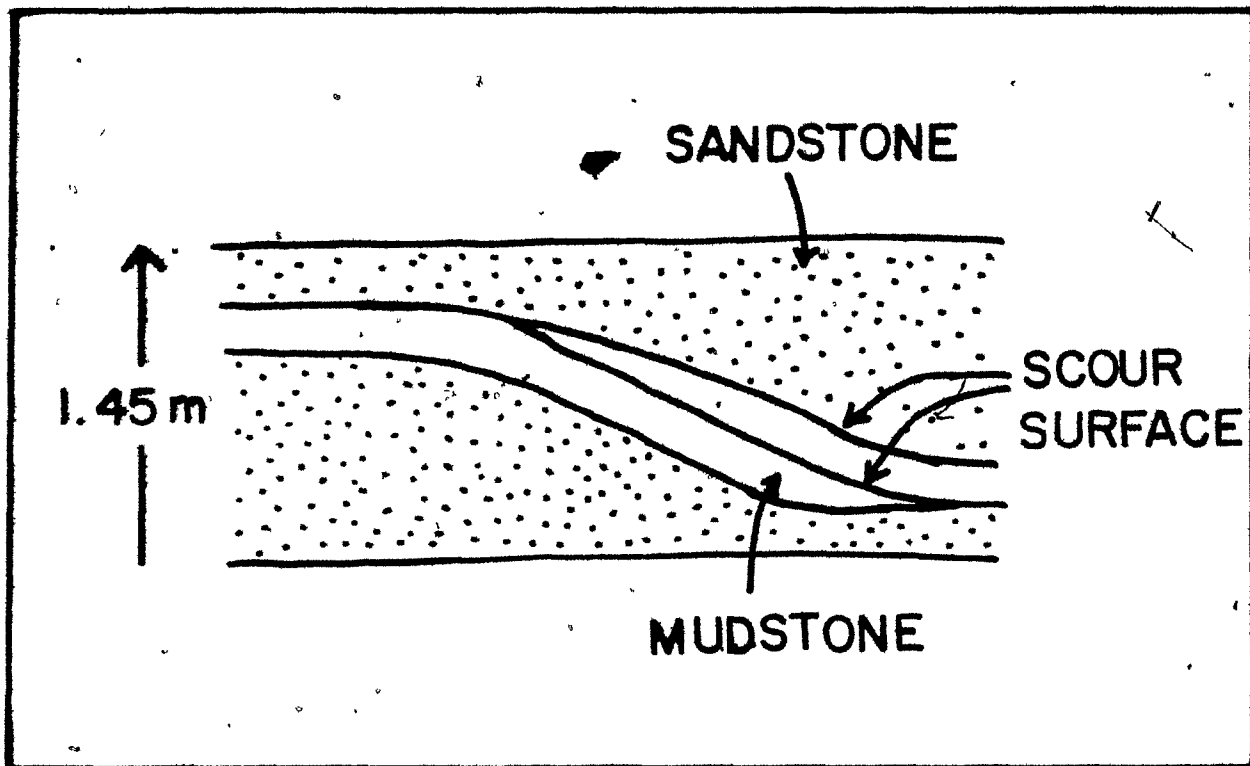


Figure 8-6. Field sketch of trough-shaped scour surfaces and dark mudstone drape and fill. From Section 5, Figure 8-5.

may have been derived from an inshore fluvial source. Periodic flood conditions could produce intervals of relatively rapid sediment supply, probably as surface plumes which bypass the shelf, in much the same way as ice-front melting supplied red-brown mud to the Scotian Slope. The light-grey silty mudstone is the major shelf lithology, which is probably remobilised to supply the slope via the bottom boundary layer.

It is interesting that the dark mudstones dominate the lower slope sequence in the Rio Dell Formation. This suggests that surface layer transport may be more efficient than bottom-layer transport in supplying mud to the deeper basin. Alternatively, fluvial supply of mud to the slope may be localised and dispersal mainly by bottom currents on the slope. This might also account for the lack of mudstone on the shelf.

## CHAPTER 9

DISCUSSION: DESTRUCTIONAL SLOPE PROCESSES

A generalised late Wisconsinan facies model for the Scotian Gulf destructional area was outlined in Figure 7-9. The upper slope is dominated by large slump and slide masses which produced a high-relief morphology. Inter-block areas were partially filled by thick sand units supplied from the shelf and uppermost slope. The mid-slope morphology is also controlled by slump deposits, which form hummocks with relief of 10-20 metres. Coarser sand and silt facies tend to fill the depressions between slumps while the slumps themselves are draped with various mud facies. On the depositional lobe, a similar facies development is seen except adjacent to the main channel, where numerous coarse graded beds dominate the sequence. It is likely that the lobe itself is constructed from thick-bedded sands similar to suprafan deposits (Nelson and Kulm, 1973).

"Hemipelagic"-type processes continue to add sediment to the destructional slope during the Wisconsinan as well as the Holocene and mud is still the most common lithology. However, various gravity driven processes, most importantly slumps, debris-flows and turbidity currents are much more important than during constructional phases of slope development. These processes, although described by simple theory, have not been studied in the detailed slope framework attempted here.

## SLUMPING

Slumping occurred at a variety of scales. The largest slump features recognised have areas of several square kilometres (Fig. 7-1). These features provide the morphological framework for the detailed facies distribution. Slumped units in cores are generally relatively thin, indicating that smaller-scale slumps are also important.

Slumping is an indication of slope instability. Several inter-related factors can lead to mechanical instability, most importantly low sediment shear strength, (often a consequence of high rates of deposition), high slope angle and sudden or cyclic loading by seismic shocks or ocean waves (Morgenstern, 1967). Sediment shear strength is itself related to a number of factors including composition, porosity and internal pore pressure. Based on infinite slope analysis, Moore (1961) predicted that slumping on most continental slopes should be a relatively rare phenomenon in intercanion areas. Subsequent surveys have demonstrated that this is not true and that slumping is or has been an important process on most continental slopes (eg. Ryan, in press). Relatively few, definitively Holocene slumps have been recorded; most are attributed to Pleistocene conditions. All the slumped beds in this Scotian Slope survey are late Wisconsinan or earlier and correlation of individual beds (Chapter 4) indicates no evidence for slumping during the Holocene.

An average Pleistocene sedimentation rate of 30-60 cm/ky is estimated from the seismic interpretations of Jansa and Wade (1975) at the shelf-edge. Rates during periods of maximum sediment supply could

have been considerably higher than this average figure. Probably, the very high sedimentation rate was ultimately responsible for the increased slumping activity during the Pleistocene. High sedimentation rates may have controlled other stability factors.

Rapid sedimentation at the shelf-edge may increase the overall slope angle. The accumulation of a shelf-edge prism during the whole of the Pleistocene could increase the slope-angle by a maximum of  $4^\circ$  (from  $3^\circ$  to  $7^\circ$ ), which would substantially increase the probability of slumping. On the other hand, evidence from seismic profiles (Fig. 2-4) suggests that slumping has occurred in several episodes during the Pleistocene, perhaps related to high glacial sediment supply. Taking an average glacial/interglacial interval of 100,000 yrs, the slope angle may have been built up in increments of  $0.3^\circ$  or less before slumping occurred.

An increase of  $0.3^\circ$  hardly seems significant, but other factors are involved. Rapid rates of sedimentation has a second important effect. With more rapid burial, the sediment has less time to expel water and may become underconsolidated (Sangrey, 1981) as a result of excess pore pressure. Such sediments have a considerably lower shear strength and may be more susceptible to loading by earthquakes or ocean waves. Prior and Suhayda (1979) demonstrate that unexpectedly high pore pressures in Mississippi Delta muds explain the occurrence of slumps at slope angles as low as  $0.5^\circ$ . However, rates of sedimentation on the Mississippi Delta are three orders of magnitude higher than the maximum conceivable rate on the Scotian Shelf unless the ice margin was

very close to the shelf edge. At low sedimentation rates, shear strength increases rapidly with burial depth (Moore, 1961) so that underconsolidation is unlikely at depth unless other factors (eg. high gas content) are important. It is possible, however, that the top few metres of the sediment pile may have sufficiently low shear strength to be susceptible to slumping. This may explain some of the small scale slumps observed in the cores. Sudden deposition of sand on the slope may sufficiently load underconsolidated areas to cause slumping. Many slumped beds (Figs. 6-11) contain sand patches, so that this mechanism may be important.

Finally, the possibility of progressive slumping should not be overlooked. A single slump will tend to increase the local slope and reduce support to sediment upslope of the slump-scar (Watkins and Kraft, 1978). This often results in further slope failure with slide-planes being generated progressively in an upslope direction. The downslope profile in Fig. 2-20(a) shows evidence for several phases of slumping which may well have occurred progressively. On a smaller scale, a similar process could act on the steeper slopes at the margin of the small depressions which formed by slump erosion and deposition.

#### DEBRIS FLOWS

The mechanism of debris flow is reasonably well understood in principle (Johnson, 1970; Hampton, 1970; Middleton and Hampton, 1976). Most theory is based on subaerial observations and little is known about the details of debris flows in subaqueous environments, their

generation or behaviour during transport.

Subaerial field observations led Hampton (1970) to suggest that debris flows were generated from slumps by agitation of the slumping mass with incorporation of additional water. The process happens relatively quickly provided that the water can be rapidly introduced to the sediment matrix. A slump can travel some distance by plastic-flow and incorporate very little water. The Hampton (1970) mechanism requires break up of the slump mass and frequent block-to-block contacts (jostling), implying brittle behaviour of the slump blocks. Slumps of dominantly muddy material show plastic deformation features (Fig. 6-11). These small-scale slump deposits are likely derived from the upper few metres of unconsolidated sediments and may never have had the potential to become debris flows. More compacted and brittle sediments in larger slumps would tend to break up rather than deform during slumping and thus may be more liable to the jostling processes involved in the transformation to debris flow.

A possible mechanism to generate debris flows from unconsolidated sediment involves the brittle behaviour of enclosed sand units in muddy slumps. Several slumped beds in Figure 6-11 contain patches of well-sorted sand. It was suggested earlier that dilatancy can cause the sand inclusions to behave in a brittle fashion. Thus individual sand inclusions could be jostled together and mixed with the intervening mud. The pore water of the sand would provide the additional fluid required to create a slurry capable of flow.

All the debris flow beds observed on the Scotian Slope contain a

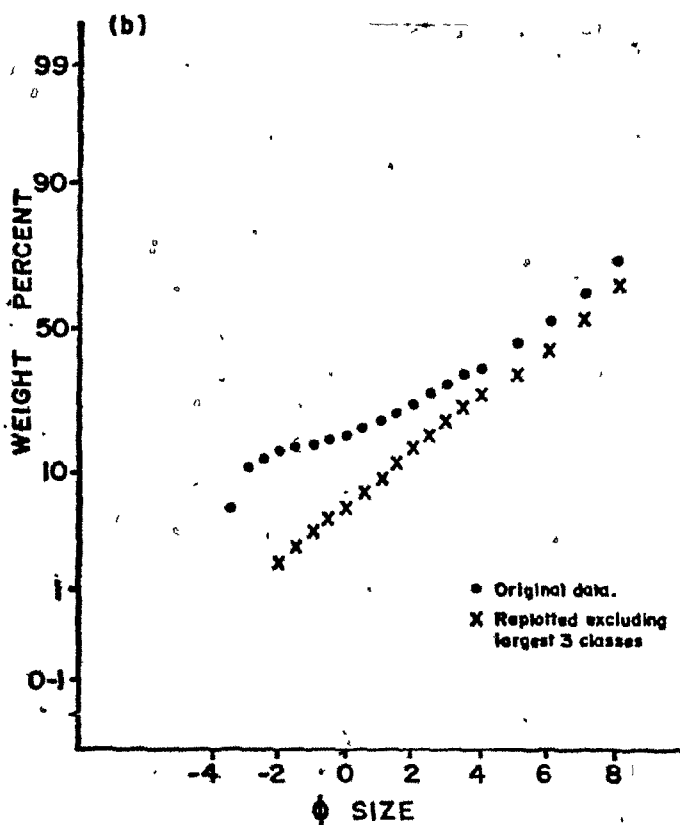
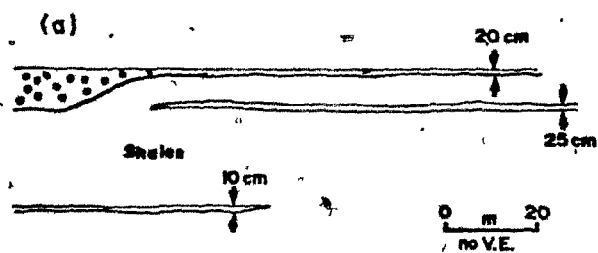
significant proportion of gravel-sized clasts (Figs. 6-9, 6-10). Gravel is relatively rare on the mid-slope area in other facies, except near the main channel and depositional lobe. Ice-rafted clasts are found in various muddy beds, sometimes in clusters, but more commonly in isolation. Thus, it seems likely that the generation of gravelly debris flows must take place on the upper slope where gravel makes up a significant part of the bedload (see Chapter 3).

Although several cores bottom out in thick beds of gravelly sandy mud, most beds are thin (< 30 cm) and relatively fine grained (compared to classical pebbly mudstones of debris-flow origin of Crowell, 1957; Aalto, 1972). They are interesting because debris flow models are based on relatively large-scale flows (Johnson, 1970; Hampton, 1970). Observations on Recent submarine debris-flows are restricted to wide, thick deposits recognised in high-resolution seismic profiles (Embley, 1980; Damuth and Embley, 1981).

Piper et al. (1978) noted some thin pebbly mudstone beds in Miocene Flysch (Fig. 9-1) that have very similar grain-size characteristics to the modern Scotian Slope beds (Fig. 9-1). Two beds in this sequence can be traced for at least 100 metres laterally, and one bed joins with a much thicker (7 metre) pebbly mudstone bed which fills a large channel.

My own observations of sediments in the Cambro-Ordovician Cow Head Group of western Newfoundland (Hubert et al., 1977; James et al., 1980) demonstrate that sheet deposits are not the only geometry of thin debris-flow deposits. Small, conformable lenses of pebbly mudstone less than 50 cm across are seen, sometimes interconnected by very thin

Figure 9-1. (a) Field sketch from Miocene Potamula Shale, Greece showing three thin pebbly mudstone beds in shale sequence. (b) Cumulative grain-size distribution of a sample from the uppermost bed in (a). The curve was replotted to exclude the two largest size intervals which contained statistically unrepresentative clast numbers (From Hill et al., 1979).



(2 to 5 cm) stringers of pebbly mudstone (Fig. 9-2). The convex shape may be the result of differential compaction, but the thickness variations cannot be ascribed to boudinage deformation (N.P. James, pers. comm.). Figure 9-2 summarises the different bed geometries (types 1 to 4) of thin-bedded debris-flow deposits observed in ancient sequences.

Cores do not provide information on the geometry of the debris flow deposits of Facies 9. However, closely spaced cores, obtained by attempting to re-occupy the site of core 80-004-29, show that the lateral extent of the bed in that core is not great (estimated at less than 500 metres).

Figure 9-3 is a speculative model of how the various bed geometries might be produced in an environment of irregular topography. It is based on subaerial observations of larger flows (Shelton, 1966; Johnson, 1970) and differs mainly in scale, and in the nature of the initial confinement of the flow.

Presumably, the slump topography would largely control the initial flow of a debris-flow. Thin sheet deposits (Types 1 and 2, Fig. 9-2) may result when the flow overtops its channel banks or moves into a more open slope area, in much the same way as subaerial flows spread and thin when they emerge from narrow valleys into a broader plain (Shelton, 1966, p. 330). Other subaerial flows are observed to deposit elongate lobes at their termination (Johnson, 1970, pp. 436, 438). These may result in the lens-shaped geometry of bed-types 3 and 4 (Fig. 9-2). Small localised spills over the channel margins may produce

Figure 9-2. Four thin debris-flow bed-geometrics recognised from ancient deposits.

- (1) Sheet deposit with convex margins
- (2) Sheet deposit associated with large channel
- (3) Lensoid, unconnected
- (4) Lensoid, connected by thin stringers.

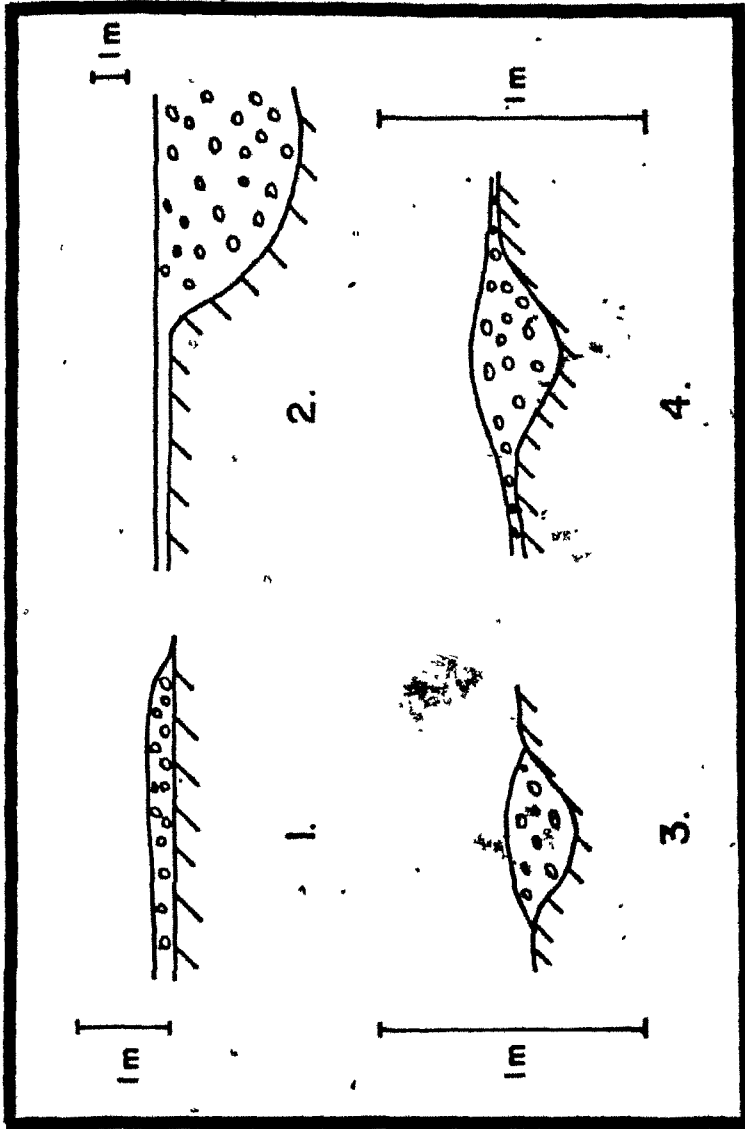
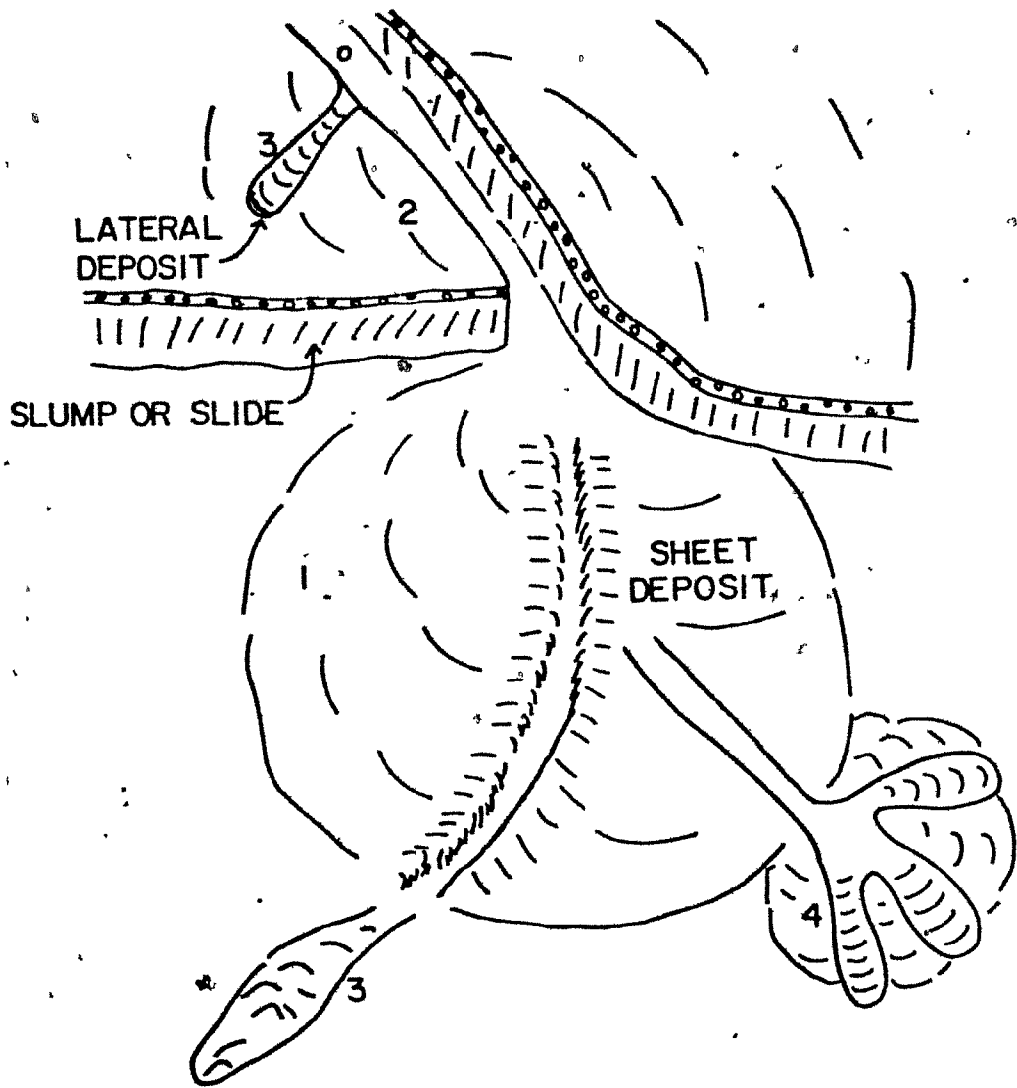


Figure 9-3. Speculative model of small-scale debris flows in the destructional slope setting. See text for detailed explanation.



elongate lateral deposits of type 3 geometry.

#### TURBIDITY CURRENTS

The general theoretical understanding of the mechanism of turbidity current flow is quite well advanced (Komar, 1969; Stow and Bowen, 1980).

The slope has been commonly thought of as a site of turbidity-current bypassing after initiation in canyon heads close to the shelfbreak.

There is strong evidence in the Scotian Slope cores that deposition from dense sandy turbidity currents also occurs on the slope under certain conditions. Three important factors are involved: (a) initiation, (b) transport paths, (c) depositional sites. The complex morphology of the destructional slope can provide favourable conditions for all three factors.

#### (a) INITIATION

There are two accepted mechanisms for initiating turbidity-currents in this situation (direct fluvial discharge can be discounted even at maximum sea-level displacements): slumping and direct current suspension. Most evidence for these mechanisms come from the heads of submarine canyons; very little is known about processes at the heads of smaller slope valleys.

Slumping of large sediment masses from the heads of canyons and canyon tributaries has been demonstrated by many authors (eg. Marshall, 1978; Valentine et al., 1980). The slumps may be triggered by earthquakes, but instability due to sediment infilling the canyon head is the underlying control. In the confined situation of a canyon, uncon-

solidated sandy sediment would rapidly incorporate water to produce an over-dense suspension which then begins to accelerate downslope as a turbidity-current. Alternatively, debris-flow may result from the initial slump. Hampton (1970) illustrated theoretically and experimentally a mechanism of shear at the debris flow surface by which a turbidity-current could be generated.

In La Jolla canyon, Shepard and Marshall (1973) reported strong down-canyon flowing currents during a large storm event. Subsequently, the current meter was lost and eventually recovered from further down the canyon, tangled amongst a mass of kelp and seagrass. This evidence led Shepard and Marshall (1973) to the conclusion that a turbidity-current had been generated during the period of downslope flowing current activity. Reimnitz (1971) made similar observations in the Rio Balsas Canyon off Mexico and demonstrated that very strong downslope currents were related to rip currents generated in the surf zone.

Autosuspension (Bagnold, 1962) is probably an important mechanism in the initiation and maintenance of turbidity-currents. The criterion for autosuspension (Bagnold, 1962) is:

$$w = \bar{U} \tan \theta$$

where  $w$  = settling velocity of a particle,  $\bar{U}$  = mean velocity and  $\theta$  = slope angle. This equation is plotted on Figure 9-4 for several slope angles. It can be seen that on a slope angle as low as  $4^\circ$ , sediment which is suspended by a particular current velocity will become immediately autosuspended. In this case, for a  $50 \text{ cm s}^{-1}$  current

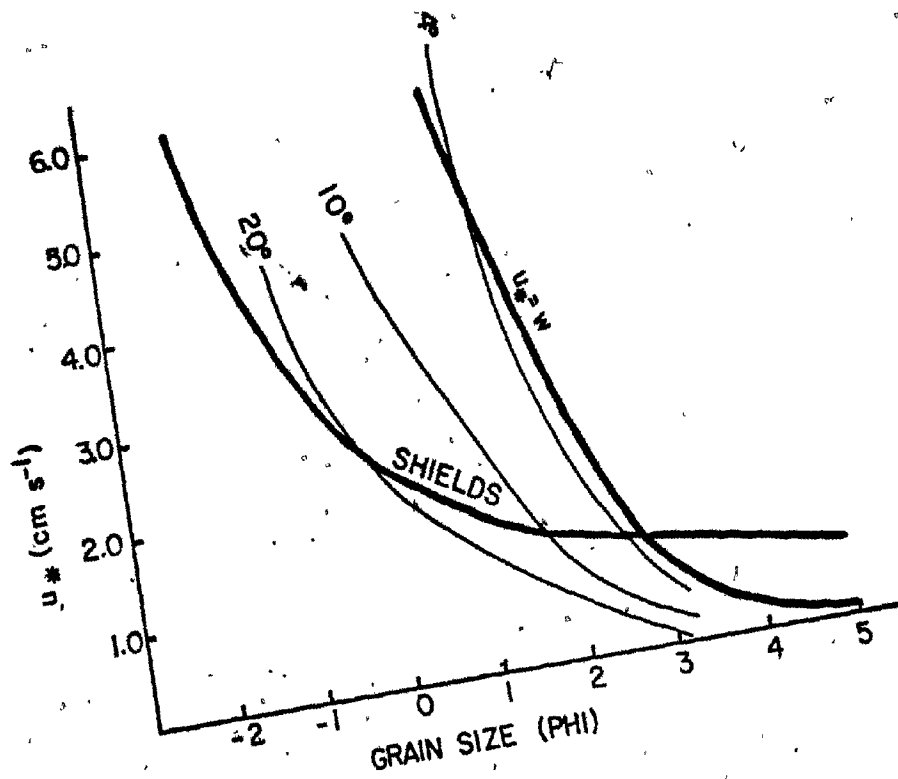


Figure 9-4. Criteria for initial movement and suspension of quartz grains in water at 20°C (after Blatt et al., 1980, p. 103) with autosuspension criterion plotted for various slope angles.

( $u_* = 2.7 \text{ cm s}^{-1}$ ), 2  $\phi$  medium sand can be autosuspended on a  $4^\circ$  slope. If this process is maintained, a sufficient concentration of particles may be entrained to cause excess density and initiate a turbidity current.

Both slump and current suspension mechanisms are potentially important on the Scotian Slope. Slumping is seen to be an active process; however it is unlikely that unconfined slumps would directly result in turbidity currents as the tendency to spread out would prevent significant turbulence developing in the slumping mass. Development of debris flows from slumps and subsequent transitions to turbidity-currents by Hampton's (1970) mechanism is also possible. Once again confinement within a channel would favour turbidity-current generation because the process would be most efficient at rapid speeds. Slump generation of turbidity currents, therefore, is probably morphologically controlled. A potential site for this mechanism is beneath the upper slope escarpment where localised slumping on the steep slope has produced a very rough topography. Unfortunately, no profiles extend across this zone in the region of the main-channel (Fig. 2-8), so it is not known whether the main channel heads into similar morphology or into tributary valleys. In either case, sediment supply from current transport is potentially high and slumping a likely process.

The present-day current regime on the uppermost slope includes periods of flow of up to  $50 \text{ cms}^{-1}$  (see Fig. 3-2). However, this velocity is directed alongslope during these periods. The potential for autosuspension is therefore high only in the alongslope direction. In

canyons, downslope flowing currents are generally considered important in the generation of turbidity-currents (Shepard and Marshall, 1973).

On the Scotian Slope, autosuspension could only occur on the margins of channels as currents flow perpendicular to the channel axis. Certainly channel-margin slopes would be high enough to achieve autosuspension of quite large particles, but the concentration of sediment would need to build up rapidly within the channel. Turbulence generated as a result of flow separation across the channel (Fig. 9-5) may keep sediment suspended and allow the density to increase sufficiently for turbidity-flow. Current velocities drop rapidly downslope so that this mechanism would have greatest potential on the uppermost slope. Sufficiently large channels are probably only present in the area of the main channel.

This mechanism is proposed because significant up and downslope currents are only observed during low-flow conditions (Fig. 3-2).

These currents may generate weak suspensions and even dilute turbidity currents (Shepard et al., 1979; see Chapter 8), but are unlikely causes of dense turbidity currents.

However, no current-meters were located within the channel itself and Shepard et al.'s (1979) observations from canyons suggest that up and down-valley currents are more important in canyons, and presumably controlled by the channel morphology. Undoubtedly, flow near the bottom in the rugged topographic area of the upper Scotian Slope, would be very complex. Furthermore, the effect of lowered sea-level and other possible oceanographic changes during the Pleistocene make the potential

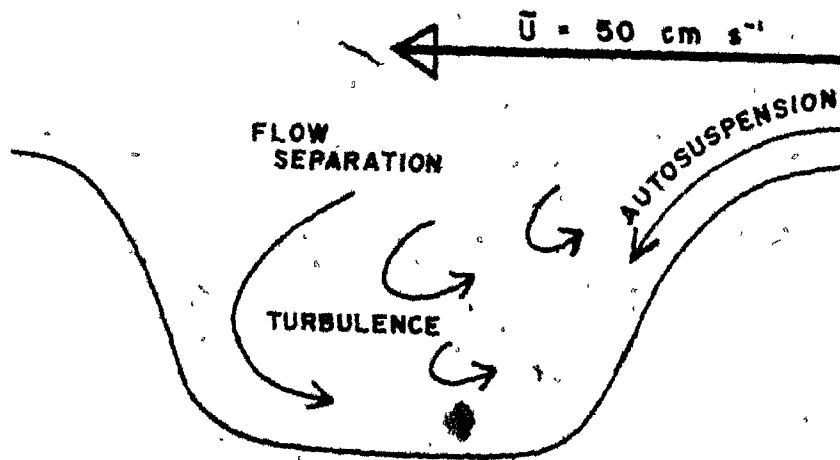


Figure 9-5. Speculative mechanism for generation of turbidity currents by cross-channel currents. Autosuspension occurs on the steep channel walls and turbulence in the channel maintains sediment in suspension until excess density is achieved.

of this autosuspension mechanism difficult to assess.

One must conclude, therefore, that slumping presents a more tangible mechanism for turbidity current generation in the Scotian Gulf area, but the autosuspension mechanism remains potentially important. The presence of a channel and the evidence for turbidity-currents in the Western Bank area where slumping is not seen to be an important process supports this conclusion. The potential for turbidity current generation by either mechanism is greatest at the head of the main channel, but the area of high-relief morphology at the base of the upper-slope escarpment may also be an important generating zone.

#### (b) TRANSPORT PATHS

It is generally thought that in order to maintain a turbidity current, the flow must remain channelised to prevent lateral dispersion and mixing (Middleton and Hampton, 1976). Deposition at the end of fan channels, in the form of suprafan lobes (Normark, 1970), stands as evidence for this. Thus, on the slope, channelised transport paths must be available to the current between the generation point (or zone) and the site of deposition.

The main channel obviously provides the most commonly used pathway on the slope. The most striking characteristic of the channel is the dramatic decrease in both width and vertical relief (Fig. 2-16). This does not correspond to the equilibrium profiles observed in other deep-sea channels (Menard, 1964) or predicted by Komar (1973). Two possibilities exist to explain this: either (a) the channel is a relatively young feature and has not had sufficient time to reach grade

or (b) the channel was at some time truncated by a slump and is presently re-equilibrating.

The second possibility cannot be ruled out, but there is no strong evidence in the deeper penetration seismic profiles for a major slump-scar (Fig. 2-4). In fact the evidence suggests bathymetric control by deep slump masses, west of the channel. Another pointer is that the channel, although diminishing rapidly, does so gradually rather than abruptly. Thus the first explanation, that the channel is a young, ungraded feature, seems more likely.

The channel profile is certainly similar to the predicted early-stage profile of Komar (1973). However, the basis of Komar's model is that the channel height is controlled by the turbidity-current height and that the channel is constructed by overspill deposition. The Scotian Slope channel in fact appears to be mainly erosional in its upper reaches, only becoming depositional as the height decreases (Figs. 2-12 to 2-14). Nevertheless, with this profile, Komar predicts that overspill of the turbidity current would be great. This would be particularly true of the lower relief section.

Komar's predictions were derived from a previous result (Komar, 1972) which indicated that the head of the turbidity current would be thicker than the body on slopes greater than  $(\sin \theta = ) 0.0022$ . At no point along its course does the channel gradient decrease to this value, so it can be said that any spillover, even from the incised channel, would most likely be from the head. Theoretical considerations predict that, in the head of a turbidity current, coarser sediments will

be concentrated while fines are lost and incorporated in the entrained body and tail of the flow (Middleton and Hampton, 1976). Thus, it follows that overspill from the upper reaches of the channel should be in the form of concentrated flows and the resulting deposit should be relatively coarse-grained and well-sorted.

These are the characteristics shown by the thin sands of Facies 7. Generally ungraded, they also have sharp tops, indicating a lack of fines in the flow that deposited the beds. The deposits are somewhat reminiscent of crevasse splay deposits in deltaic environments (Elliott, 1978). In the deltaic situation, crevassing only occurs by breach of levee walls. The process on the slope is probably different in this respect, as breach of the levee or channel wall would allow sediment from a lower level of the flow to discharge. This might sample sediment from the body of the flow to produce more typically graded beds. Simple overspill from the larger flows best explains the characteristics of Facies 7.

After overspill, the turbidity current may continue flowing as long as it has the gradient and confinement to do so. Morphological lows would tend to channelise the flow at least for short distances (Fig. 9-6). Slump-head depressions and inter-slump depressions are available to channelise any such waning flows on the mid-destructive slope surface. Hence one might expect these overspill deposits to be restricted to depressions. This trend was noted in the distribution of facies.

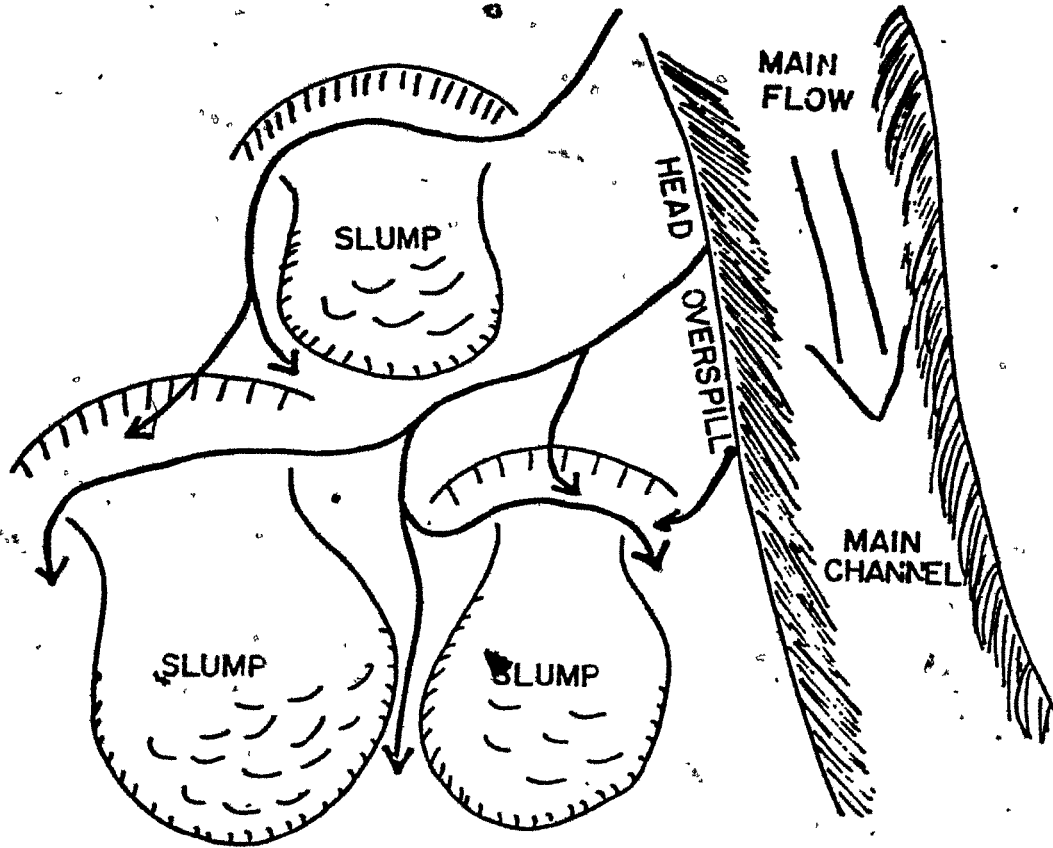


Figure 9-6. Conceptual illustration of the flow paths of mid-slope turbidity currents. See text for explanation

Although the main channel is probably the site of a majority of turbidity-flows, areas other than the channel head have the potential for generation of turbidity currents. If turbidity currents are initiated on the upper slope escarpment at points distant from the main channel, they may become channelised within the slump block morphology of the upper slope (Fig. 2-8). Infilling of valleys between slump-blocks (Fig. 2-18) with thick sand deposits (Fig. 7-9) strongly indicate that turbidity currents have flowed in these upper slope valleys. The actual routes taken by individual flows would be quite complex; flow divergence and convergence would probably be common.

The flows on reaching the more open mid-slope area would behave in much the same way as overspill flows from the main channel. The flow, however, may be expected in a series of pulses and complete head, body and tail portions of the current would arrive. Thus, these flows may deposit muddier, more complex graded and perhaps multiple-graded beds of Facies 5 and 8. Some of the sequences of Facies 5 couplets may represent amalgamations of several pulses of the same flow. Others, however, show discrete hemipelagic interbeds so were deposited from discrete events.

These specific interpretations of the turbidite facies are attractive because of their tidiness. However, they are dependent on certain assumptions concerning size and frequency of flows down a main channel which is out of equilibrium. All three facies can be produced by overspill of the channel. Core 58 from close to the channel margin (Fig. 7-4) contains several graded muddy units, presumably derived from the

channel. Flows from the upper slope blocky area are nevertheless still thought to be important contributors of sediment to the mid-slope depressions. Supply in the depositional lobe area is presumably much more directly related to flows in the main channel. A similar facies development is seen in the lobe area (Fig. 7-7), but the channel at that point is much reduced in size, so that both head- and body-transported sediment is probably supplied directly. Also, slumping has modified the lobe surface and processes analogous to those on other midslope areas may operate.

#### (c) DEPOSITIONAL SITES

Three different sites are available for turbidity current deposition: (a) depositional lobe, (b) flat channel margins, (c) hummocky mid-slope areas.

(a) The construction of the depositional lobe cannot be determined from this study. The lobe was built during an early stage of channel development and represents the adjustment of the channel to grade in much the same way as a river will construct an alluvial plain in the flat reaches of its profile (Schumm, 1977, p. 58). The lobe is morphologically similar to a suprafan lobe (Normark, 1970) and was probably similarly constructed (see summary in Rupke, 1978). Subsequently, the channel has built up and now crosses the lobe (Fig. 7-1). Overspill of the shallow channel however, was undoubtedly a major depositional process and was the main levee-building mechanism. Core 80 from the channel margin provides evidence for this process in the form of frequent thin sand and gravel beds (Fig. 7-7).

(b) Deposition on the relatively flat regions surrounding the main channel in its upper reaches consisted of fairly regular overspill and deposition of both sand and muddy sand turbidites (Core 28, Fig. 7-4) separated by units of hemipelagic mud. This provides a good indication of the number of overspill events from the main channel through time. The frequency of turbidite beds is relatively low compared to the sequence from the morphologically more complex area to the west (Fig. 7-4). This provides more strong evidence for turbidity currents generated and flowing independent of the main channel.

(c) In the mid slope hummocky area, meso-scale morphology exerts the strongest control on deposition from turbidity currents. As well as acting as transport paths, the interslump and slump head depressions will be active sites of deposition. The relief of the depressions ranges from 5 to 15 metres in depth and generally less than a kilometre in width. Confinement of turbidity currents in channels with these dimensions will be minimal, so that deposition will be prevalent.

Several authors have described channel-fill deposits in ancient turbidite sequences (eg. Hall and Stanley, 1973; Mutti, 1973; Carter, 1979). Most of the described examples are similar in scale to the Scotian Slope features, largely because this is the scale of a single large outcrop. The channels are from trench slope (Carter, 1979), base of slope (Hall and Stanley, 1973) and deep-sea fan (Mutti, 1977) environments, and the type of fill varies accordingly. None of the examples are specifically associated with slump or slide controlled morphology.

In Carter's (1979) study of the Jurassic Otekura Formation (New Zealand), the channels lie in a background of massive, graded and rippled mudstones and siltstones. Packets of thicker-bedded sandstones are inferred to have been deposited in slope-channels (Carter et al., 1978). Channel facies comprise massive and thick-bedded sandstones, graded sandstone to siltstone units and thin-bedded graded sandstones and mudstones. The channel fill sequences are characterised by single massive beds at the base, overlain by a "spasmodically" varying sequence of graded sandstones and siltstones. Alternating packets of thick sandstone units and thin sandstone/siltstone beds are present, but no systematic fining or coarsening sequences are apparent. The sequence is generally overlain by thin bedded sandstone/mudstone units, which are thought to represent the abandonment stage of the channel fill sequence.

Hall and Stanley (1973) describe two channels with a finer-grained fill sequence from the Devonian Seboomook Formation of northern Maine. The channels are filled by graded and parallel-laminated siltstone with minor mudstone. One channel contains a thick (1 metre) sandstone bed which thickens slightly and coarsens significantly toward the channel margin. The other, shallower channel contains an amalgamated siltstone "upper sedimentation unit" which continues beyond the channel as a thin bed. Outside the channel, the bed forms part of a sequence of similar (generally graded) thin sandstone and siltstone beds. Thus, the channel appears to have been filled relatively quickly by preferential deposition of thicker siltstone units, the time equivalents of thinner sedimentation units outside of the channel.

Mutti's (1977) study of the Eocene Hecho Group (Spain) is useful because of his consideration of lateral facies changes. The channels are filled by coarse-grained, thick-bedded deposits with complex internal organisation. The thick beds pinch out laterally toward the channel margins into thinner, finer beds which as a sequence, onlap the channel wall (Fig. 9-7). Single beds may pinch out completely before the channel wall. The channel margin facies consists of thin-bedded, laminated fine sandstones and siltstones. Bedding surfaces are often indistinct due either to a lack of mudstone partings or to bioturbation but the bedding surface may also have slightly undulating surfaces. Starved-, climbing- and sinusoidal-ripple laminations are observed.

These examples are cited because they represent channels which have been filled subsequent to rather than penecontemporaneous with erosion. Slump bounded depressions can be considered analogies to these examples as the depression is filled by later turbidity current deposition. A significant characteristic of both coarse- and fine-filled channels is the continuity of beds from the centre of the channel to the margin and outside of the channel. According to Mutti (1977), this indicates that although the main current passed down the channel axis, relatively dilute lateral suspensions partly overflow the channels and deposit finer sediment on the margin.

The sequences in cores from slump-bounded depressions (core 56, 75, Fig. 7-4; core 52, Fig. 7-5) are probably representative of the more marginal fill. The presence of thin slumped beds in all three

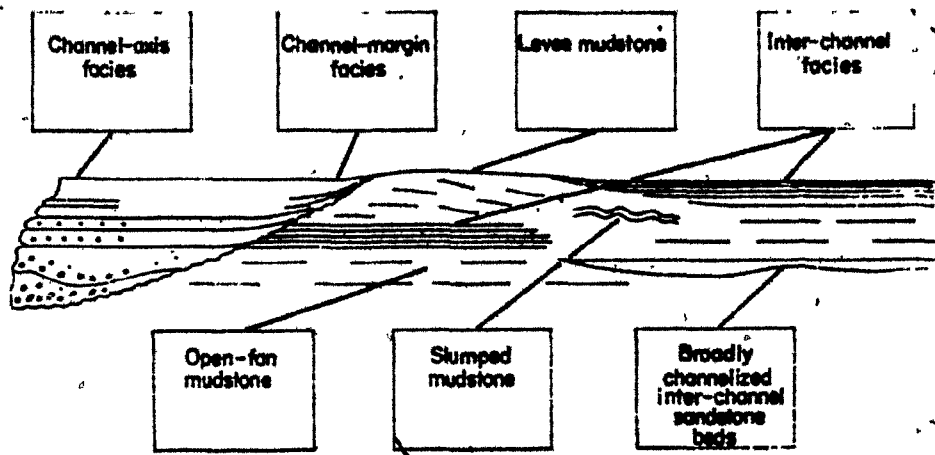


Figure 9-7. Model of thin-bedded channel fill sequences of Mutti (1977).

cores tends to support this. Core 56 has a thick sand bed at its base which may be more typical of the axial-fill deposition. The main sequence of the same core is dominated by graded sand/silt to mud couplets of Facies 5. Both cores 52 and 75 are finer-grained. Core 52 contains three, well-sorted sand beds, perhaps due to its proximity to the main channel.

Thus, the fill of slump-bounded depressions is probably similar to small-scale channels described from the ancient record (Fig. 9-8). It can be speculated that the deepest part of the depressions are filled with thicker sand beds. However, if most turbidity currents are relatively small in scale, as is likely in the mid-slope area, thin-bedded sands and silt/mud couplets may dominate the fill. Depressions rarely experiencing turbidity currents may contain a muddy fill. Sequences will tend to fine (and probably thin) across the margins of the depression, as a result of individual beds thinning and pinching out laterally.

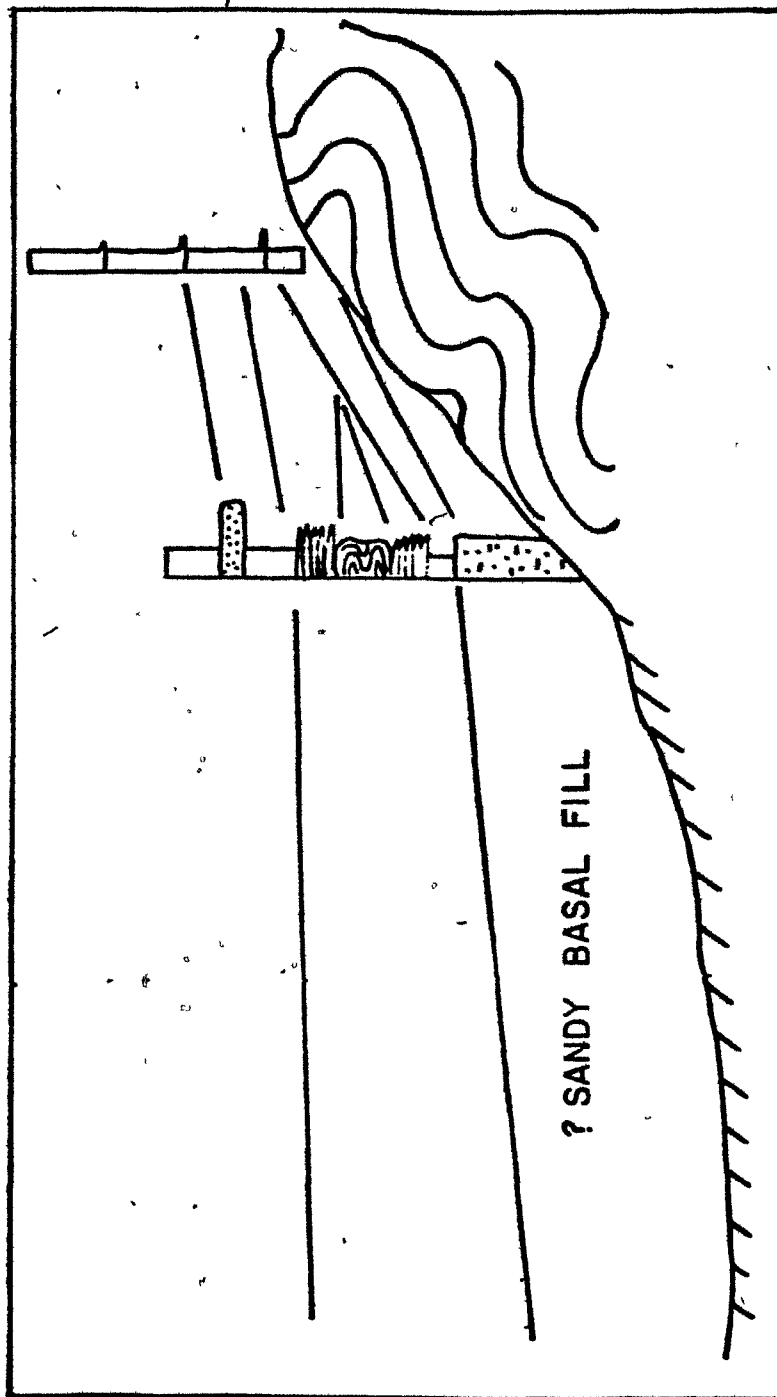


Figure 9-8. Schematic illustration of the mode of inter-slump depression fill on the Nova Scotian slope (Scotian Gulf destructional area).

CHAPTER 10CONCLUSIONS

The continental slope, even in intercanyon areas is a sedimentologically complex environment. The use of coring and shallow-penetration seismic profiling allows the study of only the top five to ten metres of the sediment pile. Slumping on various scales can create a variety of meso-scale sub-environments which accumulate distinctive facies associations.

This study has been carried out in an exploratory and opportunistic fashion, and much advantage would be gained from a more methodical approach. The size of the study areas was close to ideal in that it allowed both detailed surveying of morphological features and the compilation of such observations into a broader framework. The three-dimensional aspect of the survey provided by combined sidescan and seismic profiling was also very important in the identification of morphological features. Groundtruthing of the GLORIA record with simple bathymetry was found to be useful and it is recommended that a detailed bathymetric survey should be an early stage in the study of a slope area. Sampling becomes a much more useful tool when it is combined with detailed bathymetric and environmental information. More accurate transponder-system navigation and digital seismic processing techniques would make interpretations much more reliable.

In the Scotian Gulf study area, the slope can be divided into five parts. (1) The upper slope has considerable relief which is created by large slide blocks accumulated in a chaotic mass at the base of a prominent escarpment 1.5 km downslope of the shelfbreak. (2) The mid-slope area has a lower hummocky relief caused by relatively shallow slump dislocations and accumulations. (3) Below this area is another zone in which larger scale slide-blocks have accumulated. (4) A prominent erosive channel cuts across the upper and midslope areas, gradually decreasing in depth and width downslope. A substantial accumulation of sediment in a suprafan-like depositional lobe is crossed by the channel in its lower course. (5) In the western part of the area, a remnant of undisturbed, constructional slope remains. A discontinuous leveed channel crosses the slope in this area.

Slumping is observed in the Western Bank area also, but the relief generated by the slumping is less. A large part of this area has been left undisturbed by destructional processes.

Modern sedimentation appears to be essentially independent of the morphological variations described above. Detailed analysis of grain size populations shows that sediment textures are in equilibrium with the observed current regime. Catastrophic events or processes need not be invoked to explain the sediment distribution. Sand and mud are transported across the shelfbreak in suspension by strong currents which are essentially directed along contours, but have a small downslope component. Sediment transport is probably intermittent, but resuspension

during stronger flows continues the transport of individual particles until they reach a current regime where resuspension is no longer possible. Current strengths decrease downslope so that a gradual decrease in modal grain-size of bottom sediment results. Bedload transport, although less efficient for sand sizes, is important for gravel sized clasts on the uppermost slope, particularly in the Scotian Gulf area. In deeper water, mud continues in suspension and will be deposited in a dynamically suitable environment in the same way as upper-slope sand. The deposition of mud, however, is usually modified by flocculation and differential settling rates of the particles.

The approach, using quantitative comparisons of grain-size populations and current parameters, was found useful and suggests that the study of sediment textures in this way can be usefully applied to interpret dynamic conditions in other areas of sandy sediment transport. On the slope, the effects of less obvious controls on the sediment dynamics, such as topographic Rossby waves, can be assessed.

Sedimentation in the last 18,000 years probably followed the modern pattern and resulted in a very uniform accumulation of sediment over the whole slope. Most of the mud was supplied by erosion of the outer-shelf banks.

A marked boundary between overlying olive-grey or yellow brown muds and underlying red-brown or brown muds is recognised and was dated at approximately 19,000 yrs B.P. The underlying unit shows a much more diverse range of sediment facies, but very poor correlation of

individual beds between even closely-spaced cores. Foraminiferan assemblages do not change significantly across this boundary, but there is a major faunal boundary at a higher stratigraphic level. The faunal boundary at approximately 11,000 yrs B.P. represents the establishment of modern bottom conditions both on the slope and in the deepest part of Emerald Basin. Previously, the shelf circulation was probably largely restricted, but with rising sea-level, cross-shelf exchange of bottom waters through the Scotian Gulf became possible.

The red-brown and brown mud deposited on the slope before 19,000 yrs B.P. was derived from Carboniferous basins of Nova Scotia and the Gulf of St. Lawrence. Most of it was probably supplied to the ocean at the margin of the Nova Scotian ice-sheet. Transport across the shelf to the slope was largely in surface water suspension, and may have been restricted by the emergence of the outer-shelf banks. Under the maximum condition of 110 metre lowering of sea level, supply would have been through the Gully and the Scotian Gulf. Wisconsinan muds are generally finer-grained than Holocene or contemporary muds suggesting that the dynamic regime during the Wisconsinan was less energetic than today.

The above constructional slope processes, are, ultimately controlled by broad environmental factors which dictate the supply and transport of sediment to the slope. The same processes and controls are active on the destructional slope areas, but in addition, the gravity driven processes of slumping, debris-flow and turbidity-flow are important and are controlled closely by the morphology.

Distinct facies associations have been recognised within the

Wisconsinan sequences of the Scotian Gulf destructional area: (1) Thick sand and mud beds are characteristic of the upper slope in valleys between slump blocks, indicating the generation and flow of turbidity currents on the upper slope. (2) Graded silt beds and thin turbidite sand units are found in the mid-slope region. Depressions between slump masses are sites of coarser sediment accumulation. Turbidity currents, from the upper slope or from overspill of the main channel, flow through the mid-slope area, controlled largely by the irregular morphology. Deposition occurs preferentially in the depressions. (3) Channel banks and levees are characterised by coarse sand and even gravel beds deposited from overspilling turbidity currents. Thick mud accumulation separate the coarser beds and suggest that only rare turbidity currents overspill the channel banks.

The complexity of sedimentation on the Nova Scotia slope (in particular the Scotian Gulf area) is probably neither a unique nor necessarily common characteristic of slopes in general. The Nova Scotian margin has been largely influenced by Pleistocene glaciation and sea-level fluctuations and the gravelly, sandy shelf-edge which probably resulted from the glacial processes, is not typical of margin environments. On a more local scale, the Scotian Gulf has certain characteristics peculiar to it and which cannot be considered typical of all slope settings. The shelfbreak in this region is relatively deep and would not be influenced by the wave regime even under the extremes of proposed sea-level lowering. Also, there is evidence that the Scotian Gulf acts as a conduit for shelf/slope water exchange, which again makes

this area anomalous even in the limited context of the Nova Scotian margin. The range of possible controls on slope sedimentation illustrated here warns against the adoption of the Nova Scotian Slope as a model for continental slope sedimentation in general.

APPENDIX 1MARKOV SEQUENCE ANALYSIS OF FINE-GRAINED FACIES

According to Harbaugh and Bonham Carter (1970, p. 98), a Markov process is one "in which the probability of the process being in a given state at a particular time may be deduced from knowledge of the immediately preceding state". Sedimentary sequences such as fluvial cyclothem or turbidite units form Markov "chains" as a result of predictable processes. Any group of facies can be analysed to determine whether the transitions between facies follow the predictable Markov sequence, by the construction of transition matrices and comparison with matrices produced by random processes. The method outlined by Miall (1973) is used here.

Ten cores from the Scotian Gulf study area were used in the analysis. Facies were identified as described above, using X-radiographs. Gradual transitions between facies were noted and used in the analysis, while sharp, possibly erosive transitions were excluded. The only boundaries to be affected by this simplification were those overlain by Facies 5 silts. The number of times that a facies passed upwards into another was counted and compiled into a Transition Count Matrix (Table A-1). These values were normalised into probabilities, to give Table A-2. A chi-squared test (Till, 1974, p. 75) of the form

$$-2 \log_e \lambda = \sum_{i=1}^m \sum_{j=1}^m n_{ij} \log_e \frac{P_{ij}}{p_j}$$

was used where  $\lambda = \prod_{i,j=1}^m \left( \frac{P_{ij}}{P_{i,j}} \right)^{n_{ij}}$

and  $P_{ij}$  = probability in cell  $ij$  (row  $i$ , column  $j$  of the matrix)

$P_j$  = marginal probability in the  $j$  th column calculated from column tally divided by total tally

$n_{ij}$  = frequency in cell  $ij$  of original tally matrix

$m$  = number of states (rows or columns) in the matrix

and  $-2 \log_e \lambda$  follows  $\chi^2$  (chi-squared) with  $(m-1)^2$  degrees of freedom.

For this analysis  $-2 \log_e \lambda$  was calculated as 51.66 with 11 degrees of freedom.  $\chi^2$  for 11 degrees of freedom (from standard tables) is 26.8 at the 0.5% probability level, so that the Markov property is significant at that level.

The five facies are not present in equal proportions, so the independent probability of different transitions will be variable according to the relative proportions of the facies. These independent probabilities can be computed (Table A-3) and their effect can be removed by subtraction from Table A-2 to give a difference matrix (Table 5-1). This then highlights the statistically significant transitions as positive values. Values lower than 0.05 cannot be considered significant (Cant and Walker, 1976). Therefore one positive value (0.01 probability between Facies 2 and 3) in this case has not been used.

A.1 TRANSITION COUNT MATRIX

	1	2	3	4	5	Row Sum
1	-	0	5	1	0	6
2	2	-	3	3	0	8
3	9	0	-	2	0	11
4	0	1	3	-	0	4
5	6	9	2	0	-	<u>17</u>
	17	10	13	6	0	46

A.2 TRANSITION PROBABILITY MATRIX

	1	2	3	4	5
1	-	0	0.83	0.17	0
2	0.25	-	0.37	0.37	0
3	0.82	0	-	0.18	0
4	0	0.25	0.75	-	0
5	0.37	0.53	0.11	0	-
	0.37	0.22	0.28	0.13	0

A.3 PROBABILITY INDEPENDENT TRIALS

	1	2	3	4	5
1	-	0.34	0.45	0.21	0
2	0.47	-	0.36	0.17	0
3	0.51	0.30	-	0.18	0
4	0.42	0.25	0.32	-	0
5	0.37	0.22	0.28	0.13	-

REFERENCES

- Aalto, K.R. (1972). Elysch pebble conglomerate of the Cap-des-Rosiers Formation (Ordovician), Gaspe Peninsula, Quebec. *J. Sed. Pet.*, v. 42, p. 922-926.
- Aksu, A.E. (1980). Late Quaternary Stratigraphy, Paleoenvironmentology and Sedimentation History of Baffin Bay and Davis Strait. Unpubl. Ph.D. Thesis, Dalhousie University, Halifax, Nova Scotia.
- Alam, M. (1979). Effect of Pleistocene Climatic Changes on the Sediments around the Grand Banks. Unpublished Ph.D. Thesis, Dalhousie University, Halifax, Nova Scotia.
- Allen, J.R.L. (1970). Studies in fluvial sedimentation: a comparison of fining-upwards cyclothems with special reference to coarse-member composition and interpretation. *J. Sedim. Petrol.*, v. 40, p. 298-323.
- Andrews, J.T., Feyling-Hanssen, R.W., Hare, P.E., Miller, G.H., Schlucter, C., Stuiver, M. and Szabo, B.J. (1976). Alternative models of early and mid-Wisconsin events, Broughton Island, N.W.T.: Toward a Quaternary chronology. *Int. Union. Geol. Sci./UNESCO, Int. Geol. Correl. Prog., Proj. 73/1/24*, Bellingham, Prague, p. 12-61.
- Bagnold, R.A. (1937). The Size Grading of Sand by Wind. *Proc. Roy. Soc. Lond., Ser. A.*, v. 163, p. 250-261.
- Bagnold, R.A. (1962). Auto suspension of transported sediment, turbidity currents. *Proc. Roy. Soc. London, Ser. A.*, v. 265, p. 315-319.
- Bagnold, R.A. and Brandorff-Nielsen, O. (1980). The pattern of natural size distributions. *Sedimentology*, v. 27, p. 199-207.
- Balsam, W.L. and Heuser, L.E. (1976). Direct correlation of sea surface palaeotemps, deep circulation and terrestrial palaeoclimates: foram and palynological evidence from two cores off Chesapeake Bay. *Mar. Geol.*, 21, 121-147.
- Banerjee, I. (1977). Experimental study on the effect of deceleration on the vertical sequence of sedimentary structures in silty sediments. *Jour. Sed. Petrol.*, v. 47, p. 771-783.
- Bates, C.C. (1953). Rational Theory of Delta Formation. *A.A.P.G. Gull.*, v. 57, p. 2119-2162.

- Biscaye, P.E. (1964). Mineralogy and sedimentation of the deep sea sediment fine fraction of the Atlantic Ocean and the adjacent seas and oceans. Unpublished Ph.D. dissertation, Yale Univ., 86 pp.
- Blatt, H., Middleton, G. and Murray, R. (1980). *Origion of Sedimentary Rocks*. Prentice-Hall, New Jersey, 782 pp.
- Bouma, A.H. (1962). *Sedimentology of some flysch deposits*. Elsevier, Amsterdam, 168 pp.
- Bouma, A.H., Moore, G.T. and Coleman, J.M. (1978). Framework, Facies and Oil-Trapping Characteristics of the Upper Continental Margin. *AAPG Studies in Geology*, No. 7, 326 pp.
- Bouma, A.H., Rezak, R. and Chmelik, R.F. (1969). Sediment transport along oceanic density interfaces. *Geol. Soc. Am. Abstr.* 7, p. 259-260.
- Brandorff-Nielsen, O. (1977). Exponentially decreasing Distributions for the Logarithm of Particle Size. *Proc. Roy. Soc. Lond., Ser. A.*, v. 358, p. 401-419.
- Brookes, I.A. (1970). New evidence for an independent Wisconsin-age ice-cap over Newfoundland. *Can. J. Earth Sci.*, v. 7, p. 1374-1382.
- Cant, D.J. and Walker, R.G. (1976). Development of a braided fluvial facies model for the Devonian Battery Point Sandstone, Quebec. *Can. J. Earth Sci.*, v. 13, p. 102-119.
- Carter, R.M. (1979). Trench-slope channels from the New Zealand Jurassic: the Otekura Formation, Sandy Bay, South Otago. *Sedimentology*, v. 26, p. 475-496.
- Carter, R.M., Hicks, M.D., Norris, R.J. and Turnbull, I.H. (1978). Sedimentation patterns in an ancient arc-trench-ocean-basin complex: Carboniferous to Jurassic Rangitata Orogen, New Zealand. *IN Sedimentation in Submarine Canyons, Fans and Trenches* (eds. D.J. Stanley and G. Kelling) Dowden, Hutchinson and Ross, Stroudsburg, Pa., p. 340-361.
- Cashman, K.V., Popenoe, P. and Chayes, D. (1981). Sidescan Sonar Depiction of Slump Features Associated with Diapirism on Continental Slope off Southeastern United States. (abstr). *AAPG-SEPM Annual Convention*, San Francisco.
- Chamberlain, C.K. (1978). Recognition of Trace Fossils in Cores. *IN Basan, P.B. (ed.) Trace Fossil Concepts*. SEPM Short Course No. 5, Oklahoma City.

- Clark, J.A. and Lingle, C.S. (1979). Predicted relative sea level changes (18,000 years B.P. to present) caused by late-glacial retreat of Antarctic ice sheet. *Quat. Res.*, v. 11, p. 279-298.
- CLIMAP, (1976). The surface of the ice-age earth. *Science*, v. 191, p. 1131-1137.
- Coleman, J.M., Suhavda, J.M., Whelan, T. and Wright, L.D. (1974). Mass movement of Mississippi river delta sediments. *Trans. Gulf-Coast Assoc. Geol. Socs.*, v. 24, p. 49-68.
- Cook, H.E. (1979). Ancient continental slope sequences and their value in understanding modern slope development. IN *Geology of Continental Slopes* (eds. Doyle, L.J. and Pilkey, O.H.) SEPM Special Publication, No. 27, p. 287-305.
- Crowell, J.C. (1957). Origin of pebbly mudstones. *Geol. Soc. Am. Bull.*, v. 68, p. 993-1009.
- Dale, C.T. (1979). A Study of High Resolution Seismology and Sedimentology on the Offshore Late Quaternary Sediments, Northeast of Newfoundland. Unpublished M.Sc. Thesis, Dalhousie University, Halifax, Nova Scotia, 180 pp.
- Dalrymple, R.W. (1977). Sediment Dynamics of Macrotidal Sand Bars, Bay of Fundy. Unpublished Ph.D. Thesis, McMaster University.
- Damuth, J.E. (1980). Use of high-frequency (3.5-12 kHz) echograms in the study of near-bottom sedimentation processes in the deep sea: a review. *Mar. Geol.*, v. 38, p. 51-75.
- Damuth, J.E. and Embley, R.W. (1981). Mass-transport Processes on Amazon Core: Western Equatorial Atlantic. *Am. Assoc. Petrol. Geol., Bull.*, v. 65, p. 629-643.
- Dietz, R.S. (1952). Geomorphic evolution of continental terrace (continental shelf and slope). *Am. Assoc. Petrol. Geol. Bull.*, v. 36, p. 1802-1819.
- Doyle, L.J. and Pilkey, O.H. (1979). Geology of continental slopes. SEPM Special Publication, No. 27, 374 p.
- Doyle, L.J., Pilkey, O.H. and Woo, C.C. (1979). Sedimentation on the Eastern United States continental slope. IN Doyle, L.J. and Pilkey, O.H. (eds.) *Geology of Continental Slopes*. SEPM Special Publ. No. 27, p. 119-129.
- Drake, D.E., Kolpack, R.L. and Fischer, P.J. (1972). Sediment transport on the Santa Barbara-Oxnard Shelf, Santa Barbara Channel, California. IN Swift, D.J.P., Duane, D.B. and Pilkey, O.H. (eds.) *Shelf Sediment Transport: Process and Pattern*. Dowden, Hutchinson and Ross Inc. Stroudsburg, Pa., p. 307-331.

- Drapeau, G. and King, L.H. (1972). Surficial Geology of the Yarmouth-Browns Bank Map Area. Marine Science Paper 2, Geol. Surv. Canada Paper 72-24, 6 p.
- Elliott, T. (1978). Deltas. IN Sedimentary Environments and Facies (ed. H.G. Reading). Elsevier, p. 97-142.
- Embley, R.W. (1980). The role of mass transport in the distribution and character of deep-ocean sediments with special reference to the North Atlantic. Mar. Geol., v. 38, p. 23-50.
- Embley, R.W. and Jacobi, R. (1977). Distribution and morphology of large sediment slides and slumps on an Atlantic continental margin. Mar. Geotech., v. 2, p. 205-228.
- Emery, K.O. (1977). Stratigraphy and Structure of pull-apart margins. IN Geology of Continental Margins (eds. McFarlan, E., Drake, C.L. and Pittman, L.S.) AAPG Continuing Education Course Note Series, No. 5, p. B1-B20.
- Enos, P. (1969). Anatomy of a Flysch. J. Sed. Pet., v. 39, p. 680-723.
- Ewing, M.S., Eittreim, S.L., Ewing, J.I. and LePichon, X., (1971). Sediment transport and distribution in the Argentine Basin. 3. Nepheloid layer and processes of sedimentation. IN L.H. Ahrens, F. Press, S.K. Runcorn and H.C. Urey (eds.) Physics and Chemistry of the Earth, 8, New York, Pergamon, p. 49-77.
- Field, M.G. and Clarke, S.H. Jr. (1979). Small-scale slumps and slides and their significance for basin slope processes, Southern California Borderland. IN Doyle, L.J. and Pilkey, O.H. (eds.) Geology of Continental Slopes, SEPM Special Publ., No. 27, p. 223-230.
- Fillon, R.H. (1976). Hamilton Bank, Labrador Shelf postglacial sediment dynamics and palaeo-oceanography. Mar. Geol., v. 20, p. 7-25.
- Flint, R.F., Demorest, M. and Washburn, A.L. (1942). Glaciation of the Schickshock Mountains, Gaspé Peninsula. GSA Bull., v. 53, p. 1211-1230.
- Folk, R.L. (1966). A review of grain-size parameters. Sedimentology, v. 6, p. 73-93.
- Foote, T.R., Mann, C.R. and Grant, A.B. (1965). Oceanographic results of cruise S-64 between the Scotian Shelf, Grand Banks of Newfoundland and the Gulf Stream. Bedford Institute Report, 65-8, 40 pp.
- Friedman, G.M. and Sanders, J.E. (1978). Principles of Sedimentology. John Wiley and Sons, New York, 792 pp.

- Fuglister, F.C. and Worthington, L.V. (1951). Some results of a multiple-ship survey of the Gulf Stream. *Tellus*, v. 3, p. 1-14.
- Gatien, M.G. (1975). A study of the slope water region, south of Halifax. Unpublished M.Sc. Thesis, Dalhousie University, Halifax, Nova Scotia.
- Grant, D.R. (1977). Glacial Style and Ice Limits, the Quaternary Stratigraphic Record and Changes of Land and Ocean Level in the Atlantic Provinces, Canada. *Géogr. Phys. Quat.*, v. XXXI, p. 247-260.
- Hall, B.A. and Stanley, D.J. (1973). Levee-bounded submarine base-of-slope channels in the lower Devonian Seboomook Formation, Northern Maine. *Geol. Soc. Amer., Bull.*, v. 84, p. 2101-2110.
- Hampton, M.A. (1970). Subaqueous debris flow and generation of turbidity currents. Unpublished Ph.D. Thesis, Stanford University, Stanford, Calif., 180 p.
- Harbaugh, J.W. and Bonham-Carter, G. (1970). *Computer Simulation in Geology*. Wiley-Interscience, New York.
- Hardy, I.A. (1975). Lithostratigraphy of the Banquereau Formation on the Scotian Shelf. *IN* van der Linden, W.J.M. and Wade, J.A. (eds.) *Offshore Geology of Eastern Canada*, v. 2, *Geol. Surv. Canada, Paper 74-30*, p. 163-174.
- Harland, W.B., Herod, K.N., and Krinsley, D.H. (1966). The Definition and Identification of Tillis and Tillites. *Earth Sci. Rev.*, v. 2, p. 225-256.
- Harris, I. McK., and Schenk, P.E. (1975). The Meguma Group. *IN* Ancient Sediments of Nova Scotia (I. McK. Harris, ed.). *SEPM Eastern Section Field Guide*, 1975.
- Hedberg, H.D. (ed.) (1976). *International Stratigraphic Guide: A Guide to Stratigraphic Classification, Terminology, and Procedure*. Wiley-Interscience, New York.
- Heezen, B.C., Hollister, C.D. and Ruddiman, W.F. (1966). Shaping of the continental rise by deep geostrophic contour currents. *Science*, v. 152, p. 502-508.
- Hesse, R. and Chough, S.K. (1980). The Northwest Atlantic Mid Ocean Channel of the Labrador Sea: II. Deposition of parallel laminated levee-muds from the viscous sublayer of low density turbidity currents. *Sedimentology*, v. 27, p. 697-711.
- Hill, P.R. (1979). Late Quaternary Sediments on the Nova Scotian Continental Slope. Unpublished report, Department of Geology, Dalhousie University, Halifax, N.S., Canada, 109 pp.

- Hill, P.R., Aksu, A.E. and Piper, D.J.W. (in press). The deposition of thin bedded subaqueous debris flow deposits. NATO Science Workshop on Marine Slides and Other Mass Movements.
- Holeman, J.N. (1968). The Sediment Yield of Major Rivers of the World. *Water Resources Res.*, v. 4, p. 737-747.
- Houghton, R.W., Smith, P.C. and Fournier, R.O. (1978). A Simple Model for Cross-Shelf Mixing on the Scotian Shelf. *Canada, Fish. Res. Board Jour.*, v. 35, p. 414-421.
- Hubert, J.F., Sucheki, R.K. and Callahan, R.K.M. (1977). The Cow Head Breccia: Sedimentology of the Cambro-Ordovician Continental Margin, Newfoundland. IN *Deep Water Carbonate Environments* (Cook, H.E. and Enos, P., eds.) SEPM Special Publ., No. 25, p. 125-154.
- Hughes, T., Denton, G.H., Anderson, B.G., Schilling, D.H., Fastook, J.L. and Lingle, C.S. (1978). The last ice sheets: a global view. IN *The last great ice sheets*. Denton, G.H. and Hughes, T., (eds.) Wiley/Interscience, New York.
- Ingram, R.L. (1954). Terminology for the thickness of stratification and parting units in sedimentary rocks. *Geol. Soc. Am., Bull.*, v. 65, p. 937-938.
- Ives, J.D. (1957). Glaciation of the Torngat Mountains, northern Labrador. *Arctic*, v. 10, p. 66-87.
- Ives, J.D. (1978). The Maximum Extent of the Laurentide Ice Sheet along the East Coast of North America during the Last Glaciation. *Arctic*, v. 31, p. 24-53.
- Jacobi, R.D. (1976). Sediment Slides on the northwestern continental margin of Africa. *Mar. Geol.*, v. 22, p. 67-173.
- James, N.P. (1966). Sediment Distribution and Dispersal Patterns on Sable Island and Sable Island Bank. Unpublished M.Sc. Thesis, Dalhousie University, Halifax, N.S., 254 pp.
- James, N.P., Klappa, C.F., Skevington, D. and Stevens, R.K. (1980). Cambro-Ordovician of West Newfoundland - Sediments and Faunas. *Geol. Assoc. Canada, Annual Meeting, Halifax, 1980, Field Trip Guidebook*, No. 13, 88 pp.
- Jansa, L.F. and Wade, J.A. (1975). Geology of the continental margin off Nova Scotia and Newfoundland. IN van der Linden, W.J.M. and Wade, J.A. (eds.) *Offshore Geology of Eastern Canada*, v. 2, *Geol. Surv. Canada, Paper* 74-30.

- Johnson, A.M. (1970). *Physical Processes in Geology*. Freeman Cooper and Co., San Francisco, California, 571 pp.
- Jopling, A.V. and Walker, R.G. (1968). Morphology and origin of ripple-drift cross-lamination, with examples from the Pleistocene of Massachusetts. *Jour. Sed. Petrol.*, v. 38, p. 971-984.
- Keen, C.E., Keen, M.J., Barrett, D.L. and Heffler, D.E. (1975). Some aspects of the ocean-continent transition at the continental margin off eastern North America. IN van der Linden, W.J.M. and Wade, J.A. (eds.) *Offshore Geology of Eastern Canada*, v. 2, Geol. Surv. Canada, Paper 74-30.
- Kelling, G. and Stanley, D.J. (1976). Sedimentation in canyon, slope, and base of slope environments. IN Stanley, D.J. and Swift, D.J.P. (eds.) *Marine Sediment Transport and Environment Management*. Wiley-Interscience New York, p. 379-435.
- King, L. H. (1969). Submarine end-moraines and associated deposits on the Scotian Shelf. *G.S.A. Bull.*, v. 80, p. 83-96.
- King, L.H. (1970). Surficial Geology of the Halifax-Sable Island Map Area. *Marine Sciences Paper 1*, Dept. of Energy, Mines and Resources, Canada, 16 pp.
- King, L.H. (1979). Aspects of regional surficial geology related to site investigation requirements - eastern Canadian shelf. *International Conference, Offshore Site Investigation*. The Society for Underwater Technology, 34 pp.
- King, L.H. and MacLean, B. (1970). Continuous seismic-reflection study of Orpheus gravity anomaly. *Am. Assoc. Petrol. Geol. Gull.*, v. 54, p. 2007-2031.
- King, L.H. and Young, J.F. (1977). Paleocoastal slopes of East Coast Geosyncline (Canadian Atlantic Margin). *Can. J. Earth Sci.*, v. 14, p. 2553-2564.
- Komar, P.D. (1969). The Channelled Flow of Turbidity Currents with Application to Monterey Deep-Sea Fan Channel. *J. Geophys. Res.*, v. 74, p. 4544-4558.
- Komar, P.D. (1972). Relative significance of Head and Body Spill from a Channelled Turbidity Current. *GSA Bull.*, v. 83, p. 1151-1156.
- Komar, P.D. (1973). Continuity of Turbidity Current Flow and Systematic Variations in Deep Sea Channel Morphology. *GSA Bull.*, v. 84, p. 3329-3338.

- Kranck, K. (1975). Sediment deposited from flocculated suspensions. *Sedimentology*, v. 22, p. 111-123.
- Kranck, K. (1981). Particulate matter grain-size characteristics and flocculation in a partially mixed estuary. *Sedimentology*, v. 28, p. 107-114.
- Kurtz, D.B. and Anderson, J.B. (1979). Recognition and sedimentologic description of recent debris flow deposits from the Ross and Weddell Seas, Antarctica. *J. Sed. Pet.*, v. 49, p. 1159-1170.
- Laird, M.G. (1968). Rotational slumps and slump-scars in Silurian rocks, western Ireland. *Sedimentology*, v. 10, p. 111-120.
- Lively, R.R. (1979). Current Meter and Meteorological Observations on the Scotian Shelf, December 1975 to January 1978. Bedford Institute of Oceanography Data Series, B1-D-79-1, 2 volumes.
- Lohmann, G.P. (1978). Abyssal benthonic foraminifera as hydrographic indicators in the western South Atlantic Ocean. *J. Foram. Res.*, v. 8, p. 6-30.
- Loken, O.H., (1966). Baffin Island refugia older than 54,000 years. *Science*, v. 153, p. 1378-1380.
- Loring, D.H. and Nota, D.J.G. (1973). Morphology and sediments of the Gulf of St. Lawrence, Canada. *Fish. Res. Board Canada Bull.*, v. 182, 147 pp.
- Louis, J.P., Petrie, B.C. and Smith, P.C. (in press). Topographic Rossby Waves on the Continental Slope off Nova Scotia.
- MacLean, B. and King, L.H. (1971). Surficial Geology of the Banquereau and Misaine Bank Map Area. *Marine Sciences, Paper 3, Geol. Surv. Canada, Paper 71-52*, 19 pp.
- Marshall, N.F. (1978). A large storm-induced sediment slump reopens an unknown Scripps Submarine Canyon tributary. *IN Sedimentation in Submarine Canyons, Fans and Trenches* (eds. D.J. Stanley and G. Kelling) Dowden, Hutchinson and Ross Inc., Stroudsburg, Pa., p. 73-84.
- McCave, I.N. (1971). Sand waves in the North Sea off the coast of Holland. *Mar. Geol.*, v. 10, p. 199-225.
- McCave, I.N. (1972). Transport and Escape of Fine-Grained Sediment from Shelf Areas. *IN Swift, D.J.P., Duane, D.B. and Pilkey, O.H. (eds.) Shelf Sediment Transport: Process and Pattern.* Dowden, Hutchinson and Ross Inc., Stroudsburg, Pa. p. 225-248.

- McCave, I.N. and Swift, S.A. (1976). A physical model for the rate of deposition of fine-grained sediments in the deep sea. *G.S.A. Bull.* v. 87, p. 541-546.
- McGregor, B.A. and Bennett, R.H. (1977). Continental slope sediment instability northeast of Wilmington Canyon. *Am. Assoc. Petrol. Geol., Bull.*, v. 61, p. 918-.
- McGregor, B.A. and Bennett, R.H. (1979). Mass movement of sediment on the continental slope and rise seaward of the Baltimore Canyon Trough. *Mar. Geol.*, v. 33, p. 163-.
- McGregor, B.A., Bennett, R.H. and Lambert, D.N. (1979). Bottom processes, morphology, and geotechnical properties of the continental slope south of Baltimore Canyon. *Applied Ocean Research*, v. 1, p. 177-187.
- McIver, N.L. (1972). Cenozoic and Mesozoic Stratigraphy of the N.S. Shelf. *Can. J. Earth Sci.*, v. 9, p. 54-70.
- McLellan, H.J. (1957). On the distinctiveness and origin of the Slope Water off the Scotian Shelf and its easterly flow south of the Grand Banks. *J. Fish. Res. Bd. Canada*, v. 14, p. 213-239.
- McLellan, H.J. (1975). *Elements of Physical Oceanography*. Pergamon Press, 151 pp.
- Menard, H.W. (1964). *Marine Geology of the Pacific*. McGraw-Hill, New York, 271 pp.
- Miall, A.D. (1973). Markov chain analysis applied to an ancient alluvial plain succession. *Sedimentology*, v. 20, p. 347-364.
- Middleton, G.V. (1976). Hydraulic interpretation of sand size distributions. *Jour. Geol.*, v. 84, p. 405-426.
- Middleton, G.V. and Hampton, M.A. (1976). Subaqueous Sediment Transport and Deposition by Sediment Gravity Flows. IN *Marine Sediment Transport and Environmental Management* (eds. D.J. Stanley and D.J.P. Swift), Wiley Interscience, N.Y., p. 197-218.
- Miller, G.H. (1977). Calibration of amino acid reactions and palaeotemperature reconstructions for eastern Baffin Island. Unpublished abstract, 6th Ann. Baffin Is./Arctic Canada Workshop, INSTAAR, Univ. of Colorado, Boulder.
- Miller, G.H. and Dyke, A.S. (1974). Proposed extent of late Wisconsin Laurentide ice on eastern Baffin Island. *Geology*, v. 2, p. 125-130.

- Moore, D.G. (1961). Submarine slumps. *J. Sed. Pet.*, v. 31, p. 343-357.
- Moore, D.G. (1969). Reflection Profiling Studies of the California Continental Borderland: Structure and Quaternary Turbidite Basins. *Geol. Soc. Am. Spec. Paper*, 107, 142 pp.
- Moore, D.G. (1977). Submarine Slides. IN *Rock Slides and Avalanches*, vol. 1: Developments in Geotechnical Engineering (ed. Voight, B.) p. 563-604.
- Morgensten, N.R. (1967). Submarine slumping and the initiation of turbidity currents. IN *Marine Geotechnique* (ed. A.F. Richards), p. 189-220, Univ. Illinois Press, Urbana.
- Moss, A.J. (1972). Bedload sediments. *Sedimentology*, v. 18, p. 159-219.
- Mudie, P.J. (1980). Palynology of Later Quaternary Marine Sediments, Eastern Canada. Unpublished Ph.D. thesis, Dalhousie University, Halifax, N. S. Canada, 464 pp.
- Mullins, H.T. and Neumann, A.C. (1979). Deep carbonate bank margin structure and sedimentation in the Northern Bahamas. IN Doyle, L.J. and Pilkey, O.H. (eds.) *Geology of continental slopes*. SEPM Special Publication No. 27, p. 165-192.
- Mutti, E. (1977). Distinctive thin-bedded turbidite facies and related depositional environments in the Eocene Hecho Grou (south-central Pyrenees, Spain). *Sedimentology*, v. 24, p. 107-131.
- Nardin, T.R., Hein, F.J., Gorsline, D.S. and Edwards, B.D. (1979). A Review of Mass Movement Processes, Sediment and Acoustic Characteristics, and Contrasts in Slope and Base-of-Slope Systems versus Canyon-Fan-Basin Floor Systems. IN Doyle, L.J. and Pilkey, O.H. (eds.) *Geology of Continental Slopes*, SEPM Special Publ., No. 27, p. 61-73.
- Needham, H.D., Habib, D. and Heezen, B.C. (1969). Upper Carboniferous palynomorphs as a tracer of red sediment dispersal patterns in the N.W. Atlantic. *J. Geol.* 77, p. 113-120.
- Nelson, C.H. and Kulm, L.D. (1973). Submarine fans and channels. IN: *Turbidites and deep-water sedimentation*. SEPM Pacific Section, Short Course, Anaheim, p. 39-78.
- Nelson, D.D., Pierce, J.W. and Colquhoun, D.D. (1973). Sediment dispersal by cascading coastal water. *Geol. Soc. Am. Abstr. Programs*, v. 8, p. 423-424.

- Nielsen, E. (1976). The composition and Origin of Wisconsin Till In Mainland Nova Scotia. Unpublished Ph.D. thesis, Dalhousie University, Halifax, N.S., 256 pp.
- Normark, W.R. (1970). Growth patterns of deep-sea fans. AAPG Bull., v. 54, p. 2170-2195.
- Normark, W.R. and Piper, D.J.W. (1972). Sediments and growth pattern of Navy deep sea fan, San Clemente Basin, California borderline: J. Geology, v. 80, p. 198-223.
- Petrie, B. and Smith, P.C. (1977). Low Frequency Motions on the Scotian Shelf and Slope. Atmosphere, v. 15, p. 117-139.
- Pickard, G.L. (1979). Descriptive Physical Oceanography. Pergamon Press, Toronto.
- Pierce, J.W. (1976). Suspended sediment transport at the shelf break and over the outer margin. IN Stanley, D.J. and Swift, D.J.P., Marine Sediment Transport and Environmental Management. Wiley Interscience, New York, p. 437-458.
- Pierson, T.C. (1980). Erosion and deposition by debris flows at Mt. Thomas, North Canterbury, New Zealand. Earth Surface Processes, v. 5, p. 227-247.
- Piper, D.J.W. (1976). Manual of Sedimentological Techniques. Dept. of Geology, Dalhousie University, 96 p.
- Piper, D.J.W. (1976). The Use of Ice-Rafted Marine Sediments in Determining Glacial Conditions. Rev. Geogr. Montr., v. XXX, p. 207-212.
- Piper, D.J.W. (1978). Turbidite Muds and Silts on Deep sea Fans and Abyssal Plains. IN Sedimentation in Submarine Canyons, Fans, and Trenches (eds. D.J. Stanley and G. Kelling).
- Piper, D.J.W. and Brisco, C.D. (1975). Deep-water continental margin sedimentation DSDP Leg 28, Antarctica. IN (Hayes, D.E., Frakes, L.A. et al.) Initial Repts. of Deep Sea Drilling Project, v. XXVII, p. 727-755.
- Piper, D.J.W. and Marshall, N.F. (1969). Bioturbation of Holocene sediment on La Jolla deep-sea fan, California. Jour. Sed. Petrol., v. 39, p. 601-606.
- Piper, D.J.W., Normark, W.R. and Ingle, J.C. (1976). The Rio Dell Formation: A Plio-Pleistocene basin slope deposit in Northern California. Sedimentology, v. 23, p. 309-328.

- Piper, D.J.W., Panagos, A.G. and Pe, G.G. (1978). Conglomeratic Miocene Flysch, Western Greece. *J. Sed. Pet.*, v. 48, p. 117-126.
- Piper, D.J.W., Mudie, P.J., Letson, J.R.J., Barnes, N., Iuliucci, R.J. and Scott, D.P. (in preparation). The Marine Geology of the South Shore, Nova Scotia. *Geol. Surv. Canada Paper*.
- Prior, D.B. and Suhayda, J.N. (1979). Application of infinite slope analysis to subaqueous sediment instability, Mississippi Delta. *Eng. Geol.*, v. 14, p. 1-10.
- Quinlan, G.M. (1981). Numerical models of postglacial relative sea level change in Atlantic Canada and the eastern Canadian Arctic. Unpublished Ph.D. thesis, Dalhousie University, Halifax, N.S. 499 pp.
- Quinlan, G. and Beaumont, C. (1981). A comparison of observed and theoretical postglacial relative sea level in Atlantic Canada. *Can. Jour. Earth Sci.*, v. 18, p. 1146-1163.
- Reading, H.G. (ed.) (1978). *Sedimentary Environments and Facies*. Elsevier, New York, 557 pp.
- Reimnitz, E. (1971). Surf-beat origin for pulsating bottom currents in the Rio Balsas submarine canyon, Mexico. *Geol. Soc. Amer., Bull.*, v. 82, p. 81-90.
- Reineck, H.-E. and Singh, I.B. (1975). *Depositional Sedimentary Environments*. Springer-Verlag, New York, 439 pp.
- Robe, R.Q. (1971). Oceanographic Observations, North Atlantic Standard Monitoring Systems A1, A2, A3 and A4, 1967-68. U.S. Coast Guard, Oceanographic Report No. 43, 227 pp.
- Robin, G. de Q. (1977). Ice cores and climatic change. *Phil. Trans., Royal Soc. London, Series B.*, v. 20, p. 169-182.
- Rona, P.A. (1969). Middle Atlantic continental slope of the U.S.: deposition erosion. *AAPG Bull.* 53, p. 1431-1465.
- Rupke, N.A. (1975). Deposition of fine-grained sediments in the abyssal environments of the Algeno-Balearic Basin, western Mediterranean Sea. *Sedimentology*, v. 22, p. 95-109.
- Rupke, N.A. (1978). Deep Clastic Seas. *IN Sedimentary Environments and Facies* (ed. H.G. Reading), Elsevier, p. 372-415.
- Ryan, W.B.F. (in press). Imaging of submarine landslides with wide-swath sonar. NATO Science Workshop on Marine Slides and Other Mass Movements.

- Sangrey, D.A. (1981). Geotechnical Engineering Link between Offshore Processes and Hazards. IN Bouma, A.H. et al. Offshore Geologic Hazards AAPG Education Course Note Series #18, p. 3-1 to 3-75.
- Schlee, J.S., Dillon, W.P. and Grow, J.A. (1979). Structure of the Continental Slope off the Eastern United States. IN Geology of Continental Slopes (eds. Doyle, L.J. and Pilkey, O.H.) SEPM Spec. Publ. No. 27, p. 95-117.
- Schneider, E.D. and Heezen, B.C. (1966). Sediments of the Caicos Outer Ridge, the Bahamas. GSA Bull., v. 77, p. 1361-1398.
- Schnitker, D. (1974). West Atlantic abyssal circulation during the past 120,000 years. Nature, v. 248, p. 385-387.
- Schnitker, D. (1979). The Deep Waters of the western North Atlantic during the past 24,000 years, and the reinitiation of the Western Boundary Undercurrent. Mar. Micropal., v. 4, p. 265-280.
- Schumm, S.A. (1977). The Fluvial System. Wiley Interscience, New York, 338 p.
- Scott, D.B.S. and Medioli, F.S. (1979). Marine Emergence and Submergence in the Maritimes. Unpublished Progress Report to Dept. of Energy, Mines and Resources.
- Scott, D.B. and Medioli, F.S. (1980). Post-glacial emergence curves in the Maritimes determined from marine sediments in raised basins. Proceedings of Canadian Coastal Conference 1980 Burlington, Ontario.
- Shelton, J.S. (1966). Geology Illustrated. W.H. Freeman & Co., San Francisco.
- Shepard, F.P. (1954). Nomenclature based on sand-silt-clay ratios. Jour. Sed. Pet., v. 24, p. 151-158.
- Shepard, F.P. (1973). Submarine Geology (3rd ed.). New York, Harper and Row, 517 p.
- Shepard, F.P. and Dill, R.F. (1966). Submarine Canyons and Other Sea Valleys. Chicago, Rand McNally and Co., 381 pp.
- Shepard, F.P. and Marshall, N.F. (1973). Storm-generated current in a LaJolla submarine canyon, California. Mar. Geol., v. 15, p. M19-M24.
- Shepard, F.P., Marshall, N.F., McLoughlin, P.A. and Sullivan, G.G. (1979). Currents in Submarine Canyons and Other Sea Valleys. AAPG Studies in Geology, No. 8, 173 pp.

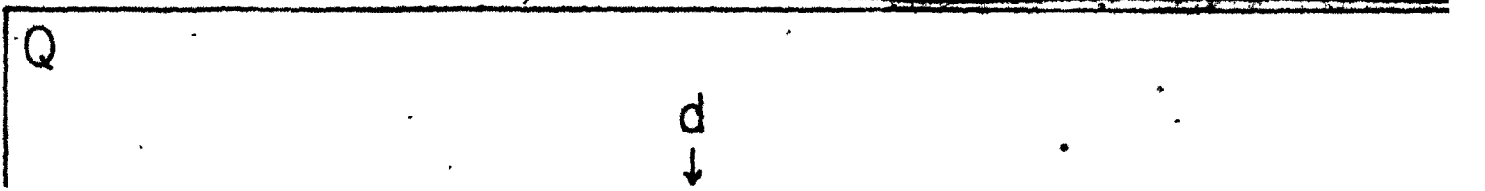
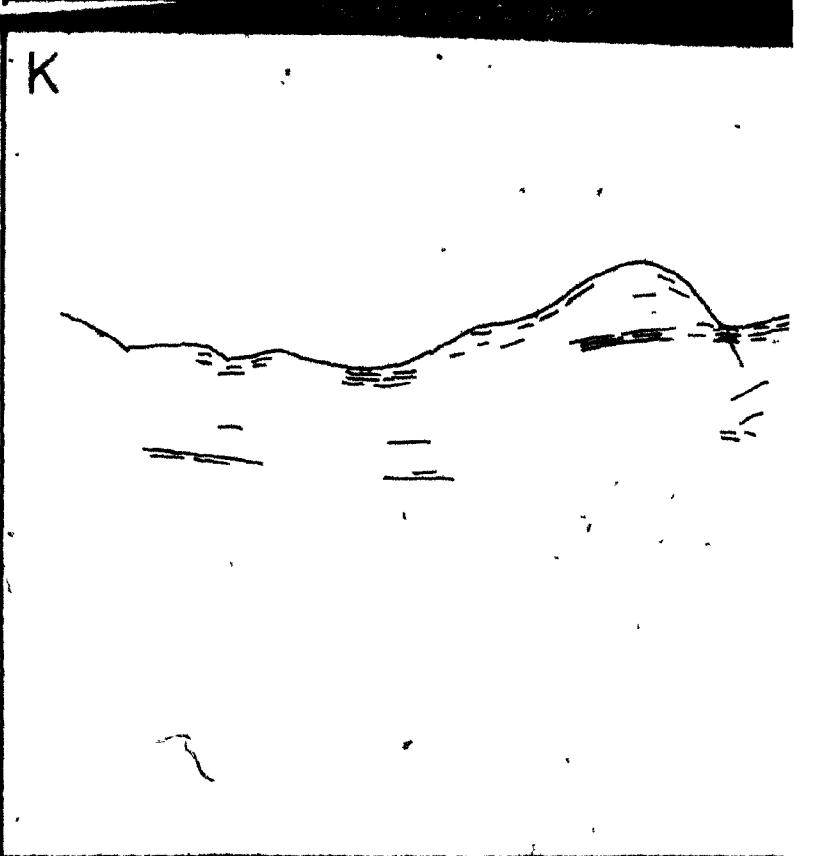
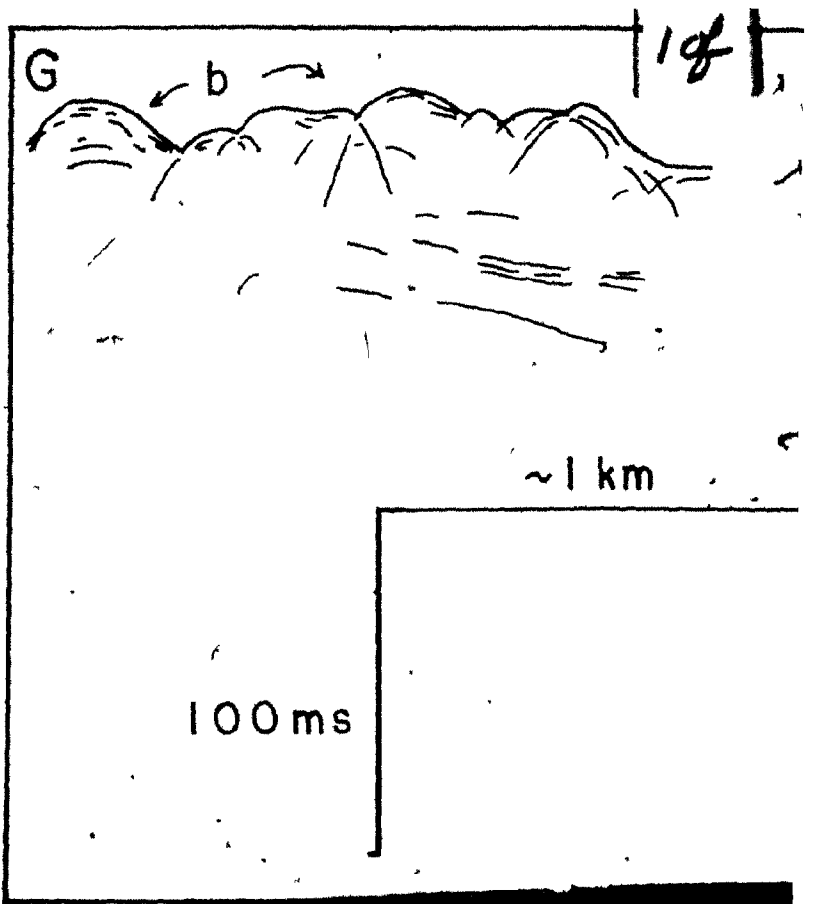
- Silverberg, N. (1965). Reconnaissance of the upper continental slope off Sable Island Bank, Nova Scotia. Unpublished M.Sc. Thesis, Dalhousie University, Halifax, Nova Scotia.
- Somers, M.L., Carson, R.M., Revie, J.A., Edge, R.H., Barrow, B.J. and Andrews, P.G. (1978). GLORIA II An improved long-range sidescan sonar. Proceedings of IEE/IERE Sub-Conference on Offshore Instrumentation Communication. Oceanology International 1978. BPS Publications Ltd., London, pp. 16-24.
- Southard, J.B. and Stanley, D.J. (1976). Shelf Break Processes and Sedimentation. IN Stanley, D.J. and Swift, D.J.P. Marine Sediment Transport and Environmental Management. Wiley-Interscience, New York, p. 351-377.
- Stanley, D.J. and Swift, D.J.P. (eds.) (1976). Marine Sediment Transport and Environmental Management. Wiley-Interscience, New York, 602 pp.
- Stanley, D.J. and Unrug, R. (1972). Submarine channel deposits, fluxoturbidites and other indicators of slope and base-of-slope environments in modern and ancient marine basins. IN Recognition of Ancient Sedimentary Environments (Rigby, J.K. and Hamblin, W.K. eds.) SEPM Special Publ. No. 16, p. 287-340.
- Stanley, D.J. and Wear, C.M. (1978). The "Mud-Line": An Erosion-Deposition Boundary on the Upper Continental Slope. Mar. Geol. v. 28, p. M19-M29.
- Stanley, D.J., Drapeau, G. and Cok, A.E. (1968). Submerged Terraces on the Nova Scotian Shelf. Zeitschrift fur Geomorphologie, Supplement 7, p. 85-94.
- Stanley, D.J., Swift, D.J.P., Silverberg, N., James, N.P. and Sutton, R.G. (1972). Late Quaternary Progradation and Sand "Spillover" on the Outer Continental Margin off Nova Scotia, Southeast Canada. Smithsonian Contrib. Earth Sci., No. 8, 88 pp.
- Stommel, H. (1965). The Gulf Stream: a physical and dynamical description. Univ. of Calif. Press, 202 pp.
- Stow, D.A.V. (1977). Late Quaternary Stratigraphy and Sedimentation on the Nova Scotia Outer Continental Margin. Unpublished Ph.D. thesis, Dalhousie University, Halifax, N.S., 360 pp.
- Stow, D.A.V. and Bowen, A.J. (1980). A physical model for the transport and sorting of fine-grained sediment by turbidity currents. Sedimentology, v. 27, p. 31-46.

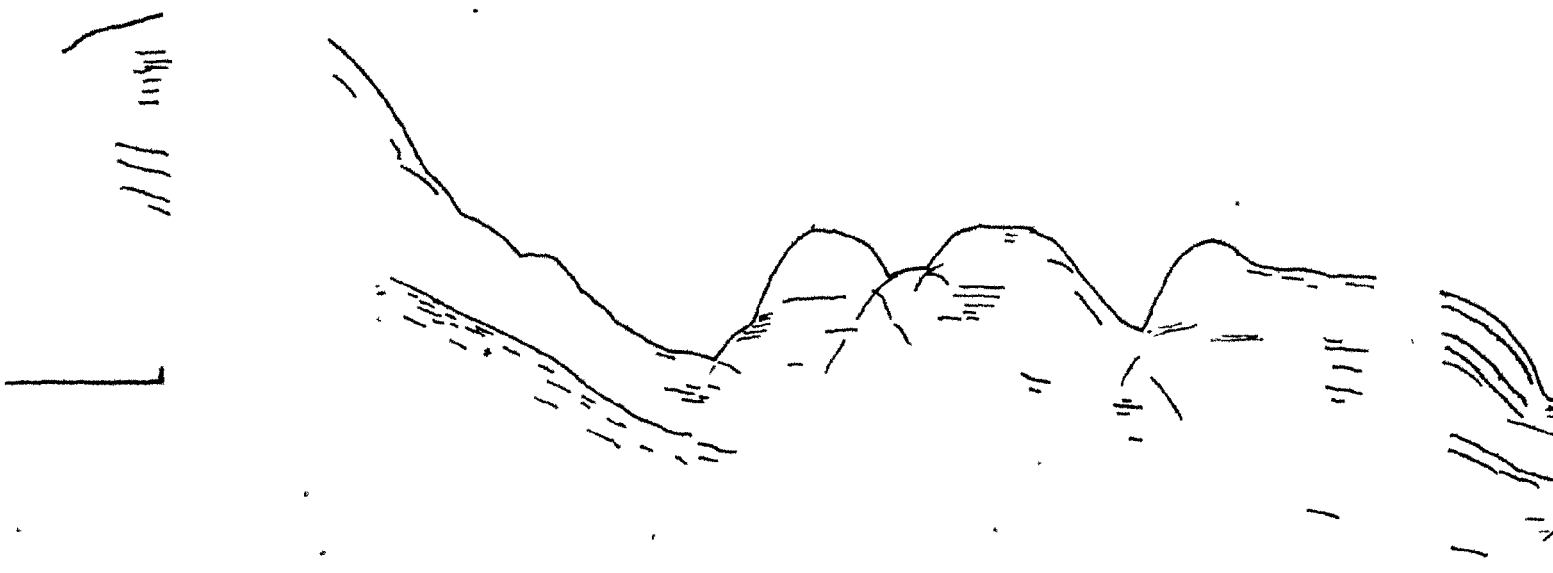
- Stow, D.A.V. and Lovell, J.P.B. (1979). Contourites: Their Recognition in Modern and Ancient Sediments. *Earth Sci. Rev.*, v. 14, p. 251-291.
- Streeter, S.S. (1973). Bottom water and benthonic foraminifera in the North Atlantic - glacial-interglacial contrasts. *Quat. Res.*, v. 3, p. 131-141.
- Streeter, S.S. and Shackleton, N.J. (1979). Paleocirculation of the Deep North Atlantic: 150,000 Year Record of Benthonic Foraminifera and Oxygen 18. *Science*, v. 208, p. 168-171.
- Till, R. (1974). *Statistical Methods for the Earth Scientist*. John Wiley, New York.
- Valentine, P.C., Uzzmann, J.R. and Cooper, R.A. (1980). Geology and biology of Oceanographer Submarine Canyon. *Mar. Geol.*, v. 3, p. 283-312.
- Vilks, G. (1981). Late Glacial-Postglacial Foraminiferal Boundary in Sediments of Eastern Canada, Denmark and Norway. *Geoscience Canada*, v. 8, p. 48-55.
- Vilks, G. and Rashid, M.A. (1976). Post-glacial paleo-oceanography of Emerald Basin, Scotian Shelf. *Can. J. Earth Sci.*, v. 13, p. 1256-1267.
- Visher, G.S. (1969). Grain Size Distribution and Depositional Processes. *J. Sed. Pet.*, v. 39, p. 1074-1106.
- Walker, R.G. (1979). Racies Models 8. Turbidites and Associated Coarse Clastic Deposits. IN *Facies Models* (R.G. Walker, ed.) *Geoscience Canada Reprint Series 1*, p. 91-103.
- Walker, R.G. and Mutti, E. (1973). Turbidite facies and facies associations. IN Middleton, G.V. and Bouma, A.H. (eds.) *Turbidites and deep water sedimentation*. Pacific Section, Soc. Econ. Paleont. Min., Short Course Notes, p. 119-157.
- Watkins, D.J. and Kraft, L.M. (1978). Stability of Continental Shelf and Slope off Louisiana and Texas: Geotechnical Aspects. IN *Framework, Facies and Oil Trapping Characteristics of the Upper Continental Margin* (eds. A.H. Bouma, G.T. Moore and J.M. Coleman). AAPG Studies in Geology, No. 7.
- Worthington, L.V. (1976). On the North Atlantic circulation. The Johns Hopkins Oceanographic Studies, No. 6, The Johns Hopkins Univ. Press., Baltimore, 110 pp.

Worthington, L.V. and Wright, W.R. (1970). North Atlantic Ocean Atlas of potential temperature and salinity in the deep water, including temperature, salinity and oxygen profiles from the Erika Dan cruise of 1962. Woods Hole Oceanographic Institute, Atlas Series, v. 2, 58 plates.

Wright, L.D. (1977). Sediment Transport and Deposition at River Mouths: A Synthesis. Geol. Soc. Am., Bull., v. 88, p. 857-868.

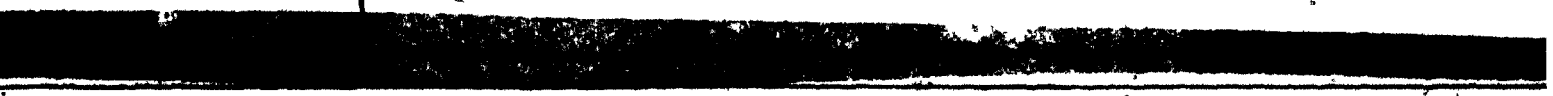
Young, R.N. and Southard, J.B. (1978). Erosion of fine-grained marine sediments: seafloor and laboratory experiments. G.S.A. Bull., v. 89, p. 663-672.





~1km

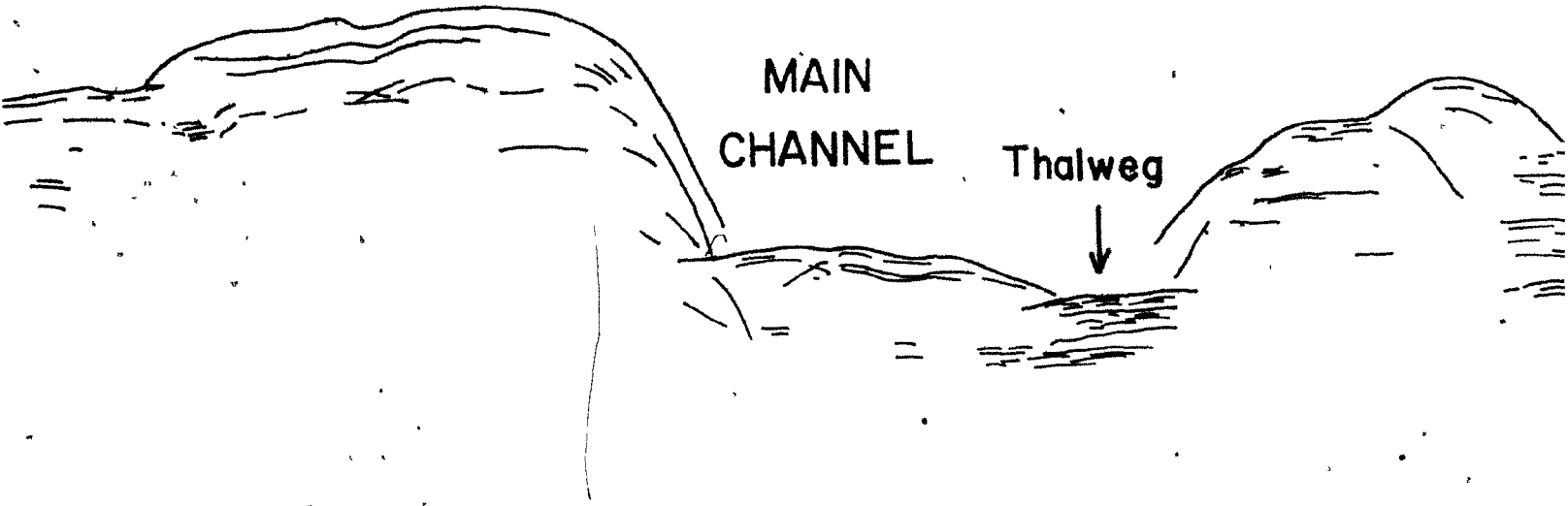
100 ms



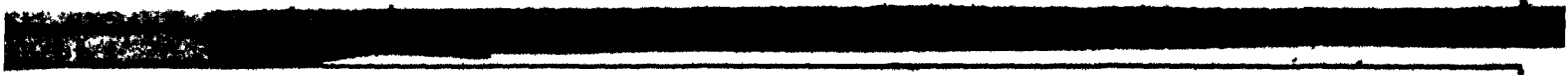
MAIN  
CHANNEL



MAIN  
CHANNEL Thalweg



10  
G



K'



— Depositional Lobe —————>

159

G'



K'

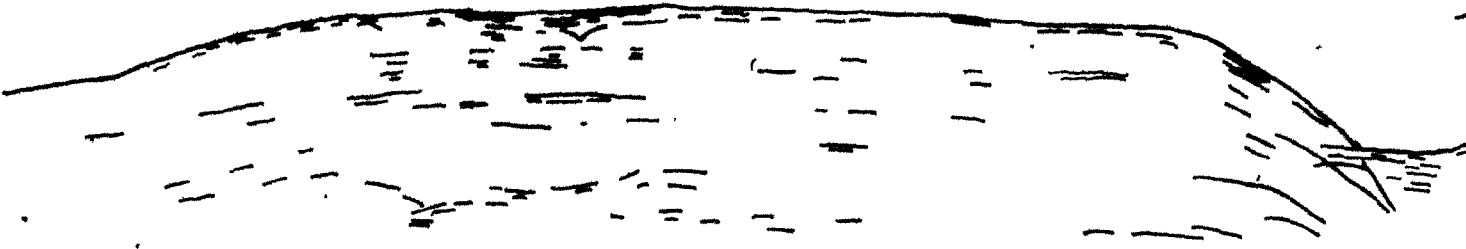


Q'



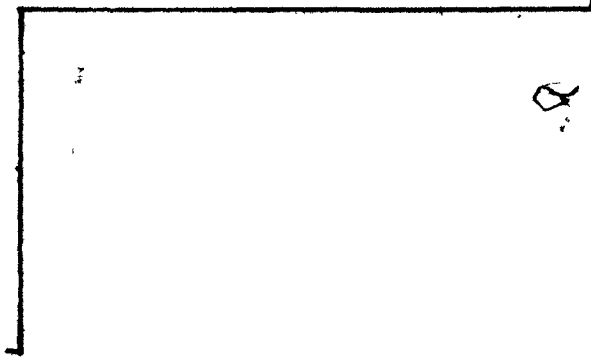
Q

d  
↓



~ 1 km

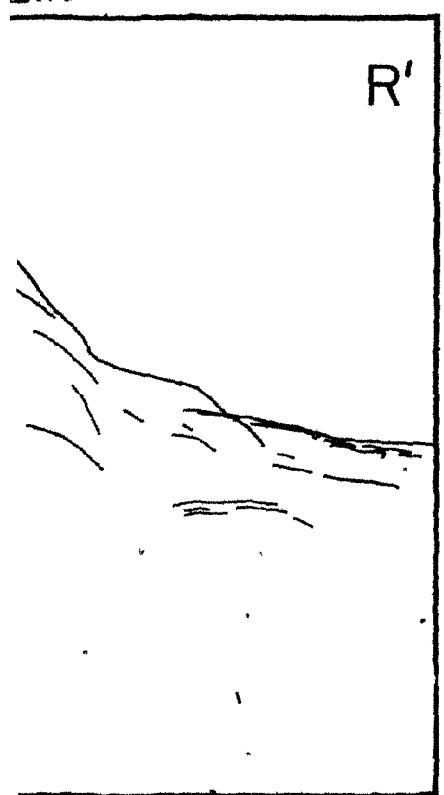
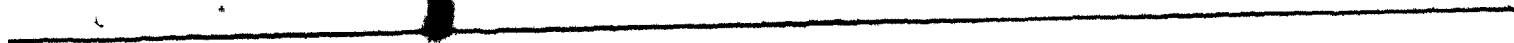
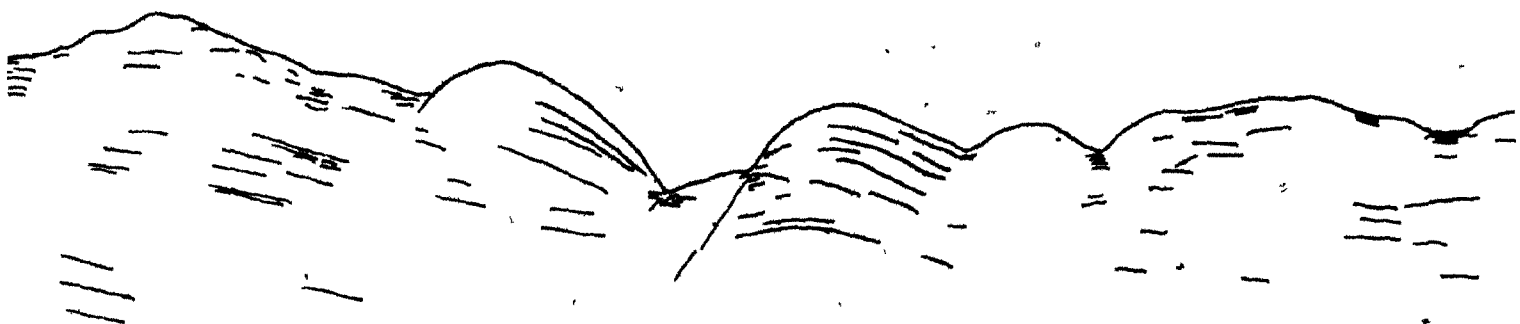
100 ms



d  
↓

~ 500 m

50 ms

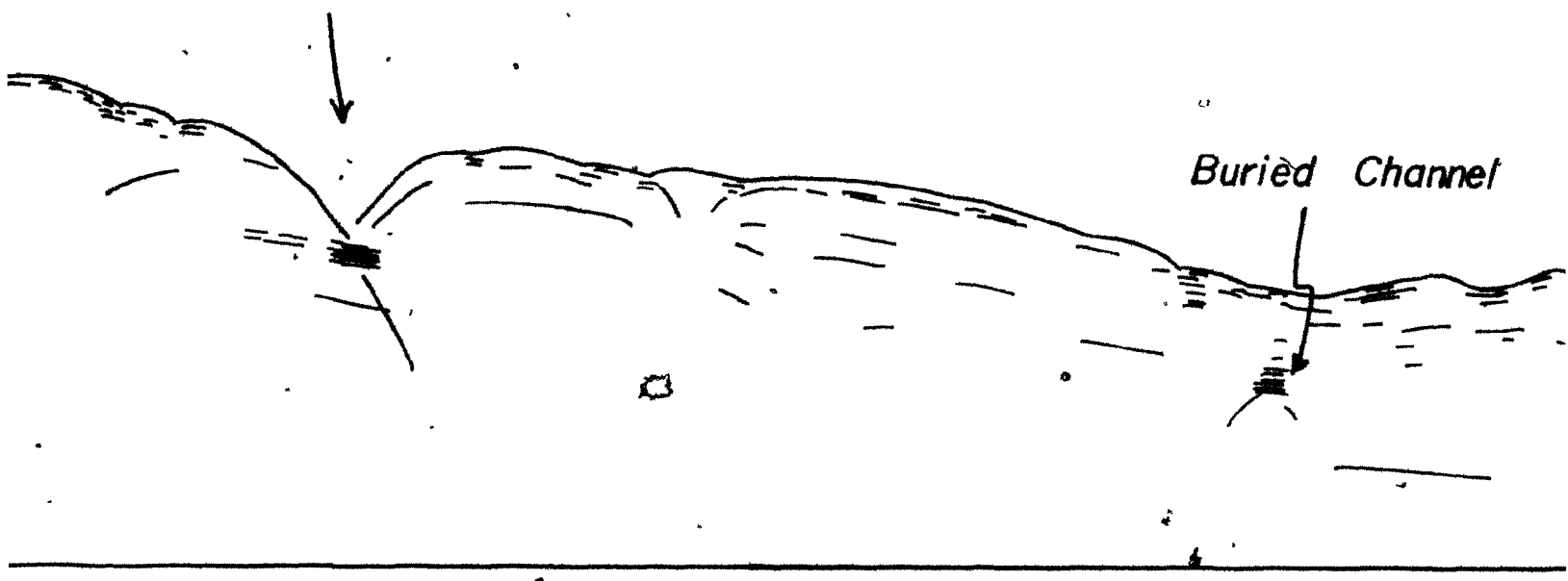




— Depositional Lobe —————>

MAIN  
CHANNEL

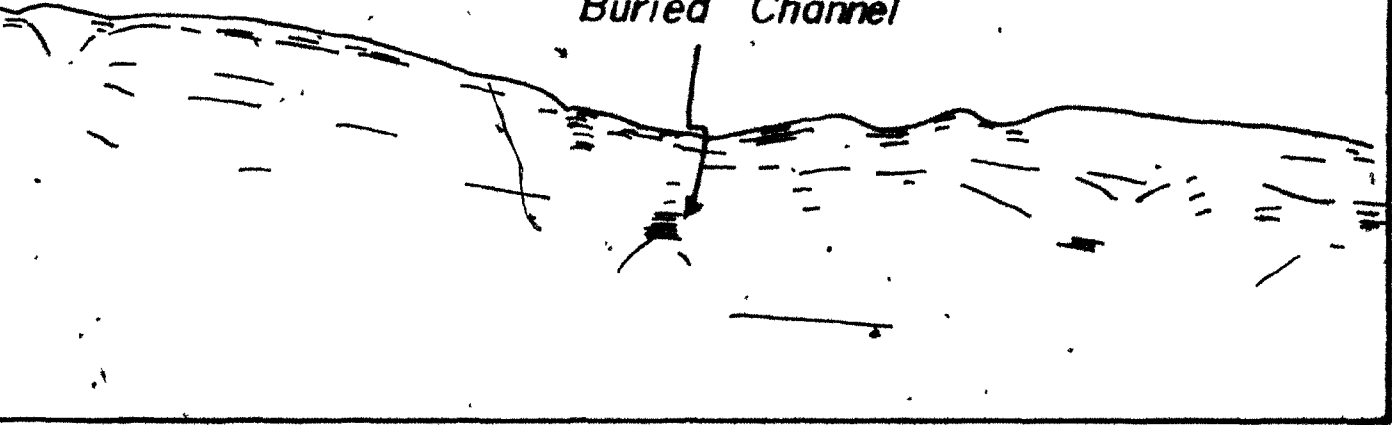
Buried Channel



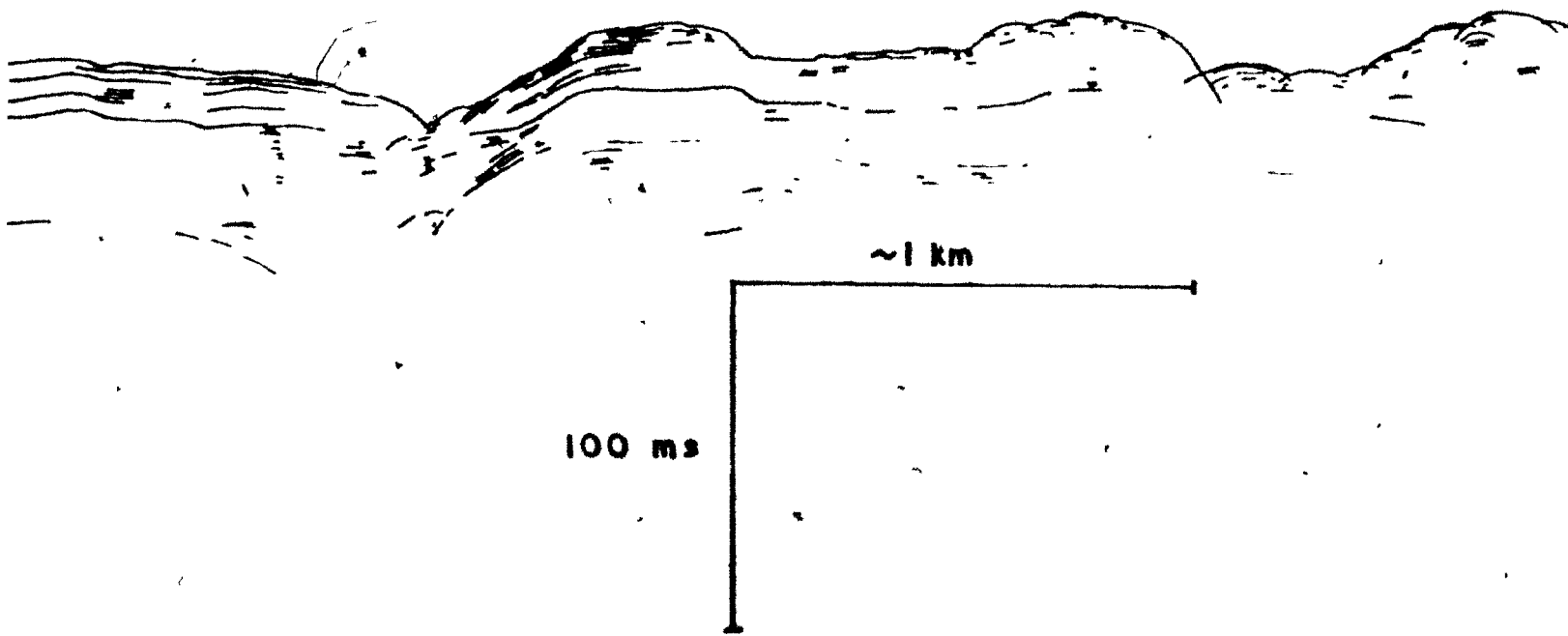
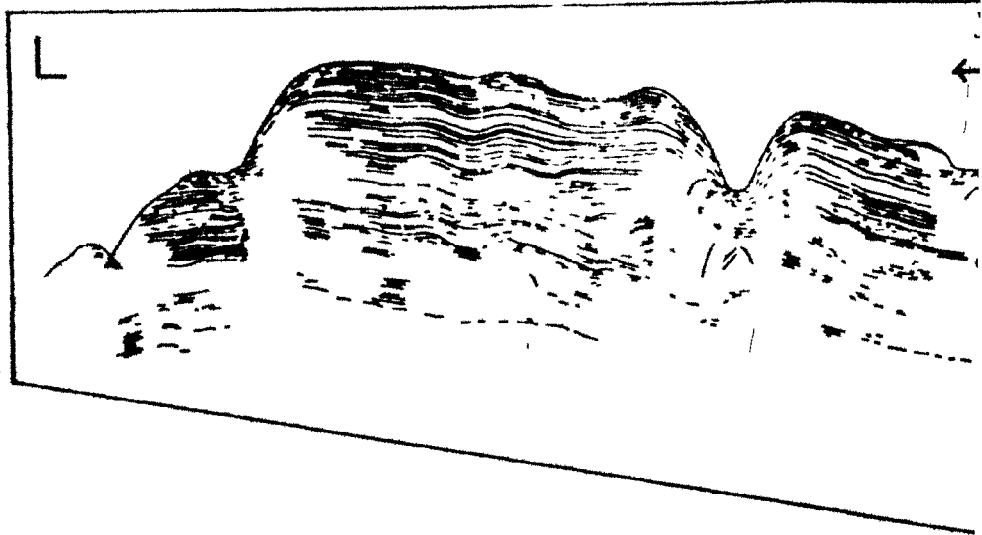
Q



Buried Channel

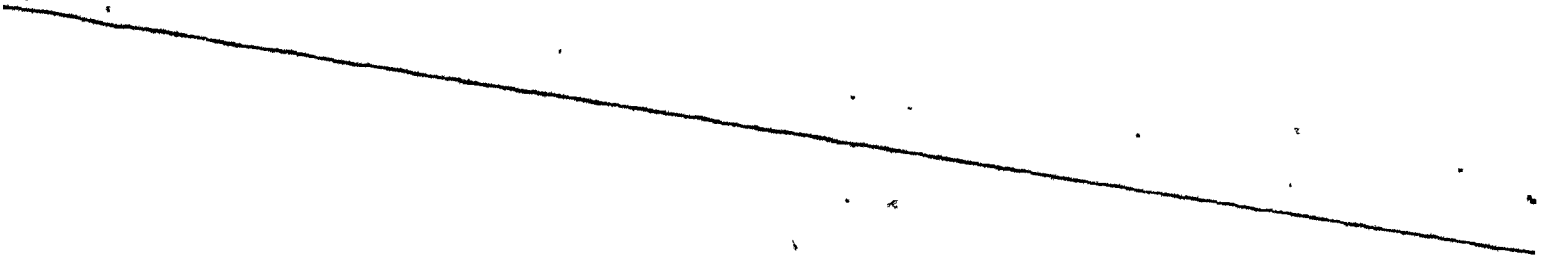


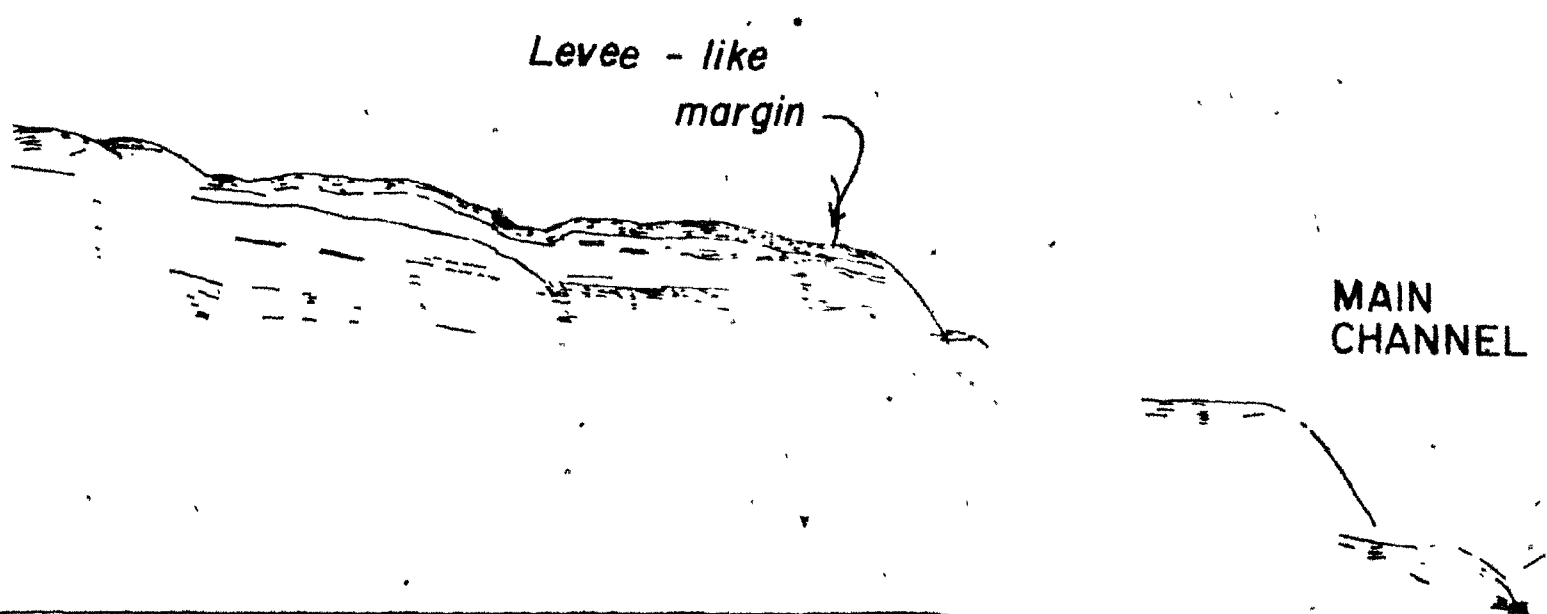
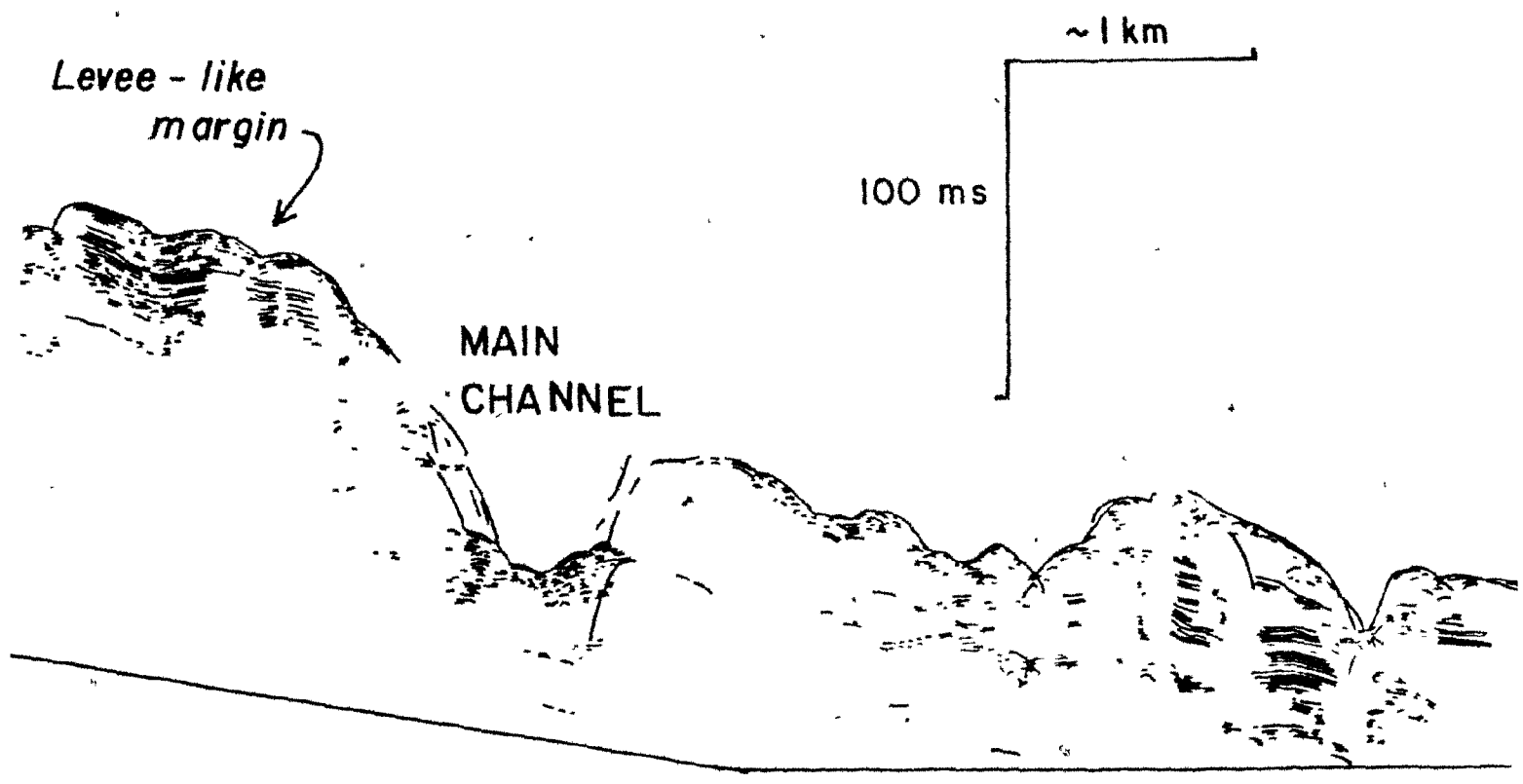
10 of 10

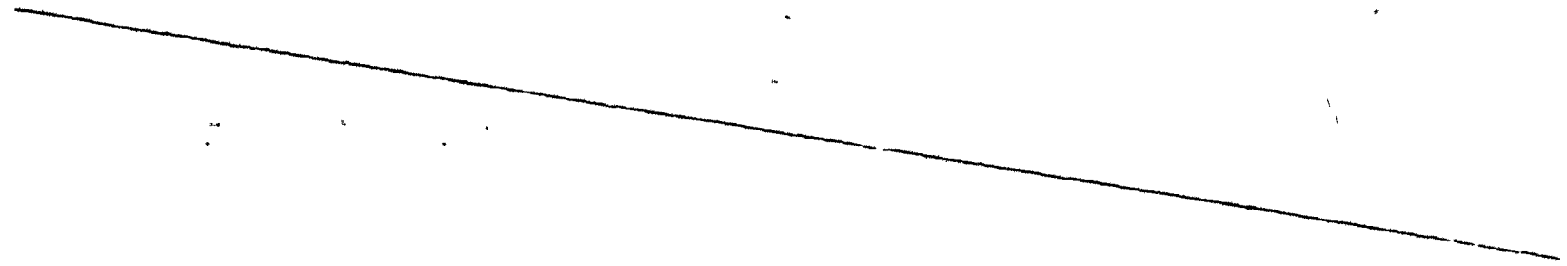
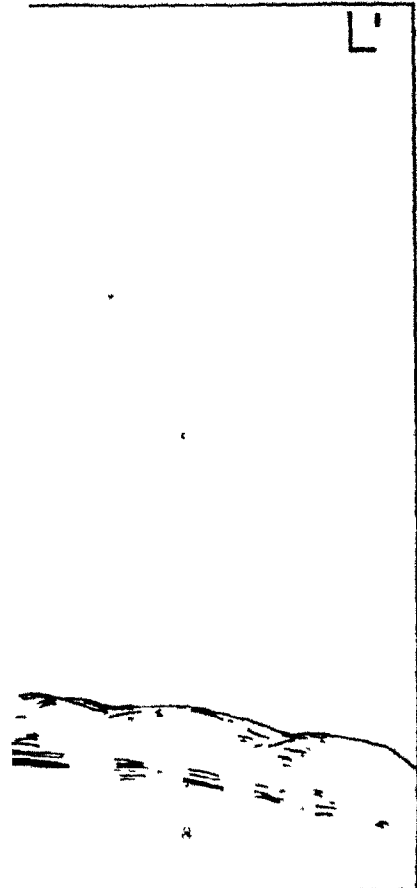


← ZONE OF REMOVAL →

L6



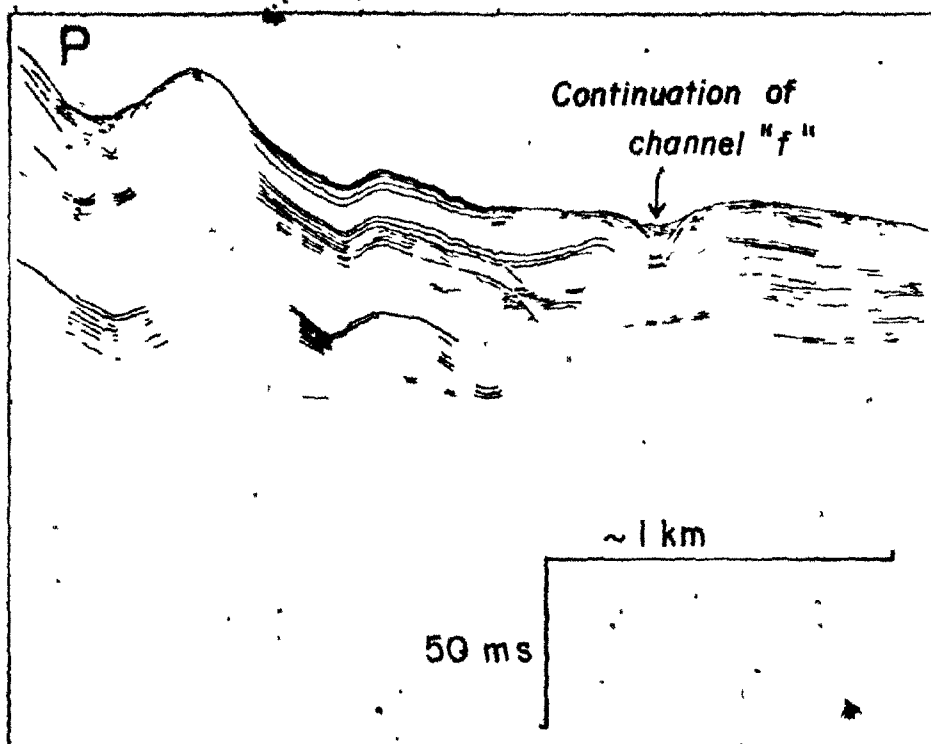




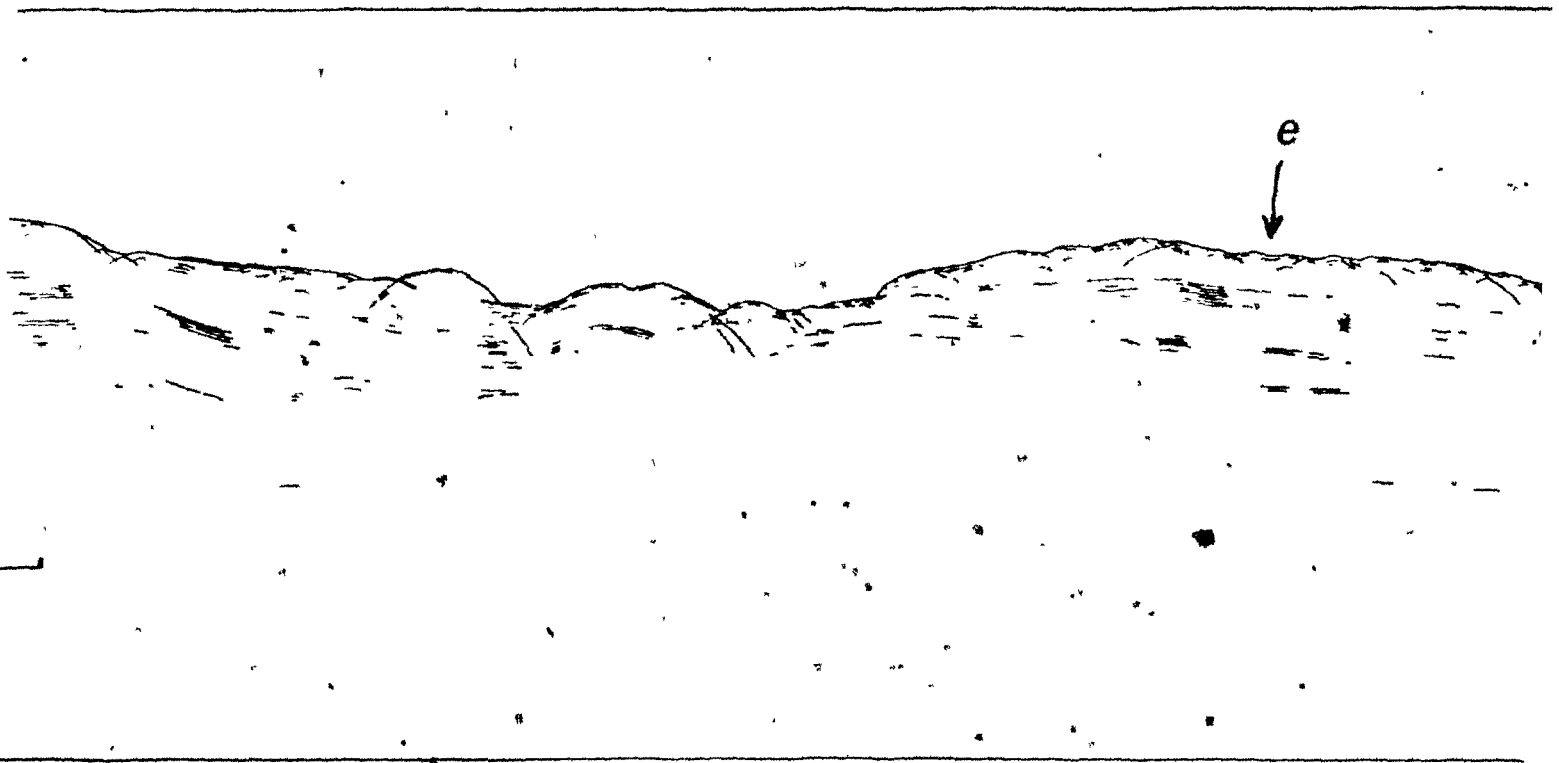
EL



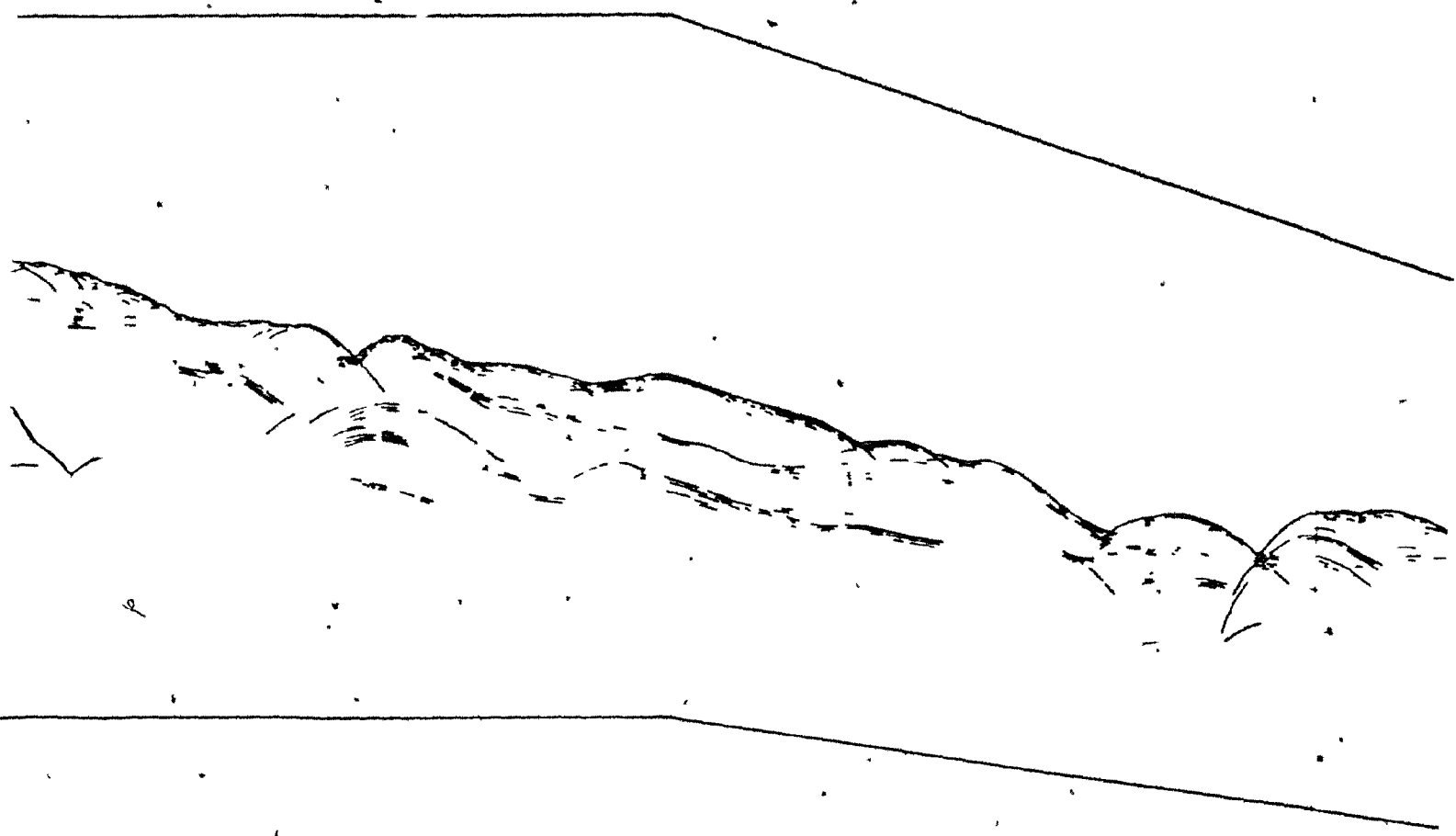
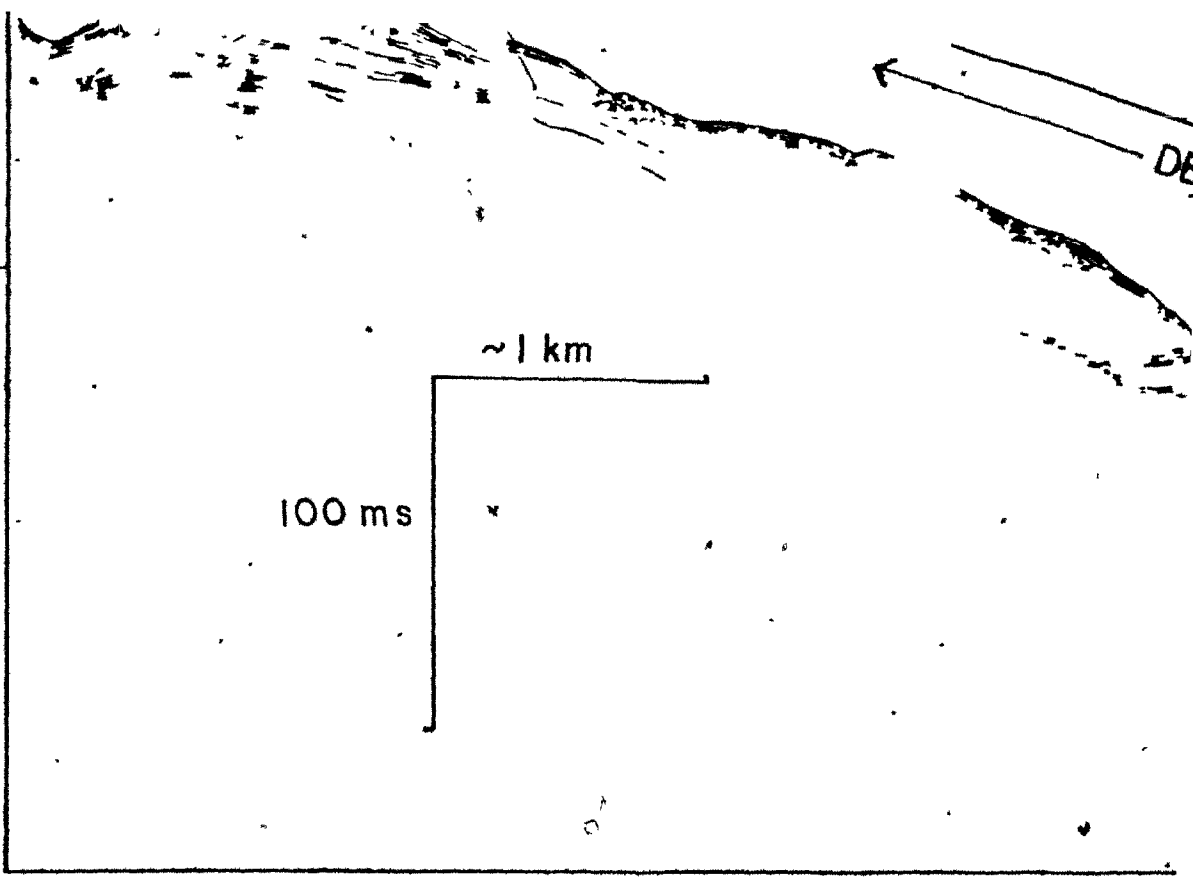




69



74



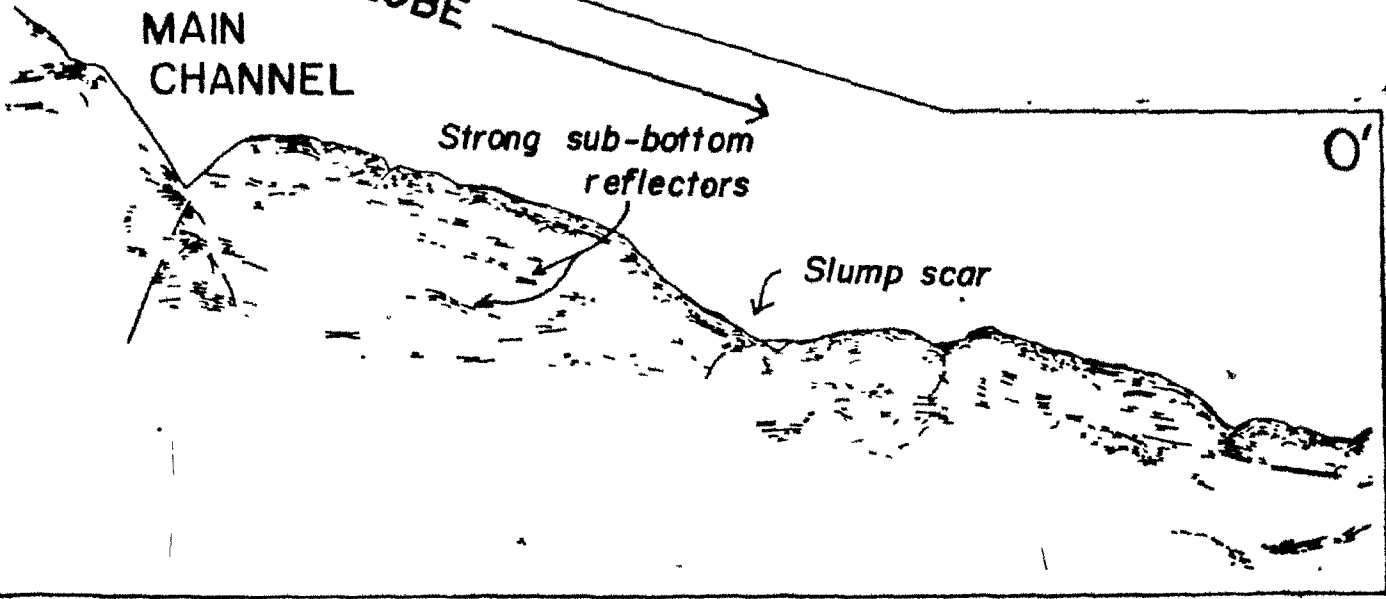
DEPOSITIONAL LOBE

MAIN CHANNEL

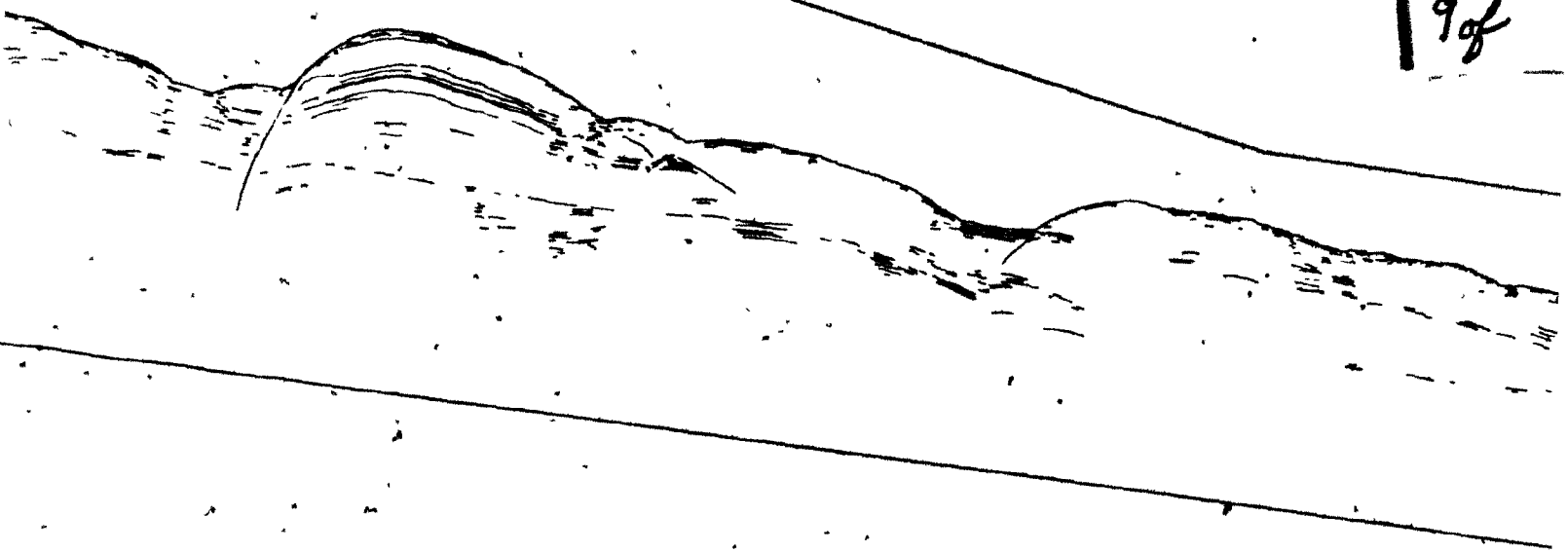
Strong sub-bottom reflectors

Slump scar

0'

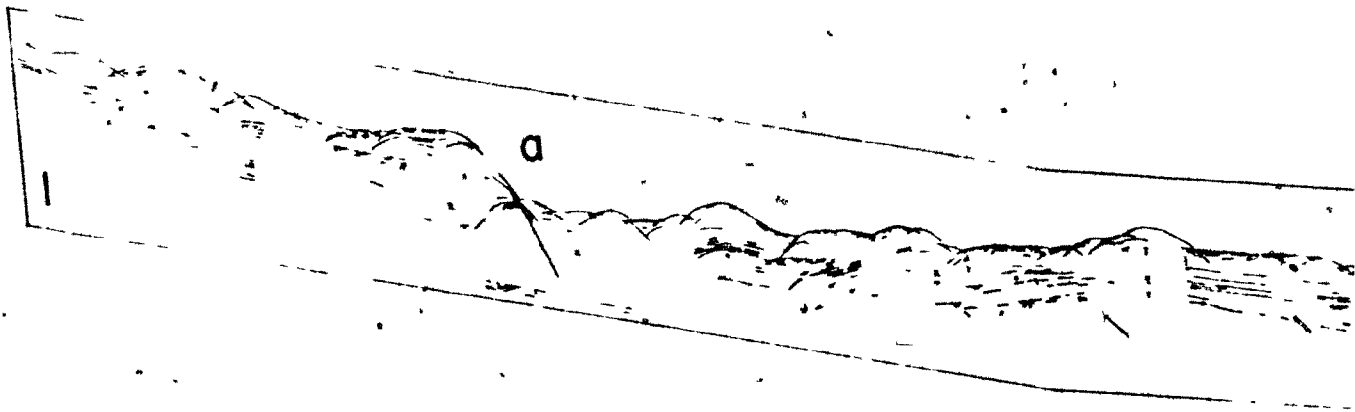
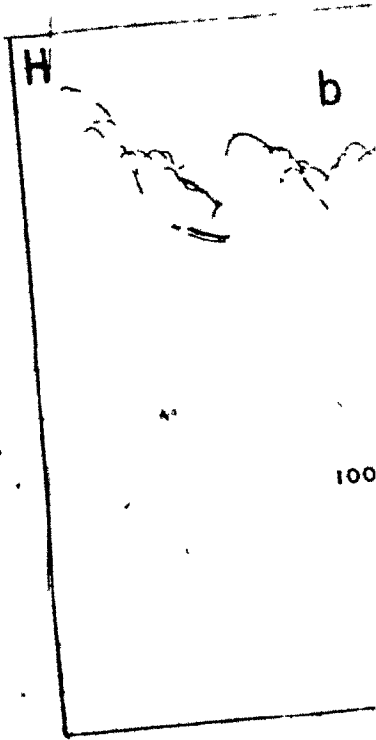


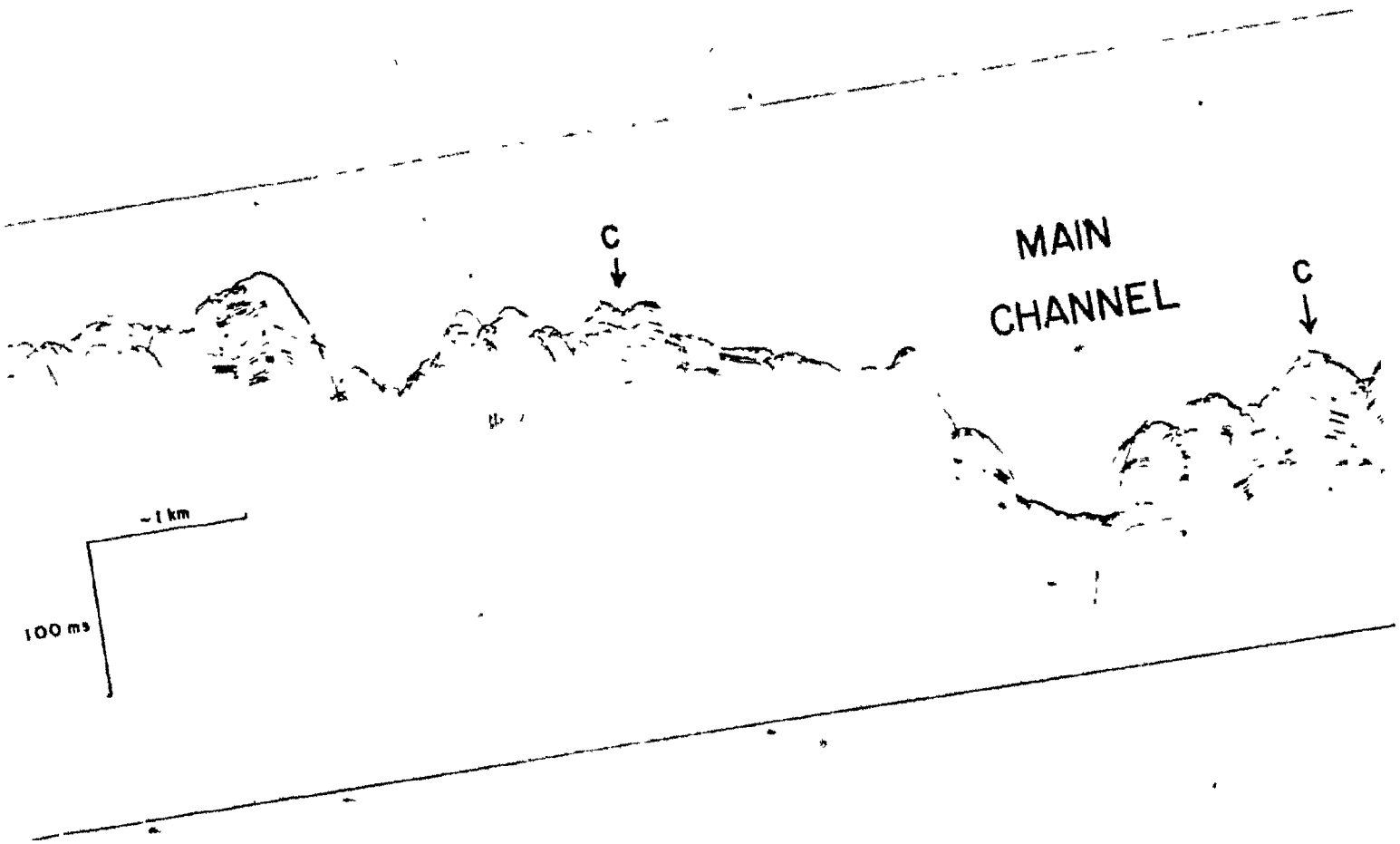
19 of



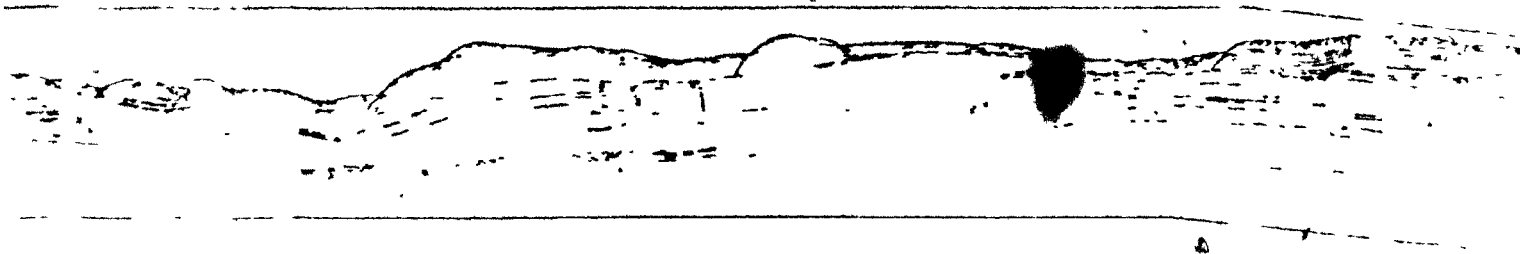


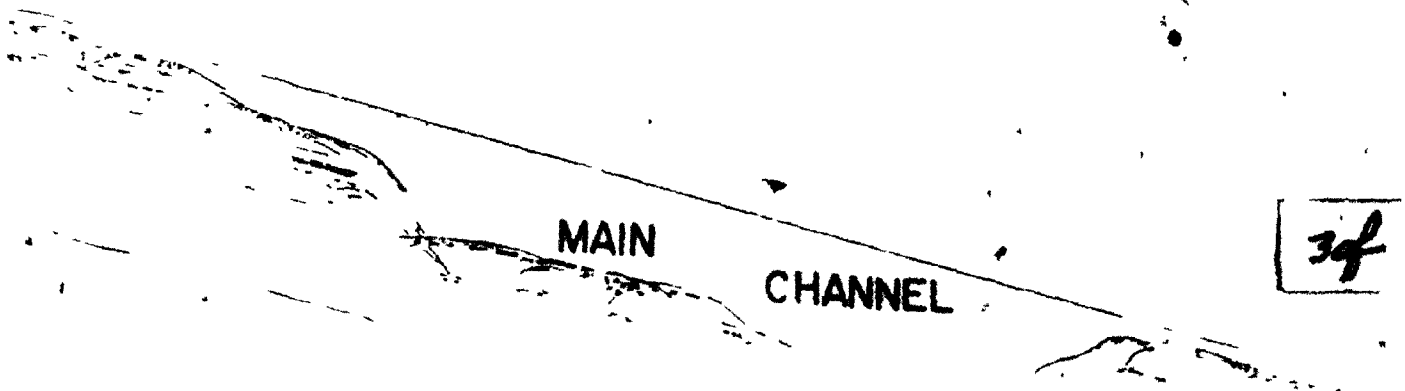
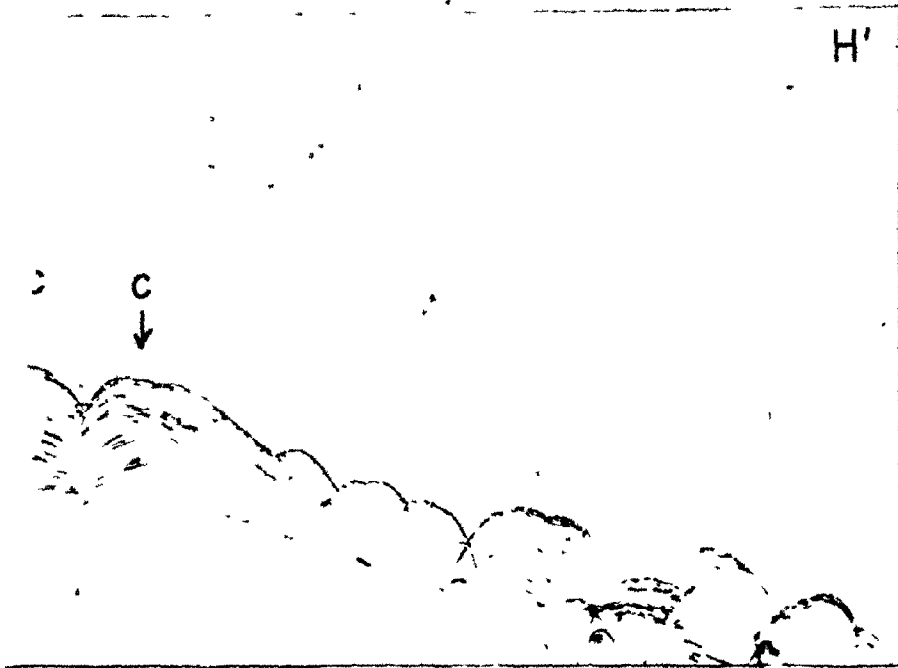
10 of 10



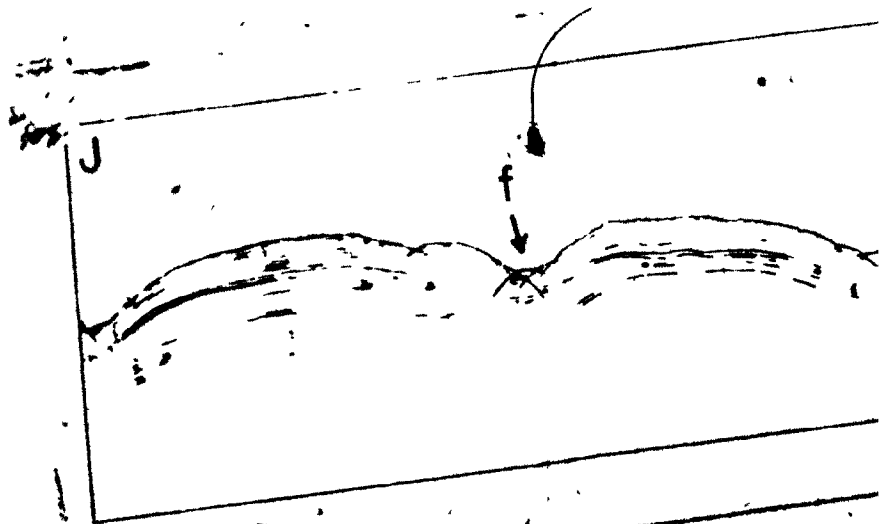


28

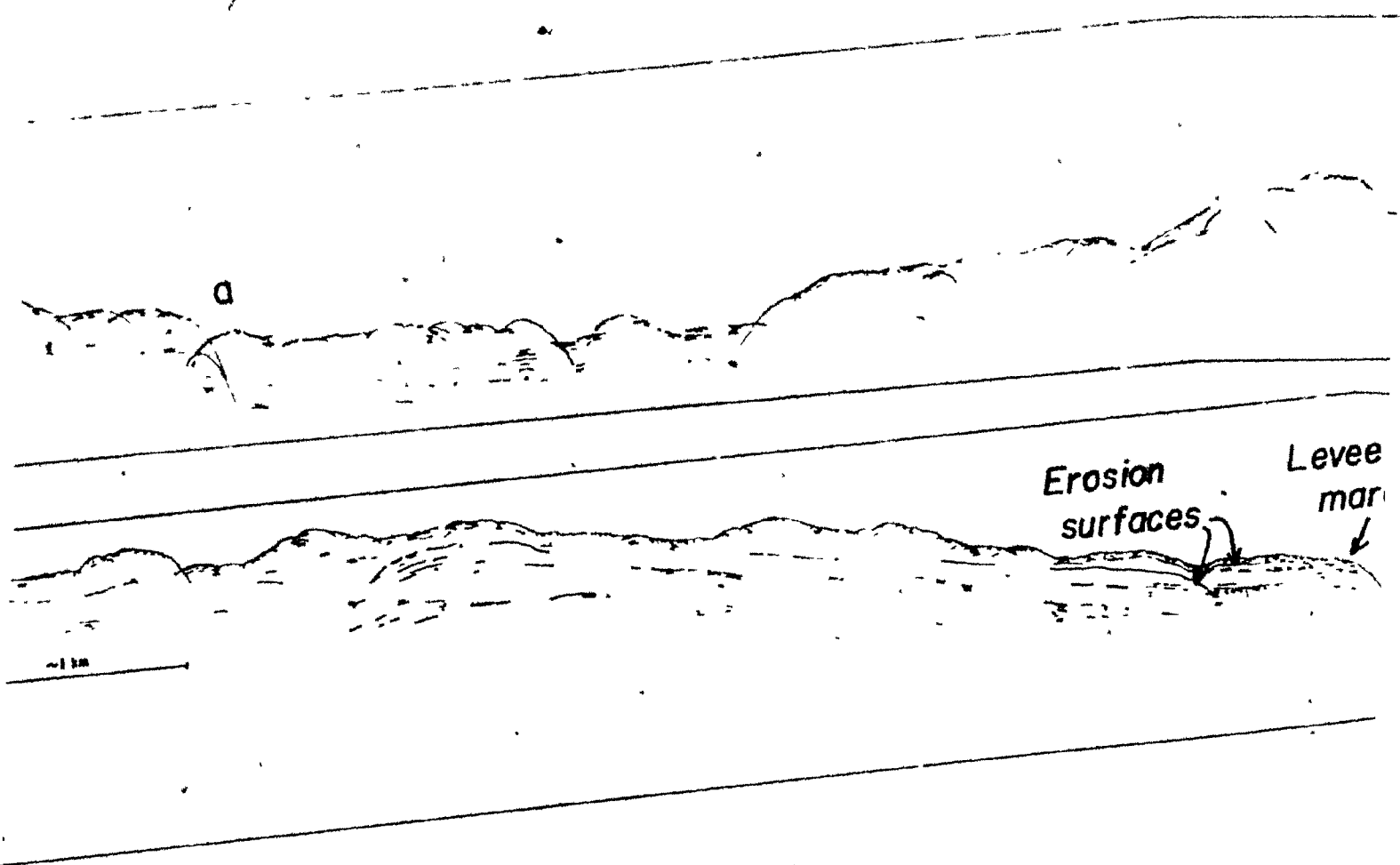








*59*



698

MAIN

CHANNEL

50 m

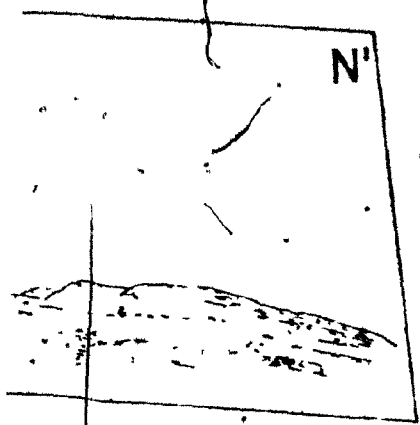
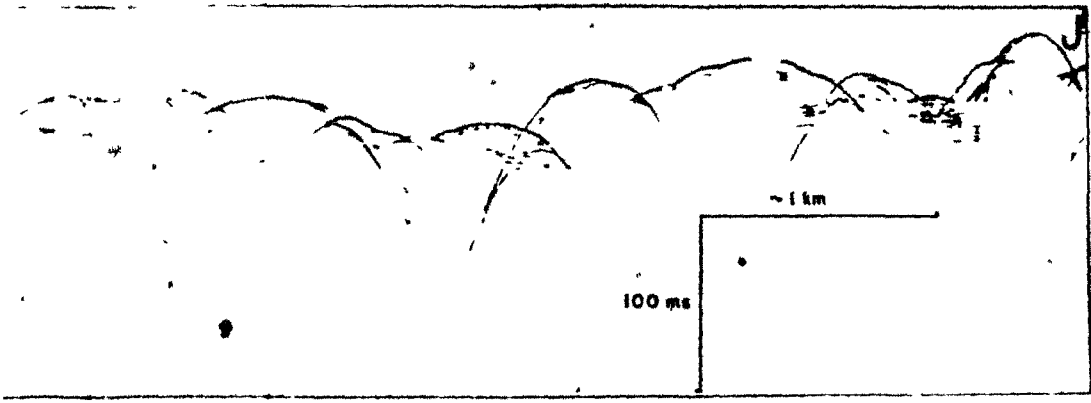
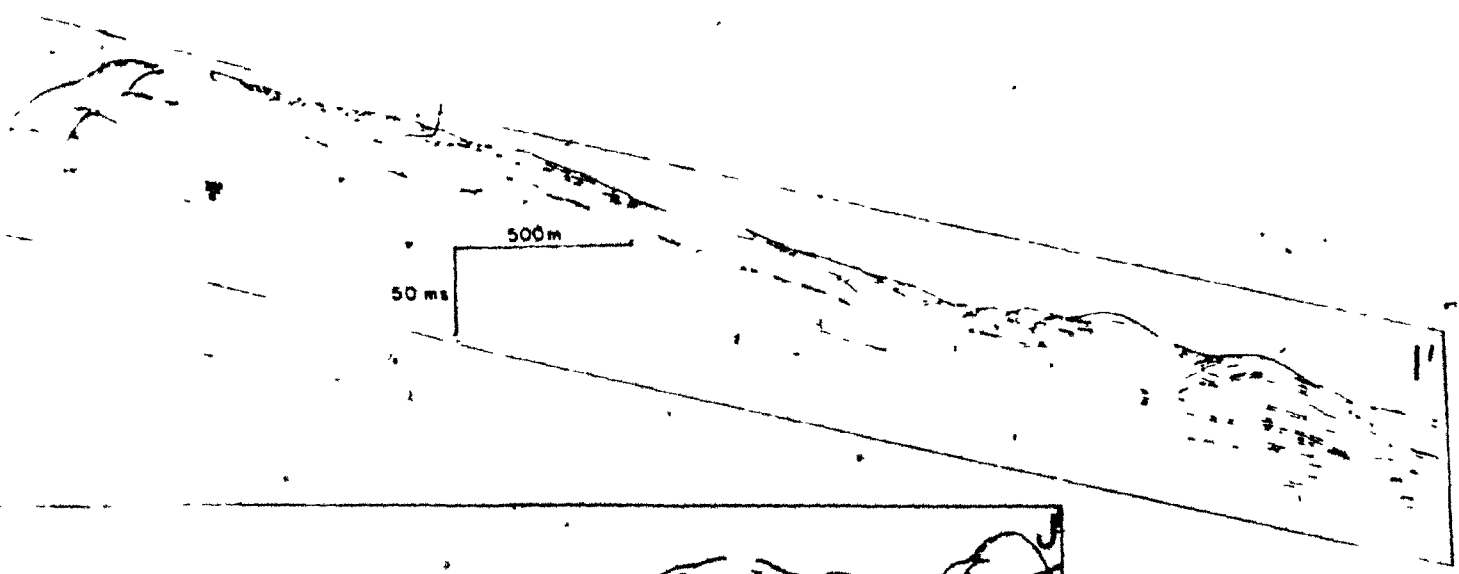
MAIN  
CHANNEL

reef-like  
margin

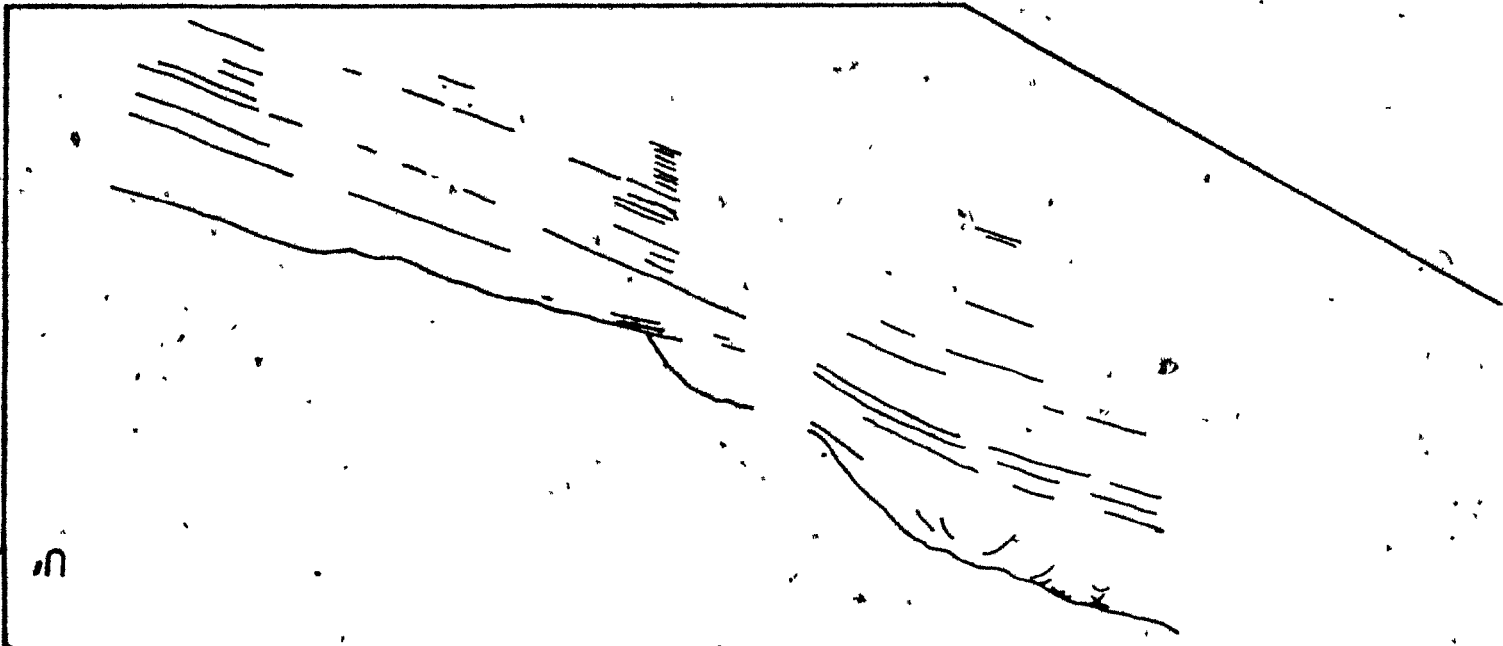
MAIN  
CHANNEL

N'

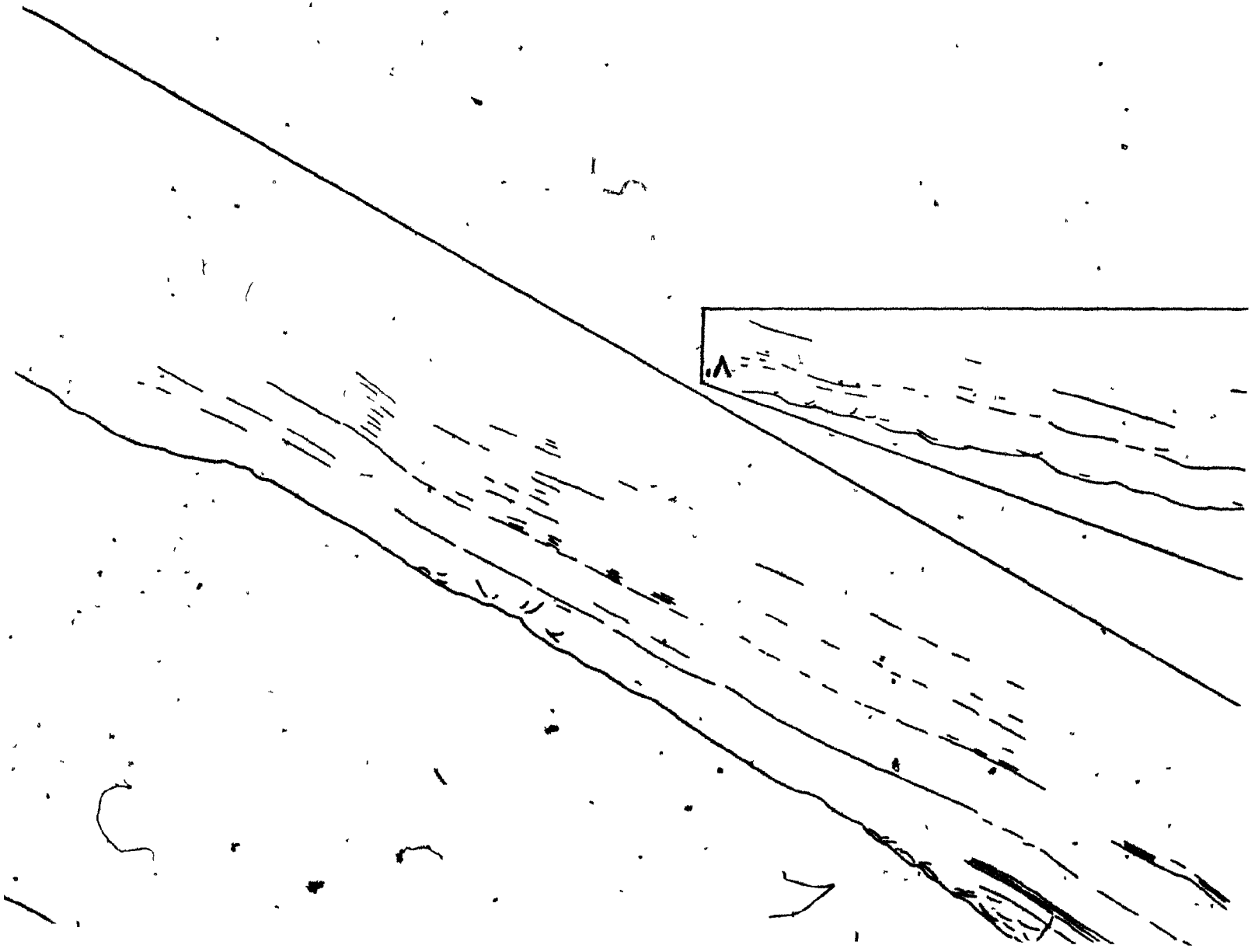
74

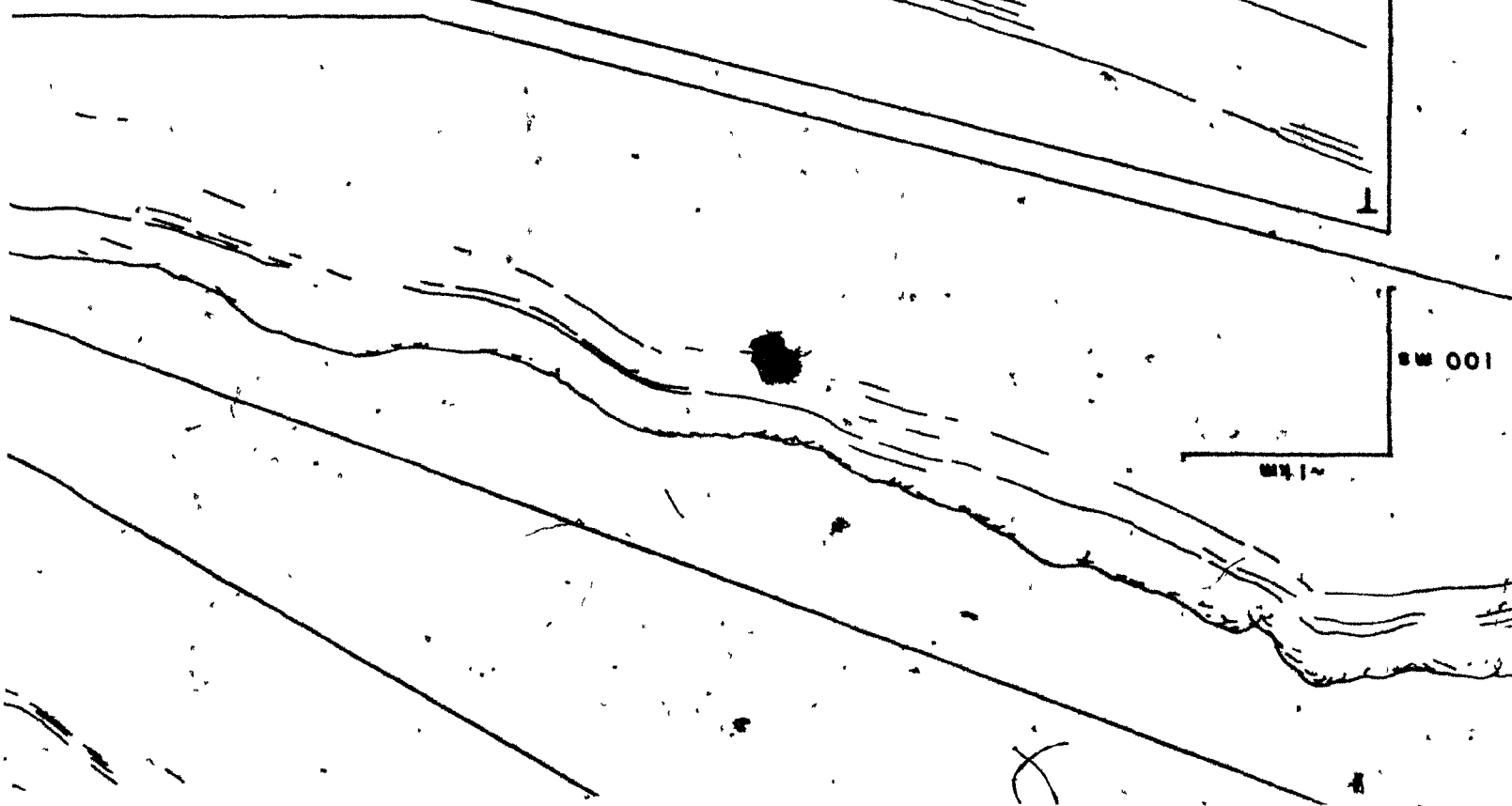
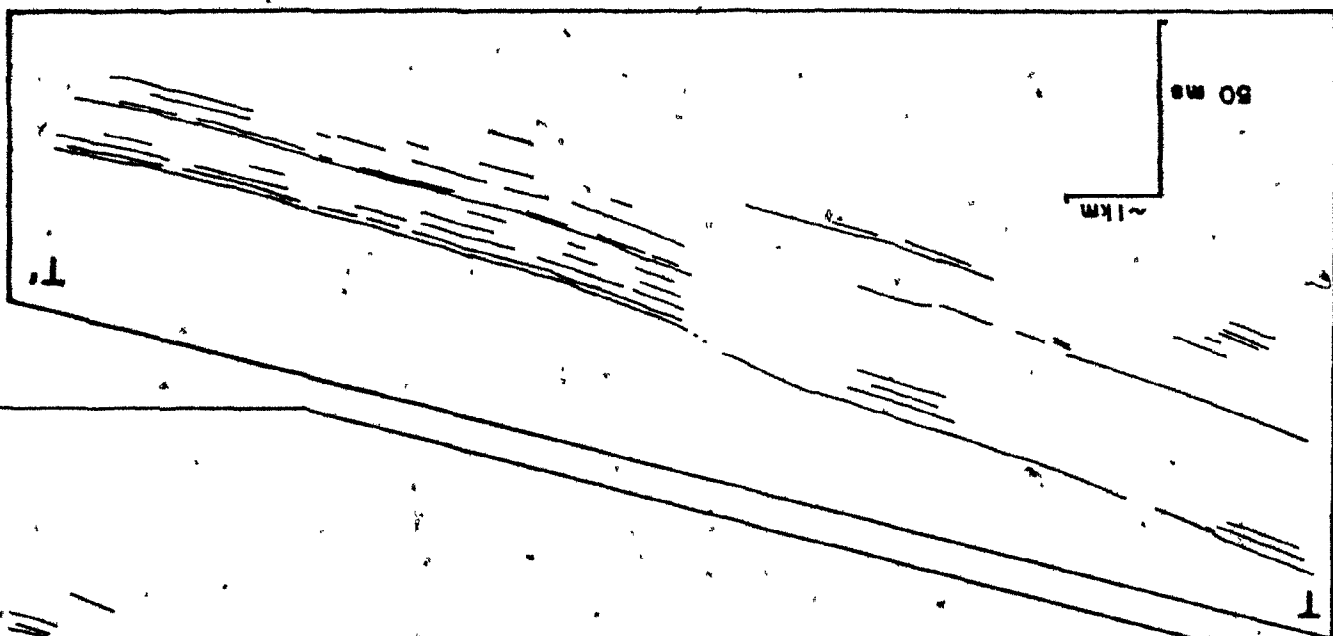


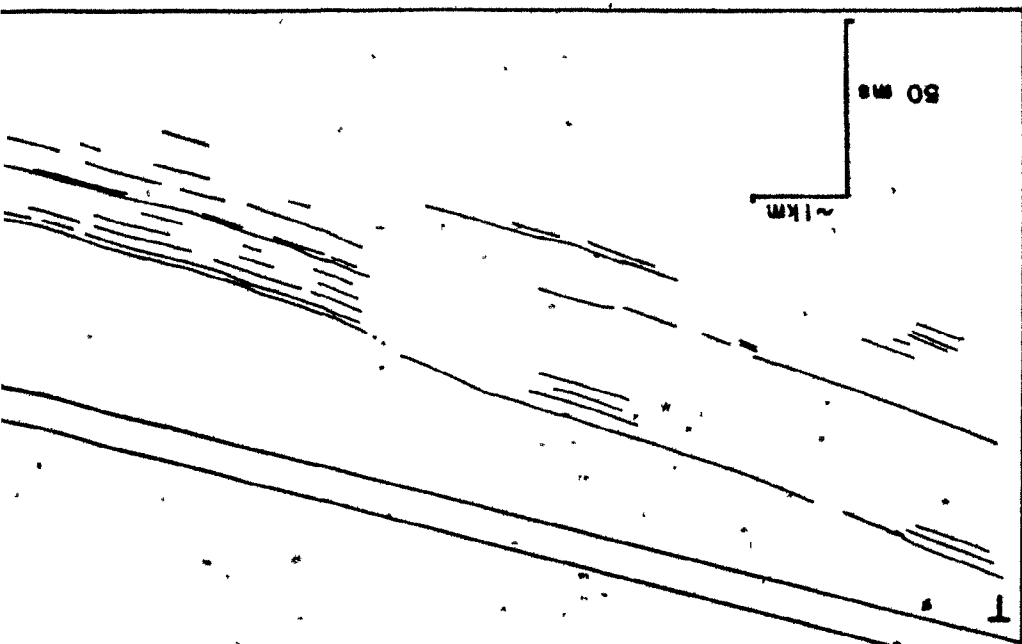
40



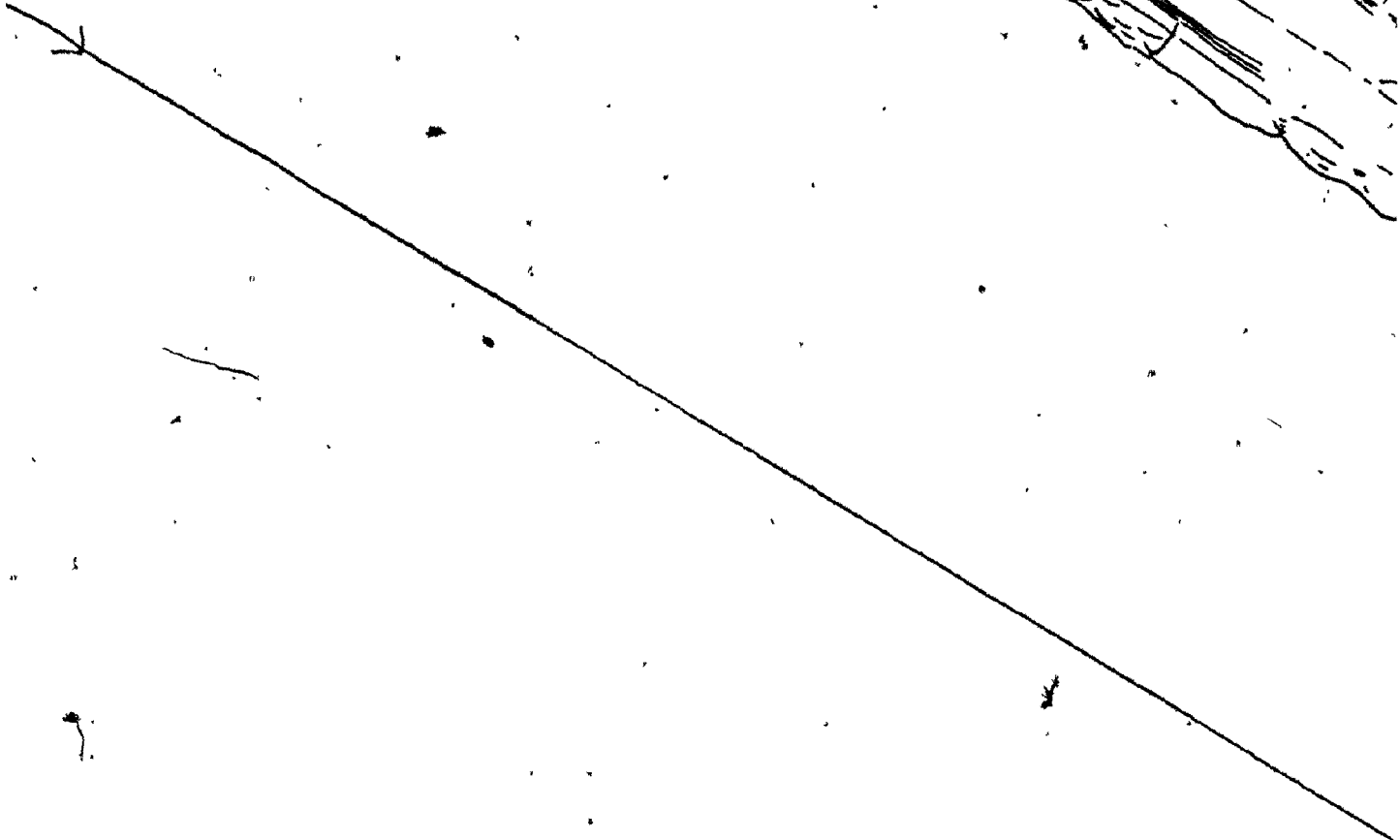
u



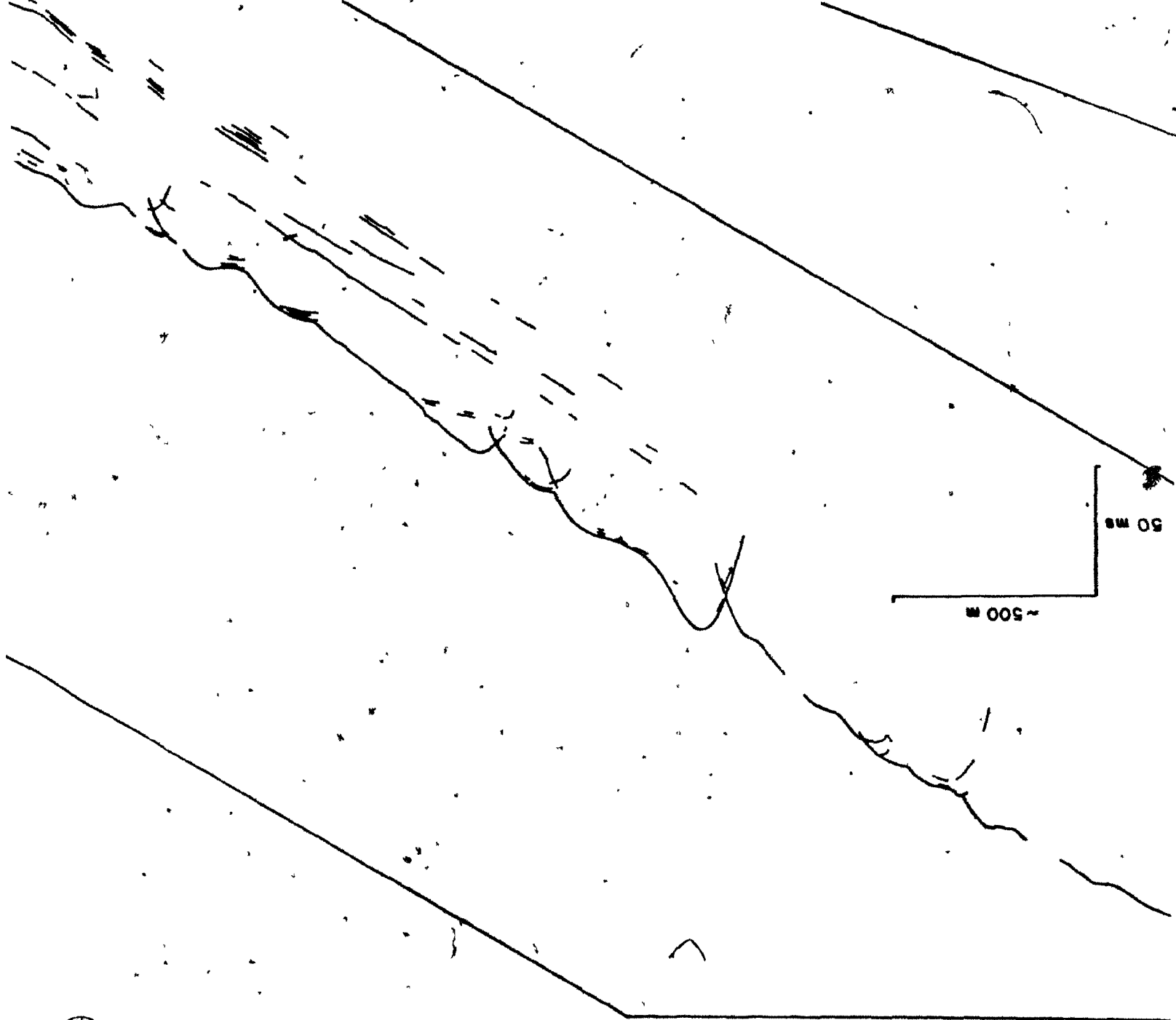




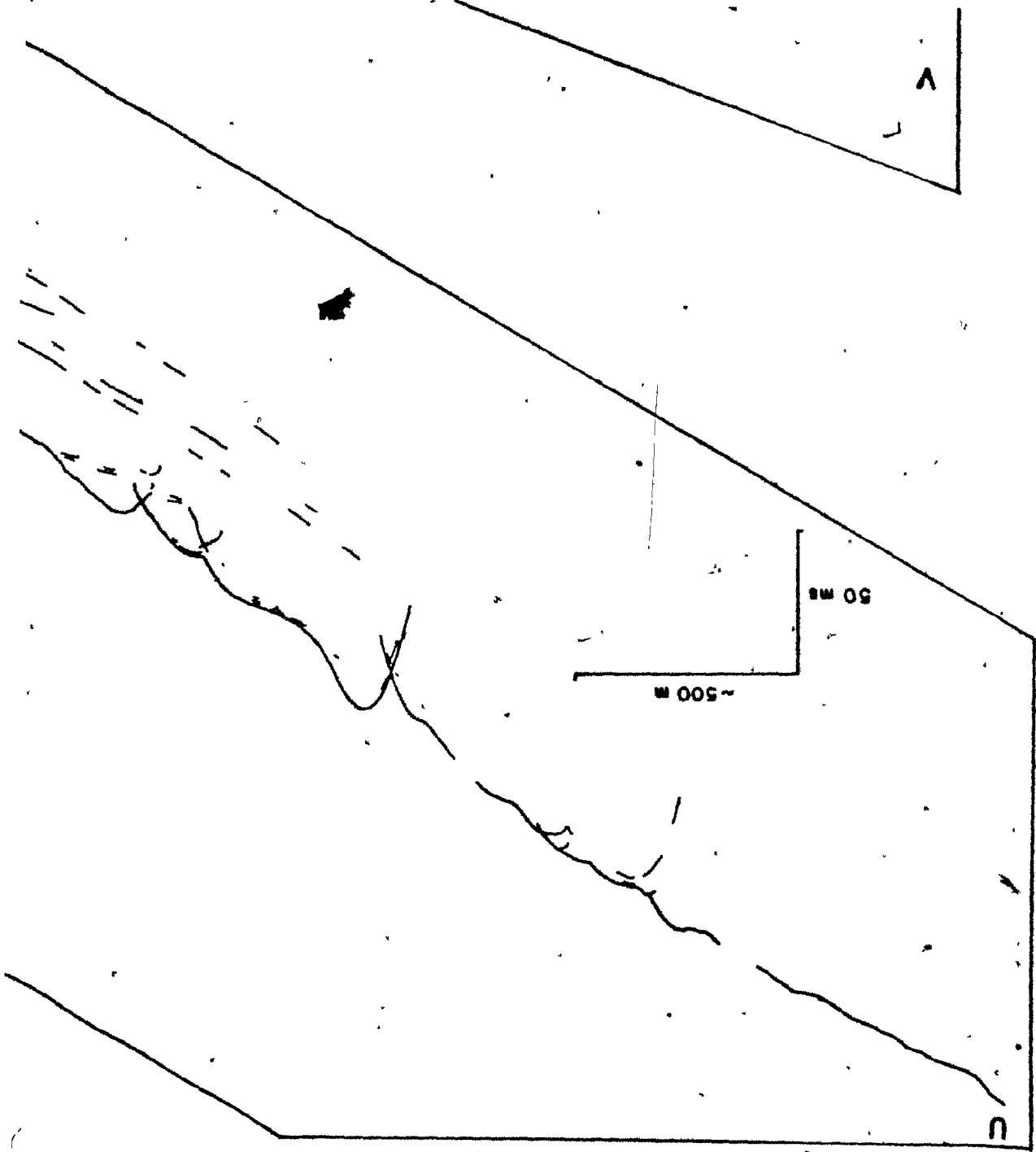
58



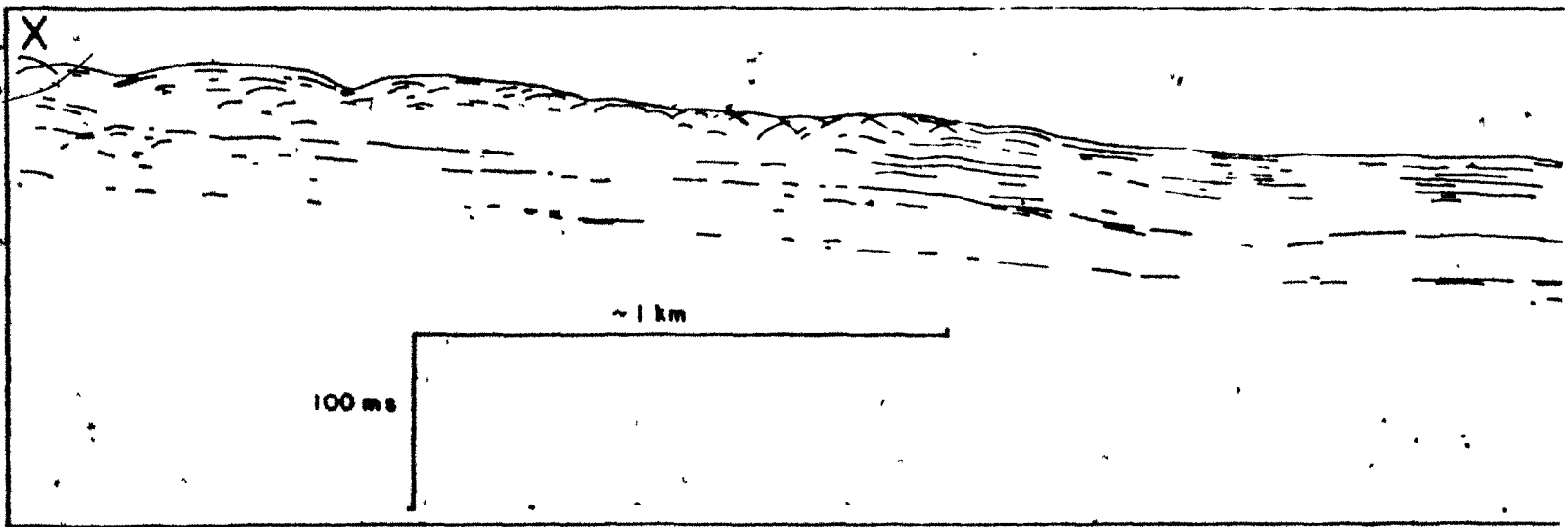
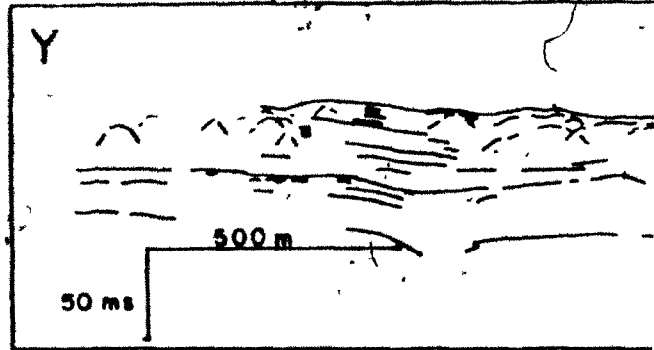
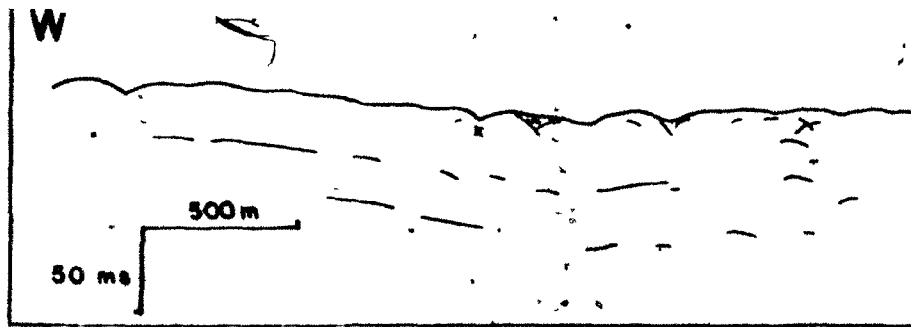
69



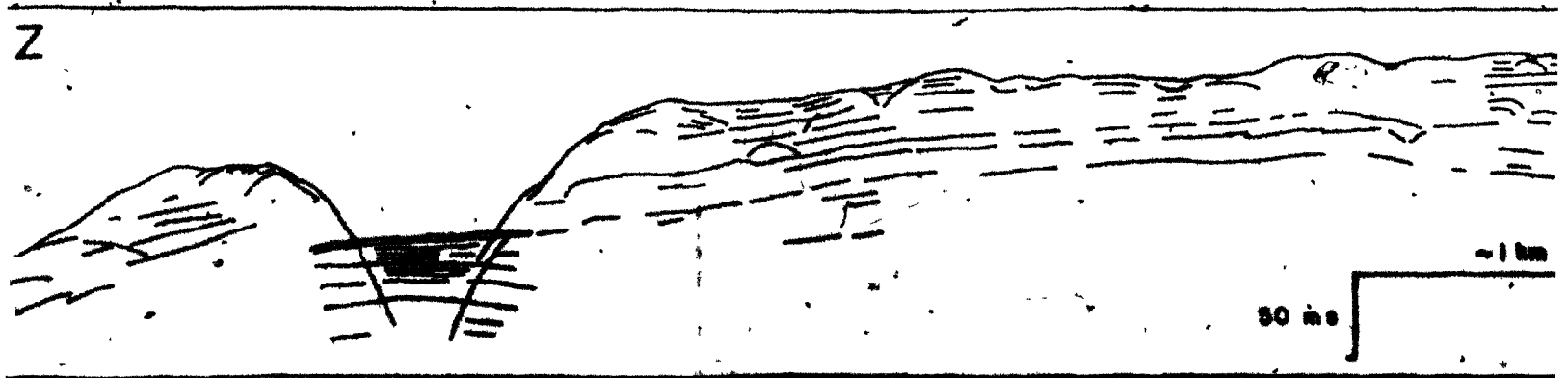
74

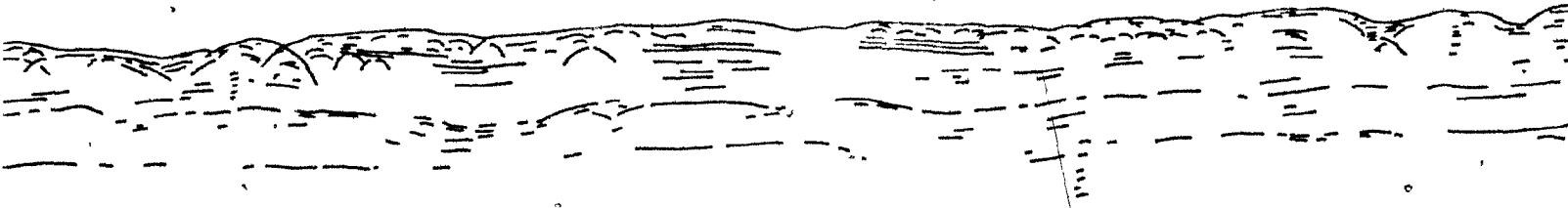
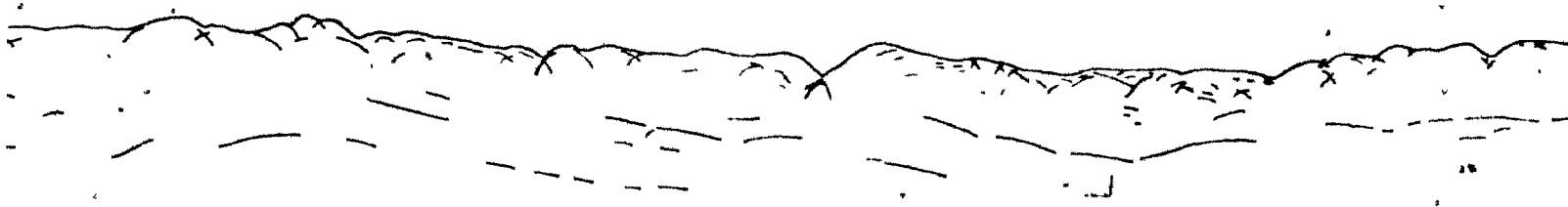


8/8



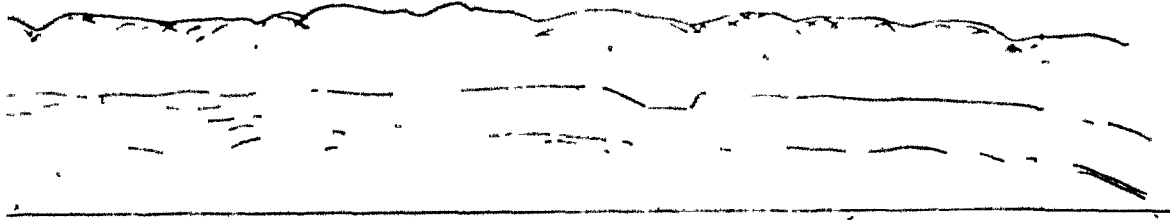
19





~1 km

W'



Y'

